FORTSCHRITTE DER CHEMIE ORGANISCHER NATURSTOFFE

92

PROGRESS IN THE CHEMISTRY OF ORGANIC NATURAL PRODUCTS

Editors
A. D. Kinghorn · H. Falk · J. Kobayashi

Authors
H. Budzikiewicz
R. Pereda-Miranda, D. Rosas-Ramírez, and J. Castañeda-Gómez

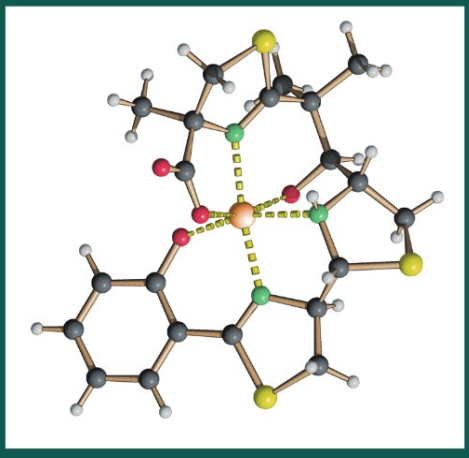

SpringerWienNewYork

SpringerWienNewYork

Fortschritte der Chemie
organischer Naturstoffe

Progress in the Chemistry
of Organic Natural Products

Founded by L. Zechmeister

92

Fortschritte der Chemie organischer Naturstoffe

Progress in the Chemistry of Organic Natural Products

Authors:
H. Budzikiewicz
R. Pereda-Miranda, D. Rosas-Ramírez,
and J. Castañeda-Gómez

SpringerWienNewYork

Prof. A. Douglas Kinghorn, College of Pharmacy,
Ohio State University, Columbus, OH, USA

em. Univ.-Prof. Dr. H. Falk, Institut für Organische Chemie,
Johannes-Kepler-Universität, Linz, Austria

Prof. Dr. J. Kobayashi, Graduate School of Pharmaceutical Sciences,
Hokkaido University, Sapporo, Japan

SpringerWienNewYork is a part of
Springer Science + Business Media
springer.at

Library of Congress Catalog Card Number 2009941525

Typesetting: SPI, Chennai

Printed on acid-free and chlorine-free bleached paper
SPIN: 12210411

With 36 (partly coloured) Figures and 10 coloured Plates

ISSN 0071-7886
ISBN 978-3-211-99660-7 e-ISBN 978-3-211-99661-4
DOI 10.1007/ 978-3-211-99661-4
SpringerWienNewYork

Brief CV – Herbert Budzikiewicz

Herbert Budzikiewicz was born on February 20, 1933 in Vienna (Austria). He received his Ph. D. in chemistry in 1959 from the University of Vienna. From 1961 to 1965, he was head of the mass spectrometry facilities of the Department of Chemistry at Stanford University (CA, USA). From 1965 to 1969, he was at the University of Braunschweig (Germany), where he received the *venia legendi* for organic chemistry. In 1970, he became *professor ordinarius* at the Institute of Organic Chemistry of the University at Köln (Germany). He was dean of the Faculty of Sciences several times and since 1998, he has been *emeritus*.

The fields of research of Herbert Budzikiewicz are mass spectrometry and natural products chemistry, in which he specialized in bacterial metabolites. He is the author of over 500 research publications and he authored and co-authored several books on mass spectrometry. In 2008, he received the Honor Medal of the German Mass Spectrometry Society.

Brief CV – Rogelio Pereda-Miranda

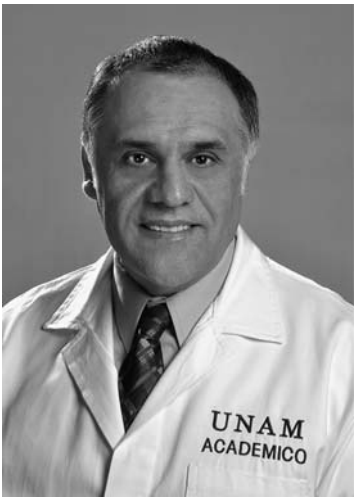

Rogelio Pereda-Miranda is a native of Mexico City and completed his undergraduate education in Biology at the Metropolitan Autonomous University in 1981. He received his Ph.D. in Chemistry from the National Autonomous University of Mexico (UNAM) in 1994. Following a postdoctoral fellowship at the Institutes of Biology and Chemistry, University of Ottawa, he joined the faculty of the Department of Pharmacy, School of Chemistry, UNAM, where he has been Full Professor of Pharmacognosy. Dr. Pereda-Miranda has published 85 papers in plant secondary metabolites with relevant medicinal and agrochemical importance. He has had a long-standing interest in developing analytical methods for the isolation of biodynamic principles by modern preparative chromatography techniques. His research interests also include determination of the tridimensional structure and molecular conformation by nuclear magnetic resonance spectroscopy and molecular modeling of carbohydrates, oligosaccharides and complex secondary metabolites. Currently, he is working in the chemical design and total synthesis of new substances with antimicrobial, cytotoxic and antineoplasic activities based on natural products.

Brief CV – Daniel Rosas-Ramírez

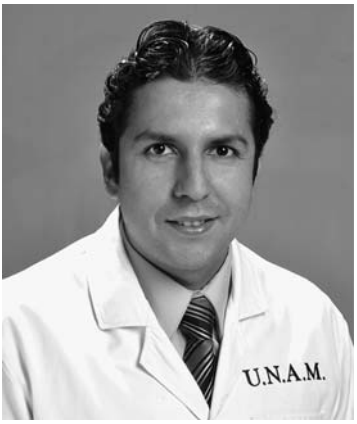

Daniel Rosas-Ramírez was born in Mexico City. He obtained his B.Sc. (2006) from La Salle University and his M.Sc. (2007) from the National Autonomous University of Mexico (UNAM). As a Ph.D. student, he has spent two years at the Department of Pharmacy, School of Chemistry, UNAM, working on the conformation by NMR spectroscopy and crystal structure of sweet potato oligosaccharides.

Brief CV – Jhon Castañeda-Gómez

Jhon Castañeda-Gómez is a native of Manizales, Colombia. He obtained his B.Sc (1999) from the University of Caldas and his M.Sc. (2007) from Del Valle University in Colombia. He has completed two years of the Ph.D. program at the School of Chemistry, National Autonomous University of Mexico, and working at the Department of Pharmacy on the development of analytical techniques for the isolation of complex polysaccharides from plant sources.

Contents

Listed in PubMed

List of Contributors

Budzikiewicz, Prof. Dr. H., Institut für Organische Chemie, Universität zu Köln, Greinstr. 4, 50939 Köln, Germany
e-mail: aco88@uni-koeln.de

Castañeda-Gómez, Dr. J., Departamento de Farmacia, Facultad de Química, Universidad Nacional Autónoma de México, Ciudad Universitaria, 04510 DF, México
e-mail: jhoncast15@yahoo.com

Pereda-Miranda, Prof. Dr. R., Departamento de Farmacia, Facultad de Química, Universidad Nacional Autónoma de México, Ciudad Universitaria, 04510 DF, México
e-mail: pereda@servidor.unam.mx

Rosas-Ramírez, Dr. D., Departamento de Farmacia, Facultad de Química, Universidad Nacional Autónoma de México, Ciudad Universitaria, 04510 DF, México
e-mail: veca@hotmail.com

Microbial Siderophores

Herbert Budzikiewicz

Contents

H. Budzikiewicz
Institut für Organische Chemie, Universität zu Köln, Greinstr. 4, 50939 Köln, Germany
e-mail: aco88@uni-koeln.de

A.D. Kinghorn et al. (eds.), *Fortschritte der Chemie organischer Naturstoffe / Progress in the Chemistry of Organic Natural Products, Vol. 92*,
DOI 10.1007/978-3-211-99661-4_1, © Springer-Verlag/Wien 2010

1. Introduction

Iron is of great importance for many metabolic processes since the redox potential between its two valence states Fe^{2+} and Fe^{3+} lies within the range of physiological processes. Actually, iron is not a rare element, it is fourth in abundance in the earth crust, but it is not readily available for microorganisms. In the soil ferric oxide hydrates are formed at *pH* values around seven and the concentration of free Fe^{3+} is at best 10^{-17} mol/dm^3 while about 10^{-6} mol/dm^3 would be needed. In living organisms iron is usually strongly bound to peptidic substances such as transferrins. To increase the supply of soluble iron microorganisms other than those living in an acidic habitat may circumvent the problem by reduction of Fe^{3+} to Fe^{2+} (*182*), which seems to be of major importance for marine phytoplankton (*151*); see also amphiphilic marine bacteria (Sect. 2.8) and Fe^{2+} binding ligands (Sect. 7) below. An important alternative is the production of Fe^{3+} chelating compounds, so-called siderophores. Siderophores are secondary metabolites with masses below 2,000 Da and a high affinity to Fe^{3+}. Small iron-siderophore complexes can enter the cell via unspecific porins, larger ones need a transport system that recognizes the ferri-siderophore at the cell surface. In the cell, iron is released mostly by reduction to the less strongly bound Fe^{2+} state (*137*), and the free siderophore is re-exported ("shuttle mechanism"); for a modified shuttle system see pyoverdins (Sect. 2.1) and amonabactins (Sect. 2.7). Rarely the siderophore is degraded in the periplasmatic space as, *e.g.* enterobactin (Sect. 2.7). Alternatively Fe^{3+} is transferred at the cell surface from the ferri-siderophore to a trans-membrane transport system ("taxi mechanism"). A probably archaic and unspecific variety of the taxi mechanism comprises the reduction of Fe^{3+} at the cell surface (see ferrichrome A, Sect. 2.6 (*99*, *105*)). The terms "shuttle" and "taxi mechanism" were coined by *Raymond* and *Carrano* (*296*).

A microbial strain may produce more than one siderophore. There are variations in fatty acid chains of a lipophilic part or in the amino acids making up the backbone, as well as released intermediates of the biosynthetic chain. These variations belong all to the same structural pattern. However, there is also the possibility that so-called secondary siderophores are encountered. They constitute a different structural type, usually less complex in their constitution but also less efficient in binding Fe^{3+} than the primary ones. Secondary siderophores will be produced when the demand for iron is not so severe or in case there is a genetic defect impeding the production of the primary ones. Examples will be found throughout the review.

Obviously siderophores can be potent virulence factors of pathogenic bacteria. Siderophores in many cases have elaborate structures providing recognition only by the receptor site of the producing species. This renders a pirating by competing microorganisms more difficult. The structural specificities of siderophores have been used for classification purposes of bacterial species (see especially pyoverdins, Sect. 2.1).

Whether a Fe^{3+} binding metabolite is actually involved in the iron transport has not always been established firmly. Criteria are the pronounced production under iron starvation and growth after feeding, or labeling studies (at best simultaneously of Fe^{3+} and of the ligand, see, *e.g.* parabactin, Sect. 3.2, and schizokinen, Sect. 4.1). Chelators whose function is uncertain will be included in this review with an explanatory remark. Incompletely characterized siderophores will be mentioned when at least some structural elements have been identified. However, the mere statement that color reactions for catecholates (*8a*) or hydroxamates (*9a*) were positive will not be sufficient. Not included will be the sideromycins, conjugates of siderophores with antibiotically active residues, produced mainly by *Streptomyces* spp., which use the iron transport paths for "Trojan Horse" strategies. For further references see (*34*, *97*, *187*).

Due to its high charge density, small ion radius, and low polarizability, Fe^{3+} is a hard *Lewis* acid and can bind strongly to hard *Lewis* bases such as oxide ions. It forms octahedral d^5 high spin complexes providing six coordination sites, which can accommodate three bidentate ligands. The major ligands types are catecholates, hydroxamates, and α-hydroxy carboxylates; other ligands are encountered occasionally. Siderophores containing different ligand types are not uncommon. Three bidentate ligands are often connected by aliphatic segments keeping them in place for complexation. This results in an entropic advantage over three non-connected ligands. Siderophores containing only two binding sites form either $(Fe^{3+})_2Lig_3$ complexes or the remaining two octahedral loci accommodate some external ligand (see, *e.g.* pyochelin, Sect. 5). For $(Fe^{3+})_2Lig_3$ structures with three bridges or with one bridging ligand have been discussed. The latter variety has been proven for alcaligin (Sect. 3.3). Three bidentate ligands can be arranged around the Fe^{3+} nucleus in two ways forming a left-handed or a right-handed screw, designated as Λ or Δ. Three identical ligands can point all in the same direction (*cis*) or one of them is reversed (*trans*). The chiral arrangement of the Fe^{3+} complex can be determined by X-ray analysis or can be deduced from the sign of the broad CD extremum at *ca.* 500 nm correlated with the metal-to-ligand charge transfer band. A positive $\Delta\varepsilon$ indicates a Λ configuration.

Ga^{3+} complexes are frequently analyzed for two reasons. Ga^{3+} also forms octahedral structures and it has almost the same ion radius as Fe^{3+} (62 *vs.* 65 pm). In contrast to Fe^{3+} it is diamagnetic and its complexes are therefore amenable to NMR analysis. Also in contrast to Fe^{3+} it cannot be reduced and therefore it is used for uptake studies interested in the fate of the complex in the cell.

Siderophores can be classified by different criteria. In this review related structural types will be grouped together. Some arbitrariness cannot be avoided due to the occurrence of "mixed types". Cross-references will then be given. Trivial names

have either been given to the free ligands or to their iron complexes. In the latter case the free ligands are referred to as "desferri" or "deferri" (sometimes in a shortened form as "desferrioxamines" for "desferriferrioxamines") or as "pro" (see Sect. 3.3). Occasionally the name applied originally to the iron complex was used later for the free ligand (*e.g.* ferribactins, Sect. 2.1). These variations should be kept in mind when literature search programs are used.

For earlier compilations of siderophores see (*97*, *255a*, *276*), specifically for fungal siderophores (*157a*, *300*, *383*), and for biosynthesis pathways (*19*, *63*, *403*). Reviews for specific classes of siderophores will be mentioned where applicable.

2. Peptide Siderophores

In this group the ligands are incorporated in a peptide chain usually containing both D- (underlined in the structural formulas below) and L-configured amino acids. Frequently the two ends of the peptide chain are blocked by the formation of cyclic structures or otherwise. This prevents the degradation by proteolytic enzymes. Non-proteinogenic amino acids are encountered (homoserine, Hse; ornithine, Orn; 2,4-diaminobutyric acid, Dab; 2,3-dehydrobutyric acid, Dhb), lysine and ornithine may be incorporated in the chain by their ε/δ- rather than by their α-amino group, and amino acids may be modified to form ligand sites (3-hydroxy-aspartic acid, OHAsp; 3-hydroxy-histidine, OHHis; N^5-acyl-N^5-hydroxy-ornithine, acylOHOrn; *N*-hydroxy-*cyclo*-ornithine, *i.e.* 3-amino-1-hydroxy-piperidone-2, cOHOrn). Diaminobutyric acid frequently condenses with the preceding amino acid (Chart 1) giving a tetrahydropyrimidine ring (*116*). These condensation products are indicated below by a parenthesis as *e.g.* (Hse-Dab) in azoverdin (Sect. 2.2).

2.1. *Pyoverdins and Related Siderophores from Pseudomonas spp.*

The most thoroughly investigated representatives are the pyoverdins, also spelled pyoverdines and occasionally named pseudobactins (*353*), produced by the fluorescent members of the genus *Pseudomonas*. For reviews see (*44*, *231*); for a detailed

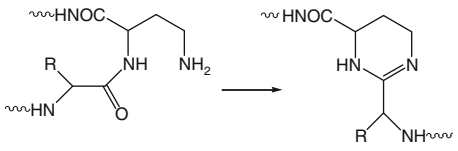

Chart 1. Condensation of a Dab residue with the preceding amino acid residue

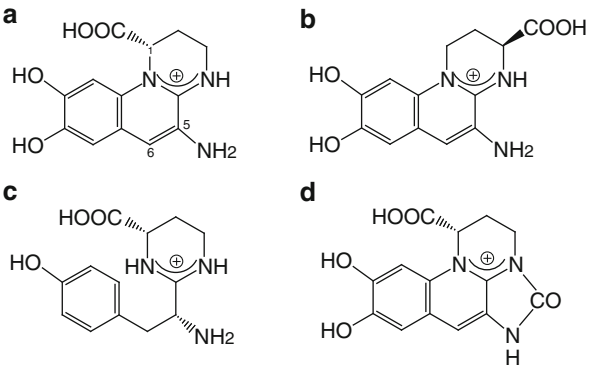

Fig. 1. Chromophore types: (**a**) pyoverdin, (**b**) isopyoverdin, (**c**) ferribactin, (**d**) azotobactin

study of the siderophores of this genus (*37*). Pyoverdins consist of three distinct structural parts, a chromophore (Chr**a**) (Fig. 1, **a**), a peptide chain comprising six to twelve amino acids, and a dicarboxylic acid (succinic acid – Suc-, malic, glutamic, and 2-oxoglutaric acid) or monoamides (succinamide, malamide). For glutamic and 2-oxoglutaric acid the binding to the chromophore by their γ-carboxyl groups has been established by chemical degradation (*124*). For malic acid some not really convincing and partially contradictory NMR arguments have been advanced (*319*) for the binding by the carboxyl group neighboring the CH_2 group. Recently mass spectrometric arguments were reported suggesting a binding *via* the other carboxyl group (*45*).

The about fifty pyoverdins for which structures have been proposed can be divided into three structural types exemplified by the three pyoverdins of *Pseudomonas aeruginosa* (*234*) (Fig. 2), *viz*. pyoverdins (a) with a C-terminal tri- or tetra-cyclopeptidic substructure (lactam formation between the C-terminal carboxyl group and an in-chain lysine or ornithine), *e.g*. ATCC 15692 (PAO1) (**1**), (b) with a C-terminal cOHOrn, *e.g*. ATCC 27853 (**2**), and (c) with a C-terminal free carboxyl group, *e.g*. Pa6 (R) (**3**). The free carboxyl group is probably the hydrolysis product of a depsipeptidic substructure (ester formation between the C-terminal carboxyl group and an in-chain serine or threonine). In several cases both the cyclic and the hydrolyzed open-chain form were found (*e.g*. (*50*)). Binding sites for Fe^{3+} are the catecholate part of the chromophore Chr**a** and two units in the peptide chain, hydroxamate (acylOHOrn, cOHOrn) and/or α-hydroxycarboxylate (OHAsp, OHHis).

Complete structural analysis requires mass spectral and NMR data as well as chemical degradation and analysis of the chirality of the constituent amino acids, determination of the mode of linkage of lysine (α- or ε-), the size of the cyclopeptide or cyclodepsipeptide ring, *etc*. (*37*). In some cases structures have been proposed based only on mass spectral data. Difficulties arising in this approach were discussed (*44*). To determine the three-dimensional structure an X-ray

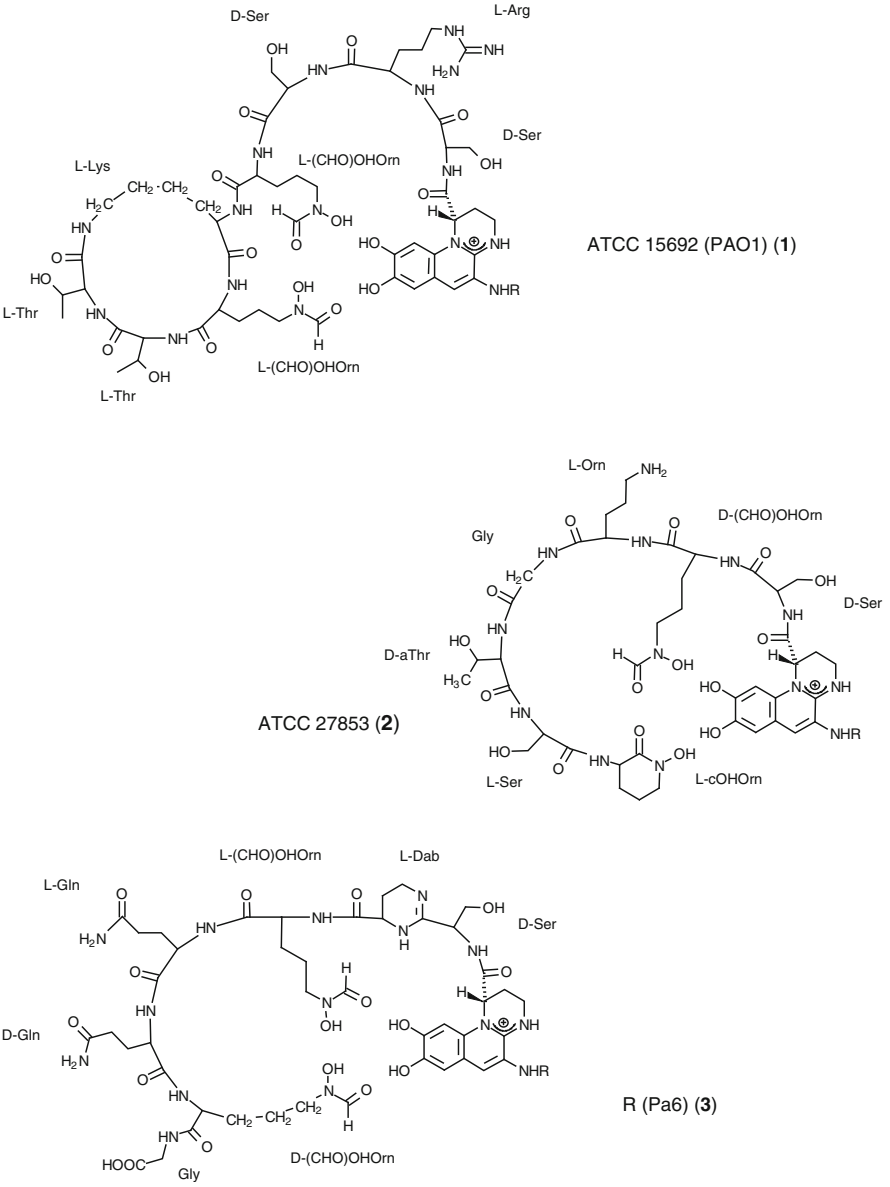

Fig. 2. Pyoverdins from *Pseudomonas aeruginosa* representing the three structural types

analysis (Plate 1) so far only of the Fe^{3+} complex of the pyoverdin B10 (**4**) was performed (*353*).

4 Suc-Chr**a**-εLys-OHAsp-Ala-aThr-Ala-cOHOrn

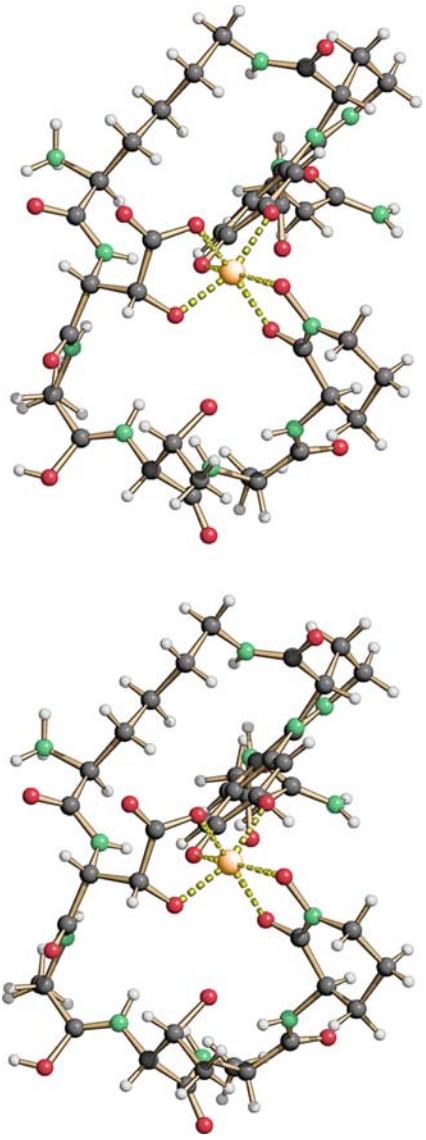

Plate 1. X-ray structure (stereo view) of ferri-pyoverdin B10 (ferri-**4**)

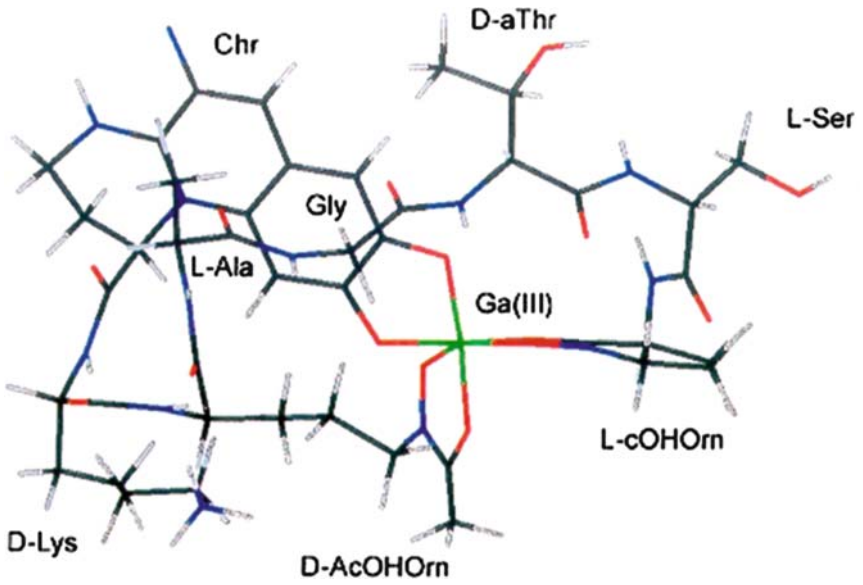

Plate 2. Calculated three-dimensional structure of the Ga^{3+}-complex of pyoverdin PL8 (without side chain) Chr**a**-Lys-acetylOHOrn-Ala-Gly-aThr-Ser-cOHOrn

As an alternative strategy the investigation of the isomorphic Ga^{3+} complexes by NMR analysis was developed (*241*) for the pyoverdin GM-II (**5**) and extended to other pyoverdins, *e.g.* PL8 (*16*) (Plate 2) (*H. Budzikiewicz*, unpublished).

5 Suc-Chr**a**-Ala-Lys-Gly-Gly-OHAsp-Gln-Ser
-Ala-Ala-Ala-Ala-cOHOrn

In all cases the metal ion was found to lie at the surface of the complex. This facilitates its uptake and release. For the pyoverdins both Λ and Δ arrangements have been reported (*37*).

Iron transport through the cell membrane follows a modified shuttle mechanism. Evidence has been presented that the iron-free siderophore of *P. aeruginosa* PAO1 (**1**, Fig. 2) binds strongly to the receptor protein (*67*, *314a*). This suggests two scenarios for the subsequent steps of iron transfer, an exchange of the ligands or a transfer or Fe^{3+} between them. By ^{3}H- and ^{55}Fe-labeling as well as fluorescence studies it was shown that an exchange between the approching ferri-pyoverdin and the bound iron-free pyoverdin occurs and that the former one enters the cell, *i.e.* that no Fe^{3+} exchange between the two ligands takes place (*314b*). Model studies with *Aeromonas* (Sect. 2.7) demonstrated there the iron-exchange variety. Binding of the iron-free siderophore to the receptor protein seems to be a common feature of the transport systems of *P. aeruginosa* and *Escherichia coli* (*145a*).

The peptide chains of the pyoverdins are responsible for the recognition of the ferri-siderophore at the cell surface of the producing species. It is usually highly strain specific. Cross-recognition between two strains is only observed when structurally closely related pyoverdins are produced (*125*, *233*). An exception seems to be *P. aeruginosa* ATCC 15692, which besides its own ferripyoverdin (Fe-**1**), accepts several foreign ones (*128a*).

Without going into structural details, the pyoverdins stemming from the saprophytic group *Pseudomonas aeruginosa/fluorescens/putida* contain either two hydroxamic acid units or one hydroxamic and one α-hydroxycarboxylic acid, and those from the phytopathogens *P. syringae etc.* two α-hydroxycarboxylic acids. Structural differences of pyoverdins have been used recently to characterize species newly defined by breaking up the classical cluster of *P. fluorescens/putida* (*e.g.* (*229*, *231*)). A listing of all pyoverdins from *Pseudomonas* spp. for which structural data have been published up to December 2009 is contained in the Appendix.

Pyoverdin-like siderophores with other chromophores have also been observed (see Fig. 1) (*45*). The 5,6-dihydropyoverdins (Chr**a** without the 5,6-double bond) and the ferribactins (Chr**c**) are considered to be biogenetic precursors of the pyoverdins (*318*) (the term "ferribactin" was originally used for the Fe^{3+} complex (*221*) and later for the free ligand). An azotobactin chromophore (Chr**d**, see also below Sect. 2.2) is occasionally found in *Pseudomonas* isolates (*e.g.* (*146*)). Siderophores produced by a specific *Pseudomonas* strain but differing in the chromophore always have identical peptide chains.

Isopyoverdins contain the siderophore Fig. 1, Chr**b** with aspartic acid as the first amino acid. They have been encountered so far only in isolates from *Pseudomonas putida* strains, *e.g.* BTP1 (*168*) (**6**).

6 Glu-Chr**b**-Asp-Ala-Asp-acetylOHOrn-Ser-cOHOrn

2.2. *Azomonas and Azotobacter Siderophores*

For a detailed discussion of this class of compounds see (*37*).

Azomonas macrozytogenes produces a siderophore with an isopyoverdin chromophore, azoverdin, but with a peptide chain **7** related to those of azotobactins, *viz.* (*236*).

7 Suc-Chr**b**-Hse-(Hse-Dab)-acetylOHOrn-Ser-acetylOHOrn

The three-dimensional structure of the Ga^{3+} complex was determined by NMR techniques as outlined above. Also here the metal ion lies at the surface of the complex (*377*).

From *Azotobacter vinelandii* the structures of two siderophores were elucidated. They contain the chromophore Chr**d** (Fig. 1) and Hse units: azotobactin 87-I (**8**) (from the three Hse in this sequence two are L and one D configured) from the strain ATCC 12837 (*314*), and azotobactin D (**9**) (*76*) from the strain CCM 289.

8 Chr**d**-Ser-Ser-Hse-Gly-OHAsp-Hse-Hse-Hse
-β-hydroxybutyrylOHOrn-Hse

9 Chr**d**-Asp-Ser-Hse-Gly-OHAsp-Ser-Cit-Hse-acetylOHOrn-Hse

Both of them are accompanied by compounds where the C-terminal Hse forms a γ-lactone ring (azotobactin 87-II and δ). An azotobactin O for which also a structure had been proposed (*120*) was shown later to be identical with azotobactin D (*272*). For secondary metabolites see protochelin and its constituents (Sect. 3.2).

Azotobacter chroococcum produces ornithine-containing hydroxamate siderophores with molecular masses 800 and 844 Da (difference of one carboxyl group?) of unknown structure (*115a*).

2.3. Anachelin

Cyanobacteria were probably the first organisms to perform oxygenic photosynthesis resulting eventually in the oxidation of environmental Fe^{2+} to Fe^{3+} with all its consequences. To cope with this problem the production of siderophores was initiated. Not much is known about the siderophores of cyanobacteria. Schizokinen (see below under citrate siderophores, Sect. 4.1) (*326*) found to be produced by several bacterial species may have been acquired by gene transfer; see however also the citrate siderophores synechobactins.

Certainly of genuine origin is anachelin, a strange compound whose biosynthesis requires *inter alia* steps from the peptide and polyketide paths. It exists in an open (anachelin H, Fig. 3, (**10**)) and two cyclic forms arising from an interaction of the carbonyl group of the salicylic acid residue with one of the neighboring

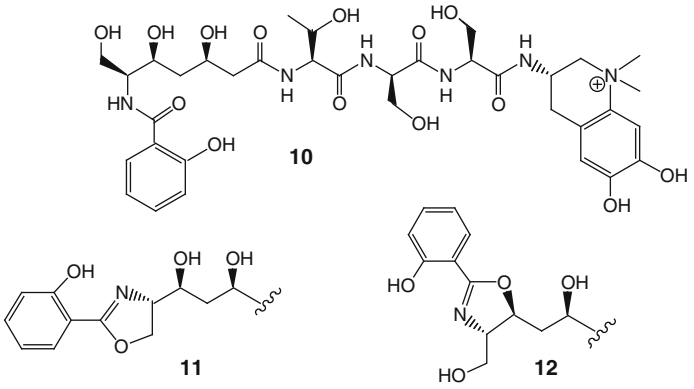

Fig. 3. Anachelin H (**10**), anachelin 1 (**11**), anachelin 2 (**12**)

hydroxy groups (anachelin 1 and 2, Fig. 3, (**11**) and (**12**)) (*22*, *167*). The relative and absolute stereochemistry of all chiral centers was established (*22*, *166*) and confirmed by synthesis (*121*) (see Sect. 8.1). In solution anachelin forms a β-turn arrangement (*122*). Mass spectrometric analysis of the Fe^{3+} complex suggests a 1:1 ratio.

2.4. Actinomycetal Metabolites

Desferrimaduraferrin is a Fe^{3+} complexing metabolite of *Actinomadura madurae* (*185*). It consists of salicylic acid, β-Ala, Gly, L-Ser and N^5-hydroxy-N^2-methyl-L-Orn, with the latter incorporated in a heterocyclic system (Fig. 4, **13**). From the same species the madurastatin group was obtained (*136*). The main representative **A1** shows the sequence salicylic acid, D-azaridine carboxylic acid, L-Ala, β-Ala, N^5-hydroxy-N^2-methyl-Orn, L-cOHOrn (Fig. 4, **14**). In **A2** the azaridine ring is opened giving a Ser residue, **A3** is an isomer of the open form with the salicylic acid bound to the hydroxy group of Ser. **B1** and **B2** are the precursors *N*-salicyloyl-azaridine carboxylic acid and *N*-salicyloyl-Ser. The madurastatin species **A1** forms a 1:1 Fe^{3+} complex as shown by mass spectrometry.

Asterobactin from *Nocardia asteroides* (*257*) contains salicylic, 2,3-dihydroxy-propionic, and 2-methyl-3-hydroxyundecanoic acid as well as derivatized Orn and Arg residues (Fig. 4, **15**). It forms a Fe^{3+} complex. The stereochemistry of the various centers was not determined but L-configuration is proposed for Orn and Arg for biosynthetic reasons (general amino acid pool) and a negative $[\alpha]_D^{25}$ of asterobactin. Whether the three compounds are involved in metal transport has not been investigated.

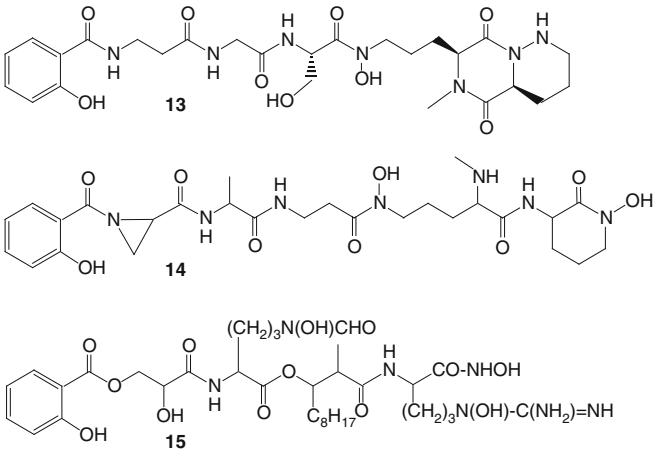

Fig. 4. Desferrimaduraferrin (**13**), madurastatin A1 (**14**), asterobactin (**15**)

2.5. *Bacterial Hydroxamate Siderophores*

Exochelins (*322*, *323*) are peptidic siderophores from *Mycobacterium* spp. (see also below mycobactins). Exochelin MS (**16**) from *M. smegmatis* comprises β-Ala and three N^5-OHOrn units, which are linked by their N^5 atoms to acyl groups thus forming hydroxamic acids.

16 N^5-formyl-N^5-OHOrn-β-Ala-N^5-OHOrn-aThr-N^5-OHOrn

Exochelin MN (**17**) from *M. neoaurum* contains N^2-methyl-N^5-hydroxy-Orn linked by its N^5 to β-Ala and by its carboxyl group to N^2 of Orn, which in turn is bound amidically to cOHOrn; all amino acids are L configured.

17 OHHis-β-Ala-β-Ala-MeOHOrn-Orn-cOHOrn

The Fe^{3+} chelating properties of exochelin MN (**17**) were investigated in detail (pK_a values, chelation constants, redox equilibria, *etc.*) (*87*). In one publication (*128*) siderophores from *Mycobacterium tuberculosis* otherwise referred to as carboxymycobactins (see below Sect. 2.8) were also named exochelins.

Vicibactin (**18**) (previously called hydroxamate K (*61a*)) from *Rhizobium leguminosarum* is a macrocyclic trilactone consisting of N^2-acetyl-N^5-hydroxy-D-Orn and (*R*)-3-hydroxybutyric acid (*91*).

18 $[\text{-O-CH(CH}_3\text{)-CH}_2\text{-CO-NOH-(CH}_2\text{)}_3\text{-CH(NHCOCH}_3\text{)-CO-}]_3$

Vicibactin 7101 from a mutant strain lacks the N-acetyl groups but shows comparable siderophore activity as demonstrated by $^{55}Fe^{3+}$ uptake studies (*91*). The answer to the question why vicibactin is biosynthesized if vicibactin 7101 is as efficient in iron sequestering may be the greater stability of the acetylated compound (*cf.* fusarinines, Sect. 2.6). Vicibactin is identical with neurosporin produced by the fungus *Neurospora crassa* for which X-ray data of the Fe^{3+} complex are available. CD spectroscopy indicates a Λ-*cis* configuration both for crystals and for solution (*108*).

A hydroxamate siderophore from *Salmonella typhimurium* is described as containing isoleucine/leucine, phenylalanine and valine, but not serine and lysine. Further details are not given (*290a*). For other *Salmonella* siderophores see Sect. 2.7.

2.6. *Fungal L-Ornithine-Based Hydroxamate Siderophores*

For other fungal siderophores see neurosporin above, pistilarin (a spermidine derivative, Sect. 3.2) and rhizoferrin (a citrate siderophore, Sect. 4.4); siderophores

produced by marine fungi are treated in (*147*). The siderophores to be discussed here can be divided in three groups, the fusarinines, the ferrichromes, and the coprogens, all based on N^5-hydroxy-N^5-acyl-L-Orn. There exist some earlier reviews (*204*, *300*, *383*); for the early days see also (*395*). Lists of sidrophores and the producing fungi have been assembled (*384*, *385*) to which the marine yeast *Aureobasidium pullulans* may be added (*374a*); see also (*139*). Chromatographic separation techniques were established (*175*, *192*). For a number of siderophores and their Fe^{3+} complexes X-ray and other structural analyses are reported (*366*). In the text and the figures, the desferri ligands will be presented without adding the prefix "desferri" to their names.

Fusarinines (**19**) produced by several fungal genera comprise the acyl unit (*Z*)-5-hydroxy-3-methyl-pent-2-enoic acid (anhydromevalonic acid) (Fig. 5, **a**) bound to N^5-hydroxy-L-ornithine. They can be a linear monomer, dimer (fusarinine A) or trimer (fusarinine B) (the monomer can also be (*E*)-configured) (*172*). Fusarinine B is possibly identical with coprogen C (*89*).

19 HO-[CO-CHNH$_2$-(CH$_2$)$_3$-NOH-CO-CH = CCH$_3$-(CH$_2$)$_2$-O]$_{1-3}$-H

The trimer by forming an ester bond between the two terminal functions results in a lactone ring (fusarinine C or fusigen) (*88*, *313*). Since the fusarinines are rather labile it is not clear whether the open forms are genuine siderophores, precursors of fusigen or just hydrolysis products (*204*). The monomers (*Z*)- and (*E*)-fusarinine form in aqueous solution at neutral *pH* (Fe^{3+})Lig_3 complexes, which are mixtures of Λ and Δ isomers (*172*).

The free α-amino groups of the ornithine units were also found in an acetylated form (*90*, *243*). Since triacetylfusigen is resistant to hydrolysis, formation of the acetylated mono-, di-, and trimeric linear acetylfusarinines is assumed to be effected by enzymatic cleavage (*103a*, *243*). X-ray and CD data of the Fe^{3+} complex of triacetylfusigen have been obtained (*152*). Depending on the solvent used for crystallization the crystals show Λ-*cis* or Δ-*cis* configuration, while in solution Δ-*cis* prevails.

The members of the ferrichrome group are cyclohexapeptides with the general structure [-(N^5-acyl-N^5-hydroxy-L-Orn)$_3$-A-B-Gly-] where A and B can be Gly, Ala, or Ser (Table 1); the various acyl groups are depicted in Fig. 5. Exceptions are tetraglycylferrichrome, a cycloheptapeptide with four Gly units in sequence and three acetyl residues in the Orn part (ferrichrome with an additional Gly) (*82*), and des(diserylglycyl)ferrirhodin, a linear tripeptide containing only the three Orn units

a. (*Z*)-CO-CH=CCH$_3$-(CH$_2$)$_2$-OH
b. (*E*)-CO-CH=CCH$_3$-(CH$_2$)$_2$-OH
c. (*E*)-CO-CH=CCH$_3$-CHOH-CH$_2$OH
d. (*E*)-CO-CH=CCH$_3$-(CH$_2$)$_2$-OCOCH$_3$
e. CO-CH$_2$-CH(CH$_3$)OH-(CH$_2$)$_2$-OH
f. (*E*)-CO-CH=CCH$_3$-CH$_2$-COOH
g. CO-CH$_2$-COOH
h. CO-(CH$_2$)$_{14}$-CH$_3$
i. COCH$_3$

Fig. 5. Acyl residues encountered in fungal hydroxamate siderophores

Table 1. The ferrichrome family[a]

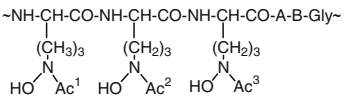

Name	A	B	Ac^1	Ac^2	Ac^3	References
ferrichrome	Gly	Gly	**i**	**i**	**i**	(*106*)
ferrichrome A	Ser	Ser	**f**	**f**	**f**	(*106*, *383*, *396*)
ferrichrome C	Gly	Ala	**i**	**i**	**i**	(*209*, *383*)
ferrichrysin	Ser	Ser	**i**	**i**	**i**	(*170*, *174*, *184*, *383*)
ferricrocin	Gly	Ser	**i**	**i**	**i**	(*184*, *383*)
ferrirubin	Ser	Ser	**b**	**b**	**b**	(*170*, *174*, *383*)
ferrirhodin	Ser	Ser	**a**	**a**	**a**	(*383*)
malonichrome	(Gly	Ala)	**g**	**g**	**g**	(*104*)
sake colorant A	Ser	Ala	**i**	**i**	**i**	(*209*)
asperochrome A	Ser	Ala	**b**	**b**	**b**	(*155*, *174*)
asperochrome B_1	Ser	Ser	**i**	**b**	**b**	(*170*, *174*)
asperochrome B_2	Ser	Ser	**b**	(**b**	**i**)	(*170*, *174*)
asperochrome B_3	Ser	Ser	**b**	(**b**	**i**)	(*170*)
asperochrome C	Ser	Ser	(**b**	**b**	**d**)	(*174*)
asperochrome D_1	Ser	Ser	**b**	**i**	**i**	(*170*, *174*)
asperochrome D_2	Ser	Ser	**i**	(**b**	**i**)	(*170*, *174*)
asperochrome D_3	Ser	Ser	**i**	(**b**	**i**)	(*170*, *174*)
asperochrome E	Ser	Ser	(**a**	**b**	**b**)	(*177*)
asperochrome F_1	Ser	Ser	(**b**	**b**	**e**)	(*177*)
asperochrome F_2	Ser	Ser	(**b**	**b**	**e**)	(*177*)
asperochrome F_3	Ser	Ser	(**b**	**b**	**e**)	(*177*)

[a]Parentheses indicate that the position of the residues is not certain. For the designation of the acyl residues see Fig. 5. Where the chirality of Ala or Ser was determined it was found to be L

of ferrirhodin (*169*). One of the members of this group, ferricrocin was identified as an intra- and intercellular iron transporter for *Aspergillus fumigatus* (*374*).

Ferrichrome (as do also at least the members of the group for which structural data are available ((*366*) and references noted in Table 1) shows Λ-, synthetic *enantio*-ferrichrome based on D-Orn Δ-configuration (*253*). Uptake studies performed with *Ustilago sphaerogena* (*103*) using $^{59}Fe^{3+}$ and [^{14}C]-ferrichrome under optimal conditions (30°C, *pH* 7) showed rapid resorption of both labels during the first 30 min. The uptake of $^{59}Fe^{3+}$ continued for further 30 min, then the level of radioactivity stayed constant, while the level of ^{14}C dropped to a lower constant value. Desferri-[^{14}C]-ferrichrome is not taken up or even bound to the cell surface. These findings are in agreement with shuttle mechanism and re-export of the ligand after detachment of iron. See also analogous experiments with parabactin (Sect. 3.2) and with schizokinen (Sect. 4.1). In contrast, ferrichrome A does not enter the cell. Fe^{3+} is rather reduced and given off at the cell surface and subsequently transported into the cell (*99*, *105*). ^{55}Fe uptake studies performed with *Neurospora crassa* showed the same incorporation rate for ferrichrome and tetraglycylferrichrome indicating that the peptide ring size is of minor importance for the acceptance by the transport system (*82*).

The third group comprises the coprogen family. Their characteristic element is a diketopiperazine ring formed by the head-to-head condensation of two N^5-acyl-N^5-hydroxy-L-Orn units. Rhodotorulic acid (**20**) first isolated from the yeast *Rhodotorula pilimanae* and subsequently found to be produced by many yeasts (*9a*) contains two acetyl groups (Fig. 6) (*9*), and dimerum acid (**21**) from *Fusarium dimerum* (*89*) and other fungi (*172*) two (*E*)-anhydromevalonyl residues (Fig. 6). An acetyl-dimerum acid of unknown structure has been encountered (*157b*). In the coprogens a third variously substituted (*E*)-fusarinine unit is added by means of an ester bond (Table 2) (*300*). Rhodotorulic and dimerum acid form $(Fe^{3+})_2Lig_3$ complexes, but also a mixed 1:1:1 complex of Fe^{3+} with dimerum acid and (*Z*)-fusarinine was observed. Various coprogens were shown to yield 1:1 complexes with Fe^{3+} (*60*, *153*, *172*). The CD-spectra of the coprogen and neocoprogen I/II Fe^{3+} complexes demonstrate Δ-configuration for the solutions and for the crystals of neocoprogen I

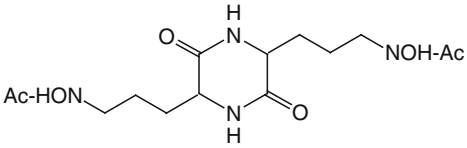

Fig. 6. Rhodotorulic acid (Ac = Fig. 5, **i**) (**20**) and dimerum acid (Ac = Fig. 5, **b**) (**21**)

Table 2. The coprogen family[a,b]

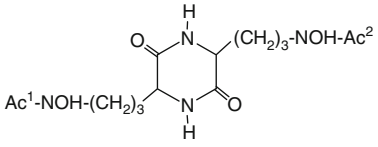

Ac^2 = CO-CH=C(CH_3)-$(CH_2)_2$-O-CO-CH(NR^1R^2)-$(CH_2)_3$-NOH-Ac^3

Name	Ac^1	Ac^3	R^1	R^2	References
coprogen	**b**	**b**	$COCH_3$	H	(*117*, *184a*)
coprogen B	**b**	**b**	H	H	(*89*)
triornicin (isoneocoprogen I)	**b**	**i**	$COCH_3$	H	(*117*)
isotriornicin (neocoprogen I)	**i**	**b**	$COCH_3$	H	(*118*, *153*)
neocoprogen II	**i**	**i**	$COCH_3$	H	(*153*)
N^2-methyl coprogen B	**b**	**b**	CH_3	H	(*30c*, *157b*)
N^2-dimethyl coprogen	**b**	**b**	CH_3	CH_3	(*173*)
N^2-dimethyl neocoprogen I	**i**	**b**	CH_3	CH_3	(*173*)
N^2-dimethyl isoneocoprogen I	**b**	**i**	CH_3	CH_3	(*173*)
hydroxycoprogen	**b**	**c**	$COCH_3$	H	(*176*)
hydroxyneocoprogen I	**i**	**c**	$COCH_3$	H	(*176*)
hydroxyisoneocoprogen I	**c**	**i**	$COCH_3$	H	(*176*)
palmitoylcoprogen	**b**	**b**	**h**	H	(*5*)

[a]For the designation of the acyl residues see Fig. 5
[b]Coprogen C is possibly identical with fusarinine B (*89*)

(*153*). Palmitoylcoprogen (Table 2 last entry) from *Trichoderma* spp. is retained in the fungal mycelium and may therefore be considered as a candidate for an iron uptake taxi mechanism (*5*).

Relationships between the structure of the siderophores and the iron transport were investigated for the fungus *Neurospora crassa* (*160*, *160a*). Apparently two different receptors exist for ferrichromes and for coprogenes. For the recognition and the binding to the cell surface the iron configuration and the nature of the acyl chains is of importance. However, the transport system seems to be the same for both siderophore types dependent on the peptide part of the molecules.

2.7. *Catecholate Siderophores*

For other catecholate siderophores see di-/tri-aminoalkane (Sect. 3.2) and citric acid (Sect. 4.3) derivatives below; for a review see (*38*).

2,3-Dihydroxybenzoic acid is produced by a series of microorganisms, *viz*. *Aerobacter aerogenes* (*291*), *Azotobacter vinelandii* (*70*, *273*), *Bacillus subtilis* (*282*), *Escherichia coli* (*261*, *291*), *Klebsiella oxytoca* (*196*), *Micrococcus denitrificans* (*347*), *Nocardia asteroides* (*112*), *Rhizobium* sp. (*74*), and *Salmonella typhimurium* (*290*), 3,4-dihydroxybenzoic acid by a mutant of *Aerobacter aerogenes* (*291*), *Azomonas macrocytogenes* (*380*), *Bacillus anthracis* (*123*), *Escherichia coli* (*291*), *Magnetospirillum magneticum* (*54*), and *Mycobacterium smegmatis* (*291*). Both dihydroxybenzoic acids can act as siderophores.

Condensation products of DHB (which usually is found also in the fermentation broth) with amino acids were reported, *viz*. with glycine from *Bacillus subtilis* (*164*) named subsequently itoic acid (*282*); with serine from *Escherichia coli* (*261*) and *Klebsiella oxytoca* (*196*); with threonine from *Klebsiella oxytoca* (*196*) and *Rhizobium* spp. (*275*, *327*); with arginine from *Pseudomonas stutzeri* (*62*); with glycine and threonine from *Rhizobium* sp. (*240*); with threonine and lysine as well as with leucine and lysine from *Azospirillum lipoferum* (*312*, *320*). In most cases the isolate (sometimes designated as being a siderophore) was hydrolyzed and the constituents were determined by paper chromatography. The relative amounts of the constituents, the chiralities of the amino acids and the molecular mass of the isolate have not been determined. Hence it is not known whether condensation products of the enterobactin type exist.

Ideally suited for Fe^{3+} complexation – exemplified by the extremely high complexing constant of 10^{49} (originally estimated as 10^{52}) (*210*) – is enterobactin (enterochelin) first isolated from *Salmonella typhimurium* (*286*) and *Escherichia coli* as well as from *Aerobacter aerogenes* (*261*) and recently from *Enterobacter cloacae* (*368*). It is a cyclic trilactone of *N*-2,3-dihydroxybenzoyl-L-serine (DHB-Ser) (Fig. 7, **22**). Syntheses have been reported (*71*, *321*). DHB-Ser by itself can act as a siderophore. In the culture medium degradation products of enterobactin also were found, and are open-chain compounds comprising two or three constitutional units. Iron release in the cell is effected by degradation of

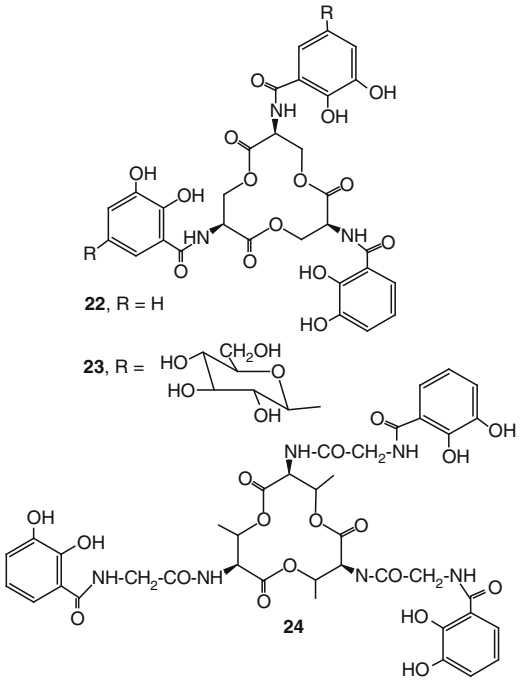

Fig. 7. Enterobactin (**22**), salmochelin S4 (**23**), corynebactin (**24**)

enterobactin. Ferri-enterobactin shows a Δ-*cis* configuration, with the synthetic ferri-*enantio*-enterobactin based on D-Ser Λ-*cis*-configuration (*256*).

Escherichia coli and *Salmonella enterica* produce a derivative of enterobactin, salmochelin S4, where two of the aromatic rings are *β*-C-glucosylated in the 5-position (Fig. 7, **23**). Also glycosylated degradation products or precursors (monomer: salmochelin SX, dimers: S1 and S5, linear trimer: S2) could be isolated (*31*, *135*, *247*). Salmochelin S4 is identical with pacifarin, a compound active against salmonellosis (*378*), and SX with pacifarinic acid, glucosylated DHB-serine (*247*).

From *Corynebacterium glutamicum* the siderophore corynebactin was obtained (*41*). It differs from enterobactin in being composed of three DHB-Gly-L-Thr units (Fig. 7, **24**). Later the same siderophore was found to be produced also by *Bacillus subtilis* and named bacillibactin (*223*). Its complexation constant is ~10^{48} (*84*). The monomeric unit DHB-Gly-Thr was isolated from *Bacillus licheniformis* (*357a*).

Azospirillum brasilense under iron starvation produces spirilobactin. Hydrolysis yields DHB, ornithine, and serine of unknown chirality in a ratio of 1:1:1. The molecular mass was not determined and hence it is not known whether spirilobactin forms a (cyclic) trimer. Iron uptake was studied with the $^{59}Fe^{3+}$ complex (*10*).

Erwinia chrysanthemi (*278*) and *Serratia marcenscens* (*101*) produce N^2-DHB-D-Lys-L-Ser named chrysobactin. The structure was confirmed by synthesis. At physiological *pH* values 2 or 3 chrysobactin residues are associated with Fe^{3+} (*280*).

From *Chryseomonas luteola* in addition to chrysobactin a derivative (chrysomonin) was isolated where C-6 of the DHB unit is substituted with the N-atom of a pyridinium cation. Chrysomonin could be synthesized from chrysobactin (*1a*).

Amonabactins (**25**) were found to be excreted by *Aeromonas hydrophila* (*355*, *356*) and by *Pseudomonas stutzeri* (*398*). They are based on the peptides Lys-Lys-Phe and Lys-Lys-Trp; N^6 of the first L-Lys residues is derivatized by DHB or by a DHB-Gly residue, and that of the second L-Lys by a DHB group (Table 3). At high *pH* values and excess ligand a $(Fe^{3+})_2Lig_3$ complex is formed, while at neutral *pH* a 1:1 ratio prevails with H_2O molecules satisfying the remaining coordination sites. The 2:3 complex is preferentially Δ-configured, and the 1:1 complex is achiral (*357*). Model uptake studies with *Aeromonas* were performed with $^{55}Fe^{3+}$ and a ^{14}C-labeled artificial synthetic siderophore. They demonstrate a modified shuttle mechanism. An iron-free siderophore molecule is strongly bound to the receptor protein and Fe^{3+} exchange occurs between an approaching ferri-siderophore and the bound one, which then is transported into the cell (*337*); *cf.* the pyoverdins (Sect. 2.1).

Alterobactin A is a cyclodepsipeptide from *Alteromonas luteoviolacea*, with N^8-DHB-(4*S*),8-diamino-(3*R*)-hydroxy-octanolyl-D-Ser-Gly-L-Arg-L-*threo*-3-hydroxy-Asp-Gly-L-*threo*-3-hydroxy-Asp having an ester bond between the C-terminal carboxyl group and Ser. It is accompanied by its hydrolysis product alterobactin B (Fig. 8, **26**, **27**) (*298*). Alterobactin A forms a 1:1 complex with Fe^{3+} with an

Table 3. Amonabactins (**25**)

R^1-NH-$(CH_2)_4$-CH(NH_2)-CO-NH-CH(COR_2)-$(CH_2)_4$-NH-DHB

Name	R^1	R^2
Amo T 789	DHB-Gly	D-Trp
Amo P 750	DHB-Gly	D-Phe
Amo T 732	DHB	D-Trp
Amo P 693	DHB	D-Phe

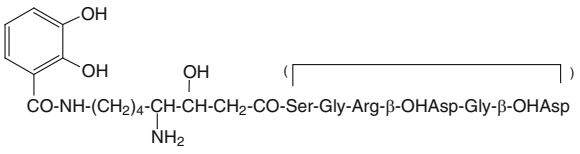

26: with ester bond between OHAsp and Ser
27: without ester bond between OHAsp and Ser

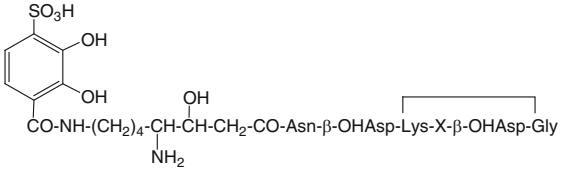

28: X = Lys, **29**: X = Arg

Fig. 8. Alterobactins (**26, 27**), pseudoalterobactins (**28, 29**)

unexpectedly high complexing constant (between 10^{49} and 10^{53}), higher than that of enterobactin above, despite the fact that two complexing sites are α-hydroxy acids which bind Fe^{3+} less efficiently than DHB units (*148*). A synthesis has been reported (*83*) (see Sect. 8.2).

Related structures are the pseudoalterobactins A and B from *Pseudoalteromonas* sp. (Fig. 8, **28**, **29**) (*183*), one of the rare examples of bacterial metabolites containing an aromatic sulfonic acid (*40*). Chiralities of the constituents were not determined.

Heterobactin A and B (**30**) are produced by *Rhodococcus erythropolis* (*59*). They are based on the sequence Orn-Gly-cOHOrn. The N^5-amino group of Orn is substituted by a DHB group. In heterobactin B, the α-amino group of Orn is free (R = H); in heterobactin A, R is probably a 2-hydroxybenzoxazolyl-carbonyl group.

30 DHB-NH-$(CH_2)_3$-CH(NHR)-CO-NH-CH_2-CO-cOHOrn

Rhodobactin (**31**) was isolated from *Rhodococcus rhodochrous* (*86*). A sequence of four Orn units derivatized in different ways is linked together. The nitrogen atoms of the N-terminal Orn are substituted with DHB groups, the N-terminal Orn is followed by two Orn moieties, for which the N^5-amino groups are transformed into urea units (NH_2CONH-), and the C-terminus is cOHOrn. The stereochemistry of the Orn units was not determined. Rhodobactin forms a 1:1 Fe^{3+}/Lig complex. Iron uptake was studied with $^{55}Fe^{3+}$.

31 DHB-NH-$(CH_2)_3$-CH(NH-DHB)-CO-(NH-CH-CO)$_2$-CO-cOHOrn
with a branch $(CH_2)_3$-NH-$CONH_2$ on the CH

Thermobifida fusca, belonging to the Actinomycetales, produces three closely related siderophores, namely, the fuscachelins (*92*). Fuscachelin B starts with the sequence DHB-Arg-Gly-Gly-Ser, which is bound to the hydroxylated N^5-amino group of Orn. Its N^2-amino group (the carboxyl group is free) is bound to the C-terminus of the sequence Gly-Gly-Arg-DHB (**32**). Fuscachelin A is considered to be the genuine metabolite, with B and C degradation products.

32 DHB-Arg-Gly-Gly-Ser-N^5-OHOrn-N^2H-Gly-Gly-Arg-N^2-DHB

In fuscachelin C the carboxyl group of Orn forms an amide, while in fuscachelin A an ester bond occurs between the carboxyl group of Orn and the hydroxy group of Ser.

2.8. Lipopeptidic Siderophores

From *Burkholderia cepacia* (formerly *Pseudomonas cepacia*) three siderophores named ornibactins (**33**) were isolated for which the structures were determined by

degradation and NMR studies (*335*, *336*) as containing 3-hydroxy fatty acid residues and putrescine that blocks the C-terminus, with acyl = R-CHOH-CH_2-CO (R = CH_3, C_3H_7, C_5H_{11}).

33 acylOHOrn-OHAsp-Ser-formylOHOrn-NH-$(CH_2)_4$-NH_2

The three ornibactins are accompanied by minor components, which contain an additional oxygen atom. Their structure has not been investigated. Ornibactins are the main siderophores of a series of *Burkholderia* strains accompanied in part by pyochelin (Sect. 5) and cepabactin (Sect. 6) (*235*). A further *B. cepacia* siderophore is cepaciachelin (Sect. 3.2) (*15*). The iron acquisition by the various siderophores of *B. cepacia* has been discussed in detail (*359*).

From *Nocardia* strains several closely related compounds (nocobactins, formobactin, amamistatins) were isolated that contain three typically Fe^{3+} binding sites, two hydroxamate units, and a hydroxyphenyloxazole structure (*cf.* Sect. 3.2 below). The C-terminus is *N*-hydroxy-*cyclo*-Lys bound to a long chain 3-hydroxy fatty acid, whose hydroxy group is esterified by N^6-acyl-N^6-hydroxy-Lys, the α-amino group of which is bound to 2-*o*-hydroxyphenyl-5-methyl-oxazole-4-carboxylic acid (Table 4). For the amamistatins the configuration of the cyclic lysine was determined as L, the open one as D, and that of C-3 of the fatty acid as (*S*). The involvement in the iron metabolism was not investigated.

Structurally related with the nocobactin family are the mycobactins and carboxymycobactins (the latter were also referred to as exochelins, Sect. 2.5 (*128*)) from *Mycobacterium* spp. For reviews see (*85*, *331*, *369*). They have the same basic skeleton as the nocobactins, but the 4,5-double bond of the oxazole ring is saturated. A series of differently substituted representatives has been isolated (see Table 5). The major group comprises mixtures carrying saturated and unsaturated long-chain fatty acid residues as substituents of the hydroxamic acid unit formed by the N^6-amino group of lysine. For some ("J", M, and N), the fatty acid residues are located in the chain, as for the nocobactins. Representatives of the MAIS group (*Mycobacterium avium*, *M. intracellulare*, *M. scrofulaceum*) possess two long

Table 4. The nocobactin family

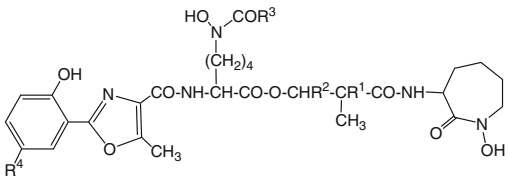

Compound	R^1	R^2	R^3	R^4	References
nocobactin NA	H	C_9H_{19},$C_{11}H_{23}$	CH_3	H	(*294*, *295*)
formobactin	CH_3	C_9H_{19}	H	H	(*252*)
amamistatin A	CH_3	C_7H_{15}	H	H	(*191*, *341*)
amamistatin B	CH_3	C_7H_{15}	H	OCH_3	(*191*, *341*)

Table 5. The mycobactin family (adapted from (*369*))

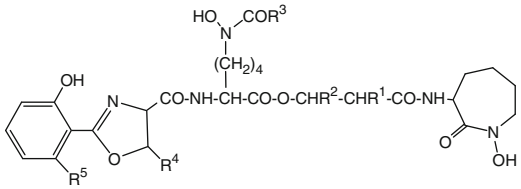

Mycobactin	R^1	R^2	R^3	R^4	R^5	References
A	H	CH_3	C_{13}	H	CH_3	(*332*)
F	H	CH_3	$C_{9\text{-}17}$	CH_3	H	(*332*)
H	H	CH_3	$C_{17,19}$	CH_3	CH_3	(*381*)
J	CH_3	$CH(CH_3)_2$	C_{15}	H	H	(*224*)
"J"	CH_3	b	a	CH_3	H	(*18*)
P	CH_3	C_2H_5	$C_{13\text{-}19}$	H	CH_3	(*329*)
R	CH_3	C_2H_5	C_{19}	H	H	(*332*)
S	H	CH_3	$C_{13\text{-}19}$	H	H	(*381*)
T	H	CH_3	$C_{14\text{-}21}$	H	H	(*330*)
M	CH_3	$C_{14\text{-}17}$	CH_3	CH_3	H	(*332*)
N	CH_3	$C_{14\text{-}17}$	C_2H_5	CH_3	H	(*332*)
MAIS	CH_3	b	a	H	H	(*18*)
	CH_3	b	a	CH_3	H	(*18*)
carboxy	H	CH_3	c	H	H	(*128*)
	H	CH_3	c	CH_3	H	(*128*)
	CH_3	C_2H_5	d	CH_3	H	(*199*, *292*)

a – unsaturated alkyl chain, b – saturated alkyl chain, c – saturated and unsaturated dicarboxylic acid methyl ester, d – unsaturated dicarboxylic acid

chain fatty acid residues. The stereochemistry of most chiral centers has been determined. For the Fe^{3+} complex of mycobactin P an X-ray analysis is available (*157*). For the carboxymycobactins the residues R^3 in Table 5 are saturated or unsaturated alkyl groups with terminal carboxyl groups or their methyl esters.

Transvalencin Z (*245a*) from *Nocardia transvalensis* could be a precursor or side product of mycobactin biosynthesis, possibly acquired from a vagabonding gene. It comprises the left part of the serine/salicylic acid based molecules (Table 5 $R^4 = R^5 = H$) and ends with N^6-formyl-Lys ($R^3 = H$, no *N*-hydroxy group). The stereochemistry of the two chiral centers was not determined. Transvalencin Z seems not to bind Fe^{3+}.

Iron uptake of *Mycobacterium smegmatis* involving mycobactin S was studied with $^{55}Fe^{3+}$ (*293*). Mycobactin is not given off into the surrounding medium but is located instead in the lipid envelope of the cell and is active in the trans-membrane transport of Fe^{3+} (taxi mechanism). Iron is relased at the inside of the membrane by a reductive mechanism. There is some evidence that salicylic acid is the extracellular siderophore.

Corrugatin (**34**) (Fig. 9) is the siderophore of *Pseudomonas corrugata* (*302*). It was also found as secondary siderophore of several pyoverdin producing *Pseudomonas* strains as *P. fluorescens*, occasionally in slightly modified forms such as

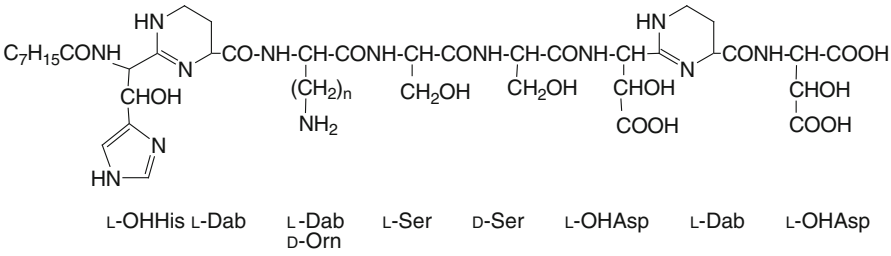

Fig. 9. Corrugatin (n = 2, L-Dab) (**34**) and ornicorrugatin (n = 3, D-Orn) (**35**)

36: RCO-OHAsp-Dab-Ser-acetylOHOrn-Ser-acetylOHOrn
37: RCO-OHAsp-Ser-Ser-Gln-acetylOHOrn-Ser-acetylOHOrn
38: RCO- acetylOHOrn-acetylOHOrn-Ser-acetylOHOrn (2 D-,1L-Orn, L-Ser)
39: RCO-OHAsp-Ser-Gln-Ser-acetylOHOrn-Dhb-Ser-cOHOrn

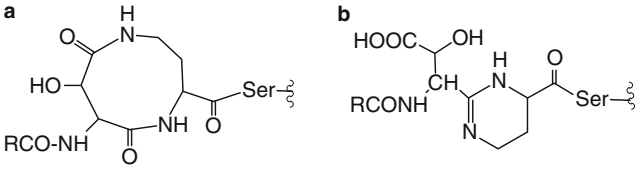

Fig. 10. Amphiphilic marine siderophores

ornicorrugatin (**35**) where one Dab is replaced by Orn (*218*), or with OHHis instead of OHAsp as the C-terminus (*S. Matthijs*, unpublished).

A group of amphiphilic siderophores was isolated from marine bacteria (*410*), the marinobactins (Fig. 10, **36**), from *Marinobacter* sp., aquachelins (Fig. 10, **37**), from *Halomonas aquamarina* (*215*, *217*), the amphibactins (Fig. 10, **38**), from *Vibrio* sp. (*216*), and the loihichelins (Fig. 10, **39**), from *Halomonas* sp. (*150*). They all comprise series of related molecules differing in the nature of the saturated or unsaturated fatty acid (for amphibactins and loihichelins also 3-hydroxy fatty acids) linked to the N-terminus (see also ochrobactins and synechobactins, Sect. 4.1). Structure elucidations were effected by spectroscopic methods and degradation studies. For the marinobactins a N-terminal nine-membered lactam ring was suggested to be formed by an amide bond between the carboxyl group of Asp and the C-4 amino group of Dab (Fig. 10, **a**). It may be suggested that rather a condensation with the amide carbonyl group had occurred (Fig. 10, **b**; *cf.* Chart 1). This would keep the α-hydroxycarboxyl grouping of OHAsp intact, which acts as a binding site for Fe^{3+} and is essential for photolytic degradation. The rather scarce structural data presented do not allow a decision to be made. The siderophores show a strong affinity to lipid membranes (*389*). The Fe^{3+} complexes of aquachelins and marinobactins suffer degradation under sunlight irradiation. For the Fe^{3+}-aquachelin complexes the formation of Fe^{2+}, of hydrophobic and of hydrophylic cleavage

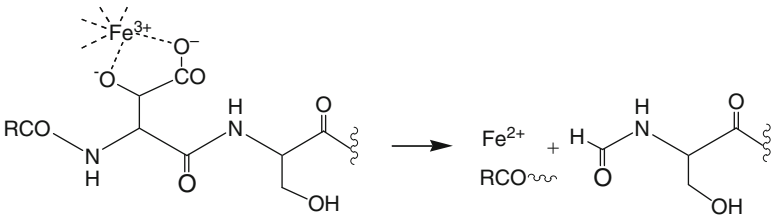

Chart 2. Light-induced degradation of Fe^{3+}-aquachelins

products was observed. For the latter a *N*-formyl-Ser terminus was suggested based on mass spectral data (Chart 2) (*12*). There is evidence that this type of photolytic degradation is common for siderophores containing α-hydroxycarboxyl ligands (*13*, *150*, *401*).

2.9. Pseudomonas mendocina Siderophores

From *Pseudomonas mendocina* five siderophores were isolated by chromatography. They are reported to have identical molecular masses of 1,152 Da (the also reported (*3a*) value of 929 Da is an error; *L. E. Hersman*, private communication) and an identical amino acid composition, which has not been revealed (*141a*). Color reactions show the presence of a hydroxamate, but not of a catecholate grouping. A gene analysis suggests a partial sequence acyl-Asp-Dab-Ser-formylOHOrn-Ser-formylOHOrn where asparagine could be OHAsp and the C-terminal ornithine cOHOrn (*9b*). In which way the five isomeric siderophores with identical molecular masses differ from each other is not clear.

3. Siderophores Based on Diamino- and Triaminoalkane Skeletons

3.1. Rhizobactin

Rhizobactin (**40**) is the siderophore of *Rhizobium meliloti* (*328*). It contains one α-hydroxycarboxylic acid and two α-amino acid units as probable binding sites for Fe^{3+}. Acid hydrolysis yields *inter alia* L-malic acid. The stereochemistry of the other two chiral centers is not known.

40 $HOOC\text{-}CH(CH_3)\text{-}NH\text{-}(CH_2)_2\text{-}NH\text{-}CH(COOH)\text{-}(CH_2)_4$
$\text{-}NH\text{-}CO\text{-}CH_2\text{-}CHOH\text{-}COOH$

3.2. *Catecholate Siderophores*

For other catecholate siderophores, see the peptide-based siderophores above (Sect. 2.7) and the citric acid derivatives below (Sect. 4.3); for a review on syntheses, see (*24*), for a general review, (*38*).

The tricatecholate siderophore protochelin (**41**) (Fig. 11) was obtained from a methanol – bacterium (*351*). Subsequently it was also found to be produced by *Azotobacter vinelandii* (*72*, *360*) together with its constituents 2,3-dihydroxybenzoic acid, azotochelin (bis-DHB lysine) (*70*) and aminochelin (mono-DHB cadaverine) (*273*). Cepaciachelin from *Burkholderia cepacia* (*15*) lacks the DHB residue from the aminochelin part of protochelin. The amino acid in all compounds is L-lysine. *Azotobacter vinelandii* shows an interesting rationale when confronted with a deficiency in iron supply. At concentrations >7 μM, 2,3-dihydroxybenzoic acid is secreted, between 3 and 7 μM, the di- and tricatecholate siderophores are produced, and at still lower concentrations, it is resorted to azotobactin D (see above Sect. 2.2) (*72*). Myxochelin A from *Angiococcus disciformis* (*197*) and *Nonomuraea pusilla* (*239a*) can be considered as a reduction product of azotochelin (lysinol instead of Lys). The absolute configuration of lysinol (*S*) was determined by synthesis. Both antipodes show about the same antitumor activity (*239a*).

Pistillarin was first isolated from *Clavariadelphus pistillaris* and from several *Ramaria* spp. (Basidiomycetes) (*334*). Recently, it was found to be produced also by the marine fungus *Penicillium bilaii* (*56*). Like siderochrome II below it is a spermidine derivative substituted only at the terminal NH_2-groups (N^1, N^{10}-di-(3,4-dihydroxy)benzoyl-spermidine). Its synthesis and that of siderochrome II was reported, their siderophore activity and their complexation with Fe^{3+} (1:1 complexes) was investigated (*102*, *299*). A derivative of pistillarin substituted at all three amino functions has not been reported yet.

When DHB is bound to serine or threonine cyclization may occur resulting in an oxazoline ring (*cf.* above anachelin, Sect. 2.3, and mycobactins, Sect. 2.8). It has been discussed whether the oxazoline nitrogen atom may act as a ligand site (see below, (*303*)). This would explain why DHB is replaced by a salicylic acid residue in some cases.

To this group of siderophores belong photobactin (**42a**) from *Photorhabdus luminescens* (Fig. 12) (*66*), derived from 1,4-diaminobutane substituted by DHB and by cyclized DHB-Thr (^{1}H-NMR data indicate that the substituents of the oxazoline ring are in *trans* positions; the absolute stereochemistry is not known),

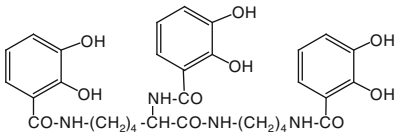

Fig. 11. Protochelin (**41**)

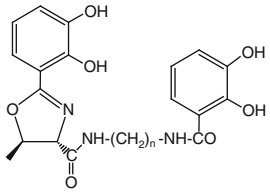

42a: n = 4
42b: n = 3

Fig. 12. Photobactin (**42a**), serratiochelin (**42b)**

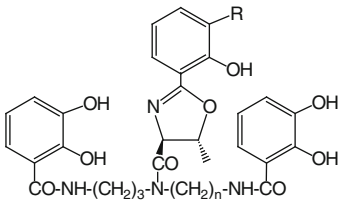

43: n = 4, R = OH
44: n = 4, R = H
45: n = 3, R = OH

Fig. 13. Agrobactin (**43**), parabactin (**44**), fluvibactin (**45**)

and its lower homolog serratiochelin (**42b**) from *Serratia marcescens* derived from 1,3-diaminopropane. Its structure including the absolute stereochemistry (L-Thr) was confirmed by synthesis (*101*).

Spermidine derivatives are agrobactin from *Agrobacterium tumefaciens* (Fig. 13, **43**) (*268*), for which the structure was confirmed by X-ray analysis (*109*) and synthesis of the hydrolyzed form (DHB-Thr) agrobactin A (*283*), and parabactin (Fig. 13, **44**) from *Paracoccus denitrificans* (*284*). Two syntheses are reported for parabactin (*28*, *28c*, *255*) (see Sect. 8.3). The open form (parabactin A) as well as the precursors 2,3-dihydroxybenzoic acid and a compound with a free central NH group (N^1, N^{10}-di-DHB-spermidine, siderochrome II) were also found (*347*). The 1:1 Ga^{3+}/Lig complex shows Λ-*cis* configuration (*28a*). Parabactin also forms a 1:1 complex with Fe^{3+} (*347*) for which the structure was investigated by X-ray photoelectron and electron spin resonance spectroscopy. In particular, the question as to whether the oxazoline nitrogen acts as a binding site has been discussed. An experimental proof seemed not to be possible (*303*).

Iron transport was studied using the $^{55}Fe^{3+}$- and ^{3}H-complexes of parabactin (*25*). After a quick uptake of 10% of both labels there was a continuing steady uptake of $^{55}Fe^{3+}$ while the amount of ^{3}H remained constant. This could either mean that after binding to the cell surface $^{55}Fe^{3+}$ only is transferred into the cell ("taxi mechanism") or there is a fast re-export of the ligand. A decision in favor of the

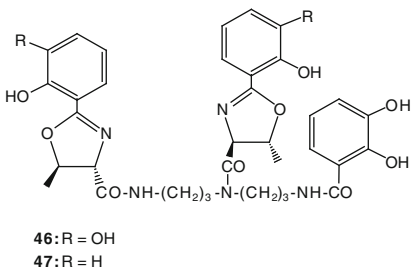

Fig. 14. Vibriobactin (**46**), vulnibactin (**47**)

taxi-mechanism could be reached by offering the Ga^{3+} complex of [^{3}H]-parabactin (Ga^{3+} cannot be released reductively in the cell and hence a re-export of the ligand is not possible). The uptake curve resembled that of ferri-[^{3}H]-parabactin: a small amount of complex is bound to the cell surface, but there is no transport of the ligand in the cell. This is in agreement with temperature studies (30 and 4°C). While the uptake of $^{55}Fe^{3+}$ decreases that of ^{3}H is not influenced.

Fluvibactin (Fig. 13, **45**) from *Vibrio fluvialis* (*391*) differs from agrobactin by replacement of spermidine by norspermidine. Also here the precursor with a free central NH group could be isolated. Vibriobactin from *Vibrio cholerae* (Fig. 14, **46**) contains two cyclized DHB-Thr substituents (*129*). Syntheses of agrobactin, fluvibactin and vibriobactin are published (*26*, *30*, *308*). In vulnibactin from *Vibrio vulnificus* (Fig. 14, **47**) (*264*) two DHB groups are replaced by salicylic acid units. The precursor with a free central NH group was also found.

3.3. Hydroxamic Acid Siderophores

Bisucaberin (**48**) from *Alteromonas haloplanktis* (*181*) is a cyclic dimer of succinyl-(*N*-hydroxycadaverin) (*348*); *cf.* the cyclic trimer proferrioxamine E (Table 6).

48 [-CO-CH_2-CH_2-CO-NH-CH_2-CH_2-CH_2-CH_2-CH_2-NOH-]$_2$

In putrebactin from *Shewanella putrefaciens* (*201*) cadaverine is replaced by putrescine (**49**, R = H). For the cyclic trimer, see proferrioxamine X_2 in Table 6. The arctic *S. gelidimarina* living in a habitat with extremely low iron supply produces a cell-associated hydroxamic acid siderophore with the mass 977 Da for $[M+H]^+$ of unknown structure (*274*).

Alcaligin from *Alcaligenes denitrificans* (*260*) and from *Bordetella* spp. (*244*) is a cyclic dimer of succinyl-N^1,3*S*-dihydroxyputrescine (**49**, R = H) confirmed by synthesis (*402*).

49 [-CO-CH_2-CH_2-CO-NH-CH_2-CHR-CH_2-CH_2-NOH-]$_2$

Table 6. Structures and nomenclature of proferrioxamines (pFO) (adapted from (*110*))[a]

H_2N-$(CH_2)_m$-NOH-CO-CH_2-CH_2-CO-NH-$(CH_2)_n$-NOH-CO-CH_2-CH_2-CO-NH-$(CH_2)_o$-NOH-CO-CH_2-CH_2-CO-NH-$(CH_2)_p$-NOH-CO-CH_2-CH_2-COOH

pFO	cyclic	m	n	o	p	N-terminus	C-terminus	Abbreviation	References
A_1	–	5	5	4	0	–	Ac	pFO_{554Ac}	(*185a*)
A_2	–	5	4	4	0	–	Ac	pFO_{544Ac}	(*185a*)
B	–	5	5	5	0	–	Ac	pFO_{555Ac}	(*30e*)
D_1	–	5	5	5	0	Ac	Ac	Ac-pFO_{555Ac}	(*185b*)
D_2	+	4	5	5	0	–	Suc	pFO_{455c}	(*185a*)
E[b]	+	5	5	5	0	–	Suc	pFO_{555c}	(*155a*, *186*)
G_1[c]	–	5	5	5	0	–	Suc	pFO_{555}	(*186a*)
G_{2a}	–	5	5	4	0	–	Suc	pFO_{554}	(*115*)
G_{2b}[c]	–	5	4	5	0	–	Suc	pFO_{545}	(*115*)
G_{2c}[c]	–	4	5	5	0	–	Suc	pFO_{455}	(*115*)
H	–	5	5	0	0	Suc	Ac	Suc-pFO_{55Ac}	(*1*)
T_1	+	5	5	5	5	–	Suc	pFO_{5555c}	(*115*)
T_2	+	4	5	5	5	–	Suc	pFO_{4555c}	(*115*)
T_3	+	3	5	5	5	–	Suc	pFO_{3555c}	(*115*)
X_1	+	4	4	5	0	–	Suc	pFO_{445c}	(*115*)
X_2	+	4	4	4	0	–	Suc	pFO_{444c}	(*115*, *398*)
X_7	+	3	5	5	0	–	Suc	pFO_{355c}	(*115*, *398*)

[a]Structures were not established for C and F (R_f values and physical constants) (*30d*), T_4-T_6, and X_8, X_9 (mass spectra) (*115*)
[b]Identical with norcardamin (*186*, *338*)
[c]Accompanied by "truncated" compounds without the terminal succinic acid unit (G_{1t}, G_{2bt}, G_{2ct}) (*115*, *398*)

Alcaligin forms at *pH* 2.0 a 1:1 and at *pH* 6.0 a 2:3 Fe-to-ligand complex. The structure (Plate 3) of the $(Fe^{3+})_2Lig_3$ complex was studied by X-ray analysis (*156*). One ligand bridges two metal ions while the remaining two are coordinated with a single Fe^{3+} each. The metal centers show Λ-configuration.

Alcaligin E from *Alcaligenes eutrophus* is described from color tests as a phenolic siderophore (*126a*). According to a recent publication (*90a*) it is identical with staphyloferrin B, a citrate siderophore (Sect. 4.2). No further information is given to resolve these discrepancies.

A group of related siderophores comprises the desferri- or deferriferrioxamines (occasionally abbreviated as desferrioxamines) or proferrioxamines. Originally they were obtained from Actinomycetes, mainly *Nocardia* and *Streptomyces* spp. (*187*) and later found to be produced also by *Erwinia* spp. (several representatives) (*e.g.* (*30a*, *113*, *115*, *180*)), *Arthrobacter simplex* (B), *Chromobacterium violaceum* (E) (*246a*), and by *Pseudomonas stutzeri* (several) (*229a*, *246*, *398*). They consist of three (or in rare cases four) mono-*N*-hydroxy-1,4-diaminobutane (putrescine), mono-*N*-hydroxy-1,5-diaminopentane (cadaverine) or (rarely) mono-*N*-hydroxy-1,3-diaminopropane units connected by succinic acid links. The hydroxylated terminus carries an acetyl or a succinyl (as in the structural formula heading Table 6)

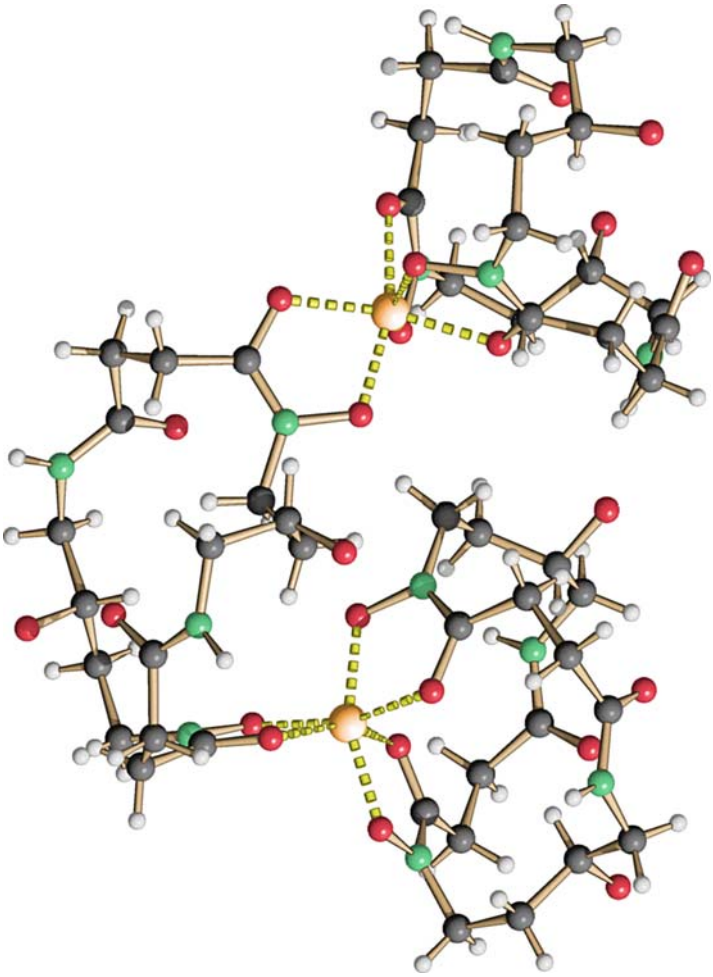

Plate 3. X-ray structure of ferri-alcaligin (ferri-**49**)

residue, and in the latter case the free carboxyl group and the free N-terminus may form a macrolactam. The terminal acid residue can also be missing (referred to as "truncated") (*115*, *398*). By feeding of suitable diamino precursors to the culture medium unnatural analogs can be obtained (*111*, *194*, *227*). At *pH* values above 6.5 $(Fe^{3+})_2Lig_3$ complexes prevail, in more acidic media Fe^{3+}Lig is formed (*194*). The crystals of the Fe^{3+}Lig complexes of ferrioxamine D_1 and E are racemic mixtures of Λ-*cis* and Δ-*cis* coordination isomers (*154*, *366a*). The outer membrane receptor protein of *Erwinia amylovora* was structurally determined (*180*). Siderophore activity was demonstrated for ^{55}Fe-labeled ferrioxamine E (*30a*). For the mass spectrometric analysis, see (*112a*).

Originally the various natural representatives had been designated by capital letters, but later a nomenclature system was proposed (*110*). In short, the indices and modifications as listed in Table 6 (p = 0 means that the entire fourth diaminoalkane-succinyl unit is missing) are grouped around the acronym pFO. The system is essentially self-explanatory; for details and possible extensions see the original publication.

4. Citrate Siderophores

For a review, see (*39*). Some citrate siderophores are accompanied by cyclic imide structures formed by the loss of water from the central carboxyl group and a lateral amide NH (Chart 3). They are usually designated by an A following the name of the siderophore. Free citric acid can be a true siderophore, *e.g.* for *Bradyrhizobium* spp. (*205*), *Pseudomonas aeruginosa* (*213*), and *Mycobacterium smegmatis* (*228a*). The mode of the uptake differs. *Bradyrhizobium* and *Pseudomonas* incorporate ferric citrate but *Pseudomonas* shows also a citrate mediated Fe^{2+} uptake, while in the case of *Mycobacterium* no citrate enters the cell. Ferric citrate is a complex system depending on the *pH* of the solution and the relative concentration of the two constituents (*333a*, *333b*). In an acidic milieu equimolar concentrations form $[FeCit]^{-}$, at about *pH* 4 polymerization starts resulting at *pH* 8–9 in an insoluble complex with an iron hydroxide core and citrate ions bound to the surface. With a citrate excess species like $[FeCit_2]^{5-}$ are discussed.

It should be mentioned that the central carbon atom of citric acid becomes chiral when the two peripheral carboxy groups are substituted differently (examples will be found below). For enzyme reactions it is a prochirality center. This has been shown for vibrioferrin (**58**) and staphyloferrin B (**59**).

4.1. Siderophores with Two Hydroxamic Acid Units

In siderophores of this series, 1,3-diaminopropane, 1,5-diaminopentane, or lysine (by its α-amino group) is connected to the outer two carboxyl groups of citric acid.

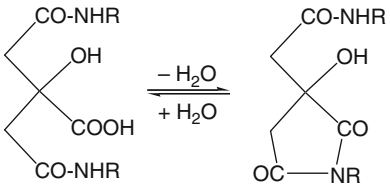

Chart 3. Cyclization of citrate siderophores to amidic structures

These spacers, in turn, are acylated and derivatized by a *N*-hydroxy group thus forming hydroxamic acids. For a synthesis concept see (*404*).

Schizokinen (Fig. 15, **50**) was first isolated from *Bacillus megaterium* (*53*), subsequently from *Ralstonia solanacearum* (*43*), *Rhizobium leguminosarum* (*339*), and several species of the cyanobacterium *Anabena* (*e.g.* (*326*)). It was named after its cell division promoting effect observed with *Bacillus* cultures (*200*). Its structure was elucidated by degradation and spectral data and confirmed by synthesis (*43*, *202*, *237*, *248*). For a compilation of details on structural data the review (*39*) should be consulted. Both natural and synthetic schizokinen is accompanied by the cyclized schizokinen A (*43*, *202*, *237*, *248*). Schizokinen forms a 1:1 complex with Fe^{3+}, but at the central hydroxy group acetylated schizokinen yields $(Fe^{3+})_2Lig_3$. This proves that the central unit is one of the binding sites (*285*). Also *N*-deoxyschizokinen from *Bacillus megaterium* lacking one hydroxamic acid unit still binds Fe^{3+} (*158*). Whether it acts as a siderophore is not known.

The schizokinen-mediated Fe^{3+} transport in *Bacillus megaterium* was studied by double labelling with ^{59}Fe and ^{3}H (*8*). At 37°C, uptake of ^{59}Fe and of ^{3}H are parallel during the first 30 sec, then that of ^{59}Fe continues until it levels off after 2 min, while that of [^{3}H]-schizokinen drops to a low constant level. At 0°C, uptake of both labels reaches this low level which is obviously due to the binding of the ferrisiderophore to the cell surface. At 37°C, transport into the cell, release of iron, and re-export of the ligand follow. Apparently a shuttle mechanism takes place, *cf.* the experimental results obtained with parabactin (Sect. 3.2) indicative of a taxi mechanism.

Arthrobactin (Fig. 15, **51**) was obtained from *Arthrobacter* spp. and originally described as the growth factor of *A. terregens*, the "terregens factor" (*51*). Its structure was elucidated (*207*) and confirmed by synthesis (*202*). Also the structure

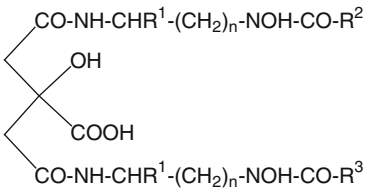

50: R^1 = H, R^2 = R^3= CH_3, n = 2
51: R^1 = H, R^2 = R^3 = CH_3, n = 4
52: R^1 = H, R^2 = R^3 = (*E*)-CH=CH-$(CH_2)_4$-CH_3 , n = 2
53: R^1 = COOH, R^2 = R^3 = CH_3, n = 4
54: R^1 = COOH, R^2 = R^3 = (*E*)-CH=CH-C_6H_5 , n = 4
55: R^1 = COOH, $R^2$and R^3 alkyl or alkenyl groups, n = 4
56: R^1 = H, R^2 = CH_3, R^3 = (*E*)-CH=CH-$(CH_2)_6$-CH_3 , n = 2
57: R^1 = H, R^2 = CH_3, R^3 = alkyl groups, n = 2

Fig. 15. Citrate siderophores with two hydroxamic acid units

of acinetoferrin from *Acinetobacter haemolyticus* was established (Fig. 16, **52**) (*265*) and confirmed by synthesis (*375*). It shows strong interaction with lipid membranes like the marine liposiderophores above (*211*) (Sect. 2.8).

Aerobactin (Fig. 15, **53**) was first isolated from *Aerobacter* (*Enterobacter*) *aerogenes* (*126*), *Enterobacter cloacae* (*368*) and subsequently from various enterobacteria such as *Escherichia* (*376*), *Salmonella* (*225*), *Shigella* (*277*), *Yersinia* (*340*), but also from *Erwinia carotovora* (*163*), *Pseudomonas* sp. (*52*) and *Vibrio* spp. (*141*, *266*). Aerobactin is an important virulence factor for enterobacteria (*75*). Aerobactin contains L-lysine. A synthesis is described (*222*). The bright orange Fe^{3+} complex was investigated in detail (predominant Λ configuration in solution, stability constant, redox potential) (*138*). Fe^{3+} transport was studied by double labelling (^{59}Fe and ^{3}H) (*8*). The results corresponded to those obtained with schizokinen. Aerobactin binds to the same receptor as the bacteriocin cloacin DF13 and thus alleviates the growth inhibiting effect of the latter (*368*).

Nannochelin C (Fig. 15, **54**) from the myxobacterium *Nannocystis exedens* contains two L-Lys and two (*E*)-cinnamic acid units. The reported mono- and di-methyl esters (nannochelin B and A) may be artifacts from the work-up (*198*). A synthesis is described (*29*) (see Sect. 8.4). The ochrobactins (Fig. 15, **55**) isolated from the sea-shore bacterium *Ochrobactrum* sp. (*214*) with the spacer L-lysine are membrane active due to the fatty acid residues (saturated C_8 and (2*E*)-unsaturated C_8 and C_{10}); *cf.* lipopeptidic siderophores in Sect. 2.8.

Rhizobactin 1021 (Fig. 15, **56**) (for rhizobactin, see diaminoalkane-based siderophores, Sect. 3.1) from *Rhizobium meliloti* (*281*), contains an acetyl and an (*E*)-decenoyl group. Its Fe^{3+} complex in aqueous solution is Λ-configured and forms an equilibrium between a monomeric and a dimeric form that can be separated by chromatography. A synthesis is described (*404*).

Synechobactins (Fig. 15, **57**) from the cyanobacterium *Synechococcus* (*165*), contain an acetyl and C_{12}-, C_{10}-, and C_8-saturated acid residues and thus belong to the amphiphilic marine siderophores (*cf.* Sect. 2.8). Both rhizobactin 1021 and the synechobactins are substituted unsymmetrically. Hence, for each, the central C-atom of citric acid is chiral, but its stereochemistry has not been determined.

Awaitins are synthetic homologs of siderophores (A: **53**, n = 3; B: **50**, n = 3; C: **53**, n = 2) "awaited" to be found in nature, so far without success (*405*).

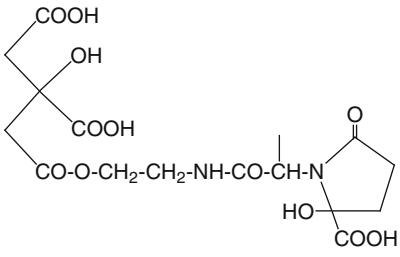

Fig. 16. Vibrioferrin (cyclic form) (**58**)

4.2. *Siderophores with 2-Oxoglutaric Acid Units*

N-Alkylated 2-oxoglutaric acid derivatives cyclize at neutral *pH* values to two epimeric 5-carboxy-5-hydroxy-2-oxopyrolidine structures (Chart 4). In this way, α-hydroxycarboxylic acid groupings are formed that can act as ligand sites for Fe^{3+}.

Vibrioferrin (**58**, Fig. 16) was isolated from *Vibrio parahaemolyticus*. The stereochemistry of the central citric acid C-atom is *R*, that of the alanine part is *S* as shown by stereospecific synthesis (*411*). Iron uptake was studied with $^{55}Fe^{3+}$ proving that vibrioferrin acts as a siderophore despite the fact that it has only five ligand sites, the two α-hydroxy acids and the free citric acid carboxyl group. Possibly a solvent molecule satisfies the eighth octahedral position (*393*, *411*). Vibrioferrin is also formed by *Marinobacter* spp. It is a week Fe^{3+} chelator (complexing constant 10^{24}). Its Fe^{3+} complex is very susceptible to photodegradation by oxidative decarboxylation of the cyclized 2-oxoglutaric acid unit yielding a succinimide ring. This species cannot bind Fe^{3+}. The concomitantly formed Fe^{2+} (*cf.* Chart 2) is reoxidized to fairly soluble Fe^{3+} hydroxo complexes, which are readily taken up by the bacteria (*410*).

Staphyloferrin B (**59**, Fig. 17) is produced together with staphyloferrin A (see below Sect. 4.4) by *Staphylococcus hyicus* and other staphylococci (*94*, *131*), by *Ralstonia eutropha* (*250*) (= *Cupriavidus metallidurans* (*90a*)). Comparison of its CD spectrum with those of model compounds suggests the (*S*)-configuration of the central citric acid C-atom. Mass spectral investigations show a 1:1 Fe^{3+}-to-ligand ratio, and NMR studies of the Ga^{3+} complex confirm the participation of the two α-hydroxy- and of the α-amino acid functions in complex formation. Uptake studies with $^{55}Fe^{3+}$ showed that staphyloferrin B acts as a siderophore, but it is less efficient than staphyloferrin A.

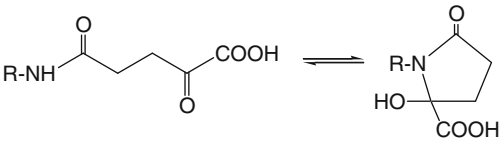

Chart 4. Cyclization of 2-oxoglutaric acid substituents

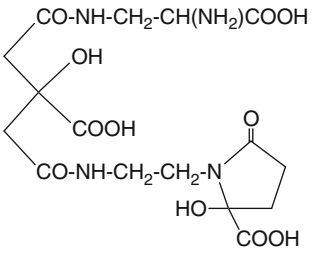

Fig. 17. Staphyloferrin B (cyclic form) (**59**)

Achromobactin (**60**, Fig. 18) is produced by *Erwinia chrysanthemi* in addition to chrysobactin (see above under the catecholate siderophores, Sect. 2.7). It has two chiral centers, a L-Dab unit and the central citric acid C-atom (not determined) (*249*). Recently, achromobactin was also found to be produced by *Pseudomonas syringae* (*30b*), a very versatile bacterial species (see pyoverdin, Sect. 2.1, and yersiniabactin, Sect. 5).

4.3. Siderophores with Two Catecholate Units

In petrobactin, spermidine residues are bound to citric acid substituted with 3,4-dihydroxybenzoyl (*27*), and not 2,3-dihydroxybenzoyl units (Fig. 19, **61**), as assumed originally (*14*). One or both of the substituents can carry a sulfonic acid group in the 2-position of the aromatic ring (Fig. 19, **62** and **63**) (*142*, *149*); *cf.* also (*40*). Petrobactin was originally obtained from *Marinobacter hydrocarbonoclasticus* (*14*) and subsequently from *Bacillus anthracis* (*195*, *382*), *B. cereus* and *B. thuringiensis* (*195a*), its sulfonated derivatives from *Marinobacter* spp. It is probably identical with the incompletely characterized anthrachelin (*123*).

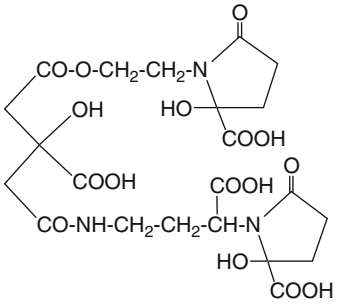

Fig. 18. Achromobactin (cyclic form) (**60**)

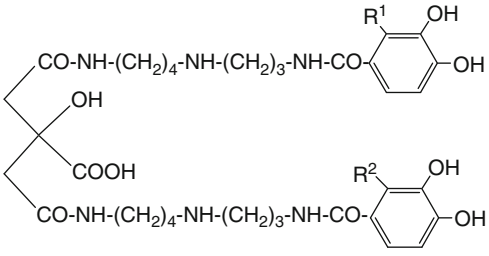

61: $R^1 = R^2 = H$
62: $R^1 = H$, $R^2 = SO_3H$
63: $R^1 = R^2 = SO_3H$

Fig. 19. Petrobactin (**61**), petrobactin monosulfonic acid (**62**), petrobactin disulfonic acid (**63**)

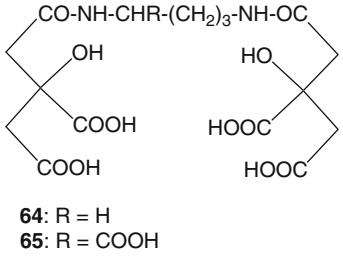

Fig. 20. Rhizoferrin (**64**), staphyloferrin A (**65**)

4.4. Siderophores with Two Citric Acid Units

(*S*,*S*)-(*enantio*)-Rhizoferrin (Fig. 20, **64**) was obtained from *Ralstonia pickettii* (*251*). It is the optical antipode of the fungal (*R*,*R*)-rhizoferrin first isolated from *Rhizopus microsporus* (*93*) and subsequently found to be a common siderophore of Zygomycetes (*358*). It is accompanied by two dehydration products, which are due to the formation of one or two imide rings (*cf.* Chart 3). UV spectral studies revealed that rhizoferrin forms a 1:1 Fe^{3+}-to-ligand complex despite the fact that it has only two α-hydroxy acid binding sites (*95*). NMR studies of the Ga^{3+} complex proved the twofold symmetry of the complex and showed that only the carboxyl groups, but not the hydroxy groups are deprotonated between *pH* 5.5 and 9.0. The Fe^{3+} complex is chiral and shows Λ-configuration (*58*). Uptake studies suggest a shuttle mechanism (*61*). While *Ralstonia* accepts both antipodes with equal rates *Rhizopus* shows a clear preference for its native (*R*,*R*)-enantiomer (*251*).

Staphyloferrin A (Fig. 20, **65**) is a second siderophore of *Staphylococcus* spp. (*226*). D-Ornithine connects the two citric acid parts. Due to the unsymmetrical link the central C-atoms of the citric acid units are chiral, but their stereochemistry has not been determined. Another consequence of the asymmetric structure is that two mono- and one di-dehydration products are observed. Staphyloferrin A forms a 1:1 Fe^{3+}-to-ligand complex, which is preferentially Λ-configured. For steric considerations only *cis*-(*SR*′) or *cis*-(*RS*′) arrangements can be considered. Uptake experiments with ^{55}Fe showed that it is a true siderophore (*193*).

4.5. Legiobactin

Legionella pneumophila produces a siderophore named legiobactin, which shows no catecholate or hydroxamate reactions (*206*). Enzymatic studies suggest a citrate structure in agreement with the data obtained by mass spectrometry (molecular mass *ca*. 350 Da) and NMR (three carbonyl and ten aliphatic C atoms). It is not clear yet as to whether legiobactin is essential for the iron acquisition in the aqueous habitat of the bacterium or during lung infection (*2*, *65*).

5. Pyochelin and Related Structures

This group comprises condensation products of salicylic acid with cysteine giving a thiazoline ring. For a review, see (*310*). Some structurally related compounds will also be mentioned here. Salicylic acid isolated from *Burkholderia* (*Pseudomonas*) *cepacia* was named azurochelin (*333*). It was found to act as a siderophore, *e.g.* for *Pseudomonas fluorescens* (*230*) and *P. syringae* (*178*); see also *Mycobacterium smegmatis* (Sect. 2.8). For details on the siderophore activity of salicylic acid, see (*359*).

The structure of pyochelin (for a detailed bibliography, see (*37*)), a secondary siderophore of *Pseudomonas aeruginosa* and of *Burkholderia cepacia* was established (*73*) as 2-(2-*o*-hydroxyphenyl-2-thiazolin-4-yl)-3-methylthiazolidine-4-carboxylic acid. It consists of a mixture of two easily interconvertible stereoisomers (pyochelin I and II) differing in the configuration of C-2″. They can be separated by chromatography, but in methanolic solution (not in DMSO) the equilibrium (*ca.* 3:1) is restored quickly. For a discussion of the mechanism of isomerization, see (*37*, *317*).

The relative and absolute stereochemistry (4′*R*,2″*R*,4″*R*) of pyochelin I (Fig. 21, **66**) were established by an X-ray analysis of its Fe^{3+} complex (*316*). Fe^{3+} is associated with the phenolate and the carboxylate oxygen ions and with the two nitrogen atoms. Two of these units are bridged by an acetate ion and a water molecule satisfying the remaining two ligand loci of Fe^{3+} (Plate 4). However, by titration a (Fe^{3+})/pyochelin ratio of 1:2 has been determined at *pH* 2.5 (*370*). This may be due to a partial protonation of the complexing sites. From *Burkholderia cepacia*, a mixed complex was obtained comprising Fe^{3+}/pyochelin/cepabactin 1:1:1 (see Sect. 6 below) (*188*). An X-ray analysis has been performed of ferri-pyochelin bound to its outer membrane receptor (*67a*). Pyochelin II has the configuration (4′*R*,2″*S*,4″*R*). It does not complex Fe^{3+} (*140*).

Several syntheses resulting in mixtures of stereoisomers (C-4′ and C-2″) have been developed (*6*, *301*, *397*) (Sect. 8.5). *Pseudomonas fluorescens* CHA0 produces *enantio*-pyochelin (*394*). The two optical antipodes are not accepted reciprocally by the two *Pseudomonas* species.

Pyochelin is a non-ribosomal condensation product of salicylic acid with two molecules of cysteine (*289*). Intermediates with one cysteine unit are aeruginoic acid (Fig. 21, **67**) first isolated from *Pseudomonas aeruginosa* (*390*), and (+)-(*S*)-4,5-dihydroaeruginoic acid, from *Pseudomonas fluorescens* (*57*). Detailed studies (*274a*) suggest that *N*-hydroxybenzoyl-L-cysteine bound to the synthetase

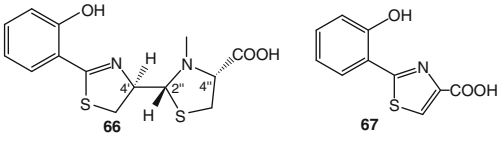

Fig. 21. Pyochelin I (**66**), aeruginoic acid (**67**)

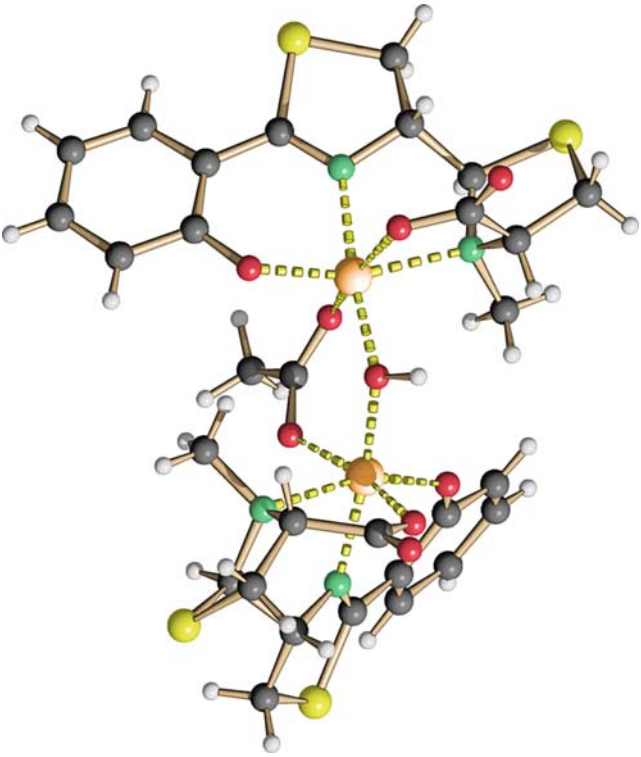

Plate 4. X-ray structure of ferri-pyochelin I (ferri-**66**)

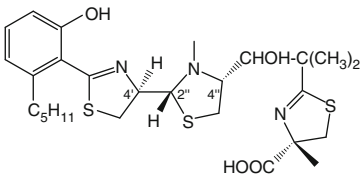

Fig. 22. Micacocidin (**68**)

racemizes, that bound dihydroaeruginoic acid is still a racemate, and that in the further steps only the 4′(*R*) isomer is used.

Micacocidin (Fig. 22, **68**) from *Pseudomonas* sp. complexes Fe^{3+} and other metal ions (*189*, *190*). Whether it acts as a siderophore has not been investigated. A stereospecific synthesis was elaborated (*161*, *161a*), but the same isomerization problems at C-4′ and C-2″ were encountered as had been observed with pyochelin (see Note 14 in (*161*)).

Yersiniabactin (Fig. 23, **69**) was obtained from *Yersinia* spp., and is produced also by *Pseudomonas syringae* (*49*) and *Escherichia coli* (*178*). Its structure was elucidated independently by two groups and given the names yersiniabactin (*96*)

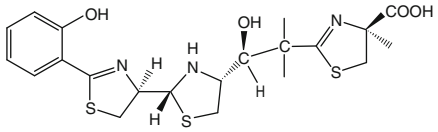

Fig. 23. Yersiniabactin (**69**)

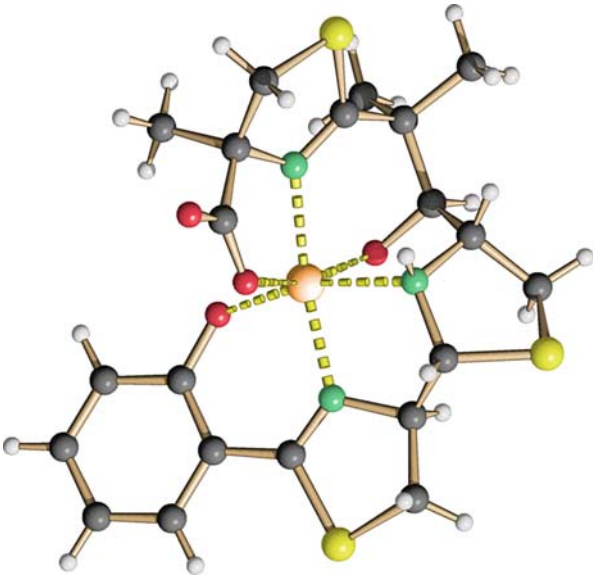

Plate 5. X-ray structure of ferri-yersiniabactin (ferri-**69**)

and yersiniophore (*64*). The configurations of the four chiral centers were not determined, but epimerization probably at C-10 (corresponding to C-2″ of pyochelin) was indicated. A recent X-ray analysis (Plate 5) of the Fe^{3+} complex (*238*) established the absolute stereochemistry [N-2 (*R*), C-9 (*R*), C-10 (*R*) as for pyochelin, C-12 (*R*), C-13 (*S*), C-19 (*S*)], with Δ-configuration.

Anguibactin (Fig. 24, **70**) from *Vibrio anguillarum* (*171*) contains DHB condensed with Cys (stereochemistry not determined). It is accompanied by a biosynthetic by-product (*311*) without the histamine part as its methyl ester.

6. Miscellaneous Siderophores

Desferri-ferrithiocin from *Streptomyces antibioticus* (Fig. 25, **71**) (*4*, *254*) is structurally related to the pyochelin group. It is (*S*)-configured and forms a $Fe^{3+}Lig_2$ complex (*131a*).

Cepabactin (Fig. 25, **72**) from *Burkholderia cepacia* (*232*) forms a $(Fe^{3+})Lig_3$ complex (*386*) and a mixed Fe^{3+} complex with pyochelin (Sect. 5).

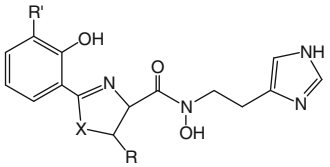

70: X = S, R = H, R' = OH
78: X = O, R = CH_3, R' = OH
79: X = O, R = CH_3, R' = H

Fig. 24. Anguibactin (**70**), pre-acinetobactin (**78**), pre-pseudomonine (**79**)

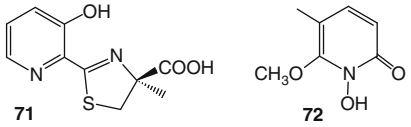

Fig. 25. Desferri-ferrithiocin (**71**), cepabactin (**72**)

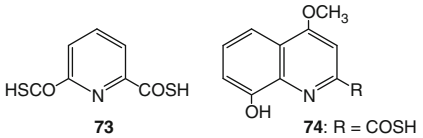

Fig. 26. Pyridine-di(monothiocarboxylic acid) (**73**), thioquinaldic (**74**), quinaldic acid (**75**)

Pyridine-2,6-di(monothiocarboxylic acid) (Fig. 26, **73**) [for a review, see (*36*), *cf*. also (*37*)] was obtained from *Pseudomonas putida* (*262*) and later from *Pseudomonas stutzeri* (*203*). It forms a brown Fe^{3+} complex and a blue Fe^{2+} complex (both $FeLig_2$) (*143*), which may be accompanied by complexes carrying two additional cyanide ions (*145*). An X-ray analysis (Plate 6) of the Fe^{3+} complex of **73** shows a distorted octahedral symmetry (*143*). There is evidence that a sulfenic acid residue (-CO-SOH) is the biosynthetic link between -COOH and -COSH (*144*).

From iron-deficient cultures of *Pseudomonas fluorescens*, 8-hydroxy-4-methoxy-monothioquinaldic acid (thioquinolobactin) together with the corresponding quinaldic acid (quinolobactin) (Fig. 26, **74** and **75**), could be isolated (*258*). Quinolobactin can act as an alternative siderophore of *Pseudomonas fluorescens* (*245*), although it is the hydrolysis product of the thioacid (*220*). Its synthesis and complex formation as $(Fe^{3+})Lig_2$ was described (*98*).

Pseudomonine (Fig. 27, **76**) is produced by *Pseudomonas fluorescens* strains (*7*, *228*) and by *P. entomophila*, where it can act as a secondary siderophore (*209*). The substituents on C-4 and C-5 of the isoxazolinone ring are in *trans* positions (*311*). The complex formation has not been studied. *In vitro* enzyme-catalyzed synthesis studies (*311*, *388*) showed that initially the intermediate pre-pseudomonine (Fig. 24, **79**) is formed, which non-enzymatically rearranges to pseudomonine.

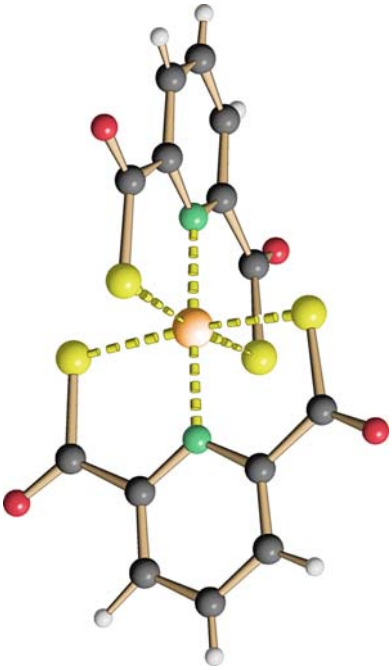

Plate 6. X-ray structure of the Fe^{3+}-complex of **73**

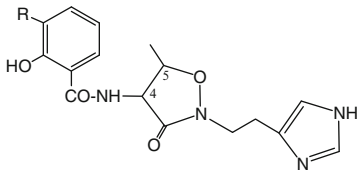

76: R = H
77: R = OH

Fig. 27. Pseudomonine (**76**), acinetobactin (**77**)

An analogous set of studies demonstrated that acinetobactin from *Acinetobacter baumannii* (*392*) has actually the structure **77** shown in Fig. 27 and that the one originally proposed (Fig. 24, **78**) is that of pre-acinetobactin. In contrast, the thiazoline ring of anguibactin (Fig. 24, **70**) (see above Sect. 5) is stable. Acinetobactin forms a 1:1 complex with Fe^{3+}.

Domoic acid (Fig. 28, **80**) (*263*) is a neuro-phycotoxin responsible for the mortality of wildlife and for amnesic shellfish poisoning (ASP) of humans during algal bloom. Domoic acid was first isolated from the red alga *Chondria armata* ("domoi" in Japanese), and it is produced also by diatoms, such as *Pseudo-nitzschia* spp. For the latter, evidence has been presented that it is involved in iron acquisition (*307*).

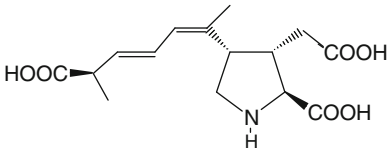

Fig. 28. Domoic acid (**80**)

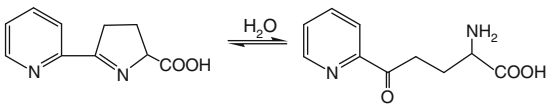

Chart 5. Proferrorosamin A (**81**)

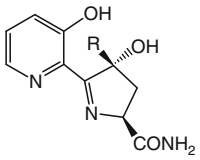

Fig. 29. Siderochelin A (R = CH_3) (**82**), B (C-3 epimer) (**83**) and C (R = C_2H_5) (**84**)

The smallest hydroxamate siderophore is *N*-methyl-*N*-thioformylhydroxylamine, CH_3-N(OH)-CHS, named thioformin (*100*) or fluopsin (*325*). The synthesis was described (CH_3-N(OH)-CHO + P_2S_5 or CH_3-N(OH)-H + HCSSK) (*100*, *166a*). It forms a purple $Fe^{3+}Lig_3$ complex. *Pseudomonas mildenbergii* produces *N*-methyl-*N*-phenylacetylhydroxylamine (CH_3-N(OH)-CO-CH_2-C_6H_5) (*159*), which also forms a purple Fe^{3+} complex.

7. Fe^{2+} Binding Ligands

Pseudomonas roseus fluorescens (*288*), *Pseudomonas* GH (*324*) and *Erwinia rhapontici* (*113*) produce pro-ferrorosamine A (**81**), also named pyrimine, which forms a red (Fe^{2+})Lig_3 complex. Under acidic conditions, an open form of pro-ferrorosamine A prevails, which cannot bind Fe^{2+} (Chart 5). Pro-ferrorosamine B is probably an artifact produced by condensation of pro-ferrorosamine A with CHO-COOH. Pro-ferrorosamine A is essential for iron uptake by *Pseudomonas* (*367*) and for the pathogenicity of *Erwinia* (*114*).

Structurally closely related is the *Nocardia* metabolite, siderochelin, for which the structure and relative and absolute stereochemistry were all established by X-ray crystallography (*208*, *267*). It is a mixture of two epimers A and B (Fig. 29, **82** and **83**). Siderochelin C, with an ethyl residue (Fig. 29, **84**), was obtained from a different actinomycete, tentatively identified as *Streptoalloteichus* sp. (*239*).

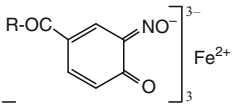

85: R = *p*-CH_2=CH-C_6H_4-O-
86: 2 R = *p*-CH_2=CH-C_6H_4-O-, 1 R = *p*-CHOH=CH-C_6H_4-O-
87: 2 R = *p*-CH_2=CH-C_6H_4-O-, 1 R = *p*-HOOC-CH=CH-C_6H_4-C-O-
88: R = NH_2

Fig. 30. Ferroverdins

The green pigments produced by *Streptomyces* spp. chelating Fe^{2+} with *o*-nitrosophenolate residues are occasionally referred to as siderophores, but whether they are really involved in iron metabolism has not been investigated. Ferroverdin A (*11*) forms a (Fe^{2+})Lig_3 complex (*55*), with the ligand being *p*-vinylphenyl-3-nitroso-4-hydroxybenzoate (Fig. 30, **85**). In ferroverdin B and C, one of the three ligands is substituted at the vinyl group (Fig. 30, **86** and **87**) (*346*, *361*). From *Streptomyces murayamaensis*, a precursor of ferroverdin was obtained (Fig. 30, **88**) (*69*).

For a further chelator of Fe^{2+}, see pyridine-2,6-di(monothiocarboxylic acid) above (Sect. 6).

8. Selected Syntheses

In this section the syntheses of several typical siderophores will be presented in a summarized form pointing out interesting features.

8.1. Anachelin H (10)

The challenge lay in the stereochemically correct synthesis of the polyketide part of the molecule. Starting from L-serine (**89**) (Chart 6) by C_2-elongation steps, reduction of the obtained keto functions including adequate protection and deprotection, and introduction of the salicylic acid residue the four stereoisomeric 3,5-diols (**90**) were obtained. Comparison of the ^{1}H-NMR data with those of anachelin (**10**) showed that the isomer with (3*R*,5*S*,6*S*) configuration was the correct starting material.

The chromophore part was prepared from Boc-protected *N*, *N*-dimethyl-L-DOPA (**91**), reduction to the diamine **92** and tellurium-mediated oxidative ring closure (**93**). The free amino group of **94** was coupled with protected L-Ser and L-Thr-D-Ser (**95**) and then the two constituent parts were connected and deprotected yielding **10** (*121*).

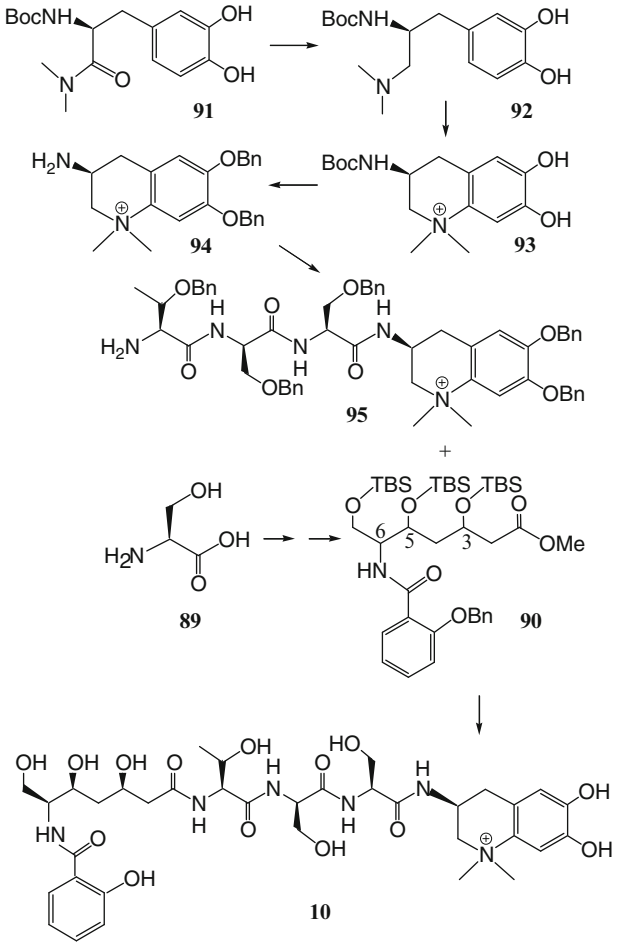

Chart 6. Synthesis scheme of anachelin H (**10**)

8.2. Alterobactin (26)

Several building blocks were prepared separately (Chart 7). Methyl *trans*-cinnamate gave by *Sharpless* enantiocontrolled dihydroxylation a diol from which by a series of stereo- and regioselective transformations (**96**) and Ru-catalyzed oxidation for transformation of the phenyl into a carboxyl group accompanied by adequate protection (**97**) and deprotection steps the protected OHAsp derivative **98** was obtained.

The protected (*S*)-4,8-diamino-3-oxooctanoic acid **99** was reduced with $NaBH_4$, the resulting mixture of diastereomers was separated and the (3*R*,4*S*)-product was derivatized with benzylated DHB (**100**). Then derivatized D-Ser-Gly was added and the serine OH-group was esterified with the protected OHAsp (**101**). The Gly carboxyl group was finally set free.

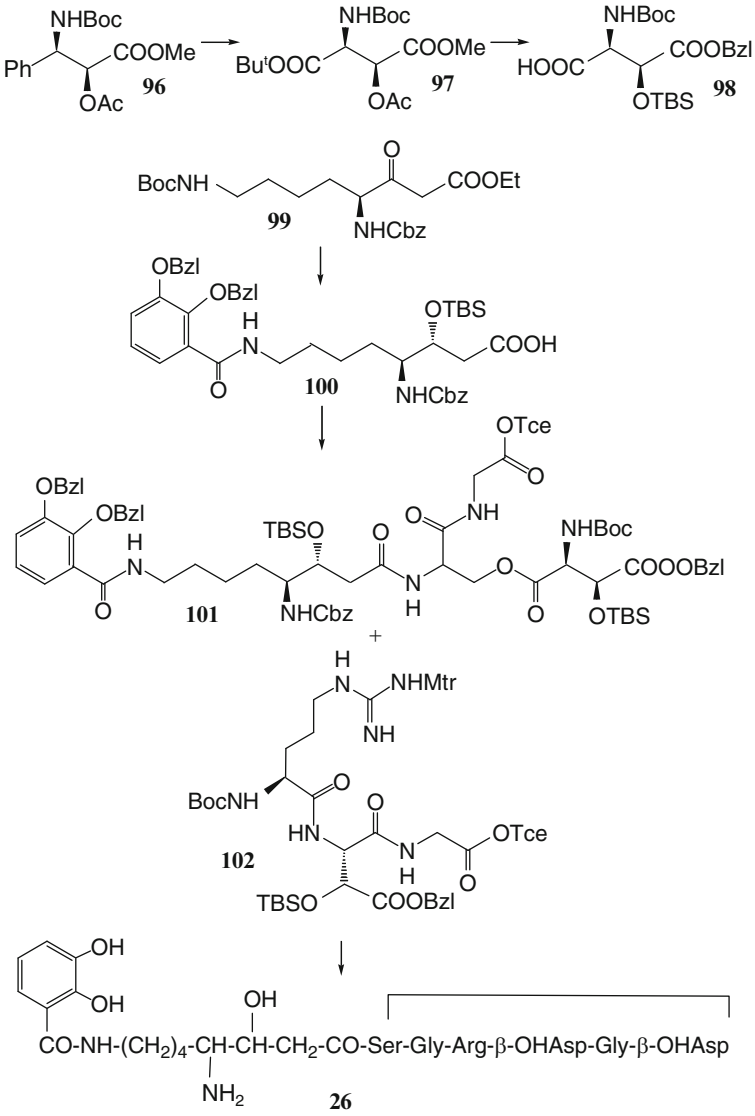

Chart 7. Synthesis scheme of alterobactin (**26**)

The synthesis of the remaining part of the molecule started from a condensation of protected Gly with the OHAsp derivative **98**, and subsequently with protected Arg (**102**). In the resulting protected tripeptide the Boc group from the Arg residue was removed. Connection of the two building blocks between Gly and Arg was followed by ring closure between Ser and Gly. Deprotection yielded finally alterobactin (**26**) (*83*).

8.3. *Parabactin (44)*

Here the critical step is the formation of the oxazoline ring. Both the stereochemistry of the two chiral centers and its acid lability had to be considered. Two approaches have been published. They can be modified for other members of this class.

The terminal NH_2-groups of N^5-benzylspermidine (Chart 8) were acylated with 2,3-dimethoxybenzyol chloride and the benzyl group was removed by hydrogenolysis (*28b*). N^1, N^{10}-bis(2,3-dimethoxy)benzoylspermidine (**103**) was then reacted with protected L-threonine (**104**). The Boc group was removed with CF_3COOH and the methoxy groups were cleaved with BF_3 (**105**). Subsequent reaction with 2-hydroxybenzimidoethyl ether (**106**) gave parabactin (**44**) (*28*, *28c*).

In the second synthesis (Chart 9) of **44** the carboxyl group of benzoyl-protected salicylic acid was activated by transformation into the 1,2-thiazolidine-2-thione derivative **107** and reacted with D-threonine. The methyl ester was debenzoylated reductively (**108**). Treatment with $SOCl_2$ resulted in cyclization accompanied by stereoinversion of C_β of threonine. The resulting *cis*-oxazoline derivative **109** was epimerized at C_α with C_2H_5ONa. Subsequent hydrolysis of the ester function gave the *trans*-carboxylic acid **110** which was reacted with N^1, N^{10}-bis(benzyloxycarbonyl)spermidine by treatment with phenylbis-(2-thioxo-1,3-thiazolidine-3-yl) phosphinoxide (**111**). The remaining steps leading to **44** (removal of the N-protecting

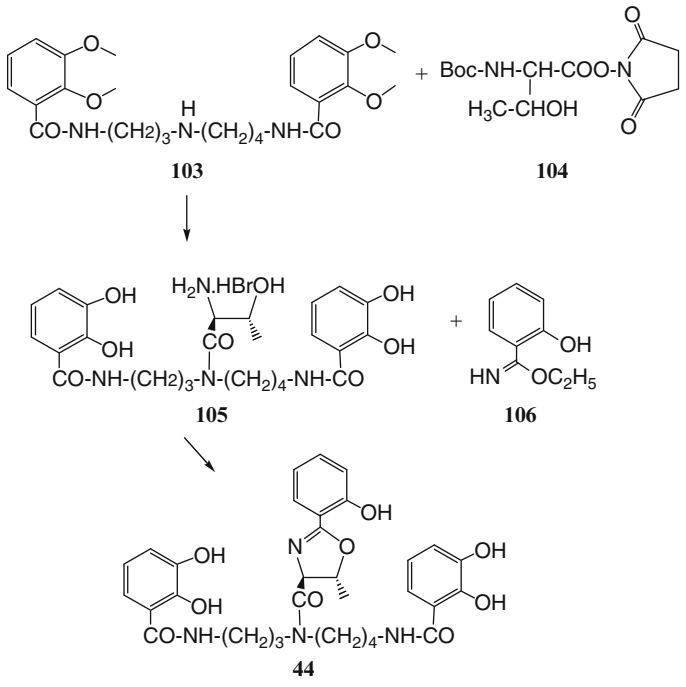

Chart 8. Synthesis I of parabactin (**44**)

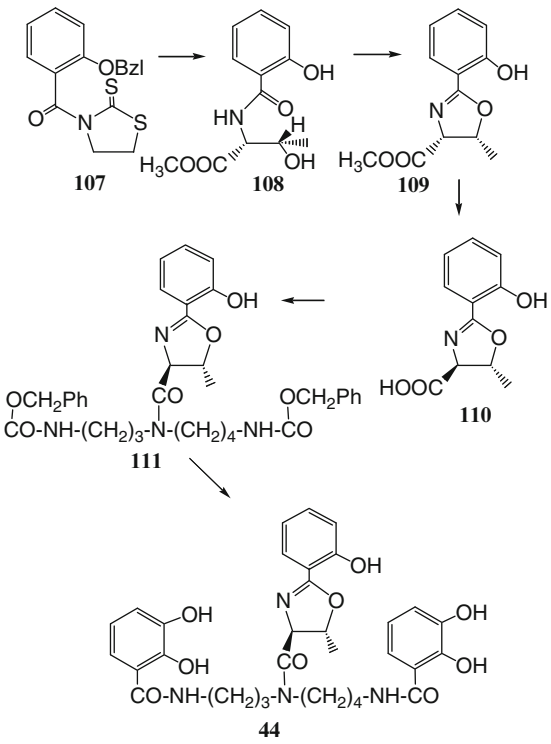

Chart 9. Synthesis II of parabactin (**44**)

groups, reaction with 2,3-diacetoxybenzyl chloride and cleavage of the acetoxyl groups) were standard operations (*255*).

In a recent modification of the second synthesis (*308*) effected for fluvibactin (**45**) an *o*-xylene protection group was proposed (reaction of 2,3-dihydroxybenzoic acid methyl ester with 1,2-di(bromomethyl)benzene) which could be removed later by hydrogenolysis. The formation of the oxazoline ring from protected DHB-L-threonine methyl ester was achieved with Mo(VI) catalysts (*e.g.* $(NH_4)_2MoO_4$) without affecting the chiral centers. Derivatization of the primary amino groups of norspermidine with the protected DHB methyl ester was catalyzed by $Sb(OC_2H_5)_3$.

8.4. Nannochelin A

For the condensation with the properly derivatized lysine part (**112**) 3′-*tert*-butyl-1,5-di-*N*-hydroxysuccinimidyl citrate (**113**) was used (Chart 10). It was prepared from 1,5-dimethyl citrate by reaction with *tert*-butyl acetate, alkaline hydrolysis of the methyl ester and coupling with *N*-hydroxysuccinimide by DCCI (*237*).

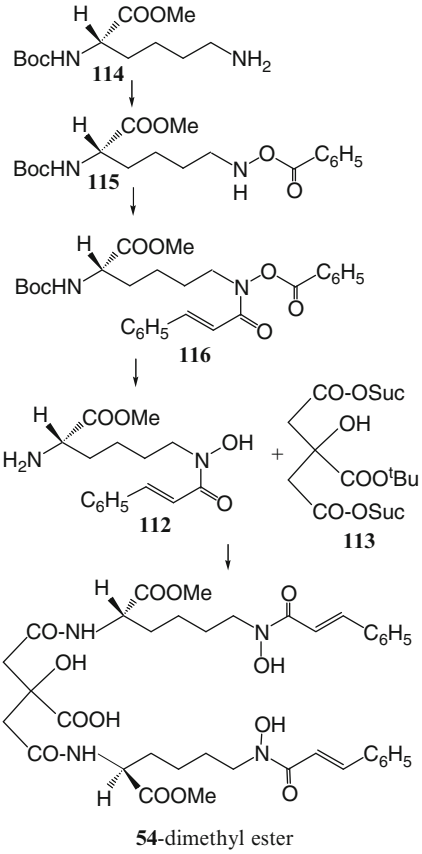

54-dimethyl ester

Chart 10. Synthesis of nannochelin A (**54**-dimethyl ester)

For the synthesis of the lysine part (**112**) N^2-Boc-L-lysine methyl ester (**114**) was treated with benzoylperoxide/Na_2CO_3 (**115**) and subsequently with *trans*-cinnamoyl chloride yielding **116**. The hydroxamate ester was deprotected with NH_3/CH_3OH at −23°C and the Boc group was removed with CF_3COOH. Condensation with the citric acid 3-*tert*-butyl ester was effected with $(C_2H_5)_3N$. After cleavage of the ester with CF_3COOH nannochelin A (**54**-dimethyl ester) was obtained (*29*). The difficulties in the synthesis lay in the various functional and protecting groups, which had to be introduced and removed in a deliberate sequence.

8.5. Pyochelin

The problem encountered with all published syntheses (*6*, *301*, *397*) is the non-stereospecific formation of C-4′ and the facile conversion of C-2″. The common approach (Chart 11) consists in the reaction of 2-hydroxybenzonitrile (**117**) with

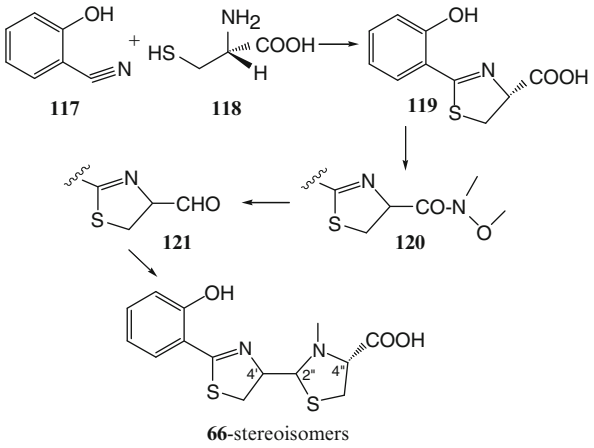

Chart 11. Synthesis of pyochelin stereoisomer mixture

L-cysteine (**118**) giving dihydroaeruginoic acid (**119**), reduction of the carboxyl group to the aldehyde **121** and condensation of the latter with L-*N*-methyl-cysteine. Details will be given for the procedure worked out by *Zamri* and *Abdallah* (*397*). The first condensation step was effected in a phosphate buffer (*pH* 6.4) to minimize epimerization at C-4′. Then the carboxyl group was reacted with *N*,*O*-dimethyl-hydroxylamine (**120**) using diethylcyanophosphonate as condensation agent. Reduction with $LiAlH_4$ yielded the aldehyde **121**, which then was treated with L-*N*-methyl-cysteine. A mixture of the four stereoisomers of (**66**), (4′*R*,2″*S*,4″*R*), (4′*S*,2″*S*,4″*R*), (4′*R*,2″*R*,4″*R*), (4′*S*,2″*R*,4″*R*) in a ratio of 2:1:2:5 was obtained.

9. Epilog

The history of siderophores actually began towards the end of the nineteenth century when laboratories engaged in bacteriological research observed that certain bacterial cultures showed a green fluorescence, and when in 1891 the first attempts were reported to isolate the fluorescent pigment (later namend pyoverdin, Sect. 2.1) produced by *Bacterium fluorescens liquefaciens* (*Pseudomonas fluorescens*), although it was not before 1978 that *J.-M. Meyer* demonstrated its being involved in the iron transport into the bacterial cell (*37*). Pyoverdins were among the centers of interest during the last decades, and other preferred topics were the fungal siderophores (Sect. 2.6), and more recently the marine lipopeptides (Sect. 2.8).

This review is mainly concerned with structural aspects of siderophores and their iron transport, intended to give a status report of what has been achieved up to late-2009. But the fields of interest in siderophores are much wider, spreading into

– genetics (identification of the genes responsible for the synthesis of the siderophores and their receptors (*e.g.* (*403*, *409*)),

- medicine (siderophores as virulence factors (*e.g.* (*75*)), but serving also as carriers for antibiotics in a Trojan Horse strategy (*e.g.* (*35a*)),
- agriculture (starving phytopathogenic bacteria by binding iron (*e.g.* (*187b*, *406*)),
- environmental problems (binding heavy metal ions (*e.g.* (*90a*)), degrading detrimental compounds (*e.g.* (*205a*)), mobilizing uranium and *trans*-uranium elements in contanimated soils (*e.g.* (*242a*)),

just to mention some areas. The diversity of scientific journals to be found in the References Section gives an idea of where information on siderophores can be hidden.

Structural work may take its time. Examples are *Pseudomonas mendocina* (Sect. 2.9) where the first structural data were reported in 2000 and the next pertinent publication appeared in 2008, or *Legionella pneumophila* (Sect. 4.5) whose legiobactin was first characterized in 2000, further details followed in 2007 and 2009, with loose ends in both cases. Only partially characterized siderophores are mentioned wherever data were available in order to stimulate further work. This would be worthwhile: siderophore research is a fascinating branch of natural products chemistry promising sometimes surprising results (*e.g.* (*311*, *388*)).

Acknowledgement Many thanks are due to Dr. *J. Neudörfl* for preparing the Plates with siderophore X-ray structures. Data bases for the X-ray structures: Plate 1: FEPSBC 10; 3: TEQKQV; 4: YELJOP; 5: VENPAC; 6: CUHGUH.

Appendix

Table 7. Pyoverdins Isolated from *Pseudomonas* spp.

P.	Name	Peptide chain[a,b,c,d]	Mass[e]	References[f]
(a) Complete or fairly complete structures				
Pyoverdins with a C-terminal cOHOrn				
		6 amino acids		
f	Ps (= B10[h])	εLys-OHAsp-Ala-aThr-Ala-cOHOrn	989	(*352–354*)
f	Py 9AW[n]	Ser-Lys-OHHis-aThr-Ser-cOHOrn	1043	(*42*)
ap	Py 4a[l] (= Py SB83)	Ala-Lys-Thr-Ser-AcOHOrn-cOHOrn	1046	(*47*)
p	iPy BTP1	Asp-Ala-Asp-AcOHOrn-Ser-cOHOrn	1047	(*168*)
		7 amino acids		
f	Py PL7	Ser-AcOHOrn-Ala-Gly-aThr-Ala-cOHOrn	1046	(*16*)
f	Py BTP2	Ser-Val-OHAsp-Gly-Thr-Ser-cOHOrn	1049	(*270*)
p	Py G4R	Asp-Orn-(OHAsp-Dab)-Gly-Ser-cOHOrn[i]	1073	(*33*, *309*)
	Py 2908	Ser-Orn-OHAsp-Ser-Ser-Ser-cOHOrn	1088	(*373*)
ae	Py T II[g] (=27853)	Ser-FoOHOrn-Orn-Gly-aThr-Ser-cOHOrn[bb]	1091	(*350*)
f	Py PL8	Lys-AcOHOrn-Ala-Gly-aThr-Ser-cOHOrn	1103	(*16*)

Table 7. *(continued)*

P.	Name	Peptide chain[a,b,c,d]	Mass[e]	References[f]
p	Py 11370	Asp−εLys-OHAsp-Ser-Ala-Ser-cOHOrn	1106	(*48*)
p	iPy 90-33	Asp-Lys-Thr-OHAsp-Thr-aThr-cOHOrn	1164	(*345*)
		8 amino acids		
p	Py 90-51	Asp-εLys-OHAsp-Ser-Gly-aThr-Lys-cOHOrn	1234	(*343*)
		9 amino acids		
c, *au*	Py Pau[u]	Ser-AcOHOrn-Gly-aThr-Thr-Gln-Gly-Ser-cOHOrn	1277	(*21*)
f	Py 2392 (= A6[h])	Lys-AcOHOrn-Gly-aThr-Thr-Gln-Gly-Ser-cOHOrn	1318	(*23*)
p	Ps 589A[o]	Asp−εLys-OHAsp-Ser-Thr-Ala-Glu-Ser-cOHOrn	1336	(*279*)
p	Py 2461 (=L1[h], WCS358[h])	Asp-εLys-OHAsp-Ser-aThr-Ala-Thr-Lys-cOHOrn[cc]	1349	(*365*)
ap	Py 3b[t]	Asp-(AcOHOrn-Dab)-Thr-Ala-Thr-Thr-Gln-cOHOrn	1358	(*349*)
		10 amino acids		
f	Py 2798 (=W[aa])	(Ser-Dab)-Gly-Ser-OHAsp-Ala-Gly-Ala-Gly-cOHOrn	1187	(*78*)
f	Py 17400	Ala-Lys-Gly-Gly-OHAsp-(Gln-Dab)-Ser-Ala-cOHOrn[i]	1299	(*77*)
p	Py 1,2	Ser-Thr-Ser-Orn-OHAsp-(Gln-Dab)-Ser-aThr-cOHOrn	1405	(*130*)
f	Py 1.3	Ala-Lys-Gly-Gly-OHAsp-(Gln-Dab)-Gly-Ser-cOHOrn	1285	(*125*)
t	Py 2192	Ser-Lys-Ser-Ser-Thr-Ser-AcOHOrn-Thr-Ser-cOHOrn	1424	(*78*)
p	iPy 90-44	Asp-Lys-AcOHOrn-Thr-Ser-Ser-Gly-Ser-Ser-cOHOrn[s]	1408	(*344*)
		11 amino acids		
f	Py 51W	Ala-Lys-Gly-Gly-OHAsp-Gln-Ser-Ala-Gly-aThr-OHOrn	1375	(*371*)

[a]In part (a) D-amino acids are underlined; a broken line indicates either that the stereochemistry of the amino acid has not been determined or that a specific amino acid occurs both in the D- and the L-form, but a localization of the the two enantiomers has not been effected. In part (b) D-amino acids are indicated only when data are available from the literature

[b]Abbreviations: *P, Pseudomonas*; *ae, aeruginosa*; *ap, aptata*; *as*, *asplenii*; *au*, *aureofaciens*; *c*, *costantinii*; *ci*, *cichoriae*; *en, entomophila*; *f, fluorescens*; *li*, *libanensis*; *m*, *marginalis*; *mo*, *monteilii*; *p, putida*; *pa, palleroniana*; *r*, *rhodesiae*; *s*, *syringae*; *t*, *tolaasii*; Ps, pseudobactin; Py, pyoverdin; iPy, isopyoverdin; amino acids: 3-letter code - in addition: OHAsp, *threo*-β-hydroxy-Asp; OHHis, *threo*-β-hydroxy-His; OHOrn, N^5-hydroxy-Orn; Ac(Fo,Bu)OHOrn, N^5-acetyl (formyl, (R)-β-hydroxy-butyryl) OHOrn; cOHOrn, *cyclo*-OHOrn (3-amino-1-hydroxy-piperidone-2); aThr, *allo*-Thr

[c]Amino acids are bound to the chromophore or to the preceding amino acid by their α-amino group or in the case of Lys occasionally by its ε-amino group (indicated as εLys)

Table 7. *(continued)*

P.	Name	Peptide chain[a,b,c,d]	Mass[e]	References[f]
		12 amino acids		
f	Py GM	Ala-Lys-Gly-Gly-OHAsp-Gln-Ser-Ala-Ala-Ala-Ala-cOHOrn	1430	(*242*)
	Py 1547	Ser-Lys-Ala-AcOHOrn-Thr-Ala-Gly-Gln-Ala-Ser-Ser-OHOrn	1547	(*304*)
Pyoverdins with a C-terminal cyclo-tetra- or tripeptide				
		cyclo-tetrapeptide		
f	Py G173	Ser-Ala-AcOHOrn-(Orn-Asp-AcOHOrn-Ser)	1175	(*363*)
	Py 96-312	Ser-Ser-FoOHOrn-(Lys-FoOHOrn-Lys-Ser)	1190	(*315*)
	Py 96.188	Ser-Lys-FoOHOrn-(Lys-FoOHOrn-Glu-Ser)	1232	(*379*)
ae	Py C-E (= PAO1[h], ATCC 15692, Pa)	Ser-Arg-Ser-FoOHOrn-(Lys-FoOHOrn-Thr-Thr)	1333	(*35*, *81*)
	Py 95-275 (= BTP7[h])	Ser-Ser-FoOHOrn-Ser-Ser-(Lys-FoOHOrn-Lys-Ser)	1364	(*342*)
f	Py 12	Ser-Lys-Gly-FoOHOrn-Ser-Ser-Gly-(Lys-FoOHOrn-Glu-Ser)	1520	(*124*)
		cyclo-tripeptide		
f	Py 13525[m]	Ser-Lys-Gly-FoOHOrn-(Lys-FoOHOrn-Ser)	1160	(*146*)
pa	Py 96-318	Ser-Orn-FoOHOrn-Ser-Ser-(Lys-FoOHOrn-Ser)	1263	(*315*)
f	Py 18-1	Ser-Lys-Gly-FoOHOrn-Ser-Ser-Gly-(Lys-FoOHOrn-Ser)	1391	(*3*)
Pyoverdins with a C-terminal cyclodepsipeptide or a free carboxyl group				
		6 amino acids		
a	PS 6.10	Ala-Orn-OHAsp-Dab-AcOHOrn-Lys	1091	(*46*)
		7 amino acids		
ae	Py R′	(Ser-Dab)-FoOHOrn-Gln-FoOHOrn-Gly	1046	(*305*)

[d]Parentheses indicate either a cycle formed by an amide or ester bond between the carboxyl group of the C-terminal amino acid and a side chain functionality of another amino acid or the condensation product of the NH_2 groups of Dab with the amide carbonyl group of the preceding amino acid giving a tetrahydropyrimidine ring (see Chart 1)

[e]Nominal molecular mass for a Py or iPy chromophore with a succinic acid side chain; the exact mass is about 0.5 Da higher

[f]References to complete structure elucidations. For further details see (*37*)

[g]Probably identical with the pyoverdin of *Pseudomonas aeruginosa* ATCC 9027 (*212*)

[h]The structure published originally had to be corrected or amended; literature references to the originally proposed structure may be found in (*37*)

[i]Accompanied by the not cyclized Dab form (M + 18)

[j]Accompanied by a non-cyclic pyoverdin with the same amino acid sequence

[k]For this pyoverdin an ε-amino Lys linkage was claimed but not substantiated. It is probably identical with the pyoverdin from *P. putida* 9AW where a α-amino Lys linkage was established

[l]*P. aptata* is a pathovar of *P. syringae*. The same pyoverdin was found produced by *P. fluorescens* SB83 (*20*). The identification of *P. aptata* may, therefore, be questioned (*cf.* also (*179*))

Table 7. *(continued)*

P.	Name	Peptide chain[a,b,c,d]	Mass[e]	References[f]
ci	PaB	εLys-OHAsp-Thr-(Thr-Gly-OHAsp-Ser)	1093	(*50*)
s	Py 19310	εLys-OHAsp-Thr-(Thr-Ser-OHAsp-Ser)[j]	1123	(*179*)
ae	Py R (=Pa6)	(Ser-Dab)-FoOHOrn-Gln-Gln-FoOHOrn-Gly	1173	(*127*)
		8 amino acids		
p	Ps A214 (= Ps 39167)	Ser-AcOHOrn-Ala-Gly-(Ser-Ala-OHAsp-Thr)[j]	1134	(*365*)
f	Py P19 (= Ps 7 SR1[h], Ps A 225)	Ser-AcOHOrn-Ala-Gly-(Ser-Ser-OHAsp- Thr)[j]	1150	(*372*)
ch	Py D-TR133	Asp-FoOHOrn-Lys-(Thr-Ala-Ala-FoOHOrn-Ala)[j,x]	1230	(*17*)
f	Py I-III	Asn-FoOHOrn-Lys-(Thr-Ala-Ala-FoOHOrn-Lys)	1286	(*287*)
f	CHAO	Asp-FoOHOrn-Lys-(Thr-Ala-Ala-FoOHOrn-Lys)	1287	(*387*)
		9 amino acids		
p	Py C	Asp-BuOHOrn-Dab-Thr-Gly-Ser-Ser-OHAsp-Thr	1370	(*319*)
p	Py BTP16	Asp-BuOHOrn-Dab-Thr-Gly-Ser-Ser-OHAsp-Thr [v]	1370	(*271*)
		10 amino acids		
as	Py fuscovaginae	εLys-OHAsp-Ala-(Thr-Dab-Gly-Gly-Thr-(OHAsp-Dab))	1316	(*49a*, *231*)
(b) Partial or tentative structures				
Pyoverdins with a C-terminal cOHOrn				
p	Thai	(Ser-Dab)-Thr-Ser-AcOHOrn-cOHOrn	1016	(*306*)
f	Py 244[k]	Ser-εLys-OHHis-aThr-Ser-cOHOrn	1043	(*132–134*)
p	Py 12633[o]	Asp-Lys-OHAsp-Ser-Thr-Ala-Glu-Ser-cOHOrn	1336	(*80*)
Pyoverdins with a C-terminal cyclo-tetra- or tripeptide				
		cyclo-tetrapeptide		
f	D47	Ser-Orn-FoOHOrn-(Lys-FoOHOrn-Glu-Ser)	1218	(*119*)
r	L25	Ser-Lys-FoOHOrn-Ser-Ser-Gly-(Lys-FoOHOrn-Ser-Ser)	1421	(*119*)

[m]The same pyoverdin was isolated from *P. chlororaphis* ATCC 9446 (*146*) and CNR15 (*162*). The reported isolation from *P. putida* KT2440 (*297*) is the result of a mix-up of strains (*J.-M. Meyer*, private communication)

[n]Probably identical also with that from *P. fluorescens* 244

[o]The Py 589A is probably identical with the pyoverdin Py Pp 12633

[p]Either the preliminary structural work or the identification of the strains may be questioned since screening of a large number of *P. aeruginosa* strains revealed the existence of only three siderovars characterized by the production of the pyoverdins Py C-E, Py R and Py Pa TII (*234*) plus probably of a mutant of Py R (R′ (*305*)). Py Pa 15152 was shown to be identical with Pa D above (*20*)

[q]The structural proposals are tentative; Orn/Asn and Lys/Gln have the same mass, Lys may be incorporated in the peptide chain by its α- or its ε-amino group

Table 7. *(continued)*

P.	Name	Peptide chain[a,b,c,d]	Mass[e]	References[f]
		cyclo-tripeptide		
m	G 76	Ser-Ser-FoOHOrn-Ser-Ser-(Lys-FoOHOrn-Ser)	1236	(*119*)
	DSM 50106	Ser-Lys-Gly-FoOHOrn-Ser-Ser-Gly-(Orn- FoOHOrn-Ser)	1377	(*119*)
Pyoverdins where only limited mass spectral data are available[q]				
p	Py GS43	Lys-OHAsp-Ser-Ser-Ser-cOHOrn	1007	(*231*)
li	Py 96.195	Ala-Orn-OHAsp-Ser-Orn-Ser-cOHOrn	1091	(*231*)
	Py G 85	Ser-Lys-OHAsp-Ser-Orn-Ser-cOHOrn	1121	(*231*)
	Py G 76	Ser-Ser-FoOHOrn-Ser-Ser-Lys-(FoOHOrn-Ser)	1236	(*231*)
	Py HR6	Asp-ε-Lys-OHAsp-Ser-Ser-Thr-Thr-Thr-cOHOrn	1238	(*231*)
	LBSA1	Asp-Arg-AcOHOrn-Lys-Ser-Asp-cOHOrn	1260	(*231*)
mo	iPy Lille 1	Asp-Lys-AcOHOrn-Ala-Ser-Ser-Gly-Ser-cOHOrn	1291	(*231*)
f	Py G153	Ser-Lys-Ala-Ser-Ser- AcOHOrn-Ser-Ser-cOHOrn	1293	(*231*)
en	L48	Ala-Asn-Dab-OHHis-Gly-Gly-Ala-Thr-Ser-cOHOrn	1298	(*219*)
p	Py G172	Ala-Lys-Dab-OHAsp-Thr-Gly- OHAsp-Gly-Thr-Thr - H_2O	1335	(*231*)
f	Pf0-1	Ala-AcOHOrn-Orn-Ser-Ser-Ser-Arg-OHAsp-Thr	1381	(*231*)
p	90-136/ G 168	Ser-Lys-Ser-Ser-Thr-Thr-AcOHOrn-Ser-Ser-cOHOrn	1424	(*231*)
	IB3	Ser-Ala-Thr-Gln-Orn-AcOHOrn-Thr-Thr-Ala-Ser-Thr-Ala-Ala-cOHOrn	1764	(*231*)
Various pyoverdins with incomplete structural data				
ae	Py UNK[p]	Ser-Thr-Ser-Gly-OHOrn-OHOrn		(*107*)
ae	Pa 15152[p]	2 Arg, 2 Orn, 3 Ser, 3 Thr		(*107*)
p	Py Pm	OHAsp, Lys, OHOrn, 2 Ser, 3 Thr		(*212a*)
s	Py Ps	Lys, OHOrn, 3 Ser, 3 Thr		(*362*)
s	Py PSS[z]	2 OHAsp, Lys, 2 Ser, 2 Thr		(*68*)
	P. mildenbergii	Glu, Lys, Ser, Thr[w]		(*259*)

[r]The reported amino acid composition cannot be correct. The minimum molecular mass calculated from it is about 120 u higher than the molecular mass determined by mass spectrometry. Also the amino acids acting as ligands for Fe^{3+} are missing

[s]2 D-Ser, 2 L-Ser

[t]Contains 2 Thr and one aThr. The amino acid analysis of the corresponding ferribactin gave D-Ala, L-Asp, L-Dab, D- and L-Glu, L-Orn, D-aThr, L-Thr and D-Tyr

[u]The same pyoverdin was isolated from *P. tolaasii* NCBBP 2192 (*P. constantinii*); the fact that the strain designated as *P. aureofaciens* does not produce phenazines casts doubts on the correct identification (*364*)

[v]1 Thr, 1 aThr

[w]Ratios of 1:1:2:4 and 1:2:3:5 are reported for the pyoverdins from two strains of *P. mildenbergii*; for the second one a blocked N-terminus was demonstrated

[x]1 D-Ala, 2L-Ala; the pyoverdin D-TR 133 is accompanied by a small amount of a pyoverdin where the second Ala is replaced by Gly

Table 7. *(continued)*

P.	Name	Peptide chain[a,b,c,d]	Mass[e]	References[f]
p	Py A1	Asx, Glx, 3 Gly, His, Lys, 4 Ser, Thr, Val[r]		(*32*)
f	BTP9[y]	2 Lys, 2 FoOHOrn, 5 Ser		(*269*)
p	BTP14[aa]	Asx, Dab, Glx, Gly, Orn, 2 Ser, Thr, aThr		(*269*)

[y]Probably identical with the pyoverdins of BTP7 and BTP16 (private communication Dr. *M. Ongena*, Liège)
[z]Probably identical with the pyoverdin Py 19310
[aa]Identical with pyoverdin W mentioned in (*79*) (private communication Dr. *J.-M. Meyer*, Strasbourg)
[bb]Accompanied by a variety with one AcOHOrn (*187a*)
[cc]Accompanied by a small amount of a pyoverdin where Ala is replaced by Gly

Notes Added in Proof

Section 2.5

Coelichelin from *Streptomyces coelicolor* comprises D-N^5-formyl-N^5-hydroxy-Orn-D-aThr bound to N^5 of L-N^5-hydroxy-Orn whose N^2 is acylated by D-N^5-formyl-N^5-hydroxy-Orn (*412*).

Section 2.6

Erythrochelin from *Saccharopolyspora erythraea* is a coprogen-type siderophore (Table 2) with Ac^1 = **i** and Ac^2 = D-Ser-D-N^2, N^5-diacetyl-N^5-hydroxy-Orn (*413*).

Section 2.7

The transport system of *Bacillus subtilis* accommodates the Fe^{3+} complexes of enterobactin (Δ-configured), *enantio*-D-enterobactin and of corynebactin (bacillibactin) (both Λ). Since only Λ complexes can be bound to the receptor a configurational change from Δ to Λ is induced. Only the natural ferri-L-siderophores can be degraded enzymatically (*399*, *408*).

From *Nocardia tenerifensis* the heterobactin JBIR-16 was obtained (**30**, R = DHB). The stereochemistry of the two Orn residues was not established. By mass spectrometry a 1:1 Fe^{3+}/Lig ratio was determined for the red complex (*407*).

References

1. Adapa S, Huber P, Keller-Schierlein W (1982) Stoffwechselprodukte von Mikroorganismen. 216. Mitteilung. Isolierung, Strukturaufklärung und Synthese von Ferrioxamin H. Helv Chim Acta **65**: 1818

1a. Adolphs M, Taraz K, Budzikiewicz H (1996) Catecholate Siderophores from *Chryseomonas luteola*. Z Naturforsch **51c**: 281
2. Allard KA, Dao J, Sanjeevaiah P, McCoy-Simandle K, Chatfield CH, Crumrine DS, Castignetti D, Cianciotto NP (2009) Purification of Legiobactin and the Importance of this Siderophore in Lung Infection by *Legionella pneumophila*. Infect Immun **77**: 2887
3. Amann C, Taraz K, Budzikiewicz H, Meyer JM (2000) The Siderophores of *Pseudomonas fluorescens* 18.1 and the Importance of Cyclopeptidic Substructures for the Recognition at the Cell Surface. Z Naturforsch **55c**: 671
3a. Ams DA, Maurice PA, Hersman LE, Forsythe JH (2002) Siderophore Production by an Aerobic *Pseudomonas mendocina* Bacterium in the Presence of Kaolinite. Chem Geol **188**: 161
4. Anderegg G, Räber M (1990) Metal Complex Formation of a New Siderophore Desferrithiocin and of Three Related Ligands. J Chem Soc Chem Commun 1194
5. Anke H, Kinn J, Bergquist KE, Sterner O (1991) Production of Siderophores by Strains of the Genus *Trichoderma*. Isolation and Characterization of the New Lipophilic Coprogen Derivative, Palmitoylcoprogen. Biol Metals **4**: 176
6. Ankenbauer RG, Toyokuni T, Staley A, Rinehard KL Jr, Cox CD (1988) Synthesis and Biological Activity of Pyochelin, a Siderophore of *Pseudomonas aeruginosa*. J Bacteriol **170**: 5344
7. Anthoni U, Christophersen C, Nielsen PH, Gram L, Petersen BO (1995) Pseudomonine, an Isoxazolidone with Siderophoric Activity from *Pseudomonas fluorescens* AH2 Isolated from a Lake Victorian Nile Perch. J Nat Prod **58**: 1786
8. Arceneau JEL, Davis WB, Downer DN, Haydon AH, Byers BR (1973) Fate of Labeled Hydroxamates during Iron Transport from Hydroxamate-Iron Chelates. J Bacteriol **115**: 919
8a. Arnow LE (1937) Colorimetric Determination of the Components of 3,4-Dihydroxyphenylalanine-Tyrosine Mixtures. J Biol Chem **118**: 531
9. Atkin CL, Neilands JB (1968) Rhodotorulic Acid, a Diketopiperazine Dihydroxamic Acid with Growth-Factor Activity. I. Isolation and Characterization. Biochemistry **7**: 3734
9a. Atkin CL, Neilands JB, Phaff HJ (1970) Rhodotorulic Acid from Species of *Leucosporidium*, *Rhodosporidium*, *Rhodotorula*, *Sporidiobolus*, and *Sporobolomyces*, and a New Alanine-containing Ferrichrome from *Cryptococcus melibiosum*. J Bacteriol **103**: 722
9b. Awaya JD, DuBois JL (2008) Identification, Isolation, and Analysis of a Gene Cluster Involved in the Iron Acquisition by *Pseudomonas mendocina* ymp. Biometals **21**: 353
10. Bachhawat AK, Ghosh S (1987) Iron Transport in *Azospirillum brasiliense*: Role of the Siderophore Spirilobactin. J Gen Microbiol **133**: 1759
11. Ballio A, Bertholdt H, Carilli A, Chain EB FRS, Di Vittorio V, Tonolo A, Vero-Barcellona L (1963) Studies on Ferroverdin, a Green Iron-containing Pigment Produced by a *Streptomyces* Wak. Species. Proc Royal Soc London; Ser B; Biol Sci **158**: 43
12. Barbeau K, Rue EL, Bruland KW, Butler A (2001) Photochemical Cycling of Iron in the Surface Ocean Mediated by Microbial Iron(III)-Binding Ligands. Nature **413**: 409
13. Barbeau K, Rue EL, Trick CG, Bruland KW, Butler A (2003) Photochemical Reactivity of Siderophores Produced by Marine Heterotrophic Bacteria and Cyanobacteria Based on Characteristic Fe(III) Binding Groups. Limnol Oceanogr **48**: 1069
14. Barbeau K, Zhang G, Live DH, Butler A (2002) Petrobactin, a Photoreactive Siderophore Produced by the Oil-Degrading Marine Bacterium *Marinobacter hydrocarbonoclasticus*. J Am Chem Soc **124**: 378
15. Barelmann I, Meyer JM, Taraz K, Budzikiewicz H (1996) Cepaciachelin, a New Catecholate Siderophore from *Burkholderia* (*Pseudomonas*) *cepacia*. Z Naturforsch **51c**: 627
16. Barelmann I, Taraz K, Budzikiewicz H, Geoffroy V, Meyer JM (2002) The Structures of the Pyoverdins from Two *Pseudomonas fluorescens* Strains Accepted Mutually by their Respective Producers. Z Naturforsch **57c**: 9
17. Barelmann I, Uría Fernández D, Budzikiewicz H, Meyer JM (2003) The Pyoverdine from *Pseudomonas chlororaphis* D-TR133 Showing Mutual Acceptance with the Pyoverdine from *Pseudomonas fluorescens* CHA0. BioMetals **16**: 263

18. Barklay R, Ewing DF, Ratledge C (1985) Isolation, Identification, and Structural Analysis of the Mycobactins of *Mycobacterium avium*, *Mycobacterium intracellulare*, *Mycobacterium scrofulaceum*, and *Mycobacterium paratuberculosis*. J Bacteriol **164**: 896
19. Barry SM, Challis GL (2009) Recent Advances in Siderophore Biosynthesis. Curr Opin Chem Biol **13**: 205
20. Beiderbeck H (1997) Untersuchung der Pyoverdine aus *Pseudomonas aeruginosa* ATCC 15152, *Pseudomonas fluorescens* CFBP 2392 und *Pseudomonas putida* 2461. Diplomarbeit, Universität zu Köln, and unpublished results
21. Beiderbeck H, Risse D, Budzikiewicz H, Taraz K (1999) A New Pyoverdin from *Pseudomonas aureofaciens*. Z Naturforsch **54c**: 1
22. Beiderbeck H, Taraz K, Budzikiewicz H, Walsby AE (2000) Anachelin, the Siderophore of the Cyanobacterium *Anabena cylindrica* CCAP 1403/2A. Z Naturforsch **55c**: 681
23. Beiderbeck H, Taraz K, Meyer JM (1999) Revised Structures of the Pyoverdins from *Pseudomonas putida* CFBP 2461 and from *Pseudomonas fluorescens* CFBP 2392. BioMetals **12**: 331-338
24. Bergeron RJ (1987) Synthesis and Properties of Polyamine Catecholamide Chelators. In: Winkelmann G, van der Helm D, Neilands JB (eds) Iron Transport in Microbes, Plants and Animals. VCH: Weinheim, p 285
25. Bergeron RJ, Dionis JB, Elliot GT, Kline SJ (1985) Mechanism and Stereospecificity of the Parabactin-mediated Iron-Transport System in *Paracoccus denitrificans*. J Biol Chem **260**: 7936
26. Bergeron RJ, Garlich JR, McManis JS (1985) Total Synthesis of Vibriobactin. Tetrahedron **41**: 507
27. Bergeron RJ, Huang G, Smith RE, Bharti N, McManis JS, Butler A (2003) Total Synthesis and Structure Revision of Petrobactin. Tetrahedron **59**: 2007
28. Bergeron RJ, Kline SJ (1982) Short Synthesis of Parabactin. J Am Chem Soc **104**: 4489
28a. Bergeron RJ, Kline SJ (1984) 300-MHz ^{1}H NMR Study of Parabactin and its Ga(III) Chelate. J Am Chem Soc **106**: 3089
28b. Bergeron RJ, Kline SJ, Stolowich NJ, McGovern KA, Burton PS (1981) Flexible Synthesis of Polyamine Catecholamides. J Org Chem **46**: 4524
28c. Bergeron RJ, McManis JS, Dionis JB, Garlich JR (1985) An Efficient Total Synthesis of Agrobactin and its Ga(III) Chelate. J Org Chem **50**: 2780
29. Bergeron RJ, Phanstiel O iv (1992) The Total Synthesis of Nannochelin, a Novel Cinnamoyl Hydroxamate-containing Siderophore. J Org Chem **57**: 7140
30. Bergeron RJ, Xin MG, Weimar WR, Smith RE, Wiegand J (2001) Significance of Asymmetric Sites in Choosing Siderophores as Deferration Agents. J Med Chem **44**: 2469
30a. Berner I, Konetschny-Rapp S, Jung G, Winkelmann G (1988) Characterization of Ferrioxamine E as the Principal Siderophore of *Erwinia herbicola* (*Enterobacter agglomerans*). Biol Metals **1**: 51
30b. Berti AD, Thomas MG (2009) Analysis of Achromobactin Biosynthesis by *Pseudomonas syringae* pv. *syringae* B728a. J Bacteriol **191**: 4594
30c. Bertrand S, Larcher G, Landreau A, Richomme P, Duval O, Bouchara JP (2009) Hydroxamate Siderophores of *Scedosporium apiospermum*. Biometals **22**: 1019
30d. Bickel H, Bosshardt R, Gäumann E, Reusser P, Vischer E, Voser W, Wettstein A, Zähner H (1960) Stoffwechselprodukte von Actinomyceten. 26. Mitteilung. Über die Isolierung und Charakterisierung der Ferrioxamine A–F, neuer Wuchsstoffe der Sideramingruppe. Helv Chim Acta **43**: 2118
30e. Bickel H, Hall GE, Keller-Schierlein W, Prelog V, Vischer E, Wettstein A (1960) Stoffwechselprodukte von Actinomyceten. 27. Mitteilung. Über die Konstitution von Ferrioxamin B. Helv Chim Acta **43**: 2129
31. Bister B, Bischoff D, Nicholson GJ, Valdebenito M, Schneider K, Winkelmann G, Hantke K, Süssmuth RD (2004) The Structure of Salmochelins: C-Glucosylated Enterobactins of *Salmonella enterica*. BioMetals **17**: 471

32. Boopathi E, Rao KS (1999) A Siderophore from *Pseudomonas putida* Type A1: Structural and Biological Characterization. Biochim Biophys Acta **1435**: 30

33. Boukhalfa H, Reilly SD, Michalczyk R, Iyer S, Neu P (2006) Iron (III) Coordination Properties of a Pyoverdin Siderophore Produced by *Pseudomonas putida* ATCC 33015. Inorg Chem **45**: 5607

34. Braun V, Pramanik A, Gwinner T, Köberle M, Bohn E (2009) Sideromycins: Tools and Antibiotics. Biometals **22**: 3

35. Briskot G, Taraz K, Budzikiewicz H (1989) Pyoverdin-Type Siderophores from *Pseudomonas aeruginosa*. Liebigs Ann Chem 375

35a. Budzikiewicz H (2001) Siderophore-Antibiotic Conjugates used as Trojan Horses against *Pseudomonas aeruginosa*. Curr Top Med Chem **1**: 73

36. Budzikiewicz H (2003) Heteroaromatic Monothiocarboxylic Acids from *Pseudomonas* spp. Biodegradation **14**: 65

37. Budzikiewicz H (2004) Siderophores of the Pseudomonadaceae *sensu stricto* (Fluorescent and Non-fluorescent *Pseudomonas* spp.). Progr Chem Org Nat Prod **87**: 81

38. Budzikiewicz H (2004) Bacterial Catecholate Siderophores. Mini-Rev Org Chem **1**: 163

39. Budzikiewicz H (2005) Bacterial Citrate Siderophores. Mini-Rev Org Chem **3**: 119

40. Budzikiewicz H (2006) Bacterial Aromatic Sulfonates – a *Bucherer* Reaction in Nature? Mini-Rev Org Chem **3**: 93

41. Budzikiewicz H, Bössenkamp A, Taraz K, Pandey A, Meyer JM (1997) Corynebactin, a Cyclic Catecholate Siderophore from *Corynebacterium glutamicum* ATCC 14067 (*Brevibacterium* sp. DSM 20411). Z Naturforsch **52c**: 551

42. Budzikiewicz H, Kilz S, Taraz K, Meyer JM (1997) Identical Pyoverdines from *Pseudomonas fluorescens* 9AW and from *Pseudomonas putida* 9BW. Z Naturforsch **52c**: 721

43. Budzikiewicz H, Münzinger M, Taraz K, Meyer JM (1997) Schizokinen, the Siderophore of the Plant Deleterious Bacterium *Ralstonia* (*Pseudomonas*) *solanacearum* ATCC 11969. Z Naturforsch **52c**: 496

44. Budzikiewicz H, Schäfer M, Meyer JM (2007) Siderotyping of Fluorescent Pseudomonads – Problems in the Determination of Molecular Masses by Mass Spectrometry. Mini-Rev Org Chem **4**: 246

45. Budzikiewicz H, Schäfer M, Uría Fernández D, Matthijs S, Cornelis P. (2007) Characterization of the Chromophores of Pyoverdins and Related Siderophores by Electrospray Tandem Mass Spectrometry. BioMetals **20**: 135

46. Budzikiewicz H, Schäfer M, Uría Fernández D, Meyer JM (2006) Structure Proposal for a New Pyoverdin from *Pseudomonas* sp. PS 6.10. Z Naturforsch C **61c**: 815

47. Budzikiewicz H, Schröder H, Taraz K (1992) Zur Biogenese der *Pseudomonas*-Siderophore: Der Nachweis analoger Strukturen eines Pyoverdin-Desferriferribactin-Paares. Z Naturforsch **47c**: 26

48. Budzikiewicz H, Uría Fernández D, Fuchs R, Michalke R, Taraz K, Ruangviriyachai C (1999) Pyoverdins with a Lys ε-Amino Link in the Peptide Chain? Z Naturforsch **54c**: 1021

49. Bultreys A, Gheysen I, de Hoffmann E (2006) Yersiniabactin Production by *Pseudomonas syringae* and *Escherichia coli*, and Description of a Second Yersiniabactin Locus Evolutionary Group. Appl Environ Microbiol **72**: 3814

49a. Bultreys A, Gheysen I, Wathelet B, Maraite H, de Hoffman E (2003) High-Performance Liquid Chromatography Analyses of Pyoverdin Siderophores Differentiate among Phytopathogenic Fluorescent *Pseudomonas* Species. Appl Environ Microbiol **69**: 1143 and unpublished material

50. Bultreys A, Gheysen I, Wathelet B, Schäfer M, Budzikiewicz H (2004) The Pyoverdins of *Pseudomonas syringae* and *Pseudomonas cichorii*. Z Naturforsch **59c**: 613

51. Burton MO, Sowden FJ, Lochhead AG (1954) The Isolation and Nature of the "Terregens Factor". Can J Biochem Physiol **32**: 400 (Chem Abstr **48**, 10839d, 1954).

52. Buyer JS, de Lorenzo V, Neilands JB (1991) Production of the Siderophore Aerobactin by a Halophilic Pseudomonad. Appl Environ Microbiology **57**: 2246

53. Byers BR, Powell MV, Lankford CE (1967) Iron-Chelating Hydroxamic Acid (Schizokinen) Active in Initiation of Cell Division in *Bacillus megaterium*. J Bacteriol **93**: 286
54. Calugay RJ, Takeyama H, Mukoyama D, Fukuda Y, Suzuki T, Kanoh K, Matsunaga T (2006) Catechol Siderophore Excretion by Magnetotactic Bacterium *Magnetospirillum magneticum* AMB-1. J Biosci Bioeng **101**: 445
55. Candeloro S, Gardenić D, Taylor N, Thompson B, Viswamitra M, Hodgkin DC (1969) Structure of Ferroverdin. Nature **224**: 589
56. Capon RJ, Steward M, Ratnayake R, Lacey E, Gill JH (2007) Citromycetins and Bilains A-C: new Aromatic Polyketides and Diketopiperazines from Australian Marine-derived and Terrestrial *Penicillium* spp. J Nat Prod **70**: 1746
57. Carmi R, Carmeli S, Levy E, Gough FJ (1994) (+)-(*S*)-Dihydroaeruginoic Acid, an Inhibitor of *Septoria tritici* and other Phytopathogenic Fungi and Bacteria, Produced by *Pseudomonas fluorescens*. J Nat Prod **57**: 1200
58. Carrano CJ, Drechsel H, Kaiser D, Jung G, Matzanke B, Winkelmann G, Rochel N, Albrecht-Gary AM (1996) Coordination Chemistry of the Carboxylate Type Siderophore Rhizoferrin: the Iron(III) Complex and its Metal Analogs. Inorg Chem **35**: 6429
59. Carrano CJ, Jordan M, Drechsl H, Schmid DG, Winkelmann G (2001) Heterobactins: a New Class of Siderophores from *Rhodococcus erythropolis* IGTS8 Containing both Hydroxamate and Catecholate Donor Groups. BioMetals **14**: 119
60. Carrano CJ, Raymond KN (1978) Coordination Chemistry of Microbial Iron Transport Compounds. 10. Characterization of the Complexes of Rhodotorulic Acid, a Dihydroxamate Siderophore. J Am Chem Soc **100**: 5371
61. Carrano CJ, Thieken A, Winkelmann G (1996) Specificity and Mechanism of Rhizoferrin-Mediated Metal Ion Uptake. BioMetals **9**: 185
61a. Carson KC, Glenn AR, Dilworth MJ (1994) Specificity of Siderophore-mediated Transport of Iron in Rhizobia. Arch Microbiol **161**: 333
62. Chakraborty RN, Patel HN, Desai SB (1990) Isolation and Partial Characterization of Catechol-Type Siderophore from *Pseudomonas stutzeri*. Curr Microbiol **20**: 283
63. Challis GL (2005) A Widely Distributed Bacterial Pathway for Siderophore Biosynthesis Independent of Nonribosomal Peptide Synthetases. ChemBioChem **6**: 601
64. Chambers CE, McIntyre DD, Mouck M, Sokol PA (1996) Physical and Structural Characterization of Yersiniophore, a Siderophore Produced by Clinical Isolates of *Yersinia enterocolitica*. BioMetals **9**: 157
65. Cianciotto NP (2007) Iron Acquisition by *Legionella pneumophila*. Biometals **20**: 323
66. Ciche TA, Blackburn M, Carney JR, Ensign JB (2003) Photobactin: a Catechol Siderophore Produced by *Photorhabdus luminescens*, an Entomopathogen Mutually Associated with *Heterorhabditis bacteriophora* NC1 Nematodes. Appl Environ Microbiol **69**: 4706
67. Cobessi D, Celia H, Folschweiller N, Schalk IJ, Abdallah MA, Pattus F (2005) The Crystal Structure of the Outer Pyoverdine Membrane Receptor FpvA from *Pseudomonas aeruginosa* at 3.6 Å Resolution. J Mol Biol **347**: 121
67a. Cobessi D, Celia H, Pattus F (2005) Crystal Structure at High Resolution of Ferric-Pyochelin and its Membrane Receptor FptA from *Pseudomonas aeruginosa.* J Mol Biol **352**: 893
68. Cody YS, Gross DC (1987) Characterization of Pyoverdin$_{pss}$, the Fluorescent Siderophore Produced by *Pseudomonas syringae* pv. *syringae*. Appl Environ Microbiol **53**: 928
69. Cone MC, Melville CR, Carney JR, Gore MP, Gould, SJ (1995) 4-Hydroxy-3-nitrosobenzamide and its Ferrous Chelate from *Streptomyces murayamaensis*. Tetrahedron **51**: 3095
70. Corbin JL, Bulen WA (1969) The Isolation and Identification of 2,3-Dihydroxybenzoic Acid and 2-*N*,6-*N*-di(2,3-dihydroxybenzoyl)-L-lysine Formed by Iron-deficient *Azozobacter vinelandii*. Biochemistry **8**: 757
71. Corey EJ, Bhattacharyya S (1977) Total Synthesis of Enterobactin, a Macrocyclic Iron Transporting Agent of Bacteria. Tetrahedron Lett 3919
72. Cornish AS, Page WJ (1995) Production of the Triacetocholate (*sic*!) Siderophore Protochelin by *Azotobacter vinelandii*. BioMetals **8**: 332

73. Cox CD, Rinehart KL Jr, Moore ML, Cook, JC Jr (1981) Pyochelin: Novel Structure of an Iron-chelating Growth Promotor for *Pseudomonas aeruginosa*. Proc Natl Acad Sci USA **78**: 4256

74. De M, Basu M, Chakrabartty PK (2003) Increased Synthesis of Dihydroxybenzoic Acid in the Presence of Aluminum by *Rhizobium* MO1. Acta Microbiol Polon **52**: 195

75. De Lorenzo V, Martinez JL (1988) Aerobactin Production as a Virulence Factor: a Reevaluation. Eur J Clin Microbiol Infect Dis **7**: 621

76. Demange P, Bateman A, Dell A, Abdallah MA (1988) Structure of Azotobactin D, a Siderophore of *Azotobacter vinelandii* Strain D (CCM 289). Biochemistry **27**: 2745

77. Demange P, Bateman A, MacLeod JK, Dell A, Abdallah MA (1990) Bacterial Siderophores: Unusual 3,4,5,6-Tetrahydropyrimidine-Based Amino Acids in Pyoverdins from *Pseudomonas fluorescens*. Tetrahedron Lett **31**: 7611

78. Demange P, Bateman A, Mertz C, Dell A, Piémont Y, Abdallah MA (1990) Bacterial Siderophores: Structure of Pyoverdins Pt, Siderophores of *Pseudomonas tolaasii* NCPPB 2192, and Pyoverdins Pf, Siderophores of *Pseudomonas fluorescens* CCM 2798. Identification of an Unusual Natural Amino Acid. Biochemistry **29**: 11041

79. Demange P, Wendenbaum S, Bateman A, Dell A, Meyer JM, Abdallah MA (1986) Bacterial Siderophores: Structure of Pyoverdins and Related Compounds. In: Swinburne TR (ed) Iron, Siderophores, and Plant Diseases. Plenum, New York, p 131

80. Demange P, Wendenbaum S, Linget C, Bateman A, MacLeod J, Dell A, Albrecht AM, Abdallah MA (1989) *Pseudomonas* Siderophores: Structure and Physicochemical Properties of Pyoverdins and Related Peptides. Second Forum on Peptides **174**: 95

81. Demange P, Wendenbaum S, Linget C, Mertz C, Cung MT, Dell A, Abdallah MA (1990) Bacterial Siderophores: Structure and NMR Assignment of Pyoverdins Pa, Siderophores of *Pseudomonas aeruginosa* ATCC 15692. Biol Metals **3**: 155

82. Deml G, Voges K, Jung G, Winkelmann G (1984) Tetraglycylferrichrome – the First Heptapeptide Ferrichrome. FEBS **173**: 53

83. Deng J, Hamada Y, Shioiri T (1995) Total Synthesis of Alterobactin A, a Super Siderophore from an Open-Ocean Bacterium. J Am Chem Soc **117**: 7824

84. Dertz EA, Xu J, Stintzi A, Raymond KN (2006) Bacillibactin-mediated Iron Transport in *Bacillus subtilis*. J Am Chem Soc **128**: 22

85. de Voss JJ, Rutter K, Schroeder BG, Barry CE III (1999) Iron Acquisition and Metabolism by Mycobacteria. J Bacteriol **181**: 4443

86. Dhungana S, Michalczyk R, Boukhalfa H, Lack JG, Koppisch AT, Fairlee JM, Johnson MT, Ruggiero CE, John SG, Cox MM, Browder CC, Forsythe JH, Vanderberg LA, Neu MP, Hersman LE (2007) Purification and Characterization of Rhodobactin: a Mixed Ligand Siderophore from *Rhodococcus rhodochrous* Strain OFS. Biometals **20**: 853

87. Dhungana S, Miller MJ, Dong L, Ratledge C, Crumbliss AL (2003) Iron Chelation Properties of an Extracellular Siderophore Exochelin MN. J Am Chem Soc **125**: 7654

88. Diekmann H (1967) Stoffwechselprodukte von Mikroorganismen. 56. Mitteilung. Fusigen – ein neues Sideramin aus Pilzen. Arch Mikrobiol **58**: 1

89. Diekmann H (1970) Stoffwechselprodukte von Mikroorganismen. 81. Mitteilung. Vorkommen und Strukturen von Coprogen B und Dimerumsäure. Arch Microbiol **73**: 65

90. Diekmann H, Krezdorn E (1975) Stoffwechselprodukte von Mikroorganismen. 150. Mitteilung. Ferricrocin, Triacetylfusigen und andere Sideramine aus Pilzen der Gattung *Aspergillus*, Gruppe *Fumigatus*. Arch Microbiol **106**: 191

90a. Diels L, Van Roy S, Taghavi S, Van Houdt R (2009) From Industrial Sites to Environmental Applications with *Cupriavidus metallidurans*. Antonie van Leeuwenhoek **96**: 247

91. Dilworth MJ, Carson KC, Giles RGF, Byrne LT, Glenn AR (1998) *Rhizobium leguminosarum* bv. *viciae* Produces a Novel Cyclic Trihydroxamate Siderophore, Vicibactin. Microbiology **144**: 781

92. Dimise EJ, Widboom PF, Bruner SD (2008) Structure Elucidation and Biosynthesis of Fuscachelins, Peptide Siderophores from the Moderate Thermophile *Thermobifida fusca*. Proc Natl Acad Sci USA **105**: 15311

93. Drechsel H, Metzger J, Freund S, Jung G, Boelaert JR, Winkelmann G (1991) Rhizoferrin – a Novel Siderophore from the Fungus *Rhizopus microsporus* var. *rhizopodiformis*. Biol Metals **4**: 238

94. Drechsel H, Freund S, Nicholson G, Haag H, Jung O, Zähner H, Jung G. (1993) Purification and Chemical Characterization of Staphyloferrin B, a Hydrophilic Siderophore from Staphylococci. BioMetals **6**: 185

95. Drechsel H, Jung G, Winkelmann G (1992) Stereochemical Characterization of Rhizoferrin and Identification of its Dehydration Products. BioMetals **5**: 141

96. Drechsel H, Stephan H, Lotz R, Haag H, Zähner H, Hantke K, Jung G (1995) Structure Elucidation of Yersiniabactin, a Siderophore from Highly Virulent *Yersinia* Strains. Liebigs Ann Chem 1727

97. Drechsel H, Winkelmann G (1997) Iron Chelation and Siderophores. In: Winkelmann G, Carrano CJ (eds) Transition Metals in Microbial Metabolism. Harwood Academic Publishers, Amsterdam, p 1

98. du Moulinet d'Hardemare A, Serratrice G, Pierre JL (2004) Synthesis and Iron-binding Properties of Quinolobactin, a Siderophore from a Pyoverdine-deficient *Pseudomonas fluorescens*. BioMetals **17**: 691

99. Ecker DJ, Lancaster JR Jr., Emery T (1982) Siderophore Iron Transport Followed by Electron Paramagnetic Resonance Spectroscopy. J Biol Chem **257**: 8623

100. Egawa Y, Umino K, Ito Y, Okuda T. (1971) Antibiotic YC 73 of *Pseudomonas* Origin. II. Structure and Synthsis of Thioformin and its Cupric Complex (YC 73). J Antibiot **24**: 124

101. Ehlert G, Taraz K, Budzikiewicz H (1994) Serratiochelin, a New Catecholate Siderophore from *Serratia marcescens*. Z Naturforsch **49c**: 11

102. El Hage Chahine JM, Bauer AM, Baraldo K, Lion C, Ramiandrasoa F, Kunesch G. (2001) Kinetics and Thermodynamics of Complex Formation between Fe^{III} and Two Synthetic Chelators of the Dicatecholspermidine Family. Eur J Inorg Chem 2287

103. Emery T (1971) Role of Ferrichrome as a Ferric Ionophore in *Ustilago sphaerogena*. Biochemistry **10**: 1483

103a. Emery T (1976) Fungal Ornthine Esterases: Relationship to Iron Transport. Biochemistry **15**: 2723

104. Emery T. (1980) Malonichrome, a New Iron Chelate from *Fusarium roseum*. Biochim Biophys Acta **629**: 382

105. Emery T (1987) Reductive Mechanisms of Iron Assimilation. In: Winkelmann G, van der Helm D, Neilands JB (eds) Iron Transport in Microbes, Plants and Animals. VCH, Weinheim, p 235

106. Emery T, Neilands JB (1961) Structure of the Ferrichrome Compounds. J Am Chem Soc **83**: 1626

107. Eng-Wilmot DL, Kerley EL, Perryman DD, Brown C, Noah WH, McDyer D, Gore M, Mergo PJ, Cockburn BA (1990) Pyoverdin Type Siderophores from Various Strains of *Pseudomonas aeruginosa*. Reported at the International Symposium on Iron Transport and Metabolism II, 20.–22. June 1990, Austin TX, USA

108. Eng-Wilmot DL, Rahman A, Mendenhall JV, Grayson SL, van der Helm D (1984) Molecular Structure of Ferric Neurosporin, a Minor Siderophore-like Compound Containing N^{δ}-hydroxy-D-ornithine. J Am Chem Soc **106**: 1285

109. Eng-Wilmot DL, van der Helm D (1980) Molecular and Crystal Structure of the Linear Tricatechol Siderophore, Agrobactin. J Am Chem Soc **102**: 7719

110. Feistner GJ (1995) Suggestion for a New, Semirational Nomenclature for the Free Chelators of Ferrioxamines. BioMetals **8**: 193

111. Feistner GJ (1995) Proferrioxamine Synthesis in *Erwinia amylovora* in Response to Precursor or Hydroxylysine Feeding: Metabolic Profiling with Liquid Chromatography-Electrospray Mass Spectrometry. BioMetals **8**: 318

112. Feistner G, Beaman BL (1987) Characterization of 2,3-Dihydroxybenzoic Acid from *Nocardia asteroides* GUH-2. J Bacteriology **169**: 3982

112a. Feistner GJ, Hsieh LL (1995) On the Collision-activated Fragmentation of Proferrioxamines: Evidence for a Succinimide-mediated Mechanism. J Am Soc Mass Spectrom **6**: 836
113. Feistner GJ, Korth H, Ko H, Pulverer G, Budzikiewicz H (1983) Ferrorosamine A from *Erwinia rhapontici*. Curr Microbiol **8**: 239
114. Feistner GJ, Mavridis A, Rudolph K (1997) Proferrorosamines and Phytopathogenicity in *Erwinia* spp. BioMetals **10**: 1
115. Feistner GJ, Stahl DC, Gabrik AH (1993) Proferrioxamine Siderophores of *Erwinia amylovora*. A Capillary Liquid Chromatographic/Electrospray Tandem Mass Spectrometric Study. Org Mass Spectrom **28**: 163
115a. Fekete FA, Lanzi RA, Beaulieu JB, Longcope DC, Sulya AW, Hayes RN, Mabbott GA (1989) Isolation and Preliminary Characterization of Hydroxamic Acids Formed by Nitrogen-fixing *Azotobacter chroococcum* B-8. Appl Envir Microbiol **55**: 298
116. Filsak G, Taraz K, Budzikiewicz H. (1994) Untersuchungen zur Struktur und Derivatisierung von Kondensationsprodukten der 2,4-Diaminobuttersäure mit anderen Aminosäuren. Z Naturforsch **49c**: 18
117. Frederick CB, Bentley MD, Shive W (1981) Structure of Triornicin, a New Siderophore. Biochemistry **20**: 2436
118. Frederick CB, Bentley MD, Shive W (1982) The Structure of the Fungal Siderophore, Isotriornicin. Biochem Biophys Res Commun **105**: 133
119. Fuchs R (2000) Massenspektrometrische Untersuchung cyclischer Pyoverdine: Strukturaufklärung und Siderotyping. Dissertation; Universität zu Köln.
120. Fukasawa K, Goto M, Sasaki K, Hirata Y, Sato S (1972) Structure of the Yellow-Green Fluorescent Peptide Produced by Iron-deficient *Azotobacter vinelandii* Strain O. Tetrahedron **28**: 5359
121. Gademann K, Bethuel Y, Locher HH, Hubschwerlen C (2007) Biomimetic Total Synthesis and Antimicrobial Evaluation of Anachelin H. J Org Chem **72**: 8361
122. Gademann K, Budzikiewicz H (2004) The Peptide Alkaloid Anachelin: NMR Spectroscopic Evidence for a β-Turn Formation in Aqueous Solution. Chimia **58**: 212
123. Garner BL, Arceneaux JEL, Byers BR (2004) Temperature Control of a 3,4-dihydroxybenzoate (Protocatechuate)-based Siderophore in *Bacillus anthracis*. Curr Microbiol **49**: 89
124. Geisen K, Taraz K, Budzikiewicz H (1992) Neue Siderophore des Pyoverdin-Typs aus *Pseudomonas fluorescens*. Monatsh Chem **123**: 151
125. Georgias H, Taraz K, Budzikiewicz H, Geoffroy V, Meyer JM (1999) The Structure of the Pyoverdin from *Pseudomonas fluorescens* 1.3. Structural and Biological Relationship of Pyoverdins from Different Strains. Z Naturforsch **54c**: 301
126. Gibson F, Magrath DI (1969) The Isolation and Characterization of a Hydroxamic Acid (Aerobactin) Formed by *Aerobacter aerogenes* 62-I. Biochim Biophys Acta **192**: 175
126a. Gilis A, Khan MA, Cornelis P, Meyer JM, Mergeay M, van der Lelie D (1996) Siderophore-mediated Iron Uptake in *Alcaligenes eutrophus* CH34 and Identification of *aleB* Encoding the Ferric Iron-Alcaligin E Receptor. J Bacteriol **178**: 5499
127. Gipp S, Hahn J, Taraz K, Budzikiewicz H (1991) Zwei Pyoverdine aus *Pseudomonas aeruginosa* R. Z Naturforsch **46c**: 534
128. Gobin J, Moore CH, Reeve JR Jr, Wong DK, Gibson BW, Horwitz MA (1995) Iron Acquisition by *Mycobacterium tuberculosis*: Isolation and Characterization of a Family of Iron-binding Exochelins. Proc Natl Acad Sci USA **92**: 5189
128a. Greenwald J, Nader M, Celia H, Gruffaz C, Geoffroy V, Meyer JM, Schalk IJ, Pattus F (2009) FpvA Bound to Non-cognate Pyoverdines: Molecular Basis of Siderophore Recognition by an Iron Transporter. Mol Microbiol **72**: 1246
129. Griffiths GL, Sigel SP, Payne SM, Neilands JB (1984) Vibriobactin, a Siderophore from *Vibrio cholerae*. J Biol Chem **10**: 383
130. Gwose I, Taraz K (1992) Pyoverdine aus *Pseudomonas putida*. Z Naturforsch **47c**: 487
131. Haag H, Fiedler HP, Meiwes J, Drechsel H, Jung G, Zähner H (1994). Isolation and Biological Characterization of Staphyloferrin B, a Compound with Siderophore Activity from Staphylococci. FEMS Microbiol Lett **115**: 125

131a. Hahn FE, McMurry TJ, Hugi A, Raymond KN (1990) Coordination Chemistry of Microbial Iron Transport. 42. Structural and Spectroscopic Characterization of Diastereomeric Cr(III) and Co(III) Complexes of Desferriferrithiocin. J Am Chem Soc **112**: 1854
132. Hancock DK (1991) Isolation and Structure of a Unique Pyoverdine-type Siderophore Containing L-*threo*-β-Hydroxyhistidine. Ph.D Thesis, University of Maryland
133. Hancock DK, Coxon B, Wang SY, White VE, Reeder DJ, Bellama JM (1993) L-*threo*-β-Hydroxyhistidine, an Unprecedented Iron (III) Ion-Binding Amino Acid in a Pyoverdine-Type Siderophore from *Pseudomonas fluorescens* 244. J Chem Soc Chem Commun 468
134. Hancock DK, Reeder DJ (1993) Analysis and Configuration Assignment of the Amino Acids in a Pyoverdine-Type Siderophore by Reversed-Phase High-Performance Liquid Chromatography. J Chromatogr **646**: 335
135. Hantke K, Nicholson G. Rabsch W, Winkelmann G (2003) Salmochelins, Siderophores of *Salmonella enterica* and Uropathogenic *Escherichia coli* Strains, are Recognized by the Outer Membrane Receptor Iron. Proc Natl Acad Sci USA **100**: 3677
136. Harada K, Tomita K, Fujii K, Masuda K, Mikami Y, Yazawa K, Komaki H (2004) Isolation and Structural Characterization of Siderophores, Madurastatins, Produced by a Pathogenic *Actinomadura madurae*. J Antibiot **57**: 125
137. Harrington, JM, Crumbliss AL (2009) The Redox Hypothesis in the Siderophore-mediated Iron Uptake. Biometals **22**: 679
138. Harris WR, Carrano CJ, Raymond KN (1979) Coordination Chemistry of Microbial Iron Transport Compounds. 16. Isolation, Characterization, and Formation Constants of Ferric Aerobactin. J Am Chem Soc **101**: 2722
139. Haselwandter K, Dobernigg B, Beck W, Jung G, Cansier A, Winkelmann G (1992) Isolation and Identification of Hydroxamate Siderophores of Ericoid Mycorrhizal Fungi. BioMetals **5**: 51
140. Hayen H, Volmer DA (2006) Different Iron-chelating Properties of Pyochelin Diastereoisomers Revealed by LC/MS. Anal Bioanal Chem **385**: 606
141. Haygood MG, Holt PD, Butler A (1993) Aerobactin Production by a Planctonic Marine *Vibrio* sp. Limnol Oceanogr **38**: 1091
141a. Hersman LE, Huang A, Maurice PA, Forsythe JH (2000) Siderophore Production and Iron Reduction by *Pseudomonas mendocina* in Response to Iron Deprivation. Geomicrobiology J **17**: 261
142. Hickford SHJ, Küpper FC, Zhang G, Carrano CJ, Blunt JW, Butler A (2004) Petrobactine Sulfonate, a New Siderophore Produced by the Marine Bacterium *Marinobacter hydrocarbonoclasticus*. J Nat Prod **67**: 1897
143. Hildebrand U, Lex J, Taraz K, Winkler S, Ockels W, Budzikiewicz H (1984) Untersuchungen zum Redox-System Bis(pyridin-2,6-dicarbothioato)-ferrat(II)/ferrat(III). Z Naturforsch **39b**: 1607
144. Hildebrand U, Taraz K, Budzikiewicz H (1986) 6-(Hydroxythio)carbonylpyridin-2-carbonsäure und Pyridin-2-carbonsäure-6-monothiocarbonsäure als biosynthetische Zwischenstufen bei der Bildung von Pyridin-2,6-di(monothiocarbonsäure) aus Pyridin-2,6-dicarbonsäure. Z Naturforsch **41c**: 691
145. Hildebrand U, Taraz K, Budzikiewicz H, Korth H, Pulverer G. (1985) Dicyano-bis(pyridin-2,6-dicarbothioato)-ferrat (II)/ferrat (III), ein weiteres eisenhaltiges Redoxsystem aus der Kulturlösung eines *Pseudomonas*-Stammes. Z Naturforsch **40c**: 201
145a. Hoegy F, Celia H, Mislin GL Vicent M, Gallay J, Schalk IJ (2005) Binding of Iron-free Siderophore, a Common Feature of Siderophore Outer Membrane Transporters of *Escherichia coli* and *Pseudomonas aeruginosa*. J Biol Chem **280**: 20222
146. Hohlneicher U, Hartmann R, Taraz K, Budzikiewicz H (1995) Pyoverdin, Ferribactin, Azotobactin – a new Triad of Siderophores from *Pseudomonas chlororaphis* ATTC 9446 and its Relation to *Pseudomonas fluorescens* ATCC 13525. Z Naturforsch **50c**: 337
147. Holinsworth B, Martin JD (2009) Siderophore Production by Marine-derived Fungi. Biometals **22**: 625

148. Holt PD, Reid RR, Lewis BL, Luther GW III, Butler A (2005) Iron(III) Coordination Chemistry of Alterobactin A: a Siderophore from the Marine Bacterium *Alteromonas luteoviolacea*. Inorg Chem **44**: 7671
149. Homann VV, Edwards KJ, Webb EA, Butler A (2009) Siderophores of *Marinobacter aquaeolei*: Petrobactin and its Sulfonated Derivatives. Biometals **22**: 565
150. Homann VV, Sandy M, Tincu JA, Templeton AS, Tebo BM, Butler A (2009) Loihichelins A-F, a Suite of Amphiphilic Siderophores Produced by the Marine Bacterium *Halomonas* LOB-5. J Nat Prod **72**: 884
151. Hopkinson BM, Morel FMM (2009) The Role of Siderophores in Iron Acquisition by Photosynthetic Marine Microorganisms. Biometals **22**: 659
152. Hossein MB, Eng-Wilmot DL, Loghry RA, van der Helm D (1980) Circular Dichroism, Crystal Sructure, and Absolute Configuration of the Siderophore Ferric *N*,*N*′,*N*″-Triacetylfusarinine, $FeC_{39}H_{57}N_6O_{15}$. J Am Chem Soc **102**: 5766
153. Hossein MB, Jalal MAF, Benson BA, Barnes CL, van der Helm D (1987) Structure and Conformation of Two Coprogen-type Siderophores: Neocoprogen I and Neocoprogen II. J Am Chem Soc **109**: 4948
154. Hossein MB, Jalal MAF, van der Helm D (1986) The Structure of Ferrioxamine D1-Ethanol-Water (1/2/1) Acta Cryst C **42**: 1305
155. Hossain MB, Jalal MAF, van der Helm D (1997) 6-L-Alanineferrirubin, a Ferrichrome-type from the Fungus *Aspergillus ochraceous*. Acta Cryst C **53**: 716
155a. Hossein MB, van der Helm D, Poling M (1983) The Structure of Deferriferrioxamine E (Norcardamin), a Cyclic Trihydroamate. Acta Cryst B **39**: 258
156. Hou Z, Sunderland CJ, Nishio T, Raymond KN (1996) Preorganization of Ferric Alcaligin, Fe_2L_3. The First Structure of a Ferric Dihydroxamate Siderophore. J Am Chem Soc **118**: 5148
157. Hough E, Rodgers D (1974) The Crystal Structure of Ferrimycobactin P, a Growth Factor for the *Mycobacteria*. Biochem Biophys Res Commun **57**: 73
157a. Howard DH (1999) Acquisition, Transport, and Storage of Iron by Pathogenic Fungi. Clin Microbiol Rev **12**: 394
157b. Howard DH, Rafie R, Tiwari A, Faull KF (2000) Hydroxamate Siderophores of *Histoplasma capsulatum*. Infect Immun **68**: 2338
158. Hu X, Boyer GL (1995) Isolation and Characterization of the Siderophore *N*-Deoxyschizokinen from *Bacillus megaterium* ATCC 19213. BioMetals **8**: 357
159. Hulcher FH (1982) Isolation and Characterization of a New Hydroxamic Acid from *Pseudomonas mildenbergii*. Biochemistry **21**: 4491
160. Huschka HG, Jalal MAF, van der Helm D, Winkelmann G (1986) Molecular Recognition of Siderophores in Fungi: Role of Iron-surrounding *N*-Acyl Residues and the Peptide Backbone During Membrane Transport in *Neurospora crassa*. J Bacteriol **167**: 1020
160a. Huschka H, Naegeli HU, Leuenberger-Ryf H, Keller-Schierlein W, Winkelmann G (1985) Evidence for a Common Siderophore Transport System but Different Siderophore Receptors in *Neurospora crassa*. J Bacteriol **162**: 715
161. Ino A, Hasegawa Y, Murabayashi A (1998) Total Synthesis of the Antimycoplasma Antibiotic Micacocidin. Tetrahedron Lett **39**: 3509
161a. Ino A, Hasegwa Y, Murabayashi A (1999) Synthetic Studies of Thiazoline- and Thiazolidine-Containing Natural Products. 2. Total Synthesis of Antimycoplasma Antibiotic Micacocidin. Tetrahedron **55**: 10283
162. Inoue H, Takimura O, Kawaguchi K, Nitoda T, Fuse H, Murakami K, Yamaoka Y (2003) Tin-Carbon Cleavage of Organotin Compounds by Pyoverdine from *Pseudomonas chlororaphis*. Appl Environ Microbiol **69**: 878
163. Ishimaru CA, Loper JE (1992) High-Affinity Iron Uptake Systems Present in *Erwinia carotovora* subsp. *carotovora* Include the Hydroxamate Siderophore Aerobactin. J Bacteriol **174**: 2993
164. Ito T, Neilands JB (1958) Products of "Low-iron Fermentation" with *Bacillus subtilis*: Isolation, Characterization and Synthesis of 2,3-Dihydroxybenzoylglycine. J Am Chem Soc **80**: 4645

165. Ito Y, Butler A (2005) Structure of Synechobactins, New Siderophores of the Marine Cyanobacterium *Synechococcus* sp. PCC 7002. Limnol Oceanogr **50**: 1918
166. Ito Y, Ishida, K, Okada S, Murakami M (2004) The Absolute Stereochemistry of Anachelins, Siderophores from the Cyanobacterium *Anabena cylindrica*. Tetrahedron **60**: 9075
166a. Ito Y, Umino K, Sekiguchi T, Miyagishima T, Egawa Y (1971) Antibiotic YC 73 of *Pseudomonas* Origin. III. Synthesis of Thioformin Analogues. J Antibiot **24**: 131
167. Itou Y, Okada S, Murakami M (2001) Two Structural Isomeric Siderophores from the Freshwater Cyanobacterium *Anabena cylindrica* (NIES-19). Tetrahedron **57**: 9093
168. Jacques P, Ongena M, Gwose I, Seinsche D, Schröder H, Delphosse P, Thonart P, Taraz K, Budzikiewicz H (1995). Structure and Characterization of Isopyoverdin from *Pseudomonas putida* BTP1 and its Relation to the Biogenetic Pathway Leading to Pyoverdins. Z Naturforsch **50c**: 622
169. Jalal MAF, Galles JL, van der Helm D (1985) Structure of Des(diserylglycyl)ferrirhodin, DDF, a Novel Siderophore from *Aspergillus ochraceous*. J Org Chem **50**: 5642
170. Jalal MAF, Hossain MB, van der Helm D, Barnes CL (1988) Structure of Ferrichrome-type Siderophores with Dissimilar N^{δ}-acyl Groups: Asperchrome B_1, B_2, B_3, D_1, D_2 and D_3. Biol Metals **1**: 77
171. Jalal MAF, Hossain MB, van der Helm D, Sanders-Loehr J, Actis LA, Crosa JH (1989) Structure of Anguibactin, a Unique Plasmid-related Siderophore from Fish-pathogen *Vibrio anguillarum*. J Am Chem Soc **111**: 292
172. Jalal MAF, Love SK, van der Helm D (1986) Siderophore Mediated Iron(III) Uptake in *Gliocladium virens*. 1. Properties of *cis*-Fusarinine, *trans*-Fusarinine, Dimerum Acid, and their Ferric Complexes. J Inorg Biochem **28**: 417
173. Jalal MAF, Love SK, van der Helm D (1988) N^{α}-Dimethylcoprogens. Three Novel Trihydroxamate Siderophores from Pathogenic Fungi. Biol Metals **1**: 4
174. Jalal MAF, Mocharla R, Barnes CL, Hossain MB, Powell DR, Eng-Wilmot DL, Grayson SL, Benson BA, van der Helm D (1984) Extracellular Siderophores from *Aspergillus ochraceous*. J Bacteriol **158**: 683
175. Jalal MAF, Mocharla R, van der Helm D (1984) Separation of Ferrichromes and Other Hydroxamate Siderophores of Fungal Origin by Reversed-phase Chromatography. J Chromatogr **301**: 247
176. Jalal MAF, van der Helm D (1989) Siderophores of Highly Phytopathogenic *Alternaria longipes*. Structures of Hydroxycoprogens. Biol Metals **2**: 11
177. Jalal MAF, van der Helm D (1991) Isolation and Spectroscopic Identification of Fungal Siderophores. In: Winkelmann G (ed) Handbook of Microbial Iron Chelates. CRC, Boca Raton, FL, p 235
178. Jones AM, Lindow SE, Wildermuth MC (2007) Salicylic Acid, Yersiniabactin, and Pyoverdin Production by the Model Phytopathogen *Pseudomonas syringae* pv. tomato DC3000: Synthesis, Regulation, and Impact on Tomato and *Arabidopsis* Host Plants. J Bacteriol **189**: 6773
179. Jülich M, Taraz K, Budzikiewicz H, Geoffroy V, Meyer JM, Gardan L (2001) The Structure of the Pyoverdin Isolated from *Pseudomonas syringae* Pathovars. Z Naturforsch **56c**: 687
180. Kachadourian R, Dellagi A, Laurent J, Bricard L, Kunesch G, Expert D (1996) Desferrioxamine-dependent Iron Transport in *Erwinia amylovora* CFBP1430: Cloning of the Gene Encoding the Ferrioxamine Receptor FoxR. BioMetals **9**: 143
181. Kameyama T, Takahashi A, Kurasawa S, Ishizuka M, Okami Y, Takeuchi T, Umezawa H (1987) Bisucaberin, a New Siderophore, Sensitizing Tumor Cells to Macrophage-mediated Cytolysis. I. Taxonomy of the Producing Organism, Isolation and Biological Properties. J Antibiotics **40**: 1664
182. Kamnev AA (1998) Reductive Solubilization of Fe(III) by Certain Products of Plant and Microbial Metabolism as a Possible Alternative to Siderophore Secretion. Dokl Biophys **358-360**, 48 (translation from Dokl Akad Nauk **359**: 691).
183. Kanoh K, Kamino K, Leleo G, Adachi K, Shizuri Y (2003) Pseudoalterobactin A and B, New Sidrophores Excreted by Marine Bacterium *Pseudoalteromonas* sp. KP20-4. J Antibiotics **56**: 871

184. Keller-Schierlein W, Deér A (1963) Stoffwechselprodukte von Mikroorganismen. 44. Mitteilung. Zur Konstitution von Ferrichrysin und Ferricrocin. Helv Chim Acta **46**: 1907
184a. Keller-Schierlein W, Diekmann H (1970) Stoffwechselprodukte von Mikroorganismen. 85. Mitteilung. Zur Konstitution des Coprogens. Helv Chim Acta **53**: 2035
185. Keller-Schierlein W, Hagmann L, Zähner H, Huhn W (1988) Stoffwechselprodukte von Mikroorganismen. 250. Mitteilung. Maduraferrin, ein neuartiger Siderophor aus *Actinomadura madurae*. Helv Chim Acta **71**: 1528
185a. Keller-Schierlein W, Mertens P, Prelog V, Walser A (1965) Stoffwechselprodukte von Mikroorganismen. 49. Mitteilung. Die Ferrioxamine A_1, A_2 und D_2. Helv Chim Acta **48**: 710
185b. Keller-Schierlein W, Prelog V (1961) Stoffwechselprodukte von Actinomyceten. 29. Mitteilung. Die Konstitution des Ferrioxamins D_1. Helv Chim Acta **44**: 709
186. Keller-Schierlein W, Prelog V (1961) Stoffwechselprodukte von Actinomyceten. 30. Mitteilung. Über das Ferrioxamin E; ein Beitrag zur Konstitution des Nocardamins. Helv Chim Acta **44**: 1981
186a. Keller-Schierlein W, Prelog V (1961) Stoffwechselprodukte von Actinomyceten. 34. Mitteilung. Ferrioxamin G. Helv Chim Acta **45**: 590
187. Keller-Schierlein W, Prelog V, Zähner H (1964) Siderochrome (Natürliche Eisen(III)-trihydroxamat-Komplexe). Progr Chem Org Nat Prod **22**: 279
187a. Kilz S, Lenz C, Fuchs R, Budzikiewicz H (1999) A Fast Screening Method for the Identification of Siderophores from Fluorescent *Pseudomonas* spp. by Liquid Chromatography/Electrospray Mass Specrtrometry. J Mass Spectrom **34**: 281
187b. Kloepper JW, Leong J, Teintze M, Schroth MN (1980) *Pseudomonas* Siderophores: A Mechanism Explaining Disease-Suppressive Soils. Curr Microbiol **4**: 317
188. Klumpp C, Burger A, Mislin GL, Abdallah MA (2005) From a Total Synthesis of Cepabactin and its 3:1 Ferric Complex to the Isolation of a 1:1:1 Mixed Complex between Iron (III), Cepabactin and Pyochelin. Bioorg Med Chem Lett **15**: 1721
189. Kobayashi S, Hidaka S, Kawamura Y, Ozaki M, Hayase Y (1998) Micacocidin A, B and C, Novel Antimycoplasma Agents from *Pseudomonas* sp. I. Taxonomy, Fermentation, Isolation, Physico-chemical Properties and Biological Activities. J Antibiotics **51**: 323
190. Kobayashi S, Nakai H, Ikenishi Y, Sun WY, Ozaki M, Hayase Y, Takeda R (1998) Micacocidin A, B and C, Novel Antimycoplasma Agents from *Pseudomonas* sp. II. Structure Elucidation. J Antibiotics **51**: 328
191. Kokubo S, Suenaga K, Shinohara C, Tsuji T, Uemura D (2000) Structures of Amamistatins A and B, Novel Growth Inhibitors of Human Tumor Cell Lines from *Nocardia asteroides*. Tetrahedron **56**: 6435
192. Konetschny-Rapp S, Huschka HG, Winkelmann G, Jung G (1988) High-performance Liquid Chromatography of Siderophores from Fungi. Biol Metals **1**: 9
193. Konetschny-Rapp S, Jung G, Meiwes J, Zähner H (1900) Staphyloferrin A: a Structurally New Siderophore from Staphylococci. Eur J Biochem **191**: 65
194. Konetschny-Rapp S, Jung G, Raymond KN, Meiwes J, Zähner H (1992) Solution Thermodynamics of the Ferric Complexes of New Desferrioxamine Siderophores by Directed Fermentation. J Am Chem Soc **114**: 2224
195. Koppisch AT, Browder CC, Moe AL, Shelley JT, Kinkel BA, Hersman LE, Iyer S, Ruggiero CE (2005) Petrobactin is the Primary Siderophore Synthesized by *Bacillus anthracis* str. *Sterne* under Conditions of Iron Starvation. BioMetals **18**: 577
195a. Koppisch AT, Dhungana S, Hill KK, Boukhalfa H, Heine HS, Colip LA, Romero RB, Shou Y, Ticknor LO, Marrone BL, Hersman LE, Iyer S, Riggiero CE (2008) Petrobactin is Produced by Both Pathogenic and Non-pathogenic Isolates of the *Bacillus cereus* Group of Bacteria. Biometals **21**: 581
196. Korth H (1970) Über das Vorkommen von 2,3-Dihydroxybenzoesäure und ihrer Aminosäurederivate in Kulturmedien von *Klebsiella oxytoca*. Arch Microbiol **70**: 297
197. Kunze B, Bedorf N, Kohl W, Höfle G, Reichenbach H (1989) Myxochelin A, a New Iron-Chelating Compound from *Angiococcus disciformis* (Myxobacterales). Production, Isolation, Physicochemical and Biological Properties. J Antibiotics **42**: 14

198. Kunze B, Trowitzsch-Kienast W, Höfle G, Reichenbach H (1992) Nannochelins A, B and C, New Iron Chelating Compounds from *Nannocystis exedens* (Myxobacteria). Production, Isolation, Physico-chemical and Biological Properties. J Antibiotics **45**: 147
199. Lane SJ, Marshall PS, Upton RJ, Ratledge C, Ewing M (1995) Novel Extracellular Mycobactins, the Carboxymycobactins from *Mycobacterium avium*. Tetrahedron Lett **36**: 4129
200. Lankford CE, Walker JR, Reeves JB, Nabbut NH, Byers BR, Jones RJ (1966) Inoculum-Dependent Division Lag of *Bacillus* Cultures and its Relation to an Endogenous Factor(s) ("Schizokinen"). J Bacteriol **91**: 1070
201. Ledyard KM, Butler A (1997) Structure of Putrebactin, a New Dihydroxamate Siderophore Produced by *Shewanella putrefaciens*. J Biol Inorg Chem **2**: 93
202. Lee BH, Miller MJ (1983) Natural Ferric Ionophores: Total Synthesis of Schizokinen, Schizokinen A, and Arthrobactin. J Org Chem **48**: 24
203. Lee CH, Lewis TA, Paszczynski A, Crawford RL (1999) Identification of an Extracellular Catalyst of Carbon Tetrachloride Dehalogenation from *Pseudomonas stutzeri* Strain KC as Pyridine-2,6-bis(thiocarboxylate). Biochem Biophys Res Commun **261**: 562
204. Leong SA, Winkelmann G (1998) Molecular Biology of Iron Transport in Fungi. In: Sigel A, Sigel H (eds) Metal Ions in Biological Systems. Marcel Dekker, New York, 147
205. Lesueur D, Diem HG, Meyer JM (1993) Iron Requirement and Siderophore Production in *Bradyrhizobium* Strains Isolated from *Acacia mangium*. J Appl Bacteriol **74**: 675
205a. Lewis TA, Crawford RL (1995) Transformation of Carbon Tetrachloride via Sulfur and Oxygen Substitution by *Pseudomonas* sp. Strain KC. J Bacteriol **177**: 2204
206. Liles MR, Scheel TA, Cianciotto NP (2000) Discovery of a Nonclassical Siderophore, Legiobactin, Produced by Strains of *Legionella pneumophila*. J Bacteriol **182**: 749
207. Linke WD, Crueger A, Diekmann H (1972) Stoffwechselprodukte von Mitroorganismen. 106. Mitteilung. Zur Konstitution des Terregens-Faktors. Arch Mikrobiol **85**: 44
208. Liu WC, Fisher SM, Wells JS Jr, Ricca CS, Principe PA, Trejo WH, Bonner DP, Gougoutos JZ, Toeplitz BK, Sykes RB (1981) Siderochelin, a New Ferrous-ion Chelating Agent Produced by *Nocardia*. J Antibiot **34**: 791
209. Llinás L, Neilands JB (1976) The Structure of Two Alanine Containing Ferrichromes: Sequence Determination by Proton Magnetic Resonance. Biophys Struct Mechanism **2**: 105
210. Loomis LD, Raymond KN (1991) Solution Equilibria of Enterobactin and Metal-enterobactin Complexes. Inorg Chem **30**: 906
211. Luo M, Fadeev EA, Groves JT (2005) Membrane Dynamics of the Amphiphilic Siderophore, Acinetoferrin. J Am Chem Soc **127**: 1726
212. MacDonald JC, Bishop GG (1984) Spectral Properties of a Mixture of Fluorescent Pigments Produced by *Pseudomonas aeruginosa*. Biochim Biophys Acta **800**: 11
212a. Maksimova NP, Blazhevich OV, Lysak VV, Fomichev YuK (1994) Characteristics of fluorescent pigment pyoverdin P_m produced by *Pseudomonas putida* bacteria. *Microbiology* **63**: 587 (Russian original:Mikrobiologia **63**: 1038)
213. Marshall B, Stintzi A, Gilmour C, Meyer JM, Poole K (2009) Citrate-mediated Iron-uptake in *Pseudomonas aeruginosa*: Involvement of the Citrate-inducible FecA Receptor and the FeoB Ferrous Iron Transporter. Microbiology **155**: 305
214. Martin JD, Ito Y, Homann VV, Haygood MG, Butler A (2006) Structure and Membrane Affinity of New Amphiphilic Siderophores Produced by *Ochrobactrum* sp. SP18. J Biol Inorg Chem **11**: 633
215. Martinez JS, Butler A (2007) Marine Amphiphilic Siderophores: Marinobactin Structure, Uptake, and Microbial Partitioning. J Inorg Biochem **101**: 1692
216. Martinez JS, Carter-Franklin JN, Mann EL, Martin JD, Haygood MG, Butler A (2003) Structure and Membrane Affinity of a Suite of Amphiphilic Siderophores Produced by a Marine Bacterium. Proc Natl Acad Sci USA **100**: 3754
217. Martinez JS, Zhang GP, Holt PD, Jung HT, Carrano CJ, Haygood MG, Butler A (2000) Self-assembling Amphiphilic Siderophores from Marine Bacteria. Science **287**: 1245
218. Matthijs S, Budzikiewicz H, Schäfer M, Wathelet B, Cornelis P (2008) Ornicorrugatin, a New Siderophore from *Pseudomonas fluorescens* AF76. Z Naturforsch **63c**: 8

219. Matthijs S, Laus G, Meyer JM, Abbaspour-Tehrani K, Schäfer M, Budzikiewicz H, Cornelis P (2009) Siderophore-mediated Iron Acquisition in the Entomopathogenic Bacterium *Pseudomonas entomophila* L48 and its Close Relative *Pseudomonas putida* KT2440. Biometals **22**: 951

220. Matthijs S, Tehrani KA, Laus G, Jackson RW, Cooper RM, Cornelis P (2007) Thioquinolobactin, a *Pseudomonas* Siderophore with Antifungal and anti-*Pythium* Activity. Environ Microbiol **9**: 425

221. Maurer B, Müller A, Keller-Schierlein W, Zähner H (1968) Stoffwechselprodukte von Mikroorganismen. 61. Ferribactin, ein Siderochrom aus *Pseudomonas fluorescens* Migula. Arch Microbiol **60**: 326

222. Maurer PJ, Miller MJ (1982) Microbial Iron Chelators: Total Synthesis of Aerobactin and its Constituent Amino Acid, N^6-Acetyl-N^6-hydroxylysine. J Am Chem Soc **104**: 3096

223. May JJ, Wendrich TM, Mahariel MA (2001) The *dhb* Operon of *Bacillus subtilis* Encodes the Biosynthetic Template for the Catecholic Siderophore 2,3-Dihydroxybenzoate-glycine-threonine Trimeric Ester Bacillibactin. J Biol Chem **276**: 7209

224. McCullough WG, Merkal RS (1982) Structure of Mycobactin J. Curr Microbiol **7**: 337

225. McDougall S, Neilands JB (1984) Plasmid- and Chromosome-coded Aerobactin Synthesis in Enteric Bacteria: Insertion Sequences Flank Operon in Plasmid-mediated Systems. J Bacteriol **159**: 300

226. Meiwes J, Fiedler HP, Haag H, Zähner H, Konetschny-Rapp S, Jung G (1990) Isolation and Characterization of Staphyloferrin A, a Compound with Siderophore Activity from *Staphylococcus hyicus* DSM 20459. FEMS Microbiol Lett **67**: 201

227. Meiwes J, Fiedler HP, Zähner H, Konetschny-Rapp S, Jung G (1990) Production of Desferrioxamine E and New Analogues by Directed Fermentation and Feeding Fermentation. Appl Microbiol Biotechnol **32**: 505

228. Mercado-Blanco J, van der Drift KMGM, Olsson PE, Thomas-Oates JE, van Loon LC, Bakker PAHM (2001) Analysis of the *pmsCEAB* Gene Cluster Involved in Biosynthesis of Salicylic Acid and the Siderophore Pseudomonine in the Biocontrol Strain *Pseudomonas fluorescens* WCS374. J Bacteriol **183**: 1909

228a. Messenger AJM, Ratledge C (1982) Iron Transport in *Mycobacterium smegmatis*: Uptake of Iron from Ferric Citrate. J Bacteriol **149**: 131

229. Meyer JM (2000) Pyoverdines: Pigments, Siderophores and Potential Taxonomic Markers of Fluorescent *Pseudomonas* Species. Arch Microbiol **174**: 135

229a. Meyer JM, Abdallah MA (1980) The Siderochromes of Non-fluorescent Pseudomonads: Production of Norcardamine by *Pseudomonas stutzeri*. J Gen Microbiol **118**: 125

230. Meyer JM, Azelvandre P, Georges C (1992). Iron Metabolism in *Pseudomonas*: Salicylic Acid, a Siderophore of *Pseudomonas fluorescens* CHAO. BioFactors **4**: 23

231. Meyer JM, Gruffaz C, Raharinosy V, Bezverbnaya I, Schäfer M, Budzikiewicz, H (2008) Siderotyping of Fluorescent *Pseudomonas*: Molecular Mass Determination by Mass Spectrometry as a Powerful Pyoverdine Siderotyping Method. Biometals **21**: 259

232. Meyer JF, Hohnadel D, Hallé F (1989) Cepabactin from *Pseudomonas cepacia*, a New Type of Siderophore. J Gen Microbiol **135**: 1479

233. Meyer JM, Stintzi A, Coulanges V, Shivaji S, Voss JA, Taraz K, Budzikiewicz H (1998) Siderotyping of Fluorescent Pseudomonads: Characterization of Pyoverdines of *Pseudomonas fluorescens* and *Pseudomonas putida* Strains from Antarctica. Microbiology **144**: 3119

234. Meyer JM, Stintzi A, De Vos D, Cornelis P, Tappe R, Taraz K, Budzikiewicz H (1997) Use of Siderophores to Type Pseudomonads: the Three *Pseudomonas aeruginosa* Pyoverdine Systems. Microbiology **143**: 35

235. Meyer JM, Van VT, Stintzi A, Berge O, Winkelmann G (1995) Ornibactin Production and Transport Properties in Strains of *Burkholderia vietnamensis* and *Burkholderia cepacia* (formerly *Pseudomonas cepacia*). BioMetals **8**: 309

236. Michalke R, Taraz K, and Budzikiewicz H (1996) Azoverdin – an Isopyoverdin. Z Naturforsch **51c**: 772

237. Milewska MJ, Chimiak A, Glowacki Z (1987) Synthesis of Shizokinen, Homoschizokinen, its Imide and the Detection of Imide with ^{13}C-N.M.R.-Spectroscopy. J Prakt Chem **329**: 447
238. Miller MC, Parkin S, Fetherston JD, Perry RD, DeMoll E (2006) Crystal Structure of Ferric-yersiniabactin, a Virulence Factor of *Yersinia pestis*. J Inorg Biochem **100**: 1495
239. Mitscher LA, Högberg T, Drake SD, Burgstahler AW, Jackson M, Lee B, Sheldon RI, Gracey HE, Kohl W, Theriault RJ (1984) Isolation and Structural Determination of Siderochelin C, a Fermentation Product of an Unusual *Actinomycetes* sp. J Antibiotics **37**:1260
239a. Miyanaga S, Obata T, Onaka H, Fujita T, Saito N, Sakurai H, Saiki I, Furumai T, Igarashi Y (2006) Absolute Configuration and Antitumor Activity of Myxochelin A Produced by *Nonomuraea pusilla* TP-A0861. J Antibiotics **59**: 698
240. Modi M, Shah KS, Modi VV (1985) Isolation and Characterization of Catechol-like Siderophore from Cowpea *Rhizobium* RA-1. Arch Microbiol **141**: 156
241. Mohn G, Koehl P, Budzikiewicz H, Lefèvre JF (1994) Solution Structure of Pyoverdin GM-II. Biochemistry **33**: 2843
242. Mohn G, Taraz K, Budzikiewicz H (1990) New Pyoverdin-Type Siderophores from *Pseudomonas fluorescens*. Z Naturforsch **45b**: 1437
242a. Moll H, Glorius M, Bernhard G, Johnsson A, Pedersen K, Schäfer M, Budzikiewicz H (2008) Characterization of Pyoverdins Secreted by a Subsurface Strain of *Pseudomonas fluorescens* and their Interactions with Uranium(VI). Geomicrobiol J **25**: 157
243. Moore RE, Emery T (1976) N^{α}-Acetylfusarinines: Isolation, Characterization, and Properties. Biochemistry **15**: 2719
244. Moore CH, Foster LA, Gerbig DG Jr, Dyer DW, Gibson BW (1995) Identification of Alcaligin as the Siderophore Produced by *Bordetella pertussis* and *B. bronchiseptica*. J Bacteriol **177**: 1116
245. Mossialos D, Meyer JM, Budzikiewicz H, Wolf U, Koedam N, Baysse C, Anjaiah V, Cornelis P (2000) Quinolobactin, a New Siderophore of *Pseudomonas fluorescens* ATCC 17400, the Production of which is Repressed by the Cognate Pyoverdine. Appl Environ Microbiol **66**: 487
245a. Mukai A, Fukai T, Matsumoto Y, Ishikawa J, Hoshino Y, Yazawa K, Harada K, Mikami Y (2006) Transvalencin Z, a New Antimicrobial Compound with Salicylic Acid Residue from *Nocardia transvalensis* IFM 10065. J Antibiotics **59**: 366
246. Mulet M, Gomila M, Gruffaz C, Meyer JM, Palleroni NJ, Lalucat J, García-Valdéz E (2008) Phylogenetic Analysis and Siderotyping as Useful Tools in the Taxonomy of *Pseudomonas stutzeri*: Description of a Novel Genovar. Int J System Evol Microbiol **58**: 2309
246a. Müller A, Zähner H (1968) Stoffwechselprodukte von Mikroorganismen. 65. Mitteilung. Ferrioxamine aus *Eubacteriales*. Arch Microbiol **62**: 257
247. Müller SI, Valdebenito M, Hantke K (2009) Salmochelin, the Long-overlooked Catecholate Siderophore of *Salmonella*. Biometals **22**: 691
248. Mullis KB, Pollack JR, Neilands JB (1971) Structure of Schizokinen, an Iron Transport Compound from *Bacillus megaterium*. Biochemistry **10**: 4894
249. Münzinger M, Budzikiewicz H, Expert D, Enard C, Meyer JM (2000) Achromobactin, a New Citrate Siderophore of *Erwinia chrysanthemi*. Z Naturforsch **55c**: 328
250. Münzinger M, Taraz K, Budzikiewicz H (1999) Staphyloferrin B, a Citrate Siderophore from *Ralstonia eutropha*. Z Naturforsch **54c**: 867
251. Münzinger M, Taraz K, Budzikiewicz H, Drechsel H, Heymann P, Winkelmann G, Meyer JM (1999). S,S-Rhizoferrin (*enantio*-rhizoferrin) a Siderophore of *Ralstonia* (*Pseudomonas*) *pickettii* DSM 6297 – the Optical Antipode of R,R-Rhizoferrin Isolated from Fungi. BioMetals **12**: 189
252. Murakami Y, Kato S, Nakajima M, Matsuoka M, Kawai H, Shin-Ya K, Seto H (1996) Formobactin, a Novel Free Radical Scavenging and Neuron Cell Protecting Substance from *Nocardia* sp. J Antibiotics **49**: 839
253. Naegli HU, Keller-Schierlein W (1978) Stoffwechselprodukte von Mikroorganismen. 174. Mitteilung. Eine neue Synthese des Ferrichroms; *enantio*-Ferrichrom. Helv Chim Acta **61**: 2088

254. Naegeli HU, Zähner H (1980) Stoffwechselprodukte von Mikroorganismen. 193. Mitteilung. Ferrithiocin. Helv Chim Acta **63**: 1400
255. Nagao Y, Miyasaka T, Hagiwara Y, Fujita E 1984 Total Synthesis of Parabactin, a Spermidine Siderophore. J Chem Soc Perkin Trans I 183
255a. Neilands JB (1981) Microbial Iron Compounds. Ann Rev Biochem **50**: 715
256. Neilands JB, Ericson TJ, Rastetter WH (1981) Stereospecifity of the Ferric Enterobactin Receptor of *Escherichia coli* K-12. J Biol Chem **256**: 3831
257. Nemoto A, Hoshino Y, Yazawa K, Ando A, Mikami Y, Komaki H, Tanaka Y, Gräfe U (2002) Asterobactin, a New Siderophore Group Antibiotic from *Nocardia asteroides*. J Antibiotics **55**: 593
258. Neuenhaus W, Budzikiewicz H, Korth H, Pulverer G (1980) 8-Hydroxy-4-methoxymonothiochinaldinsäure – eine weitere Thiosäure aus *Pseudomonas*. Z Naturforsch **35b**: 1569
259. Newkirk JD, Hulcher FH (1969) Isolation and Properties of a Fluorescent Pigment from *Pseudomonas mildenbergii*. Arch Biochem Biophys **134**: 395
260. Nishio T, Tanaka N, Hiratake J, Katsube Y, Ishida Y, Oda J (1988) Isolation and Structure of the Novel Dihydroxamate Siderophore Alcaligin. J Am Chem Soc **110**: 8733
261. O'Brian IG, Gibson F (1970) The Structure of Enterochelin and Related 2,3-Dihydroxy-N-benzoylserine Conjugates from *Escherichia coli*. Biochem Biophys Acta **215**: 393
262. Ockels W, Römer A, Budzikiewicz H, Korth H, Pulverer G (1978) An Fe(II) Complex of Pyridine-2,6-di(monothiocarboxylic acid) – a Novel Bacterial Metabolic Product. Tetrahedron Lett 3341
263. Ohfune Y, Tomita M (1982) Total Synthesis of (−)-Domoic acid. A Revision of the Original Structure. J Am Chem Soc **104**: 3511
264. Okujo N, Saito M, Yamamoto S, Yoshida T, Miyoshi S, Shinoda S (1994) Structure of Vulnibactin, a New Polyamine-containing Siderophore from *Vibrio vulnificus*. BioMetals **7**: 109
265. Okujo N, Sakakibara Y, Yoshida T, Yamamoto S. (1994) Structure of Acinetoferrin, a New Citrate-based Dihydroxamate Siderophore from *Acinetobacter haemolyticus*. BioMetals **7**: 170
266. Okujo N, Yamamoto S (1994) Identification of the Siderophores from *Vibrio hollisae* and *Vibrio mimicus* as Aerobactin. FEMS Microbial Lett **118**: 187
267. Okuyama D, Nakamura H, Naganawa H, Takita T, Umezawa H, Iitaka, Y (1982) Isolation, Racemization and Absolute Configuration of Siderochelin A. J Antibiotics **35**: 1240
268. Ong SA, Peterson T, Neilands JB (1979) Agrobactin, a Siderophore from *Agrobacterium tumefaciens*. J Biol Chem **25**: 1860
269. Ongena M, Jacques P, Delfosse P, Thonart P (2002) Unusual Traits of the Pyoverdin-Mediated Iron Acquisition System in *Pseudomonas putida* Strain BTP1. BioMetals **15**: 1
270. Ongena M, Jacques P, Thonart P, Gwose I, Uría Fernández D, Schäfer M, Budzikiewicz H (2001) The Pyoverdin of *Pseudomonas fluorescens* BTP2, a Novel Structural Type. Tetrahedron Lett **42**: 5849
271. Ongena M, Jacques P, van Vyncht G, Charlier P, de Pauw E, Thonart P, Budzikiewicz H (1998) Structural Analysis of Two Pyoverdins by Electrospray and FAB Mass Spectrometry. J Mass Spectrom Soc Jpn **46**: 53
272. Page WJ, Collinson SK, Demange P, Dell A, Abdallah MA (1991) *Azotobacter vinelandii* Strains of Disparate Origin Produce Azotobactin Siderophores with Identical Structures. Biol Metals **4**: 217
273. Page WJ, von Tigerstrom M (1988) Aminochelin, a Catecholamine Siderophore Produced by *Azotobacter vinelandii*. J Gen Microbiol **134**: 453
274. Pakchung AAH, Soe CZ, Codd R (2008) Studies of Iron-uptake Mechanisms in Two Bacterial Species of the *Shewanella* Genus Adapted to Middle-range (*Shewanella putrefaciens*) or Antarctic (*Shewanella gelidimarina*) Temperatures. Chem Biodivers **5**: 2113
274a. Patel HM, Tao J, Walsh CT (2003) Epimerization of an L-Cysteinyl to a D-Cysteinyl Residue during Thiazoline Ring Formation in Siderophore Chain Elongation by Pyochelin Synthetase from *Pseudomonas aeruginosa*. Biochem **42**: 10514

275. Patel HN, Chakraborty RN, Desai SB (1988) Isolation and Partial Characterization of Phenolate Siderophore from *Rhizobium leguminosarum* IARI 102. FEMS Microbiol Lett **56**: 131.
276. Pattus F, Abdallah MA (2000) Siderophores and Iron-transport in Microorganisms. J Chin Chem Soc **47**: 1
277. Payne SM, Niesel DW, Peixotto SS, Lawlor KM (1983) Expression of Hydroxamate and Phenolate Siderophores by *Shigella flexneri*. J Bacteriol **155**: 949
278. Persmark M, Expert D, Neilands JB (1989) Isolation, Characterization, and Synthesis of Chrysobactin, a Compound with Siderophore Activity from *Erwinia chrysanthemi*. J Biol Chem **264**: 3187
279. Persmark M, Frejd T, Mattiasson B (1990) Purification, Characterization, and Structure of Pseudobactin 589A, a Siderophore from a Plant Growth Promoting *Pseudomonas*. Biochemistry **29**: 7348
280. Persmark M, Neilands JB (1992) Iron(III) Complexes of Chrysobactin, the Siderophore of *Erwinia chrysanthemi*. BioMetals **5**: 29
281. Persmark M, Pittman P, Buyer JS, Schwyn B, Gill PR Jr, Neilands JB (1993) Isolation and Structure of Rhizobactin 1021, a Siderophore from the Alfalfa Symbiont *Rhizobium meliloti* 1021. J Am Chem Soc **115**: 3950
282. Peters WJ, Warren RAJ (1968) Itoic Acid Synthesis in *Bacillus subtilis*. J Bacteriol **95**: 360
283. Peterson T, Falk KE, Leong SA, Klein MP, Neilands JB (1980). Structure and Behavior of Spermidine Siderophores. J Am Chem Soc **102**: 7715
284. Peterson T, Neilands JB (1979) Revised Structure of a Catecholamide Spermidine Siderophore from *Paracoccus denitrificans*. Tetrahedron Lett 4805
285. Plowman JE, Loehr TM, Goldman SJ, Sanders-Loehr J (1984) Structure and Siderophore Activity of Ferric Schizokinen. J Inorg Biochem **20**: 183
286. Pollak JR, Neilands JB (1970) Enterobactin, an Iron Transport Compound from *Salmonella typhimurium*. Biochem Biophys Res Commun **38**: 989
287. Poppe K, Taraz K, Budzikiewicz H (1987) Pyoverdine Type Siderophores from *Pseudomonas fluorescens*. Tetrahedron **43**: 2261
288. Pouteau-Thouvenot M, Gaudemer A, Barbier M (1968). Structure chimique de la proferrorosamine. Bull Soc Chim Biol **50**: 222
289. Quadri LEN, Keating TA, Patel HM, Walsh CT (1999) Assembly of *Pseudomonas aeruginosa* Nonribosomal Peptide Siderophore Pyochelin: in vitro Reconstitution of Aryl-4, 2-bisthiazoline Synthetase Activity from PchD, PchE, and PChF. Biochemistry **38**: 14941
290. Rabsch W, Paul P, Reissbrodt R (1986) DHBA (2,3-Dihydroxybenzoesäure)-Ausscheidung durch einen enterobactinnegativen multiresistenten *Salmonella typhimurium*-Wildstamm. J Basic Microbiol **26**: 113
290a. Rabsch W, Paul P, Reissbrodt R (1987) A New Hydroxamate Siderophore for Iron Supply of *Salmonella*. Acta Microbiol Hungar **34**: 85
291. Ratledge C (1964) Relationship between the Products of Aromatic Biosynthesis in *Mycobacterium smegmatis* and *Aerobacter aerogenes*. Nature **203**: 428
292. Ratledge C, Ewing M (1996) The Occurrence of Carboxymycobactin, the Siderophore of Pathogenic Mycobacteria, as a Second Extracellular Siderophore in *Mycobacterium smegmatis*. Microbiology **142**: 2207
293. Ratledge C, Marshall BJ (1972) Iron Transport in *Mycobacterium smegmatis*: the Role of Mycobactin. Biochim Biophys Acta **279**: 58
294. Ratledge C, Patel PV (1976) The Isolation, Properties and Taxonomic Relevance of Lipid-soluble, Iron-binding Compounds (the Nocobactins) from *Nocardia*. J Gen Microbiology **93**: 141
295. Ratledge C, Snow GA (1974) Isolation and Structure of Nocobactin NA, a Lipid-soluble Iron-binding Compound from *Nocardia asteroides*. Biochem J **139**: 407
296. Raymond KN, Carrano CJ (1979) Coordination Chemistry and Microbial Iron Transport. Acc Chem Res **12**: 183

297. Regenhardt D, Heuer H, Heim S, Fernández DU, Strömpl C, Moore ERB, Timmis KN (2002) Pedigree and Taxonomic Credentials of *Pseudomonas putida* Strain KT2440. Environ Microbiol **4**: 912
298. Reid RT, Live DH, Faulkner DJ, Butler A (1993) A Siderophore from a Marine Bacterium with an Exceptional Ferric Ion Affinity Constant. Nature **366**: 455
299. Reissbrodt R, Ramiandrasoa F, Bricard L, Kunesch G (1997) Siderophore Activity of Chemically Synthesized Dihydroxybenzoyl Derivatives of Spermidines and Cystamide. BioMetals **10**: 95
300. Renshaw JC, Robson GD, Trinci APJ, Wiebe MG, Livens FR, Collison D, Taylor RJ (2002) Fungal Siderophores: Structures, Functions and Application. Mycol Res **106**: 1123
301. Rinehart KL, Staley AL, Wilson SR, Ankenbauer RG, Cox CD (1995) Stereochemical Assignment of the Pyochelins. J Org Chem **60**: 2786
302. Risse D, Beiderbeck H, Taraz K, Budzikiewicz H, Gustin D (1998) Corrugatin, a Lipopeptide Siderophore from *Pseudomonas corrugata*. Z Naturforsch **53c**: 295
303. Robinson JP, Wawrousek EF, McArdle JV, Coyle G, Adler I (1984) X-ray Photoelectron and Electron Spin Resonance Spectra of Iron(III) Parabactin. Inorg Chim Acta **92**: L19
304. Ruangviryachai C, Barelmann I, Fuchs R, Budzikiewicz H (2000) An Exceptionally Large Pyoverdin from a *Pseudomonas* Strain Collected in Thailand. Z Naturforsch **55c**: 323
305. Ruangviriyachai C, Uría Fernández D, Fuchs R, Meyer JM, Budzikiewicz H (2001) A New Pyoverdin from *Pseudomonas aeruginosa* R'. Z Naturforsch **56c**: 933
306. Ruangviriyachai C, Uría Fernández D, Schäfer M, Budzikiewicz H (2004) Structure Proposal for a New Pyoverdin from a Thai *Pseudomonas putida* Strain. Spectroscopy **18**: 453
307. Rue E, Bruland K (2001) Domoic Acid Binds Iron and Copper: a Possible Role for the Toxin Produced by the Marine Diatom *Pseudo-nitzschia*. Mar Chem **76**: 127
308. Sakakura A, Umemura S, Ishihara K (2008) Convergent Total Syntheses of Fluvibactin and Vibriobactin Using Molybdenum(VI) Oxide-catalyzed Dehydrative Cyclization as a Key Step. Chem Commun 3561
309. Salah-el-Din ALM, Kyslík P, Stephan D, Abdallah MA (1997) Bacterial Iron Transport: Structure Elucidation by FAB-MS and by 2D NMR (^{1}H, ^{13}C, ^{15}N) of Pyoverdin G4R, a Peptidic Siderophore Produced by a Nitrogen-Fixing Strain of *Pseudomonas putida*. Tetrahedron **53**: 12539
310. Sansinenea E, Ortiz A (2009) Bacterial Siderophores Containing a Thiazoline Ring. Mini-Rev Org Chem **6**: 120
311. Sattely ES, Walsh CT (2008) A Latent Oxazoline Electrophile for N-O-C Bond Formation in Pseudomonine Biosynthesis. J Am Chem Soc **130**: 12282
312. Saxena B, Modi M, Modi VV (1986) Isolation and Characterization of Siderophores from *Azospirillum lipoferum* D-2. J Gen Microbiol **132**: 2219
313. Sayer JM, Emery TF (1968) Structures of the Naturally Occurring Hydroxamic Acids, Fusarinines A and B. Biochemistry **7**: 184
314. Schaffner EM, Hartmann R, Taraz K, Budzikiewicz H (1996) Structure Elucidation of Azotobactin 87, Isolated from *Azotobacter vinelandii* ATCC 12837. Z Naturforsch **51c**: 139
314a. Schalk IJ, Hennard C, Dugave C, Poole K, Abdallah MA, Pattus F (2001) Iron-free Pyoverdin Binds to its Outer Membrane Receptor FpvA in *Pseudomonas aeruginosa*: a New Mechanism for Membrane Iron Transport. Mol Microbiol **39**: 351
314b. Schalk IJ, Kyslik P, Prome D, van Dorsselaer A, Poole K, Abdallah MA, Pattus F (1999) Copurification of the FpvA Ferric Pyoverdin Receptor of *Pseudomonas aeruginosa* with its Iron-Free Ligand: Implications for Siderophore-Mediated Iron Transport. Biochemistry **38**: 9357
315. Schlegel K, Fuchs R, Schäfer M, Taraz K, Budzikiewicz H, Geoffroy V, Meyer JM (2001) The Pyoverdins of *Pseudomonas* sp. 96-312 and 96-318. Z Naturforsch **56c**: 680
316. Schlegel K, Lex J, Taraz K, Budzikiewicz H (2006) The X-ray Structure of the Pyochelin Fe^{3+} Complex. Z Naturforsch **61c**: 263

317. Schlegel K, Taraz K, Budzikiewicz H (2004) The Stereoisomers of Pyochelin, a Siderophore of *Pseudomonas aeruginosa*. BioMetals **17**: 409
318. Schröder H, Adam J, Taraz K, Budzikiewicz H (1995) Dihydropyoverdinsulfonsäuren – Zwischenstufen bei der Biogenese? Z Naturforsch **50c**: 616
319. Seinsche D, Taraz K, Budzikiewicz H, Gondol D (1993) Neue Pyoverdin-Siderophore aus *Pseudomonas putida* C. J Prakt Chem **335**: 157
320. Shah S, Rao KK, Desai A (1993) Production of Catecholate Type of Siderophores by *Azospirillum lipoferum* M. Indian J Exp Biol **31**: 41
321. Shanzer A, Libman J (1983) Total Synthesis of Enterobactin *via* an Organotin Template. J Chem Soc Chem Commun 846
322. Sharman GJ, Williams DH, Ewing DF, Ratledge C (1995) Isolation, Purification and Structures of Exochelin MS, the Extracellular Siderophore from *Mycobacterium smegmatis*. Biochem J **305**: 187
323. Sharman GJ, Williams DH, Ewing DF, Ratledge C (1995) Determination of the Structure of Exochelin MN, the Extracellular Siderophore from *Mycobacterium neoaurum*. Chem Biol **2**: 553
324. Shiman R, Neilands JB (1965) Isolation, Characterization and Synthesis of Pyrimine, an Iron(II) Binding Agent from *Pseudomonas* GH. Biochemistry **4**: 2233
325. Shirahata K, Deguchi T, Hayashi T, Matsubara I, Suzuki T (1970). The Structures of Fluopsins C and F. J Antibiotics **23**: 546
326. Simpson FB, Neilands JB (1976) Siderochromes in Cyanophyceae: Isolation and Characterization of Schizokinen from *Anabena* sp. J Phycol **12**: 44
327. Skorupska A, Choma A, Derylo M, Lorkiewicz Z (1988) Siderophore Containing 2,3-Dihydroxybenzoic Acid and Threonine Formed by *Rhizobium trifolli* (*sic*!). *Acta Biochim Polon* **35**: 119
328. Smith MJ, Shoolery JN, Schwyn B, Holden I, Neilands JB (1985) Rhizobactin, a Structurally Novel Siderophore from *Rhizobium meliloti*. J Am Chem Soc **107**: 1739
329. Snow GA (1965) The Structure of Mycobactin P, a Growth Factor for *Mycobacterium johnei*, and the Significance of its Iron Complex. Biochem J **94**: 160
330. Snow GA (1965) Isolation and Structure of Mycobactin T, a Growth Factor from *Mycobacterium tuberculosis*. Biochem J **97**: 166
331. Snow GA (1970) Mycobactins: Iron-chelating Growth Factors from Mycobacteria. Bacteriol Rev **34**: 99
332. Snow GA, White AJ (1969) Chemical and Biological Properties of Mycobactins Isolated from Various Mycobacteria. Biochem J **115**: 1031
333. Sokol PA, Lewis CJ, Dennis JJ (1992) Isolation of a Novel Siderophore from *Pseudomonas cepacia*. J Med Microbiol **36**: 184
333a. Spiro TG, Bates G, Saltman P (1989) The Hydrolytic Polymerization of Ferric Citrate. II. The Influence of Excess Citrate. J Am Chem Soc **89**: 5559
333b. Spiro TG, Pape L, Saltman P (1989) The Hydrolytic Polymerization of Ferric Citrate. I. The Chemistry of the Polymer. J Am Chem Soc **89**: 5555
334. Steglich W, Steffan B, Stroech K, Wolf M (1984) Pistillarin, ein charakteristischer Inhaltsstoff der Herkuleskeule (*Clavariadelphus pistillaris*) und einiger *Ramaria*-Arten (Basidiomycetes). Z Naturforsch. **39c**: 10
335. Stephan H, Freund S, Beck W, Jung G, Meyer JM, Winkelmann G (1993) Ornibactins – a New Family of Siderophores from *Pseudomonas*. BioMetals **6**: 93
336. Stephan H, Freund S, Meyer JM, Winkelmann G, Jung G (1993) Structure Elucidation of the Gallium-Ornibactin Complex by 2D-NMR Spectroscopy. Liebigs Ann Chem 43
337. Stintzi A, Barnes C, Xu J, Raymond KN (2000) Microbial Iron Transport via a Siderophore Shuttle: a Membrane Ion Transport Paradigm. Proc Natl Acad Sci USA **97**: 10691
338. Stoll A, Renz J, Brack A (1951) Beiträge zur Konstitutionsaufklärung des Nocardamins. 10. Mitteilung über antibakterielle Stoffe. Helv Chim Acta **34**: 862
339. Storey EP, Boghozian R, Little JL, Lowman DW, Charkraborty R (2006) Characterization of 'Schizokinen'; a Dihydroxamate-type Siderophore Produced by *Rhizobium leguminosarum* IARI 917. BioMetals **19**: 637

340. Stuart SJ, Prpic JK, Robins-Browne RM (1986) Production of Aerobactin by some Species of the Genus *Yersinia*. J Bacteriol **166**: 1131
341. Suenaga K, Kokubo S, Shinohara C, Tsuji T, Uemura D (1999) Structures of Amamistatins A and B, Novel Growth Inhibitors of Human Tumor Cell Lines from an Actinomycete. Tetrahedron Lett **40**: 1945
342. Sultana R, Fuchs R, Schmickler H, Schlegel K, Budzikiewicz H, Siddiqui BS, Geoffroy V, Meyer JM (2000) A Pyoverdin from *Pseudomonas* sp. CFML 95-275. Z Naturforsch **55c**: 857
343. Sultana R, Siddiqui BS, Taraz K, Budzikiewicz H, Meyer JM (2000) A Pyoverdine from *Pseudomonas putida* CFML 90-51 with a Lys ε-Amino Link in the Peptide Chain. BioMetals **13**: 147
344. Sultana R, Siddiqui BS, Taraz K, Budzikiewicz H, Meyer JM (2001) An Isopyoverdin from *Pseudomonas putida* CFML 90-44. Z Naturforsch **56c**: 303
345. Sultana R, Siddiqui BS, Taraz K, Budzikiewicz H, Meyer JM (2001) An Isopyoverdin from *Pseudomonas putida* CFML 90-33. Tetrahedron **57**: 1019
346. Tabata N, Tomoda H, Ōmura S (1999) Ferroverdins, Inhibitors of Cholesteryl Ester Transfer Protein Produced by *Streptomyces* sp. WK-5344. II. Structure Elucidation. J Antibiotics **52**: 1108
347. Tait GH (1975) The Identification and Biosynthesis of Siderochromes Formed by *Micrococcus denitrificans*. Biochem J **146**: 191
348. Takahashi A, Nakamura H, Kameyama T, Kurasawa S, Naganawa H, Okami Y, Takeuchi T, Umezawa H, Iitaka Y (1987) Bisucaberin, a New Siderophore, Sensitizing Tumor Cells to Macrophage-mediated Cytolysis. II. Physico-chemical Properties and Structure Determination. J Antibiotics **40**: 1671
349. Tappe R (1991) Ferribactin 3b, ein Siderophor von *Pseudomonas aptata* 3b. Diplomarbeit, Universität zu Köln
350. Tappe R, Taraz K, Budzikiewicz H, Meyer JM, Lefèvre JF (1993) Structure Elucidation of a Pyoverdin Produced by *Pseudomonas aeruginosa* ATCC 27853. J Prakt Chem **335**: 83
351. Taraz K, Ehlert G, Geisen K, Budzikiewicz H, Korth H, Pulverer G (1990) Protochelin, ein Catecholat-Siderophor aus einem Bakterium (DMS Nr. 5746). Z Naturforsch **45b**: 1327
352. Taraz K, Seinsche D, Budzikiewicz H (1991) Pseudobactin- und Pseudobactin A-Varianten: Neue Peptidsiderophore vom Pyoverdin-Typ aus *Pseudomonas fluorescens* "E2". Z Naturforsch **46c**: 522
353. Teintze M, Hossain MB, Barnes CL, Leong J, van der Helm D (1981) Structure of Ferric Pseudobactin, a Siderophore from a Plant Growth Promoting *Pseudomonas*. Biochemistry **20**: 6446
354. Teintze M, Leong J (1981) Structure of Pseudobactin A, a Second Siderophore from Plant Growth Promoting *Pseudomonas* B10. Biochemistry **20**: 6457
355. Telford JR, Leary JA, Tunstad LMG, Byers BR, Raymond KN (1994) Amonabactin: Characterization of a Series of Siderophores from *Aeromonas hydrophila*. J Am Chem Soc **116**: 4499
356. Telford JR, Raymond KN (1997) Amonabactin: a Family of Novel Siderophores from a Pathogenic Bacterium. J Biol Inorg Chem **2**: 750
357. Telford JR, Raymond KN (1998) Coordination Chemistry of the Amonabactins, Bis(catecholate) Siderophores from *Aeromonas hydrophila*. Inorg Chem **37**: 4578
357a. Temirov YuV, Esikova TZ, Kashporov IA, Balashova TA, Vinokurov LM, Alakhov YuB (2003) A Catecholic Siderophore Produced by the Thermoresistant *Bacillus licheniformis* VK21 Strain. Russian J Bioorg Chem **29**: 542 (translated from Bioorg Khim **29**: 597)
358. Thieken A, Winkelmann G (1992) Rhizoferrin: a Complexon Type Siderophore of the Mucorales and Entomophthorales (Zygomycetes). FEMS Microbiol Lett **94**: 37
359. Thomas MS (2007) Iron Acquisition Mechanisms of the *Burkholderia cepacia* Complex. Biometals **20**: 431

360. Tindale AE, Mehrotra M, Ottem D, Page WJ (2000) Dual Regulation of Catecholate Siderophore Biosynthesis in *Azotobacter vinelandii* by Iron and Oxidative Stress. Microbiology **146**: 1617

361. Tomada H, Tabata N, Shinose M, Takahashi Y, Woodruff HB, Ōmura S (1999) Ferroverdins, Inhibitors of Cholesteryl Ester Transfer Protein Produced by *Streptomyces* sp. WK-5344. I. Production, Isolation and Biological Properties. J Antibiotics **52**: 1101

362. Torres L, Pérez-Ortín JE, Tordera V, Beltrán JP (1986) Isolation and Characterization of an Fe(III)-Chelating Compound Produced by *Pseudomonas syringae*. Appl Environ Microbiol **2**: 157

363. Uría Fernández D**,** Fuchs R**,** Schäfer M, Budzikiewicz H**,** Meyer JM (2003) The Pyoverdin of *Pseudomonas fluorescens* G173, a Novel Structural Type Accompanied by Unexpected Natural Derivatives of the Corresponding Ferribactin. Z Naturforsch **58c**: 1

364. Uría Fernández D, Fuchs R, Taraz K, Budzikiewicz H, Munsch P, Meyer JM (2001) The Structure of a Pyoverdine Produced by a *Pseudomonas tolaasii*-like Isolate. BioMetals **14**: 81

365. Uría Fernández D, Geoffroy V; Schäfer M, Meyer JM, Budzikiewicz H (2003) Structure Revision of Several Pyoverdines Produced by Plant-Growth Promoting and Plant-Deleterious *Pseudomonas* Species. Monatsh Chem **134**: 1421

366. van der Helm D, Jalal MAF, Hossain MB (1987) The Crystal Structures, Conformations, and Configurations of Siderophores. In: Winkelmann G, van der Helm D, Neilands JB (eds) Iron Transport in Microbes, Plants and Animals. VCH, Weinheim, p 135

366a. van der Helm D, Poling M (1976) The Crystal Structure of Ferrioxamine E. J Am Chem Soc **98**: 82

367. van de Woestyne M, Bruyneel B, Mergeay M, Verstraete W (1991) The Fe^{2+} Chelator Proferrorosamine A is Essential for the Siderophore-mediated Uptake of Iron by *Pseudomonas roseus fluorescens*. Appl Environ Microbiol **57**: 949

368. Van Tiel-Menkveld GJ, Mentjox-Vervuurt JM, Oudega B, de Graaf FK (1982) Siderophore Production by *Enterobacter cloacae* and a Common Receptor Protein for the Uptake of Aerobactin and Cloacin DF13. J Bacteriol **150**: 490

369. Vergne AF, Walz AJ, Miller MJ (2000) Iron Chelators from Mycobacteria (1954-1999) and Potential Therapeutic Applications. Nat Prod Rep **17**: 99

370. Visca P, Colotti G, Serino L, Verzili D, Orsi N, Chiancone E (1992) Metal Regulation of Siderophore Synthesis in *Pseudomonas aeruginosa* and Functional Effects of Siderophore-Metal Complexes. Appl Environ Microbiol **58**: 2886

371. Voss J, Taraz K, Budzikiewicz H (1999) A Pyoverdin from the Antarctica Strain 51W of *Pseudomonas fluorescens*. Z Naturforsch **54c**: 156

372. Voßen W, Fuchs R, Taraz K, Budzikiewicz H (2000) Can the Peptide Chain of a Pyoverdin be Bound by an Ester Bond to the Chromophore? – The Old Problem of Pseudobactin 7SR1. Z Naturforsch **55c**: 153

373. Voßen W, Taraz K (1999) Structure of the Pyoverdin PVD 2908 – a New Pyoverdin from *Pseudomonas* sp. 2908. BioMetals **12**: 323

374. Wallner A, Blatzer M, Schrettl M, Sarg B, Lindner H, Haas H (2009) Ferricrocin – a Siderophore Involved in Intra- and Transcellular Iron Distribution in *Aspergillus fumigatus*. Appl Envir Microbiol **75**: 4194

374a. Wang W, Chi Z, Liu G., Buzdar MA, Chi Z, Gu Q (2009) Chemical and Biological Characterization of Siderophores Produced by the Marine-derived *Aureobasidium pullulans* HN6.2 and its Antibacterial Activity. Biometals **22**: 965

375. Wang QX, Phanstiel O IV (1998) Total Synthesis of Acinetoferrin. J Org Chem **63**: 1491

376. Warner PJ, Williams PH, Bindereif A, Neilands JB (1981) CoIV Plasmid-Specific Aerobactin Synthesis by Invasive Strains of *Escherichia coli*. Infect Immunol **33**: 540

377. Wasielewski E, Adkinson RA, Abdallah MA, Kieffer B (2002). The Three-Dimensional Structure of the Gallium Complex of Azoverdin, a Siderophore of *Azomonas macrozytogenes* ATCC 12334, Determined by NMR Using Residual Dipolar Coupling Constants. Biochemistry **41**: 12488

378. Wawszkiewicz EJ, Schneider HA (1975) Control of Salmonellosis Pacifarin Biosynthesis by Iron. Infect Immunol **11**: 69
379. Weber M, Taraz K, Budzikiewicz H, Geoffroy V, Meyer JM (2000) The Structure of a Pyoverdine from *Pseudomonas* sp. CFML 96.188 and its Relation to other Pyoverdines with a Cyclic C-terminus. *BioMetals* **13**: 301
380. Westervelt P, Bloom ML, Mabbott GA, Fekete FA (1985) The Isolation and Identification of 3,4-Dihydroxybenzoic Acid Formed by Nitrogen-fixing *Azomonas macrocytogenes*. FEMS Microbiol Lett **30**: 331
381. White AJ, Snow GA (1969) Isolation of Mycobactins from Various Mycobacteria. The Properties of Mycobactins S and H. Biochem J **111**: 785
382. Wilson MK, Abergel RJ, Raymon J, Arceneaux JE, Byers BR (2006) Siderophores from *Bacillus anthracis*, *Bacillus cereus*, and *Bacillus thuringiensis*. Biochem Biophys Res Commun **348**: 320
383. Winkelmann G (1990) Structural and Stereochemical Aspects of Iron Transport in Fungi. Biotech Adv **8**: 207
384. Winkelmann G (1991) Specificity of Iron Transport in Bacteria and Fungi. In: Winkelmann G (ed) CRC Handbook of Microbial Iron Chelates. CRC, Boca Raton, FL, p 65
385. Winkelmann G, Huschka HG (1989) Molecular Recognition and Transport of Siderophores in Fungi. In: Winkelmann G, van der Helm D, Neilands JB (eds) Iron Transport in Microbes, Plants and Animals. VCH, Weinheim, p 317
386. Winkler S, Ockels W, Budzikiewicz H, Korth H, Pulverer G (1986) 2-Hydroxy-4-methoxy-5-methylpyridin-N-oxid, ein Al^{3+}-bindender Metabolit von *Pseudomonas cepacia*. Z Naturforsch **41c**: 807
387. Wong-Lun-Sang S, Bernardini JJ, Hennard C, Kyslík P, Dell A, Abdallah MA (1996) Bacterial Siderophores: Structure Elucidation, 2D ^{1}H and ^{13}C NMR Assignments of Pyoverdins Produced by *Pseudomonas fluorescens* CHA0. Tetrahedron Lett **37**: 3329
388. Wuest WM, Sattely ES, Walsh CT (2009) Three Siderophores from one Bacterial Enzymatic Assembly Line. J Am Chem Soc **131**: 5056
389. Xu G, Martinez JS, Groves JT, Butler A (2002) Membrane Affinity of the Amphiphilic Marinobactin Siderophores. J Am Chem Soc **124**:13408
390. Yamada Y, Seki N, Kitahara T, Takahashi M, Matsui M (1970) Structure and Synthesis of Aeruginoic Acid (2-*o*-hydroxyphenylthiazole-4-carboxylic acid). Agric Biol Chem **34**: 780
391. Yamamoto S, Okujo N, Fujita Y, Saito M, Yoshida T, Shinoda S (1993) Structures of Two Polyamine-containing Catecholate Siderophores from *Vibrio fluvialis*. J Biochem **113**: 538
392. Yamamoto S, Okujo N, Sakakibara Y (1994) Isolation and Structure Elucidation of Acinetobactin, a Novel Siderophore from *Acinetobacter baumannii*. Arch Mikrobiol **162**: 249
393. Yamamoto S, Okujo N, Yoshida T, Matsuura S, Shinoda S (1994) Structure and Iron Transport Activity of Vibrioferrin, a New Siderophore of *Vibrio parahaemolyticus*. J Biochem **115**: 868
394. Youard ZA, Mislin GLA, Majcherczyk PA, Schalk IJ, Reimmann C (2007) *Pseudomonas fluorescens* CHA0 Produces enantio-Pyochelin, the Optical Antipode of the *Pseudomonas aeruginosa* Siderophore Pyochelin. J Biol Chem **282**: 35546
395. Zähner H, Keller-Schierlein W, Hütter R, Hess-Leisinger K, Deér A (1963) Stoffwechselprodukte von Mikroorganismen. 40. Mitteilung. Sideramine aus Aspergillaceen. Arch Mikrobiol **45**: 119
396. Zalkin A, Forrester JD, Templeton DH (1966) Ferrichrome A Tetrahydrate. Determination of Crystal and Molecular Structure. J Am Chem Soc **88**: 1810
397. Zamri A, Abdallah MA (2000) An Improved Stereocontrolled Synthesis of Pyochelin, Siderophore of *Pseudomonas aeruginosa* and *Burkholderia cepacia*. Tetrahedron **56**: 249
398. Zawadzka AM, Vandecasteele FPJ, Crawford RL, Paszczynski AJ (2006) Identification of Siderophores from *Pseudomonas stutzeri*. Can J Microbiol **52**: 1164

399. Abergel RJ, Zawadzka AM, Hoette TM, Raymond KM (2009) Enzymatic Hydrolysis of Trilactone Siderophores: Where Chiral Recognition Occurs in Enterobactin and Bacillibactin Iron Transport. J Am Chem Soc **131**: 12682
400. Amin SA, Green DH, Küpper FC, Carrano CJ (2009) Vibrioferrin, an Unusual Marine Siderophore: Iron Binding, Photochemistry and Biological Implications. Inorg Chem **48**: 11451
401. Barbeau K (2006) Photochemistry of Organic Iron (III) Complexing Ligands in Oceanic Systems. Photochem Photobiol **82**: 1505
402. Bergeron RJ, McManis JS, Perumal PT, Algee SE (1991) The Total Synthesis of Alcaligin. J Org Chem **56**: 5560
403. Crosa JH, Walsh CT (2002) Genetics and Assembly Line Enzymology of Siderophore Biosynthesis in Bacteria. Microbiol Mol Biol Rev **66**: 223
404. Fadeev E, Luo M, Groves JT (2005) Synthesis and Structural Modeling of the Amphiphilic Siderophore Rhizobactin-1021 and its Analogs. Bioorg Med Chem Lett **15**: 3771
405. Ghosh A, Miller MJ (1993) Synthesis of Novel Citrate-Based Siderophores and Siderophore-β-lactam Conjugates. Iron Transport-mediated Drug Delivery Systems. J Org Chem **58**: 7652
406. Lemenceau P, Expert D, Gaymard F, Bakker PAHM, Briat JF (2009) Role of Iron in Plant-Microbe Interaction. Adv Bot Res **51**: 491
407. Mukai A, Komaki H, Takagi M, Shin-ya K (2009) Novel Siderophore, JBIR-16, Isolated from *Nocardia tenerifensis* 101015. J Antibiot **62**: 601
408. Peuckert F, Miethke M, Albrecht AG, Essen LO, Marahiel MA (2009) Structural Basis and Stereochemistry of Tricatecholate Siderophore Binding by FeuA. Angew Chemie Int Ed **48**: 7924
409. Ravel J, Cornelis P (2003) Genomics of Pyoverdin-mediated Iron Uptake in Pseudomonads. Trends Microbiol **11**: 195
410. Sandy M, Butler A (2009) Microbial Iron Acquisition: Marine and Terrestrial Siderophores. Chem Rev **109**: 4580
411. Takeuchi Y, Nagao Y, Toma K, Yoshikawa Y, Akiyama T, Nishioka H, Abe H, Harayama T, Yamamoto S (1999) Synthesis and Siderophore Activity of Vibrioferrin and One of its Diastereomeric Isomers. Chem Pharm Bull **47**: 1284
412. Lautru S, Deeth RJ, Bailey LM, Challis GL (2005) Discovery of a New Peptide Natural Product by *Streptomyces coelicolor* Genome Mining. Nature Chem Biol **1**: 65
413. Robbel L, Knappe TA, Linne U, Xie X, Marahiel MA (2009) Erythrochelin - a Hydroxamate-type Siderophore Predicted from the Genome of *Saccharopolyspora erythraea*. FEBS J published online DOI 10.1111/j.1742-4658.2009.07512.x

Resin Glycosides from the Morning Glory Family

Rogelio Pereda-Miranda, Daniel Rosas-Ramírez, and *Jhon Castañeda-Gómez*

Contents

R. Pereda-Miranda
Departamento de Farmacia, Facultad de Química, Universidad Nacional Autónoma de México, Ciudad Universitaria, 04510 DF, México
e-mail: pereda@servidor.unam.mx

D. Rosas-Ramírez
Departamento de Farmacia, Facultad de Química, Universidad Nacional Autónoma de México, Ciudad Universitaria, 04510 DF, México
e-mail: veca@hotmail.com

J. Castañeda-Gómez
Departamento de Farmacia, Facultad de Química, Universidad Nacional Autónoma de México, Ciudad Universitaria, 04510 DF, México
e-mail: jhoncast15@yahoo.com

A.D. Kinghorn et al. (eds.), *Fortschritte der Chemie organischer Naturstoffe / Progress in the Chemistry of Organic Natural Products, Vol. 92*,
DOI 10.1007/978-3-211-99661-4_2,

Plate 1. Ethnobotany and Background. Convolvulaceae, the botanical name for the morning glory family, derives from the Latin *convolvo*, referring to its growth of intertwining vines (A: Heavenly blue, *Ipomoea tricolor*). The purgative properties of the Mexican roots were readily accepted in Europe when introduced in the sixteenth century, since pre-Christian folk tradition had already proclaimed the virtues of *skammonia* as found in *Dioscorides*' work *De Materia Medica*, *ca.* 50–68 A.D.

1. Introduction

Resin glycosides are part of a very extensive family of secondary metabolites known as glycolipids or lipo-oligosaccharides and are constituents of complex resins (glycoresins) (*1*) unique to the morning glory family, Convolvulaceae (*2*). These active principles are responsible for the drastic purgative action of all the important Convolvulaceous species used in traditional medicine throughout the world since ancient times. Several commercial purgative crude drugs can be prepared from the roots of different species of Mexican morning glories. Their incorporation as therapeutic agents in Europe is an outstanding example of the assimilation of botanical drugs from the Americas as substitutes for traditional Old World remedies (*3*). Even though phytochemical investigations on the constituents of these drugs were initiated during the second half of the nineteenth century, the structure of their active ingredients still remains poorly known for some examples of these purgative roots. During the last two decades, the higher resolution capabilities of modern analytical isolation techniques used in conjunction with powerful spectroscopic methods have facilitated the elucidation of the active principles of these relevant herbal products.

This chapter describes the ethnobotanical information associated with the purgative morning glory species and how traditional usages were instrumental in plant selection for chemical studies. The advantages and limitations of available analytical techniques for the isolation, purification, and structure characterization of the individual constituents of these complex glycoconjugates are also discussed. Structure elucidation has been conducted on resin glycoside mixtures of 34 convolvulaceus species pertaining to the subfamily Convolvuloideae, with the exception of *Cuscuta* (two species), and include five genera: *Ipomoea* (23 spp.), *Merremia* (three spp.), *Convolvulus* (three spp.), *Operculina* (two spp.), and *Calystegia* (one sp.). A reliable compilation of the structures of the individual resin glycosides and their glycosidic acid derivatives known to date is provided.

2. Ethnobotanical Background and Discovery

The botanical name Convolvulaceae for the morning glory family derives from the Latin *convolvo*, meaning interlaced, and describes a growth pattern of intertwining vines wrapping around a support, and is characteristic of the majority of the species

Plate 1. (*continued*) (B: Skammonia, *Convolvulus scammonia*; Juliana Anicia Codex, Vienna, Österreichische Nationalbibliothek, Cod. med. gr. I, fol. 331v). The jalap root was the main purgative ingredient in pre-Hispanic herbal medicine (C: *Ipomoea purga*, the Latin description of this illustration in the *Badianus* Manuscript reads *Purgatio ventris*, "to purge the stomach"; *Libellus de Medicinalibus Indorum Herbis*, 1552. Fol. 32r. CONACULTA-INAH-MEX, with permission of the "Instituto Nacional de Antropología e Historia", Mexico) and launched the continuing major commercial enterprises between the Americas and Europe. The Indian Rhubarb in herbals also known as "root of Michoacan" (*Ipomoea jalapa*) became a New World substitute for the drastic purgative scammony because of its milder effects (D: *I. jalapa*. *Gerald*'s *Herbal*. London. J. Norton, 1597. Dover. Reproduced from reference (*7*) with permission of Dover Publications, Inc.)

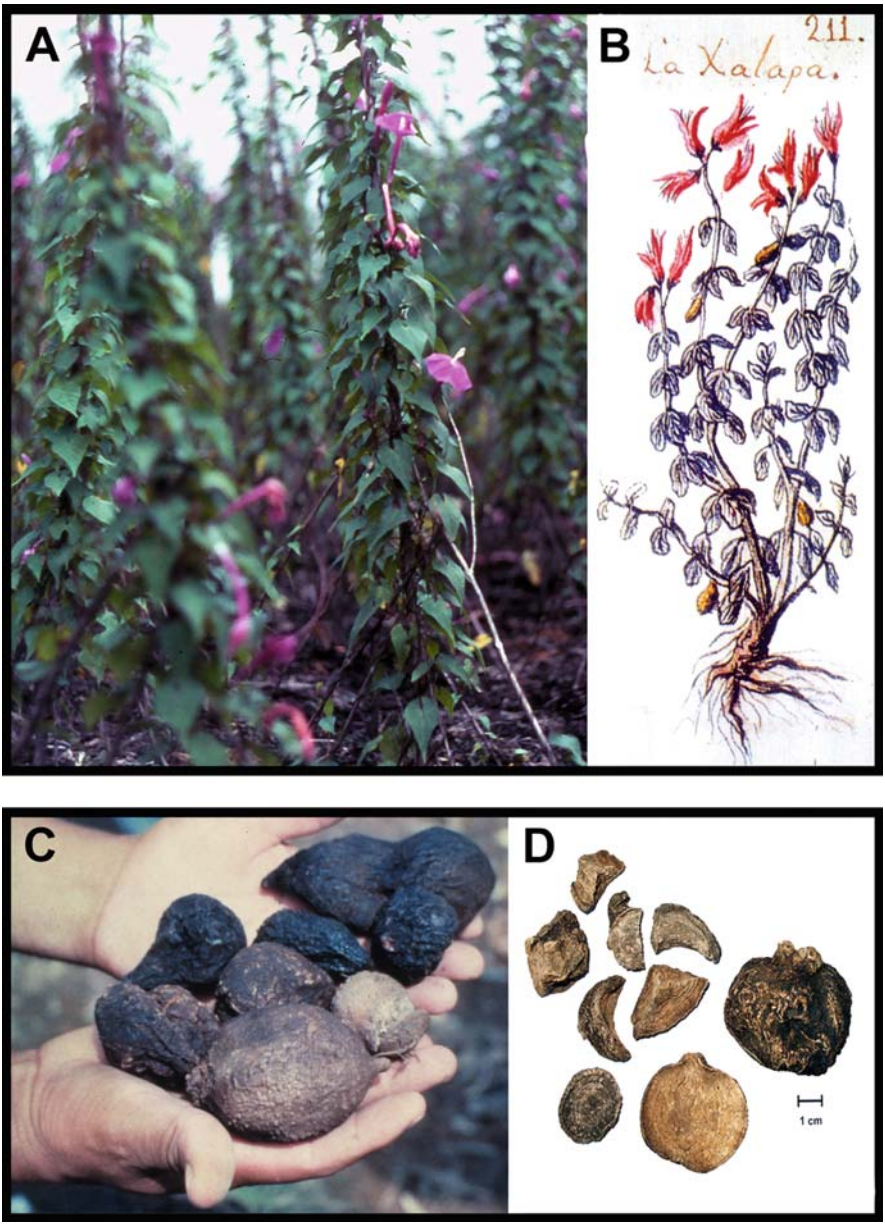

Plate 2. Jalap ("*Rhizoma Jalapae*"), the root of *Ipomoea purga*. The root of this evergreen vine (A: Traditional production system in Central Veracruz, Mexico) is one of several distantly related tuberous New World *Ipomoea* species, including *I. orizabensis*, *I. stans*, *I. jalapa*, and *I. simulans,* which are the source of a group of valued purgative remedies known as "jalaps". The therapeutic benefits were recognized early as illustrated by this eighteenth century illustration (B: *Juan Navarro*'s Natural History. Historia Natural o Jardín Americano, a manuscript of 1801 fol. 211, with permission of UNAM). Fresh and darker smoke-dried roots of "*Rhizoma Jalapae*" (C) of which the drug consists. Examples of the fragmented roots into which they are offered commercially (D)

(Plate 1). The most noticeable anatomical characteristics of this family are the presence of cells in foliar and floral tissues, seeds, and the periderm of tuberous roots, which secrete glycoresins. The ethnopharmacological knowledge of plant containing-resin glycosides strongly influenced early phytochemical investigation and the discovery of these bioactive principles. In Mesoamerica, purgative remedies, known to the pre-Hispanic Aztecs as "*cacamotli tlanoquiloni"*, consisted of diverse kinds of tuber-shaped roots, which varied in morphological characteristics, habitat, and potency of effects. Contemporary investigations have identified these roots as belonging to the genus *Ipomoea,* currently recognized as *I. purga*, *I. orizabensis*, *I. stans*, and *I. jalapa*, together with a few others less often used. The Spanish colonists took notice of these perennial, herbaceous bindweeds with cathartic, acrid-tasting, and resin-producing roots because their purgative properties were important to sixteenth century European galenic medicine (*4*, *5*). These Mexican purgative roots were readily accepted as a New World succedaneum of scammony (*Convolvulus scammonia*), an Eastern Mediterranean herb, known in English as Syrian or purging bindweed, which had been used since pre-Christian times (*6*). In addition, several field (*Convolvulus arvensis*), hedge (*C. sepium*), and sea (*Calystegia soldanella*) bindweed types were likewise extensively documented in European herbals for their purgative properties.

In fact, a major commercial enterprise was launched between the Americas and Europe that continues to this day from the introduction to the Old World of the so-called "root of Michoacan", named after the Western province of New Spain where it was thought to have been originally found and known in English herbals as "rhubarb of the Indies" (*7*). The mild effects of this new drug gained a rapid and widespread acceptance in Europe, as well as being subsequently viewed and known as a panacea (*8*). The precise identification of this root is still much disputed, although it is now generally agreed that it is *I. purga* (Plate 2). In recognition of its important benefits, the colonists bestowed the vernacular name "Jalapa" on this signature species ("officinal jalap" or "*Rhizoma Jalapa*"), for they found it in abundance in the tropical region of Xalapa, in the state of Veracruz. A second purgative root likewise restricted to the tropical areas in the Gulf of Mexico, "Orizaba jalap", identified as *I. orizabensis*, often has been used as a substitute or adulterant for the true jalap, producing a moderately strong cathartic. Even today, this root is referred to as false jalap or Mexican scammony. The jalap medicinal plant complex included "jalapa hembra" or "oficinal" (*I. purga*), "jalapa macho" (*I. orizabensis*) and "jalapa de Tampico" (*I. simulans*) (*9*), although in the ethnobotany of the neotropical and Indomalayan ecozones, several morning glories belonging to the genera *Ipomoea*, *Merremia,* and *Operculina* are also employed.

The cathartic crude drugs are derived from the roots, which are rich in glycoresins (10–18% dry weight), and provoke peristaltic movements in the small intestine. Pharmaceutical products come in the form of liquid alcoholic extracts, root or resins powders that are consumed singly or in combination with other ingredients to modify the therapeutic effect (*10*). Once the demand for these roots declined due to various reasons, German and Italian herbalists introduced to the world market other plants such as Brazilian-grown jalap, *I. operculata* (syn. *Operculina macrocarpa*),

and "Indian jalap", the roots of *Ipomoea turpethum* (syn. *O. turpethum*), which are available as milder but still very effective laxatives.

Phytochemical reports for jalap root were published as early as the second half of the nineteenth century (*2*), although most of the botanical and chemical descriptions found in the literature up to even recently are confusing and not scientifically reliable. The structural complexity of the resin glycosides seriously hampered the isolation of individual analogues limiting these chemical studies to the characterization of only their products of chemical degradation (*11*). Resin glycosides were seen as very large, high molecular weight polymers of oligosaccharides glycosidically linked to a hydroxylated fatty acid (*12*). In the 1980s, the application of high-performance liquid chromatography (HPLC) led to the isolation of four pure natural constituents from a resin glycoside mixture for the first time. They were collectively called orizabins from the Mexican scammony (*I. orizabensis*), their supposed source (*13*). The use of contemporary techniques such as high-field nuclear magnetic resonance (NMR) and high-resolution mass spectrometry (MS) allowed for the structure characterization of the above-mentioned compounds as individual macrolactones of a distinctive glycosidic acid and forced the rethinking of the long sustained hypothesis of a polymeric structure for this class of compounds.

3. Structural Diversity

3.1. Chemical Composition

Resin glycosides are glycosyl derivatives of monohydroxy and dihydroxy C_{14} and C_{16} fatty acids. Their structures are unusual for they are amphipatic metabolites, meaning that their structure contains hydrophobic (fatty acid aglycones) as well as hydrophilic (sugar or glycone) moieties. The latter are composed by a heteropolysaccharide of only a few residues (up to six), which are of no more than four different monosaccharides. Sugar units found in these metabolites are D-glucose and epimers of pentoses (L-rhamnose, D-fucose, D-quinovose, and D-xylose) in their pyranose forms. The *O*-glycosidic linkage is the only type connecting the monosaccharide residues between each other and with the aglycone. L-Rha-(1→2)-D-Fuc, L-Rha-(1→4)-L-Rha, and D-Glc-(1→2)-D-Fuc moieties represent highly conserved disaccharide subunits. The structural complexity arises from the variable linkage positions as (1→2), (1→3), (1→4), and (1→6). Short-chain aliphatic acids, *e.g.*, acetic (ac), propionic (pa), *n*-butyric (ba), isobutyric (iba), (2*S*)-methylbutyric (mba), 3-methylbutyric (3-mba), (−)-(2*R*,3*R*)-3-hydroxy-2-methylbutyric (nilic acid, nla), and tiglic (tga) acids, arylalkyl acids such as (*E*)-cinnamic acid (ca), and

saturated fatty acids with different chain lengths, *e.g.*, *n*-hexanoic (hexa) or caproic, *n*-octanoic (octa) or caprylic, *n*-decanoic (deca) or capric, *n*-dodecanoic (dodeca) or lauric, *n*-hexadecanoic (hexadeca) or palmitic, *n*-octadecanoic (octadeca) or stearic, and *n*-eicosanoic (eicosa) or arachidic acids, are among the most frequently found ester substituents linked to the oligosaccharide cores. Most of them contain jalapinolic acid, (11*S*)-hydroxyhexadecanoic acid, as the aglycone, which is always arranged to form a macrolactone ring spanning two or more units of their saccharide backbones. The chemical diversity of these oligosaccharides is further increased by the diverging possibilities of cyclization of the glycosidic acid cores into corresponding macrolactones. In addition, the multiple variations caused by acylation considerably increase their structural variety. In fact, on the whole, a large number of resin glycoside congeners occur in the Convolvulaceae family as well as a remarkable number in each species.

3.2. Resin Glycosides

The presence of resin glycosides in Convolvulaceous plants has been established through two approaches. The first one was by means of an ethnomedical rationale associated with the laxative properties of the herbal drugs (*3*). The second one was the isolation of the crude resins and the identification of their hydrolysis products (*2*), mainly through isolation of the glycosidic acid produced under saponification (*10*). Resin glycosides were classified into two groups based on their solubility in ether: jalapin (soluble) and convolvulin (insoluble). The jalapin group shares the common structure of a macrolactone composed by one acylated glycosidic acid. Members of the convolvulin group possess larger molecular weights, which could be a result of being oligomers of glycosidic acids (*12*).

Up to now, Convolvulaceae resin glycosides have not been reviewed *per se* but have been included in two reviews (*2*, *11*). The latest is not comprehensive, dealing only with the structural composition of resin glycosides through their products of hydrolysis (*2*). Since 239 of these compounds are presently known, a comprehensive review is presented in this chapter. The chemical diversity of these resin glycosides has been divided into groups based on the size of their oligosaccharide cores, thus imposing a logical sequence of structural complexity among congeners and listed in alphabetical order. To date, 53 different glycosidic acids have been identified, of which a large number have been accorded trivial names based on their plant source. In the present review, individual glycosidic acids are named according to the rules established by the Chemical Abstracts Service and only the structures for intact resin glycosides are presented. They are not IUPAC names but clearly describe the fragments of which each oligosaccharide is composed. For example, the correct IUPAC name for compound **1** would be (2*R*,3*R*)-((3*S*,4*S*,4a*R*,16*S*,17a*R*)-2-methyl-6-oxo-16-propyl-4-((2*S*,3*R*,4*S*,5*R*)-3,

4,5-trihydroxy-6-methyltetrahydro-2*H*-pyran-2-yloxy)hexadecahydropyrano-[3,2-*b*][1,4]dioxacyclopentadecin-3-yl)-3-hydroxy-2-methylbutanoate.

3.2.1. Disaccharides

Cuscutic Resinoside A

Cuscutic resinoside A (**1**; tetradecanoic acid, (11*S*)-[[6-deoxy-3-*O*-(6-deoxy-α-L-mannopyranosyl)-4-*O*-[(2*R*,3*R*)-3-hydroxy-2-methyl-1-oxobutyl]-α-L-mannopyranosyl]oxy]-intramol. 1,2′-ester) was obtained from the ethyl acetate-soluble fraction of a methanol extract prepared from the seeds of *Cuscuta chinensis* Lam. The purification of this compound employed a combination of column and preparative-scale HPLC. The structure was deduced from spectroscopic evidence and acid hydrolysis (*14*). The degradative process gave convolvulinolic acid, nilic acid, and L-rhamnose. The sugar components were identified by GC analysis after being converted to their thiazolidine derivatives. This disaccharide has a unique macrocyclic lactone, which is placed between C-1 and C-2 of the first rhamnose moiety.

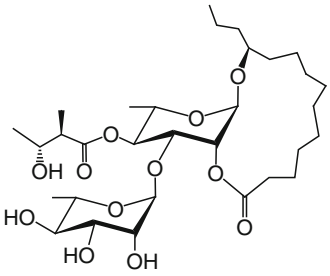

1

Ipomoeassins A–F

Six individual disaccharides have been isolated from the glycoresin of the leaves of *Ipomoea squamosa* Choisy collected in the Suriname rainforest, ipomoeassins A–F (**2–7**). The ethyl acetate-soluble extract was subjected to flash column chromatography over C_{18} silica gel and the fraction successively purified by HPLC on C_{18} and phenyl columns. The structures for the ipomoeassin series were elucidated by spectroscopic data and chemical degradation. The alkaline hydrolysis of ipomoeassin A gave two acids, cinnamic and tiglic acids, identified by GC-CIMS. Acid hydrolysis also gave the 11-hydroxy-4-oxo-tetradecanoic acid as the aglycone and two sugars, D-glucose and D-fucose. The absolute configurations of the aglycone stereogenic centers at C-5 (ipomoeassins C–E) and C-11 (ipomoeassins A and B) were determined by *Mosher*'s ester formation (*15*, *16*).

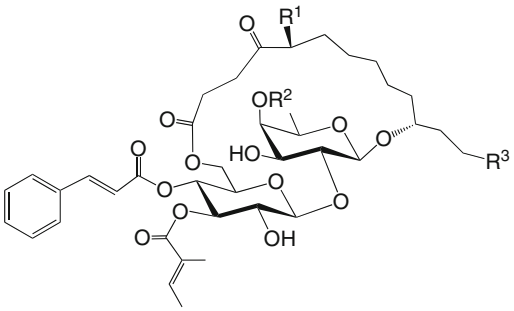

Compound	R^1	R^2	R^3
2	H	ac	CH_3
3	H	H	CH_3
4	OH	ac	CH_3
5	Oac	ac	CH_3
6	Oac	H	CH_3
7	H	ac	C_3H_7

Muricatin B

Misra and *Tewari* studied the alcoholic extract from seeds of *Ipomoea turbinata* Lag., sub nom. *Ipomoea muricata* (L.) Jacq., and isolated a resin glycoside named muricatin A (*17*, *18*). The structures of muricatin A and of its alkaline hydrolysis product, muricatin B, were not elucidated. Later, *Khanna* and *Gupta* found that muricatin A was actually a resin glycoside mixture, which by alkaline hydrolysis liberated *n*-caproic, palmitic and stearic acids, and muricatin B (hexadecanoic acid, 11-[[6-deoxy-4-*O*-(6-deoxy-α-L-mannopyranosyl)-α-L-mannopyranosyl]-oxy]) as the glycosidic acid. Acid hydrolysis of this derivative gave L-rhamnose as the only sugar component and jalapinolic acid as the aglycone (*19*).

3.2.2. Trisaccharides

Cus-1 and Cus-2

The acylated trisaccharides cus 1 and cus 2 were isolated from the $CHCl_3$-soluble extract of the seeds of *Cuscuta chinensis*. The extract was fractionated over Sephadex LH-20 and the fractions rich in resin glycosides were chromatographed by column chromatography using normal and reversed phases, followed by preparative HPLC. The oligosaccharide cores of both cus-1 (**8**) and cus-2 (**9**) are composed of two L-rhamnoses and one D-glucose. Cus-1 (D-glucose, *O*-6-deoxy-α-L-mannopyranosyl-(1→3)-*O*-[2(*S*), 4(2*R*,3*R*)]-6-deoxy-4-*O*-(3-hydroxy-2-methyl-1-oxobutyl)-2-*O*-(11-hydroxy-1-oxotetradecyl)-α-L-mannopyranosyl-(1→2)-6-acetate) has convolvulinolic acid as the aglycone,

which is linked at the C-2 of the first rhamnose unit, while cus-2 (D-glucose, *O*-6-deoxy-α-L-mannopyranosyl-(1→3)-*O*-[2(*S*),4(2*R*,3*R*)]-6-deoxy-4-*O*-(3-hydroxy-2-methyl-1-oxobutyl)-2-*O*-(11-hydroxy-1-oxohexadecyl)-α-L-mannopyranosyl-(1→2)-6-acetate) has jalapinolic acid. Acylation is found at C-4 of the first rhamnose by nilic acid and at C-6 of glucose by acetic acid. These compounds were characterized as a new group of resin glycosides since their aglycone hydroxy group at C-11 is not linked to the oligosaccharide chain (*20*).

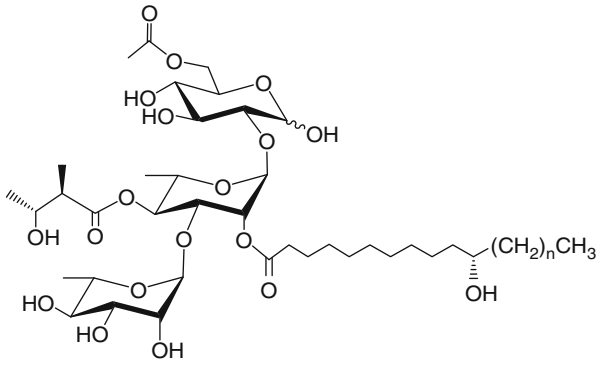

Compound	n
8	2
9	4

Cuscutic Acids A_1–A_3

An ether-insoluble resin glycoside fraction was obtained from the seeds of *Cuscuta australis* R. Br. Identification and characterization of the alkaline hydrolysis products revealed the material to be composed of three glycosidic acids, cuscutic acids A_1–A_3. In acid A_1 (hexadecanoic acid, (11*S*)-[(*O*-6-deoxy-α-L-mannopyranosyl-(1→2)-*O*-β-D-glucopyranosyl-(1→2)-6-deoxy-β-D-galactopyranosyl)oxy]) the aglycone is jalapinolic acid. Two triglycosides with convolvulinolic acid were also identified: cuscutic acids A_2 (tetradecanoic acid, (11*S*)-[(*O*-6-deoxy-α-L-mannopyranosyl-(1→2)-*O*-β-D-glucopyranosyl-(1→2)-6-deoxy-β-D-galactopyranosyl)oxy]) and A_3 (tetradecanoic acid, (11*S*)-[(*O*-6-deoxy-α-L-mannopyranosyl-(1→2)-*O*-β-D-glucopyranosyl-(1→2)-β-D-glucopyranosyl)oxy]). So far, no intact resin glycosides have been isolated containing these glycosidic acids. It is possible that the glycosidic resin found in *C. australis* is a complex mixture of glycosidic ester-type oligomers (up to heptamers). Their core consists of the above-mentioned cuscutic acids acylated at various positions (*21*).

Tricoloric Acid C

Two trisaccharide macrolactones have been characterized from the aerial parts of *Ipomoea tricolor* Cav. (syn. *Ipomoea violacea* L.) (heavenly blue), namely, tricolorins

F (**10**) and G (**11**). Tricoloric acid C (hexadecanoic acid, (11*S*)-[(*O*-6-deoxy-*β*-D-glucopyranosyl-(1→2)-*O*-*β*-D-glucopyranosyl-(1→2)-6-deoxy-*β*-D-galactopyranosyl)-oxy]) is the glycosidic acid of tricolorin F and was obtained by the alkaline hydrolysis of the natural product. It is a linear hetero-trisaccharide of jalapinolic acid formed by one unit of D-glucose, one D-fucose, and one D-quinovose. The glycosidic acid of tricolorin G has not yet been obtained in free form. However, the structure of the oligosaccharide core of this natural product was also characterized by spectroscopic analysis as being related to tricolorin C with the difference of containing a L-rhamnose unit instead of the terminal quinovose. The lactonization in both tricolorins F (**10**) and G (**11**) was located at C-2 of the terminal sugar unit (*22*).

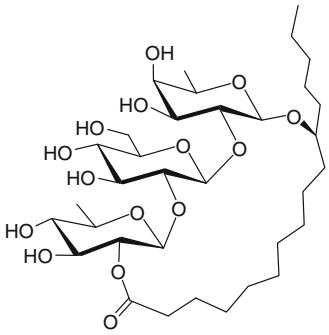

10

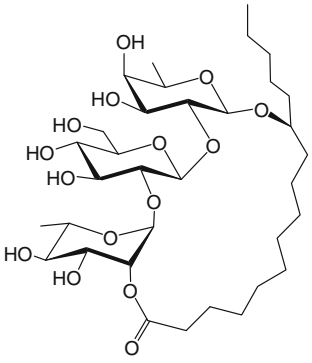

11

3.2.3. Tetrasaccharides

Cuscutic Acids A–D

Cuscutic acids A (tetradecanoic acid, (11*S*)-[(*O*-6-deoxy-α-L-mannopyranosyl-(1→3)-*O*-6-deoxy-α-L-mannopyranosyl-(1→2)-*O*-*β*-D-glucopyranosyl-(1→2)-*β*-

D-glucopyranosyl)oxy]), B (tetradecanoic acid, (11*S*)-[(*O*-6-deoxy-α-L-mannopyranosyl-(1→3)-*O*-6-deoxy-α-L-mannopyranosyl-(1→2)-*O*-β-D-glucopyranosyl-(1→2)-β-D-xylopyranosyl)oxy]), C (tetradecanoic acid, (11*S*)-[(*O*-6-deoxy-α-L-mannopyranosyl-(1→3)-*O*-6-deoxy-α-L-mannopyranosyl-(1→2)-*O*-β-D-glucopyranosyl-(1→2)-6-deoxy-β-D-glucopyranosyl)oxy]), and D (hexadecanoic acid, (11*S*)-[(*O*-6-deoxy-α-L-mannopyranosyl-(1→3)-*O*-6-deoxy-α-L-mannopyranosyl-(1→2)-*O*-β-D-glucopyranosyl-(1→2)-β-D-glucopyranosyl)oxy]) were isolated as the alkaline hydrolysis products of the ether-insoluble resin glycosides of the seeds of crude *Cuscuta chinensis* (*23*). The organic portion obtained from the basic hydrolysis revealed the presence of acetic, propionic, (2*S*)-methylbutyric, tiglic, and nilic acids as the esterifying residues of the resin glycoside mixture. All glycosidic acids have two rhamnose units and one glucose as well as convolvulinolic acid as the aglycone moiety, with the exception of cuscutic acid D, which has jalapinolic acid. So far, no intact resin glycosides have been isolated with these glycosidic acids.

Merremoside I

Merremoside I (hexadecanoic acid, (11*S*)-[(*O*-6-deoxy-α-L-mannopyranosyl-(1→4)-*O*-6-deoxy-α-L-mannopyranosyl-(1→4)-*O*-6-deoxy-α-L-mannopyranosyl-(1→4)-6-deoxy-α-L-mannopyranosyl)oxy]) is the glycosidic acid derivative from basic hydrolysis of the resin glycoside mixtures prepared from fresh tubers of *Merremia mammosa* (Lour.) Hallier f. Merremosides A–E (**12–16**) were isolated as the major intact diacylated resin glycosides after repeated separation by silica gel column chromatography and reversed-phase HPLC. L-Rhamnose units are the only sugar moieties present in the oligosaccharide core, which has jalapinolic acid as the aglycone. In these macrocyclic compounds, the lactonization site was placed at C-3 of the second rhamnose unit and the oligosaccharide core was esterified by 2-methylpropanoyl and (2*S*)-methylbutanoyl residues either at C-2 or C-3 of the third sugar and at C-3 or C-4 of the terminal saccharide unit (*24*).

Mammoside I (Operculinic Acid C)

Mammoside I (hexadecanoic acid, (11*S*)-[*O*-6-deoxy-α-L-mannopyranosyl-(1→4)-*O*-6-deoxy-α-L-mannopyranosyl-(1→4)-*O*-6-deoxy-α-L-mannopyranosyl-(1→2)-6-deoxy-β-D-galactopyranosyl]oxy) is a linear heterotetrasaccharide of jalapinolic acid composed of three L-rhamnose units and one D-fucose moiety. This glycosidic acid was originally isolated by basic hydrolysis of the resin glycosides from *Merremia mammosa* (*25*) and was later named as operculinic acid C after its isolation from *Ipomoea operculata* Mart. & Spix. (syn. *Operculina macrocarpa* (L.) Urban) (*26*). The general macrocyclic structures of mammoside A (**17**) and B (**18**) are similar to those of merremosides A (**12**) and B (**13**) with the only difference

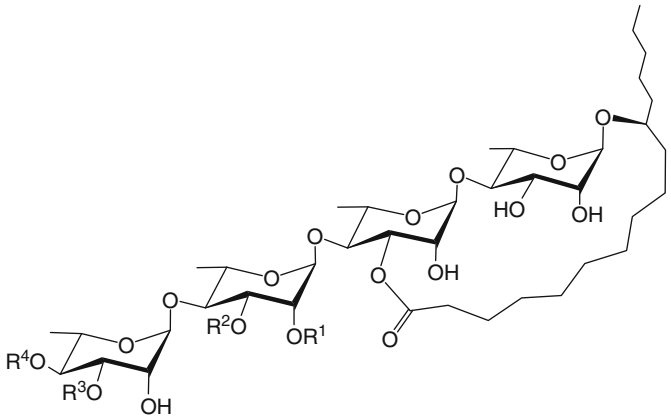

Compound	R^1	R^2	R^3	R^4
12	mba	H	H	mba
13	iba	H	H	iba
14	H	mba	H	iba
15	H	iba	H	iba
16	H	iba	iba	H

being D-fucose instead of L-rhamnose as the initial sugar for the glycosylation linkage with the aglycone (*26*).

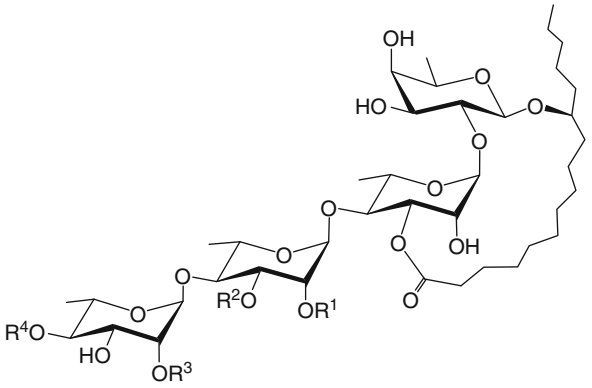

Compound	R^1	R^2	R^3	R^4
17	mba	H	H	mba
18	iba	H	H	iba
20	dodeca	H	H	dodeca
21	H	dodeca	H	dodeca
22	H	deca	H	mba
24	dodeca	H	H	mba
25	H	mba	dodeca	H
26	H	dodeca	H	mba
30	H	deca	H	H
31	H	H	H	dodeca

Ipomoea operculata has afforded three resin glycosides containing this glycosidic acid, operculins VI (**19**), XI (**20**), and XII (**21**). The macrolactone site was located at C-2 of the first rhamnose unit for **19** while in compounds **20** and **21** the lactonization was placed at C-3, the same site for mammosides A (**17**) and B (**18**). Two dodecanoyl residues are the fatty acids present in these resin glycosides and located at C-2 of the second rhamnose and at C-4 of the third rhamnose for operculin VI (**19**). For operculins XI (**20**) and XII (**21**), they were placed at C-2 or C-3 of the second rhamnose and C-4 at the third rhamnose (*27*).

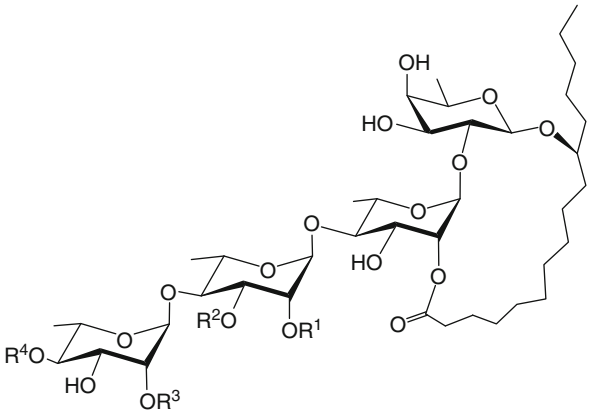

Compound	R^1	R^2	R^3	R^4
19	dodeca	H	H	dodeca
23	deca	H	H	mba
27	mba	H	H	mba
28	H	mba	H	mba
29	deca	H	CA	deca

The basic hydrolysis of stoloniferins XI (**22**) and XII (**23**), isolated from *Ipomoea stolonifera* (Cyrill) J. F. Gmel., afforded operculinic acid C (*28*). The lactonization site was placed at C-3 of the second monosaccharide unit for **22**, while for **23** it was placed at C-2. These diacylated resins contain decanoic acid esterifying position C-3 on the second rhamnose unit for **22** and C-2 for **23**. Both compounds contain (2*S*)-methylbutyric acid at C-4 on the third rhamnose. Pescapreins V (**24**) and VI (**25**) are diastereomeric tetraglycosidic lactones of operculinic acid C, obtained from the hexane-soluble extract of the aerial parts of *Ipomoea pescaprae* (L.) R. Br. Both compounds contain the lactonization site at C-3 of the second monosaccharide unit and (2*S*)-methylbutyric and *n*-dodecanoic acids as their esterifying residues (*29*). The methyl ester of operculinic acid C has been obtained by basic hydrolysis and methylation of the crude resin glycoside mixture of *Ipomoea murucoides* Roem. and Schult. (*30*). Murucoidins XIV–XVI (**26–28**), linear diacylated hetero-tetraglycosides, were isolated from the $CHCl_3$-soluble fraction prepared from flowers by column chromatography over silica gel then repeated preparative HPLC over reversed-phase C_{18} silica gel. The lactonization

site by the aglycone was placed at C-3 of the first rhamnose unit for **26**, for **27** and **28** at C-2 of the first rhamnose. All these murucoidins contain an esterifying residue that is composed of dodecanoic or (2*S*)-methylbutyric acids at the C-2 or C-3 positions on the second rhamnose unit of the oligosaccharide core and a (2*S*)-methylbutyric acid at C-4 on the third rhamnose moiety. Operculinic acid C is also present as the oligosaccharide core of the lipophilic simonin I (**29**) and batatinosides II (**30**) and III (**31**) from *I. batatas* (*31*, *32*). These monoacylated batatinosides were purified by preparative-scale recycling HPLC of the hexane extract prepared from powdered dry roots. The lactonization site of the aglycone was placed at C-3 of the first rhamnose unit, except for simonin I (**29**), where it was placed at C-2. Batatinoside II (**30**) has an *n*-decanoyl residue linked at C-3 of the third saccharide unit and batatinoside III (**31**) has a *n*-dodecanoyl group at C-4 of the last saccharide unit.

Muricatic Acids A–C

Alkaline hydrolysis of the ether-soluble glycoside fraction obtained from the seeds of *I. muricata* (L.) Jacq. provided muricatic acids A–C (*33*). These muricatic acids were purified by repeated normal-phase column chromatography. The linear tetrasaccharide muricatic acid A (hexadecanoic acid, (11*S*)-[(*O*-6-deoxy-*β*-D-galactopyranosyl-(1→4)-*O*-6-deoxy-α-L-mannopyranosyl-(1→2)-*O*-6-deoxy-*β*-D-glucopyranosyl-(1→2)-6-deoxy-*β*-D-glucopyranosyl)oxy] gave one D-fucose, one L-rhamnose, and two D-quinovose units. Muricatic acid B (hexadecanoic acid, (11*S*)-[(*O*-6-deoxy-*β*-D-glucopyranosyl-(1→4)-*O*-6-deoxy-α-L-mannopyranosyl-(1→2)]-*O*-6-deoxy-*β*-D-glucopyranosyl-(1→2)-6-deoxy-*β*-D-glucopyranosyl)-oxy]) differs only in the presence of a D-quinovose instead of the terminal fucose. Muricatic acid C (hexadecanoic acid, (11*S*)-[(*O*-6-deoxy-*β*-D-glucopyranosyl-(1→3)-*O*-[6-deoxy-α-L-mannopyranosyl-(1→2)-*O*-6-deoxy-*β*-D-glucopyranosyl-(1→2)-6-deoxy-*β*-D-glucopyranosyl)oxy] is a branched heterosaccharide and has one L-rhamnose and three D-quinovose units. For all of these compounds, jalapinolic acid is the aglycone moiety. Muricatic acid A is the oligosaccharide core of muricatins I–V (**32–36**) and VII (**37**). Muricatic acids B and C are the saccharide cores of muricatins VI (**38**) and VIII (**39**), respectively (*34*, *35*).

Muricatic acid C has also been found to be the glycosidic acid core of calonyctin A, a plant growth regulator isolated from dried leaves of *Calonyction aculeatum* L. House (*36*). It is important to note that calonyctin A has been separated into two pure components, the homologous glycosides containing the convolvulinolic and jalapinolic acids as their aglycone moieties, calonyctins A_1 (**40**) and A_2 (**41**). The lactonization site was placed at C-3 of the second quinovose unit in muricatins I–VII (**32–38**), and for muricatin VIII (**39**) and calonyctins A_1 (**40**) and A_2 (**41**) at C-2 of the third quinovose unit. The esterifying residues in **32–38** are isobutyric, (2*S*)-methylbutyric, and nilic acids (*34*, *35*) while 2-methylbutyric acid is the only esterifying group in **40** and **41** (*36*).

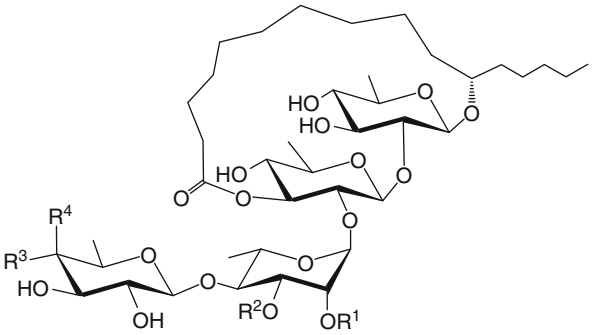

Compound	R^1	R^2	R^3	R^4
32	mba	H	H	Omba
33	mba	H	H	Oiba
34	H	mba	H	Omba
35	H	mba	H	Oiba
36	mba	H	H	OH
37	mba	H	H	Onla
38	mba	H	OH	H

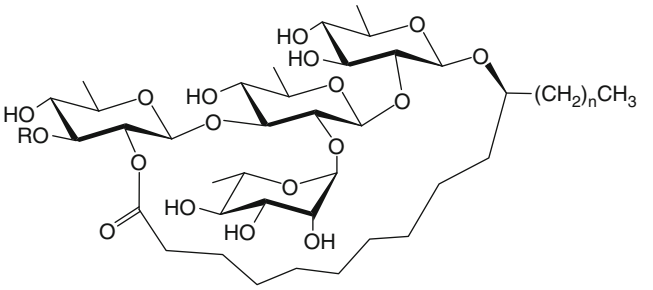

Compound	R^1	n
39	H	4
40	mba	4
41	mba	2

Operculinic Acids E and F

Operculinic acids E (hexadecanoic acid, (11*S*)-[(*O*-6-deoxy-α-L-mannopyranosyl-(1→4)-*O*-6-deoxy-α-L-mannopyranosyl-(1→4)-*O*-6-deoxy-α-L-mannopyranosyl-(1→2)-*β*-D-glucopyranosyl)oxy]) and F (hexadecanoic acid, (11*S*)-[(*O*-6-deoxy-α-L-mannopyranosyl-(1→4)-*O*-6-deoxy-α-L-mannopyranosyl-(1→4)-*O*-6-deoxy-α-L-mannopyranosyl-(1→2)-*β*-D-xylopyranosyl)oxy]) were obtained by alkaline hydrolysis of the ether-soluble crude resin glycosides from the roots of *Ipomoea*

operculata (*37*). Operculinic acid E has one D-glucose and three L-rhamnose units, while operculinic acid F has one D-xylose and three L-rhamnoses. In both, the aglycone moiety is jalapinolic acid. So far, no intact resin glycosides have been isolated containing operculinic acid F. The methyl ester of operculinic acid E was obtained by alkaline hydrolysis and methylation of the resin glycoside fraction prepared from the aerial parts of *Ipomoea purpurea* (L.) Roth (syn. *Pharbitis purpurea* Voigt.). The marubajalapins I–XI (**42–52**), named after the Japanese term "maruba-asagao" for this crude drug, were the first examples of resin glycosides based on operculinic acid E, isolated by preparative reversed-phase HPLC. The lactonization site was placed at C-2 of the first rhamnose, except for marubajalapins V (**50**), X (**51**), and XI (**52**), where it was placed at C-3. *n*-Octanoyl and *n*-decanoyl are the esterifying residues (*38*, *39*).

The methyl ester of operculinic acid E was obtained by basic hydrolysis and methylation of the crude resin glycoside mixture of *I. murucoides*. Murucoidins XII (**53**) and XIII (**54**) afford operculinic acid E as their oligosaccharide core. The lactonization site was placed at C-3 of the first rhamnose unit. These resin glycosides contain an esterifying residue that is composed of *n*-dodecanoic or (2*S*)-methylbutyric acids at the C-2 or C-3 positions on the second rhamnose unit of the oligosaccharide core and (2*S*)-methylbutyric acid at C-4 on the third rhamnose (*30*).

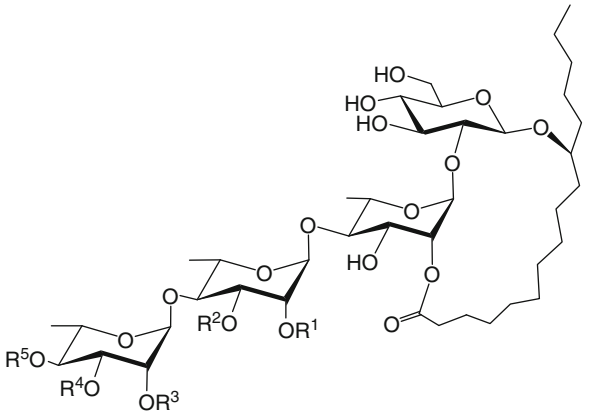

Compound	R^1	R^2	R^3	R^4	R^5
42	octa	H	H	H	octa
43	H	octa	H	H	octa
44	octa	H	H	H	deca
45	H	octa	H	H	deca
46	H	deca	H	H	deca
47	octa	H	octa	H	octa
48	H	octa	octa	H	octa
49	H	octa	H	octa	octa
55	dodeca	H	CA	H	deca
56	H	mba	CA	H	dodeca
57	mba	H	CA	H	dodeca

The jalapin-like chloroform-soluble material from the dried tubers of *I. batatas* was subjected to successive column chromatography over silica gel and HPLC to yield batatosides J–L (**55–57**) with the oligosaccharide core based on operculinic acid E. The lactonization site was placed at C-2 of the first rhamnose unit. Cinnamic acid was present as the esterifying residue at the C-2 position of the third rhamnose unit. These resin glycosides also contain esterifying residues composed of *n*-dodecanoic or (2*S*)-methylbutyric acids at the C-2 or C-3 positions on the second rhamnose unit of the oligosaccharide core as well as *n*-decanoic or *n*-dodecanoic acids at C-4 on the third rhamnose (*40*).

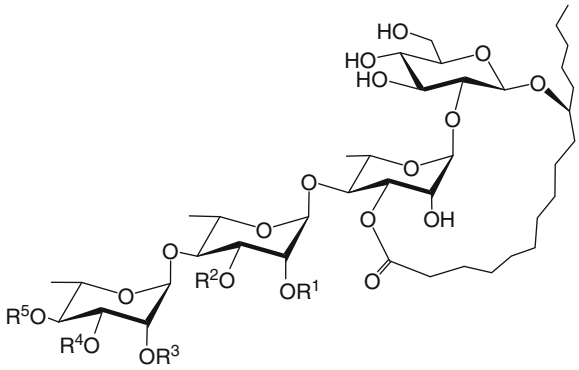

Compound	R^1	R^2	R^3	R^4	R^5
50	H	octa	H	H	deca
51	H	octa	octa	H	octa
52	octa	H	H	octa	octa
53	dodeca	H	H	H	mba
54	H	dodeca	H	H	mba

Orizabic Acid A

Basic hydrolysis of orizabins I–IV (**58–61**), isolated by preparative HPLC from the ether-soluble resins of the root of *Ipomoea orizabensis* Pelletan, Lebed. ex Steud afforded orizabic acid A (hexadecanoic acid, (11*S*)-[(*O*-6-deoxy-*β*-D-glucopyranosyl-(1→4)-*O*-6-deoxy-α-L-mannopyranosyl-(1→2)-*O*-*β*-D-glucopyranosyl-(1→2)-6-deoxy-*β*-D-galactopyranosyl)oxy]) (*13*). This oligosaccharide afforded one D-quinovose, one L-rhamnose, one D-glucose, and one D-fucose unit. Jalapinolic acid is the aglycone moiety, which is linked to the fucose C-1. The triacylated resin glycosides have (2*S*)-methylbutanoyl, tigloyl, isobutyl, and niloyl residues as short-chain esterifying moieties of the oligosaccharide core. The lactonization site were placed at C-3 of the rhamnose unit. The acylation sites for orizabins I–III (**58–60**) were located at C-6 of the glucose unit, C-2 of the third sugar, and C-4 of the quinovose unit, the terminal monosaccharide. For orizabin IV (**61**), the esterifying residues were placed at C-6 of the glucose residue, the second sugar unit, and at C-3 of the last residue.

Scammonin VII (**62**), as a minor ether-soluble resin glycoside, was isolated by reversed-phase HPLC from *Convulvulus scammonia* L. (*41*). Under basic hydrolysis, it gave orizabic acid A as well as 2-methylbutyric and tiglic acids. Compound **62** exhibits lactonization at C-3 of the rhamnose unit and is acylated by a (2*S*)-methylbutanoyl residue at C-2 of the rhamnose unit and a tigloyl residue at C-4 of the terminal quinovose.

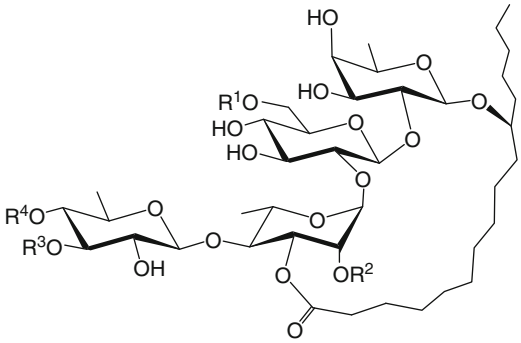

Compound	R^1	R^2	R^3	R^4
58	nla	tga	H	mba
59	nla	tga	H	iba
60	nla	tga	H	nla
61	nla	tga	iba	H
62	H	mba	H	tga

Scammonic Acid A

Alkaline hydrolysis of the ether-soluble resin glycosides from the seeds of *Convulvulus scammonia* produced scammonic acid A (hexadecanoic acid, (11*S*)-[(*O*-6-deoxy-*β*-D-glucopyranosyl-(1→4)-*O*-6-deoxy-α-L-mannopyranosyl-(1→2)-*O*-*β*-D-glucopyranosyl-(1→2)-6-deoxy-*β*-D-glucopyranosyl)oxy]), a major oligosaccharide formed by jalapinolic acid as the aglycone and two D-quinovoses, one L-rhamnose, and one D-glucose from the sugar core. The scammonin series of diacetylated macrocyclic resin glycosides was obtained by column chromatography and HPLC (*42*, *43*). The lactonization site of the aglycone in scammonins I–VI (**63–68**) was placed at C-3 of the third sugar unit. This series results from variations in the type of esterification by isobutyric, (2*S*)-methylbutyric, and tiglic acids at C-2 of the rhamnose and C-4 of the terminal quinovose. Scammonins III–VI (**65–68**) were obtained in the form of peracetates because of the great difficulties associated with their purification as intact products (*43*).

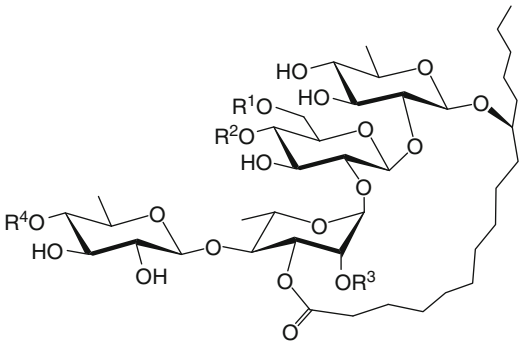

Compound	R^1	R^2	R^3	R^4
63	H	H	mba	tga
64	H	H	mba	H
65	H	H	iba	tga
66	H	H	tga	tga
67	H	H	iba	H
68	H	H	tga	H
69	H	H	mba	nla
70	H	mba	nla	H
71	H	nla	mba	H
72	nla	H	mba	tga
73	H	iba	nla	tga
74	H	iba	(+)-nla	tga
75	H	nla	iba	tga
76	H	(+)-nla	iba	tga
77	H	mba	nla	tga
78	H	mba	(+)-nla	tga
79	H	nla	mba	tga
80	H	(+)-nla	mba	tga
81	H	mba	nla	mba
82	H	mba	(+)-nla	mba
83	H	nla	mba	mba
84	H	(+)-nla	mba	mba
86	H	nla	nla	mba
87	H	nla	nla	tga
88	H	nla	nla	tga
89	H	nla	ba	tga
90	H	H	nla	nla
91	H	H	ba	mba
92	H	H	nla	H
93	H	H	pa	H
96	H	nla	iba	iba
97	H	nla	mba	iba
98	H	nla	3-mba	mba
99	H	nla	iba	nla
100	H	nla	3-mba	nla
101	H	nla	mba	nla
102	H	H	mba	iba
103	H	H	mba	mba

Scammonic acid A was also obtained by alkaline hydrolysis of the resin glycoside fraction obtained from the Mexican scammony root or false jalap (*Ipomoea orizabensis*). The $CHCl_3$-soluble resin glycoside fractions were separated by recycling preparative HPLC using a combination of C_{18} and aminopropyl silica-based bonded phases, resulting in the isolation of orizabins V–XXI. The major difference between each sample was the extent of esterification by (2*S*)-methylbutyric, tiglic, and nilic acids. The lactonization site of the aglycone was placed at C-3 of the L-rhamnose for orizabins V–VII (**69–71**) and IX–XXI (**72–84**). Orizabin VIII (**85**) is the only member of this series with lactonization at C-3 of the glucose, the second saccharide unit (*44*, *45*). This series illustrates the application of preparative-scale recycling HPLC (*45*) for the complete resolution of diastereomeric mixtures of niloyl esters involving both the (2*R*,3*R*) and (2*S*,3*S*) enantiomers of 3-hydroxy-2-methylbutanoic acid.

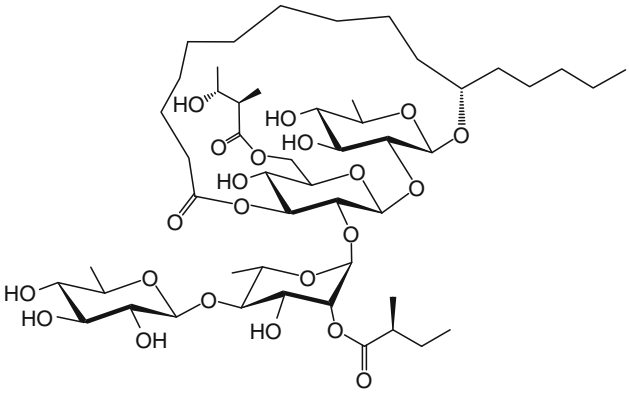

85

Basic hydrolysis of the resin glycoside fractions obtained from roots of *I. tyrianthina* afforded scammonic acid A. However, the botanical name used in this chemical study for the analyzed plant material was an invalid synonym for *I. orizabensis* (*46*), therefore, as expected, the major components of its lipophilic fractions, tyrianthins I–VII (**86–92**), represented only variations in the substitution pattern of the previously described orizabins (*44*, *45*) since the tyrianthin series was characterized through esterification as containing butyric, (2*S*)-methylbutyric, tiglic, and nilic acids (*47*). The polar fractions from this resin glycoside mixture yielded two macrocyclic resins, the known scammonin VI (**68**, misreported as the new tyrianthin VIII) and tyrianthin IX (**93**), a monosubstituted oligosaccharide acylated by propionic acid, as well as two acylated derivatives of scammonic acid A, tyrianthinic acids I (**94**) and II (**95**) (*48*). This type of non-macrocyclic resin glycoside has only been identified in three other species apart from Mexican scammony. Two are members of the Convolvulaceae family. The first of these yielded cuscutic acids A–D, tetrasaccharides isolated from the seeds of *Cuscuta chinensis* (*20*). The second yielded pescaprosides A and B, two pentasaccharides

purified from the aerial parts of *I. pes-caprae* (*29*, *49*). The third example came from the aerial parts of *Scrophularia crypthophila*, a species taxonomically unrelated to Convolvulaceae and belonging to the Scrophulariaceae, which yielded the tetrasaccharides, crypthophilic acids A–C (*50*).

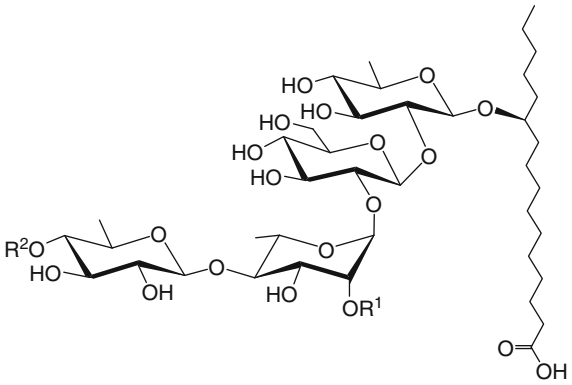

Compound	R^1	R^2
94	mba	nla
95	mba	tga

Another confusion arises in relation to the tetrasaccharides isolated from an ethyl acetate-soluble fraction of the roots of *Ipomoea stans* (*51*–*53*) since in reality the analyzed crude drug corresponds to *I. orizabensis* (*10*). Three unnamed macrocyclic resin glycosides (**96–98**) and five members of the stancin series (**99–103**) were obtained with the same lactonization and substitution pattern observed for the orizabins (*45*) with isobutyric, (2*S*)-methylbutyric, 3-methylbutyric, and nilic acids as the esterifying residues (*51*–*53*). Information was not provided to support the absolute configuration of the chiral esterifying residues and thus these products could represent diastereomeric mixtures due to the presence of both enantiomeric forms of nilic acid (*45*, *51*).

Scammonic Acid B

Scammonin VIII (**104**), isolated from *Convulvulus scammonia,* is a linear tetrasaccharide of jalapinolic acid with two glucoses, one rhamnose, and one quinovose. This compound represents the only macrocyclic resin glycoside of scammonic acid B (hexadecanoic acid, (11*S*)-[(*O*-*β*-D-glucopyranosyl-(1→4)-*O*-6-deoxy-α-L-mannopyranosyl-(1→2)-*O*-*β*-D-glucopyranosyl-(1→2)-6-deoxy-*β*-D-glucopyranosyl)oxy]).

The lactonization and acylation by (2*S*)-methylbutyric acid were placed at C-3 and C-2 of the third saccharide unit. Tiglic acid was located at C-4 of the terminal glucose (*41*).

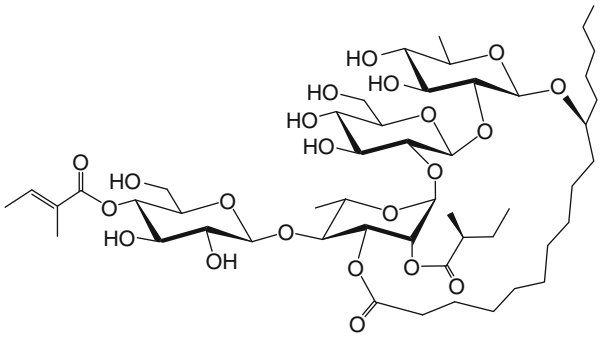

104

Soldanellic Acid B

Alkaline hydrolysis of soldanelline B (**105**), isolated from the chloroform extract of the roots of *Calystegia soldanella* (L.) Roem. and Schult. (*54*), gave soldanellic acid B (hexadecanoic acid, (11*S*)-[(*O*-6-deoxy-α-L-mannopyranosyl-(1→2)-*O*-[*β*-D-glucopyranosyl-(1→3)]-*O*-*β*-D-glucopyranosyl-(1→2)-6-deoxy-*β*-D-glucopyranosyl)-oxy]). This acid is a nonlinear tetrasaccharide composed by one quinovose, two glucoses, and one rhamnose, and the aglycone moiety is jalapinolic acid. The lactonization of the natural product was placed at C-2 of the branched glucose unit while the three acylated substituents were located at C-2 (nilic acid) and C-4 (tiglic acid) of the terminal rhamnose and at C-3 (2*S*-methylburyric acid) of the terminal glucose.

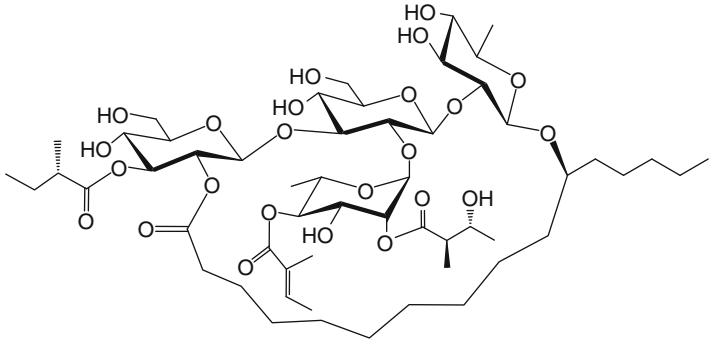

105

Tricoloric Acids A and B

Tricoloric acids A and B were produced by alkaline hydrolysis of the $CHCl_3$-soluble resin glycosides obtained from aerial parts of *Ipomoea tricolor* Cav. (*Ipomoea violacea* L.) (*55*, *56*). Tricoloric acid A (hexadecanoic acid, (11*S*)-[(*O*-6-deoxy-α-L-mannopyranosyl-(1→3)-*O*-6-deoxy-α-L-mannopyranosyl-(1→2)-*O*-*β*-D-glucopyranosyl-(1→2)-6-deoxy-*β*-D-galactopyranosyl)oxy]) has one D-fucose, one D-glucose, and two L-rhamnose monosaccharide units (*55*). Tricoloric acid B (hexadecanoic acid, (11*S*)-[(*O*-6-deoxy-α-L-mannopyranosyl-(1→3)-*O*-6-deoxy-α-L-mannopyranosyl-(1→2)-*O*-*β*-D-glucopyranosyl-(1→2)-6-deoxy-*β*-D-glucopyranosyl)oxy]) has one D-quinovose, one D-glucose, and two L-rhamnose units. Jalapinolic acid is the aglycone moiety in these glycoresins. The key to the successful separation of tricolorin A (**106**) and its analogues, tricolorins B–E (**107–110**), was the use of an amino bonded-phase by HPLC in the recycle mode (*56*). The lactonization site of the aglycone was placed at C-3 of the second saccharide unit in all compounds except tricolorin D (**109**) at C-6. Tricolorins B–D (**107–109**) differ from the general structure of compound **106** in the type of short-chain acids ester-linked at C-2 and C-4 of the third saccharide unit. These residues are (2*S*)-methylbutyric, isobutyric, and nilic acids. The structure of tricolorin E (**110**) was based on tricoloric acid B (*56*).

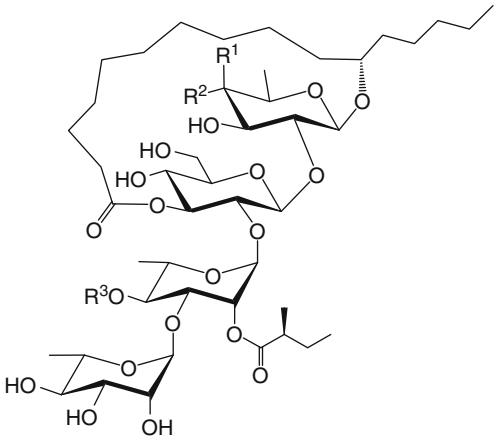

Compound	R^1	R^2	R^3
106	OH	H	mba
107	OH	H	iba
108	OH	H	nla
110	H	OH	mba

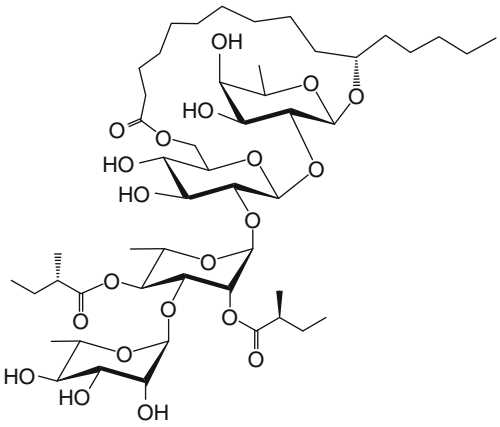

109

Turpethinic Acids A–E

Turpethinic acids A (pentadecanoic acid, 12-[(*O*-*β*-D-glucopyranosyl-(1→3)-*O*-6-deoxy-α-L-mannopyranosyl-(1→3)-*O*-*β*-D-glucopyranosyl-(1→3)-*β*-D-glucopyranosyl)oxy]-3-hydroxy), B (pentadecanoic acid 12-[(*O*-*β*-D-glucopyranosyl-(1→3)-*O*-6-deoxy-α-L-mannopyranosyl-(1→3)-*O*-*β*-D-glucopyranosyl-(1→3)-*β*-D-glucopyranosyl)oxy]-4-hydroxy), C (hexadecanoic acid, 12-[(*O*-*β*-D-glucopyranosyl-(1→3)-*O*-6-deoxy-α-L-mannopyranosyl-(1→3)-*O*-*β*-D-glucopyranosyl-(1→3)-*β*-D-glucopyranosyl)oxy]-4-hydroxy), D (hexadecanoic acid, 12-[(*O*-*β*-D-glucopyranosyl-(1→3)-*O*-6-deoxy-α-L-mannopyranosyl-(1→3)-*O*-*β*-D-glucopyranosyl-(1→3)-*β*-D-glucopyranosyl)oxy]-3-hydroxy), and E (hexadecanoic acid, 11-[(*O*-*β*-D-glucopyranosyl-(1→3)-*O*-6-deoxy-α-L-mannopyranosyl-(1→3)-*O*-*β*-D-glucopyranosyl-(1→3)-*β*-D-glucopyranosyl)oxy]) were obtained by alkaline hydrolysis of the ethanol-soluble resin glycosides of *Ipomoea turphetum* (L.) R. Br. (*57*). These glycosidic acids are composed of one rhamnose and three glucose units with 3,12-dihydroxypentadecanoic, 4,12-dihydroxypentadecanoic, 4,12-dihydroxyhexadecanoic, 3,12-dihydroxyhexadecanoic, and 11-hydroxyhexadecanoic acids, as their aglycones.

3.2.4. Pentasaccharides

Arboresinic Acid

The $CHCl_3$ extracts from roots of *Ipomoea arborescens* Humb. and Bonpl. were fractionated by column chromatography on silica gel. The alkaline hydrolysis of

the less polar fractions produced arboresinic acid (hexadecanoic acid, (11*S*)-[(*O*-6-deoxy-α-L-mannopyranosyl-(1→4)-*O*-[*β*-D-glucopyranosyl-(1→2)]-*O*-6-deoxy-α-L-mannopyranosyl-(1→4)-*O*-6-deoxy-α-L-mannopyranosyl-(1→2)-*β*-D-glucopyranosyl)oxy]) with a linear oligosaccharide core of two D-glucoses and three L-rhamnoses, as well as jalapinolic acid as the aglycone moiety. Six intact acylated resin glycosides derived from this glycosidic acid were isolated by HPLC and named arboresins I–VI (**111–116**). For all, the lactonization site was placed at C-2 of the second sugar unit, a *n*-dodecanoyl group at C-2 of the third sugar, and a niloyl residue at C-3 of the fourth sugar. The presence of congeners in this species is a consequence of variations in the type of acylating groups at C-4 of the fourth saccharide, *i.e.*, acetic, propionic, butanoic, (2*S*)-methylbutanoic, or tiglic acids (*58*).

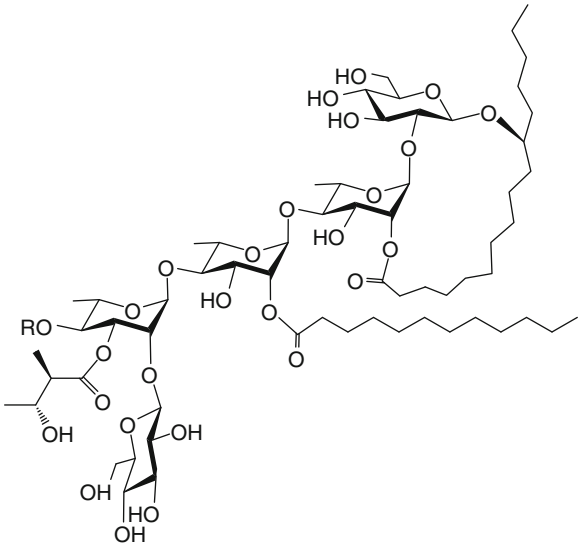

Compound	R
111	H
112	ac
113	pa
114	ba
115	mba
116	tga

Dichroside D

The EtOH extract of *Ipomoea dichroa* Choisy was fractionated into different organic solvents. The *n*-hexane-soluble fraction was resolved by column chromatography to afford dichrosides A–D. The major component dichroside D (hexadecanoic acid, (11*S*)-[(*O*-6-deoxy-α-L-mannopyranosyl-(1→3)-O-[*β*-D-glucopyranosyl-(1→4)]-*O*-6-deoxy-α-L-mannopyranosyl-(1→4)-*O*-6-deoxy-α-L-mannopyranosyl-(1→2)-6-deoxy-α-L-mannopyranosyl)oxy]) was subjected to catalytic hydrogenation.

Its chemical structure, characterized by degradative chemical procedures in conjunction with spectroscopic and spectrometric techniques, corresponded to a pentasaccharide of jalapinolic acid with one unit of D-glucose and four L-rhamnoses. The structures of the intact dichrosides A–D remain unsolved (*59*).

Merremoside J

Merremoside J (hexadecanoic acid, (11*S*)-[(*O*-6-deoxy-α-L-mannopyranosyl-(1→4)-*O*-[*β*-D-glucopyranosyl-(1→3)]-*O*-6-deoxy-α-L-mannopyranosyl-(1→4)-*O*-6-deoxy-α-L-mannopyranosyl-(1→4)-6-deoxy-α-L-mannopyranosyl)oxy]), one of the alkaline hydrolysis products from the resin glycoside mixture of *Ipomoea mammosa* (Lour.) Hallier f. (*syn*. *Merremia mammosa* (Lour.) Hallier), is a branched pentasaccharide of jalapinolic acid with one D-glucose and four L-rhamnoses. The methanol extract obtained from the crude drug gave four resin glycosides, merremosides f, g, h_1, and h_2 (**117–120**). The lactonization site of the aglycone was placed at C-3 of the second saccharide unit in merremosides f and g and at C-2 of the same sugar residue in merremosides h_1 and h_2. Differences in the acylation pattern at C-2 of the third rhamnose as well as at C-4 of the terminal rhamnose are responsible for the chemical diversity in the merremoside series with isobutyric and (2*S*)-methylbutyric acids at these two positions (*60*).

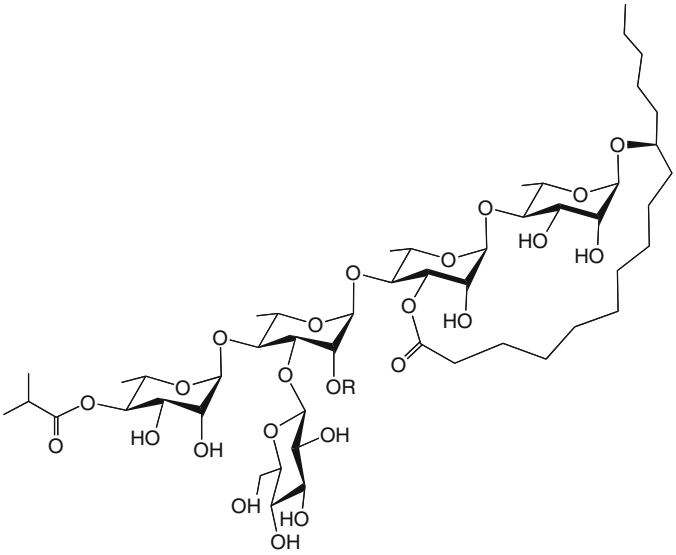

Compound	R
117	iba
118	mba

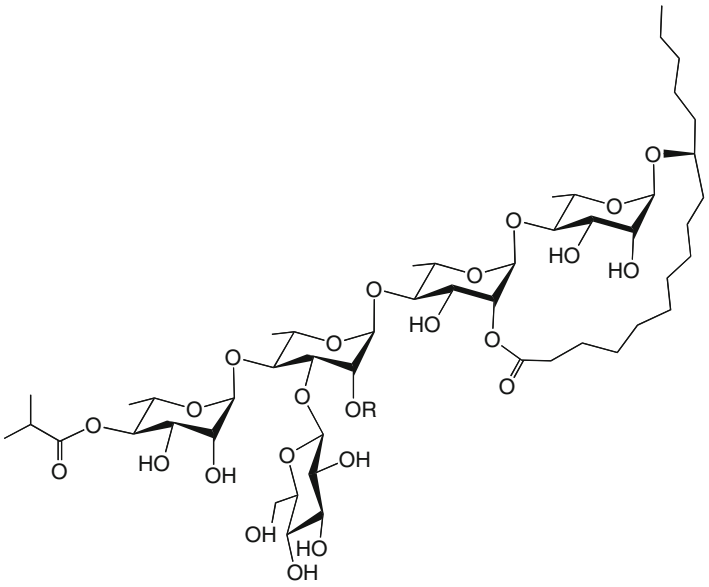

Compound	R
119	mba
120	iba

Microphyllic Acid

The alkaline hydrolysis of resins from *Convolvulus microphyllus* Sieb. *ex* Spreng. yielded microphyllic acid (hexadecanoic acid, (11*S*)-[(*O*-6-deoxy-α-L-mannopyranosyl-(1→4)-*O*-[6-deoxy-α-L-mannopyranosyl-(1→6)]-*O*-*β*-D-glucopyranosyl-(1→3)-*O*-6-deoxy-α-L-mannopyranosyl-(1→3)-6-deoxy-*β*-D-galactopyranosyl)oxy]), a nonlinear oligosaccharide with three L-rhamnose, one D-fucose, and one D-glucose units, as well as jalapinolic acid. Derivatization was used to elucidate its structure by application of GC-MS (*61*).

Multifidinic Acids A and B

Ipomoea multifida Cardinal Climber (syn. *Quamoclit multifida* Raf.) is an ornamental hybrid of *Quamoclit pinnata* and *Q. coccinea*. Alkaline hydrolysis of the ether-soluble resin glycosides obtained from seeds gave multifidinic acids A (tetradecanoic acid, (11*S*)-[(*O*-6-deoxy-α-L-mannopyranosyl-(1→4)-*O*-[*β*-D-glucopyranosyl-(1→3)]-*O*-6-deoxy-α-L-mannopyranosyl-(1→4)-*O*-6-deoxy-α-L-mannopyranosyl-

(1→2)-6-deoxy-*β*-D-glucopyranosyl)oxy]) and B (hexadecanoic acid, (11*S*)-[(*O*-6-deoxy-α-L-mannopyranosyl-(1→4)]-*O*-[*β*-D-glucopyranosyl-(1→3)]-*O*-6-deoxy-α-L-mannopyranosyl-(1→4)-*O*-6-deoxy-α-L-mannopyranosyl-(1→2)-6-deoxy-*β*-D-glucopyranosyl)oxy]). The sugar core of both is similar except for the aglycone moiety, convolvulinolic acid for A and jalapinolic acid for B. The nonlinear oligosaccharide has one D-glucose, one D-quinovose, and three L-rhamnose units. Two intact acylated resin glycosides derived from A were isolated and named multifidins I (**121**) and II (**122**). The lactonization site of the aglycone was placed at C-2 of the second saccharide unit and a (2*S*)-methylbutyric acid was located at C-4 of the fourth unit. Variations in the length of the acylating fatty acids at C-2 of the second rhamnose were observed, with *n*-decanoic acid as the esterifying residue in **121** and *n*-dodecanoic acid in **122** (*62*).

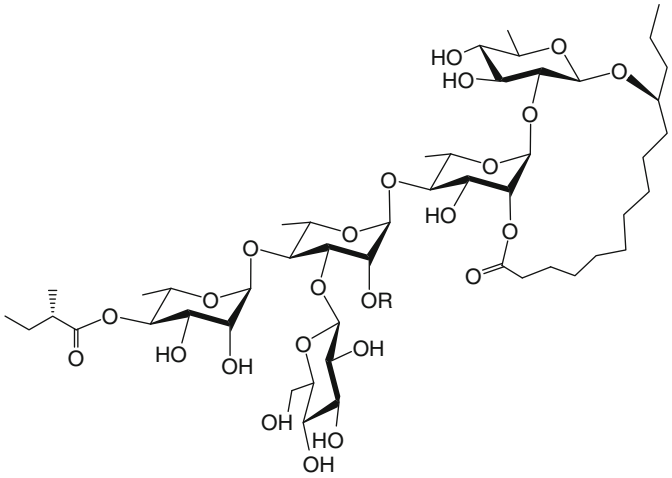

Compound	R
121	deca
122	dodeca

Murucinic Acid

The roots of the misidentified plant material *Ipomoea murucoides* were dried, pulverized, and macerated in chloroform. In reality, the analyzed plant material was *I. arborescens* as revealed by its chemistry which proved to be totally different from that identified for *I. murucoides* (*63*), when the latter was fractionated by column chromatography. The basic hydrolysis of the resinous chromatographic fractions of this sample produced the same glycosidic acid derivative ultimately found in *I. arborescens*, i.e., murucinic acid (hexadecanoic acid, (11*S*)-[(*O*-*β*-D-

glucopyranosyl-(1→2)-*O*-6-deoxy-α-L-mannopyranosyl-(1→4)-*O*-6-deoxy-α-L-mannopyranosyl-(1→4)-*O*-6-deoxy-α-L-mannopyranosyl-(1→2)-*O*-6-deoxy-*β*-D-glucopyranosyl)oxy]) (*58*). Nine intact acylated resin glycosides, murucins I–IX (**123–131**), derived from this glycosidic acid have been isolated and characterized. For all murucins the lactonization site of the aglycone was placed at C-2 of the second saccharide unit, and *n*-dodecanoic acid as the esterifying group at C-2 of the third saccharide unit. The presence of congeners in the murucin series is a consequence of the variations in the type of acylating groups at C-3 and C-4 of the fourth saccharide unit; a niloyl residue could be an esterifying group at C-3. Acetyl, propanoyl, butanoyl, (2*S*)-methylbutanoyl, 3-hydroxy-2-methylbutanoyl, or tigloyl residues could be the esterifying group at C-4 (*63*).

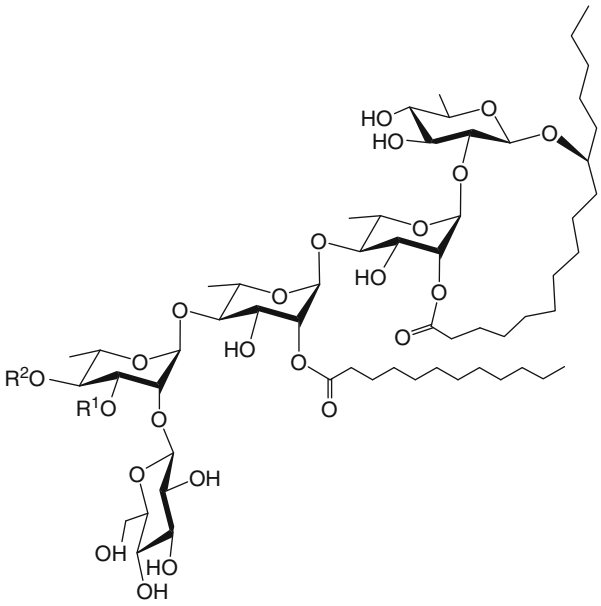

Compound	R^1	R^2
123	H	ac
124	H	pa
125	H	ba
126	H	mba
127	H	nla
128	nla	ac
129	nla	ba
130	nla	tga
131	H	H

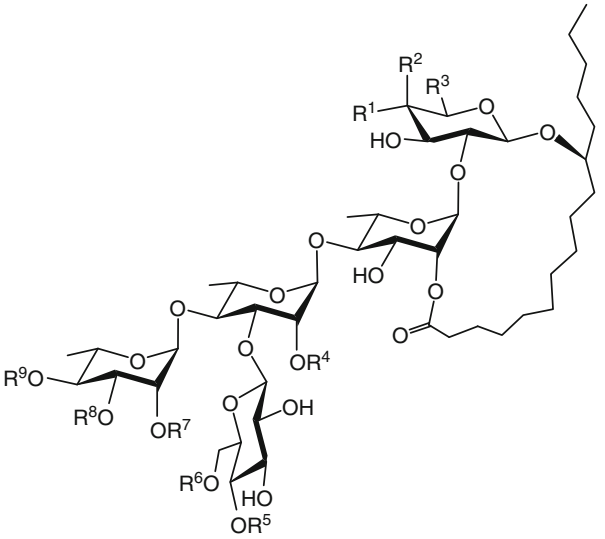

Compound	R^1	R^2	R^3	R^4	R^5	R^6	R^7	R^8	R^9
132	H	OH	CH_3	deca	H	H	H	H	H
133	H	OH	CH_3	mba	H	H	H	CA	dodeca
134	H	OH	CH_3	mba	H	H	CA	H	dodeca
135	H	OH	CH_3	mba	H	H	H	CA	mba
136	H	OH	CH_3	mba	H	H	H	CA	octa
137	H	OH	CH_3	Octa	H	H	H	CA	octa
138	H	OH	CH_3	dodeca	H	H	H	CA	(-)-(2*R*)-mba
139	H	OH	CH_3	dodeca	H	H	H	CA	mba
140	H	OH	CH_3	dodeca	H	H	H	mba	CA
141	H	OH	CH_3	dodeca	H	H	H	CA	octa
142	H	OH	CH_3	dodeca	H	H	CA	H	propa
143	H	OH	CH_3	dodeca	H	H	H	H	propa
144	H	OH	CH_3	dodeca	H	H	H	H	dodeca
145	H	OH	CH_3	deca	H	H	H	H	deca
146	OH	H	CH_2OH	dodeca	H	H	H	H	dodeca
147	OH	H	CH_2OH	deca	H	H	H	H	deca
149	H	OH	CH_3	dodeca	H	H	H	H	deca
150	H	OH	CH_3	deca	H	H	H	H	dodeca
151	OH	H	CH_2OH	dodeca	H	H	H	H	deca
152	OH	H	CH_2OH	deca	H	H	H	H	dodeca
153	OH	H	CH_2OH	dodeca	H	H	H	H	H
154	OH	H	CH_2OH	deca	H	H	H	H	H
155	OH	H	CH_2OH	H	H	H	H	H	dodeca
156	H	OH	CH_3	deca	H	H	H	H	mba
157	H	OH	CH_3	deca	H	H	H	H	mba
158	H	OH	CH_3	deca	H	H	H	H	hexa
159	H	OH	CH_3	deca	H	H	H	H	hexa
160	H	OH	CH_3	mba	H	H	H	H	iba
161	H	OH	CH_3	iba	H	H	H	H	iba
162	H	OH	CH_3	mba	H	H	H	H	mba
165	H	OH	CH_3	dodeca	H	H	H	H	mba
166	H	OH	CH_3	hexadeca	H	hexadeca	H	H	hexadeca
167	H	OH	CH_3	hexadeca	hexadeca	H	H	H	hexadeca
168	H	OH	CH_3	hexadeca	H	hexadeca	H	H	hexadeca
169	H	OH	CH_3	hexadeca	octadeca	H	H	H	hexadeca
170	H	OH	CH_3	hexadeca	octadeca	H	H	H	hexadeca
171	H	OH	CH_3	hexadeca	H	octadeca	H	H	hexadeca
172	H	OH	CH_3	hexadeca	eicosa	H	H	H	hexadeca
173	H	OH	CH_3	hexadeca	H	eicosa	H	H	hexadeca
174	H	OH	CH_3	hexadeca	H	H	H	H	hexadeca
175	H	OH	CH_3	hexadeca	H	H	H	H	hexadeca
176	H	OH	CH_3	dodeca	H	H	H	H	tga

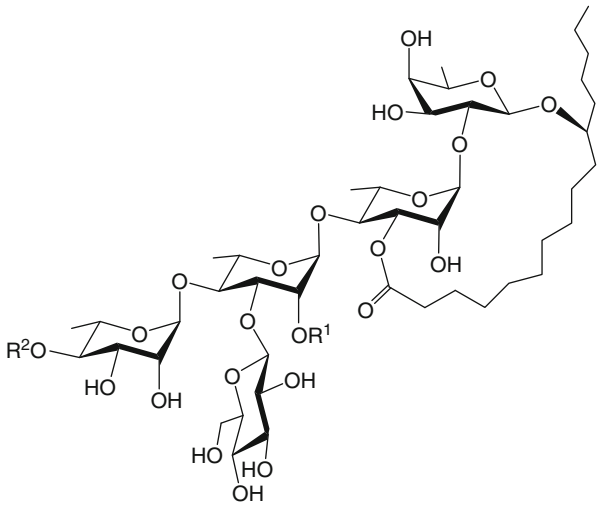

Compound	R^1	R^2
148	dodeca	dodeca
163	mba	mba
164	dodeca	mba

Operculinic Acids A, B, D, and G

Alkaline hydrolysis of the ether-soluble resin glycosides from Brazilian jalap, the roots of *Ipomoea operculata* (Gomes) Mart., gave four pentasaccharides of jalapinolic acid, named operculinic acids A (hexadecanoic acid, (11*S*)-[(*O*-6-deoxy-α-L-mannopyranosyl-(1→4)]-*O*-[β-D-glucopyranosyl-(1→3)]-*O*-6-deoxy-α-L-mannopyranosyl-(1→4)-*O*-6-deoxy-α-L-mannopyranosyl-(1→2)-6-deoxy-β-D-galactopyranosyl)oxy]), B (hexadecanoic acid, (11*S*)-[(*O*-6-deoxy-α-L-mannopyranosyl-(1→4)-*O*-[β-D-glucopyranosyl-(1→3)]-*O*-6-deoxy-α-L-mannopyranosyl-(1→4)-*O*-6-deoxy-α-L-mannopyranosyl-(1→2)-β-D-glucopyranosyl)oxy]), D (hexadecanoic acid, (11*S*)-[(*O*-6-deoxy-α-L-mannopyranosyl-(1→4)-*O*-[β-D-glucopyranosyl-(1→3)]-*O*-6-deoxy-α-L-mannopyranosyl-(1→4)-O-6-deoxy-α-L-mannopyranosyl-(1→2)-β-D-xylopyranosyl)oxy]), and G (hexadecanoic acid, (11*S*)-[(*O*-6-deoxy-α-L-mannopyranosyl-(1→4)-*O*-[2-*O*-methyl-β-D-glucopyranosyl-(1→3)]-*O*-6-deoxy-α-L-mannopyranosyl-(1→4)-*O*-6-deoxy-α-L-mannopyranosyl-(1→2)-6-deoxy-β-D-galactopyranosyl)oxy]) (*26*). Their structures are similar, only differing in the first monosaccharide unit: for acid A this is D-fucose, for acid B, D-glucose, and for acid D, D-xylose. The general structure of operculinic acid G is similar to that elucidated for operculinic acid A, differing only in the methylation of the hydroxy group at position C-2 of the terminal monosaccharide unit. Thus, this glycosidic acid seems to represent an artifact of solvent extraction.

Thirty-eight intact acylated resin glycosides derived from operculinic acid A have been isolated: batatinoside VI (**132**), batatoside H (**133**) and batatoside I (**134**) from *I. batatas* (L.) Lam. (*40*, *64*), intrapilosins I–VII (**135–141**) from *I. intrapilosa* Rose (*65*), leptophyllins A (**142**) and B (**143**) from *I. leptophylla* Torr. (*66*), operculins I (**144**), II (**145**), V (**148**), VII (**149**), and VIII (**150**) from *I. operculata* (Gomes) Mart. (*67*, *68*), stoloniferins IV–VII (**156–159**) from *I. stolonifera* (Cyrill.) J. F. Gmel. (*69*), mammosides H_1 (**160**) and H_2 (**161**) from *I. mammosa* Choisy (syn. *Merremia mammosa* (Lour.) Hall. f.) (*25*), murucoidins IV (**162**), V (**163**), and XI (**164**) from *I. murucoides* (Roem and Schult) (*70*, *71*), quamoclin IV (**165**) from *I. quamoclit* L. (syn. *Quamoclit pennata* Bojer) (*72*), tuguajalapins I–X (**166–175**) from *M. hungaiensis* Lingelish and Borza (*73*), and digitatajalapin I (**176**) from *I. digitata* L. (*74*). Seven intact acylated resin glycosides derived from operculinic acid B have also been isolated, namely, operculins III (**146**), IV (**147**), IX (**151**), X (**152**), XVI (**153**), XVII (**154**), and XVIII (**155**). The lactonization site of the aglycone was placed at C-2 of the second saccharide unit in all compounds except for operculin V (**148**) and murucoidins V (**163**) and XI (**164**), where it was placed at C-3. Different types of acylating groups at C-2 of the third saccharide unit, and at C-2, C-3, and/or C-4 of the fourth saccharide, contribute to the chemical diversity of these pentasaccharides.

Pescaprosides A, B, C, and E

The *n*-hexane-soluble extract from the aerial parts of the Mexican herbal drug "riñonina", *Ipomoea pes-caprae* var. *brasiliensis* (L.) Oost., the "beach morning glory" when separated using preparative-scale recycling HPLC, yielded two lipophilic glycosides, pescaprosides A (**177**) and B (**178**). The structure of pescaproside A (hexadecanoic acid, (11*S*)-[[*O*-6-deoxy-α-L-mannopyranosyl-(1→3)-*O*-[6-deoxy-α-L-mannopyranosyl-(1→4)]-*O*-6-deoxy-2-*O*-(1-oxododecyl)-α-L-mannopyranosyl-(1→4)-*O*-6-deoxy-α-L-mannopyranosyl-(1→2)-6-deoxy-*β*-D-galactopyranosyl)oxy]-methyl ester) is similar to that of pescaproside B (hexadecanoic acid, (11*S*)-[[(*O*-6-deoxy-α-L-mannopyranosyl-(1→3)-*O*-[6-deoxy-4-*O*-[(2*S*)-2-methyl-1-oxobutyl]-α-L-mannopyranosyl-(1→4)]-*O*-6-deoxy-2-*O*-dodecyl-α-L-mannopyranosyl-(1→4)-*O*-6-deoxy-α-L-mannopyranosyl-(1→2)-6-deoxy-*β*-D-galactopyranosyl]oxy]-methyl ester), with the only variation being the substitution by a (2*S*)-methylbutyric acid residue at position C-4 of the terminal rhamnose unit in pescaproside B (*29*, *49*). The structure of pescaproside C is similar to that of simonic acids A and B with the only difference being the presence of D-xylopyranose as the first monosaccharide in the oligosaccharide core. The four remaining sugars in this nonlinear glycosidic acid were identified as L-rhamnose (*75*).

Pescaprein XVIII (**179**) was isolated from the lipophilic fractions of the beach morning glory and its oligosaccharide core was characterized as pescaproside C (hexadecanoic acid, (11*S*)-[[*O*-6-deoxy-α-L-mannopyranosyl-(1→3)-*O*-[6-deoxy-α-L-mannopyranosyl-(1→4)]-*O*-6-deoxy-α-L-mannopyranosyl-(1→4)-*O*-6-deoxy-α-L-mannopyranosyl-(1→3)-*β*-D-xylopyranosyl]oxy]). The lactonization site of the

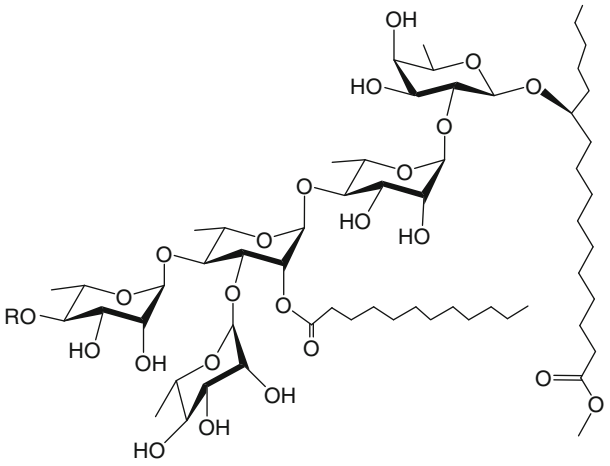

Compound	R
177	H
178	mba

aglycone was placed at C-3 of the second saccharide unit. An *n*-dodecanoyl group was located at C-2 of the third saccharide and a (2*S*)-methylbutanoyl residue at C-4 of the fourth sugar (*75*). The structure of pescaproside E (hexadecanoic acid, (11*S*)-[[*O*-6-deoxy-α-L-mannopyranosyl-(1→3)-*O*-[6-deoxy-α-L-mannopyranosyl-(1→4)]-*O*-6-deoxy-α-L-mannopyranosyl-(1→4)-*O*-6-deoxy-*β*-D-galactopyranosyl-(1→2)-6-deoxy-α-L-mannopyranosyl]oxy]) was proposed for the major saponification product of a mixture of resin glycosides isolated from a collection of beach morning glories from India. However, the glycosidation sequence, which was mainly characterized by the use of chemical degradations, seems to be not properly deduced (*76*). The D-Fuc-(1→2)-L-Rha disaccharide subunit, proposed instead of the highly preserved L-Rha-(1→2)-D-Fuc moiety, has not been reported in any other resin glycoside.

Pharbitic Acid C

The alkaline hydrolysis of the ether-insoluble resin glycoside fraction from seeds of *Ipomoea nil* (L.) Roth (*syn*. *Pharbitis nil* Choisy) yielded a pentasaccharide of ipurolic acid, which was named pharbitic acid C (tetradecanoic acid, 11-[(*O*-6-deoxy-*β*-D-glucopyranosyl-(1→4)-*O*-6-deoxy-α-L-mannopyranosyl-(1→6)-*O*-[6-deoxy-α-L-mannopyranosyl-(1→2)-O-*β*-D-glucopyranosyl-(1→2)]-*β*-D-glucopyranosyl)oxy]-3-hydroxy). On complete hydrolysis, it produced two D-glucoses, two L-rhamnoses, one D-quinovose, and the aglycone moiety (*77*).

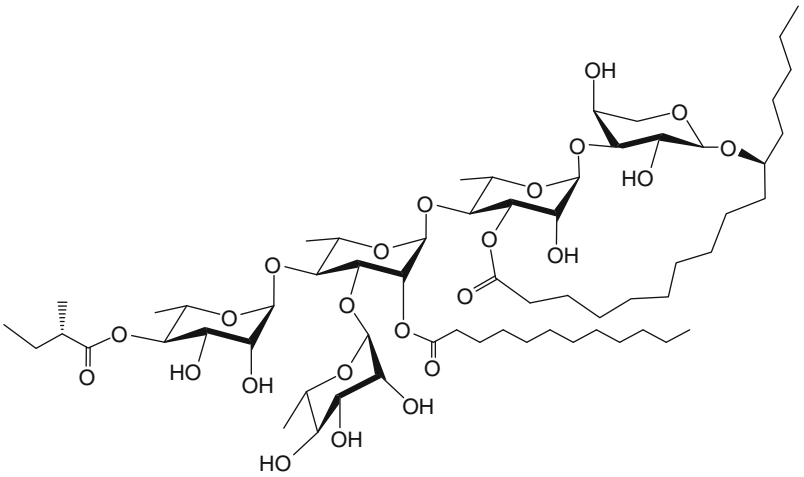

179

Quamoclinic Acid A

The MeOH extracts from seeds of *Ipomoea quamoclit* L. (syn. *Quamoclit pennata* Bojer) were partitioned between diethyl ether and H_2O. The alkaline hydrolysis of the ether-soluble fraction gave quamoclinic acid A (tetradecanoic acid, (11*S*)-[(*O*-6-deoxy-α-L-mannopyranosyl-(1→4)-*O*-[*β*-D-glucopyranosyl-(1→3)]-*O*-6-deoxy-α-L-mannopyranosyl-(1→4)-*O*-6-deoxy-α-L-mannopyranosyl-(1→2)-6-deoxy-*β*-D-galactopyranosyl)oxy], the structure of which is similar to that of operculinic acid A, with the only difference being in the aglycone moiety, namely, convolvulinolic acid for quamoclinic acid A and jalapinolic acid for operculinic acid A. Three intact acylated resin glycosides were isolated and elucidated structurally, quamoclins I–III (**180–182**). The lactonization site of the aglycone was placed at C-2 of the second saccharide unit in compounds **180** and **182**, while in **181** it was placed at C-3. In all quamoclins, a (2*S*)-methylbutanoyl group was located at C-4 of the fourth saccharide unit (*72*). These were the first examples described of ether-soluble resin glycosides in which methylbutyric acid coexists with long-chain fatty acids such as *n*-decanoic or *n*-dodecanoic acids at C-2 of the third saccharide unit.

Simonic Acids A and B

Alkaline hydrolysis of the $CHCl_3$-soluble resin glycoside mixture from dry roots of sweet potato (*Ipomoea batatas*) afforded two glycosidic acids, simonic acids A (hexadecanoic acid, (11*S*)-[(*O*-6-deoxy-α-L-mannopyranosyl-(1→3)-*O*-[6-deoxy-α-L-mannopyranosyl-(1→4)]-*O*-6-deoxy-α-L-mannopyranosyl-(1→4)-*O*-6-deoxy-

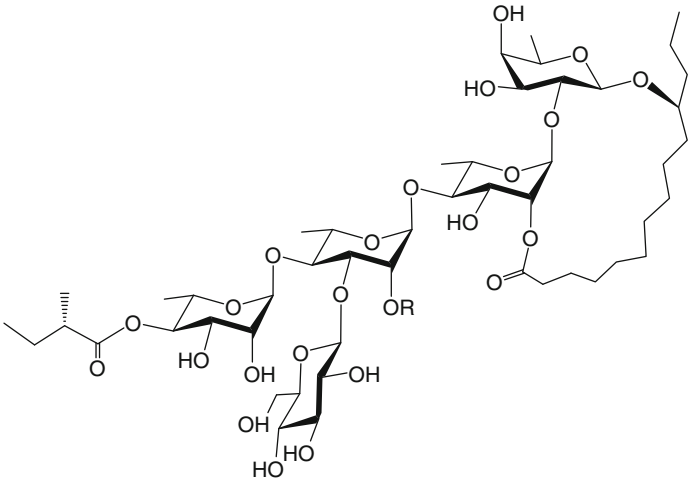

Compound	R
180	dodeca
182	deca

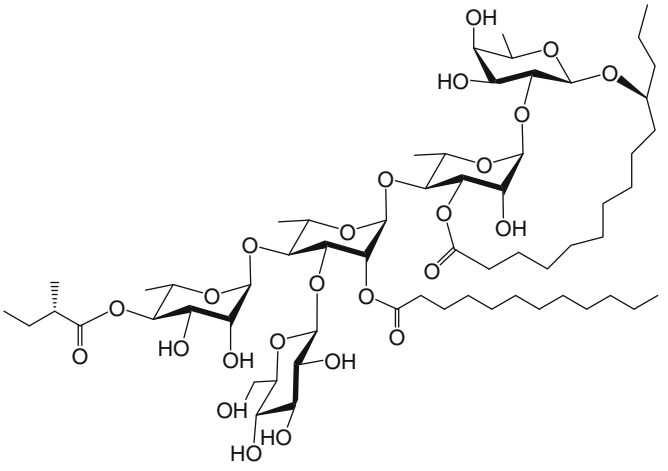

181

α-L-mannopyranosyl-(1→2)-*β*-D-glucopyranosyl)oxy]) and B (hexadecanoic acid, (11*S*)-[(*O*-6-deoxy-α-L-mannopyranosyl-(1→3)-*O*-[6-deoxy-α-L-mannopyranosyl-(1→4)]-*O*-6-deoxy-α-L-mannopyranosyl-(1→4)-*O*-6-deoxy-α-L-mannopyranosyl-(1→2)-6-deoxy-*β*-D-galactopyranosyl)oxy]) (*31*). The structures of these compounds are similar, with the difference being the presence of D-glucopyranose as the first monosaccharide of the sugar chain for simonic acid A and

D-fucopyranoside for simonic acid B. The other four monosaccharide units in the nonlinear oligosaccharide core were identified as L-rhamnoses, and their aglycone moiety was jalapinolic acid.

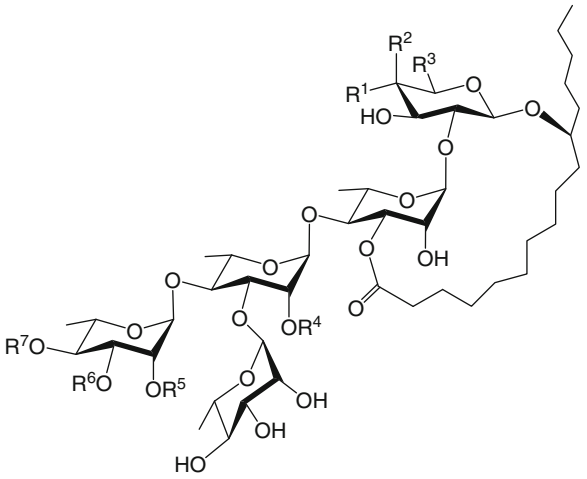

Compound	R^1	R^2	R^3	R^4	R^5	R^6	R^7
183	OH	H	CH_2OH	mba	H	H	dodeca
184	H	OH	CH_3	mba	H	H	dodeca
185	H	OH	CH_3	dodeca	H	H	dodeca
186	H	OH	CH_3	octa	H	H	dodeca
187	H	OH	CH_3	mba	H	CA	dodeca
188	H	OH	CH_3	mba	H	H	dodeca
190	H	OH	CH_3	mba	CA	iba	H
191	H	OH	CH_3	ba	H	CA	iba
192	H	OH	CH_3	mba	CA	dodeca	H
204	OH	H	CH_2OH	dodeca	H	H	mba
207	H	OH	CH_3	mba	H	H	iba
208	H	OH	CH_3	(8*R*)-hydroxy-dodeca	H	H	mba
209	H	OH	CH_3	dodeca	H	H	H
210	H	OH	CH_3	dodeca	H	H	iba
211	H	OH	CH_3	dodeca	H	H	mba
212	H	OH	CH_3	deca	H	H	hexa
213	H	OH	CH_3	deca	H	H	H
214	H	OH	CH_3	iba	H	H	dodeca
215	H	OH	CH_3	deca	H	H	hexa
216	H	OH	CH_3	deca	H	CA	mba
217	H	OH	CH_3	deca	CA	H	mba
218	H	OH	CH_3	deca	H	CA	iba
219	H	OH	CH_3	deca	CA	H	iba
220	H	OH	CH_3	dodeca	H	CA	iba
221	H	OH	CH_3	dodeca	CA	H	iba
222	H	OH	CH_3	dodeca	H	CA	mba
223	H	OH	CH_3	dodeca	CA	H	mba
224	H	OH	CH_3	mba	H	H	mba
225	H	OH	CH_3	deca	H	H	iba
226	H	OH	CH_3	deca	H	H	mba

Six intact acylated resin glycosides containing simonic acid A have been isolated: simonin II (**183**), batatosides M (**197**) and N (**198**) from *I. batatas* (*31*, *40*)

and murucoidins VI–VIII (**204–206**) from *I. murucoides* (*71*). Simonic acid B has been found to be the glycosidic acid core in the following resin glycosides: simonins III–V (**184–186**), batatinosides I (**187**), IV (**188**) and V (**189**), and batatosides A–G (**190–196**) and O–P (**199–200**) from *I. batatas* (*40*, *64*, *78*, *79*), murucoidins I–III (**201–203**), IX (**207**) and X (**208**) from *I. murucoides* (*70*, *71*), and pescapreins I–IV (**209–212**), VII–IX (**213–215**) and X–XVII (**216–223**) from *I. pescaprae* (*29*, *49*, *80*), and stoloniferins I–III (**224–226**) from *I. stolonifera* (*69*). The lactonization site of the aglycone was placed at C-3 of the second saccharide unit in all these compounds except for batatinoside V (**189**), batatosides D–G (**193–196**) and M–P (**197–200**), and murucoidins I–III (**201–203**) and VII–VIII (**205–206**), where it was placed at C-2. The presence of congeners in these series is a consequence of the variations in the type of acylating groups at C-2 of the third saccharide unit, and at C-2, C-3 and C-4 of the fourth saccharide unit. It has been reported that this diastereomerism at positions C-2 and C-3 could be a result of a transesterification via an *ortho*-acid ester intermediate that can take place in slightly acidic or neutral aqueous solution (*80*).

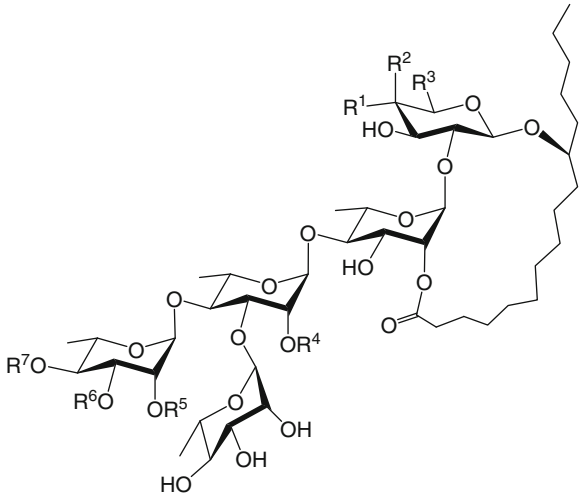

Compound	R^1	R^2	R^3	R^4	R^5	R^6	R^7
189	H	OH	CH_3	deca	H	H	H
193	H	OH	CH_3	mba	H	CA	dodeca
194	H	OH	CH_3	mba	CA	H	dodeca
195	H	OH	CH_3	mba	CA	dodeca	H
196	H	OH	CH_3	dodeca	H	CA	ba
197	OH	H	CH_2OH	dodeca	CA	H	mba
198	OH	H	CH_2OH	mba	H	CA	iba
199	H	OH	CH_3	iba	CA	H	dode
200	H	OH	CH_3	deca	CA	H	iba
201	H	OH	CH_3	mba	H	H	H
202	H	OH	CH_3	mba	H	H	iba
203	H	OH	CH_3	mba	H	H	mba
205	OH	H	CH_2OH	mba	H	H	iba
206	OH	H	CH_2OH	mba	H	H	mba

Soldanellic Acid A

From the chloroform-soluble extract obtained from the lyophilized root of *Calystegia soldanella,* an intact acylated resin glycoside, soldanelline A (**227**), was isolated (*81*). Its nonlinear pentasaccharide core has one D-quinovose, three D-glucoses, and one L-rhamnose, and as glycosidic acid, soldanellic acid. A (hexadecanoic acid, (11*S*)-[(*O*-*β*-D-glucopyranosyl-(1→3)-*O*-6-deoxy-α-L-mannopyranosyl-(1→2)-*O*-[*β*-D-glucopyranosyl-(1→3)]-*O*-*β*-D-glucopyranosyl-(1→2)-6-deoxy-*β*-D-glucopyranosyl) oxy]). The aglycone moiety is jalapinolic acid and the lactonization site of the aglycone was placed at C-2 of the second glucose unit, which represents the terminal and branched sugar for this pentasaccharide. Three sites of acylation were identified: nilic and tiglic acids at C-2 and C-4 of the third sugar (rhamnose), and (2*S*)-methylbutyric acid at C-3 of the branched glucose.

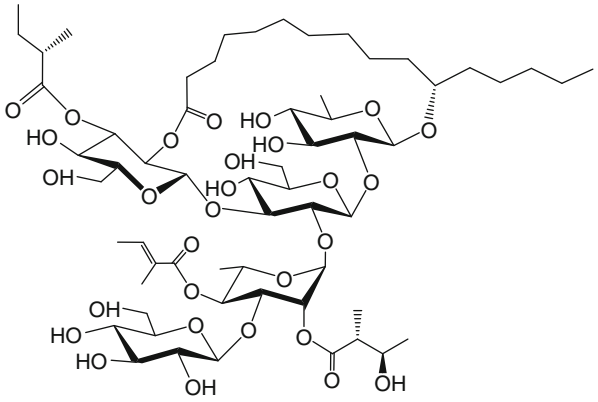

227

Woodrosinic Acid A

Two ether-insoluble resin glycosides named woodrosins I (**228**) and II (**229**) were isolated from the stems of *Ipomoea tuberosa* L. (syn. *Merremia tuberosa* (L.) Rendle) (*82*). Their oligosaccharide core was identified as a branched heteropentasaccharide, woodrosinic acid A (hexadecanoic acid, (11*S*)-[(*O*-6-deoxy-α-L-mannopyranosyl-(1→2)-*O*-[*β*-D-glucopyranosyl-(1→6)-*β*-D-glucopyranosyl-(1→3)]-*O*-*β*-D-glucopyranosyl-(1→2)-*β*-D-glucopyranosyl)oxy]), composed by four D-glucoses and one L-rhamnose. Jalapinolic acid is the aglycone. For **228** and **229**, the lactonization site was placed at C-2 of the fourth D-glucose unit. The branched monosaccharide represents the desoxyhexose unit diacylated by (2*S*)-methylbutyric acid at C-2 and C-4. The type of acylating groups at C-3 of the third saccharide unit leads to the structural difference between natural products **228** and **229**.

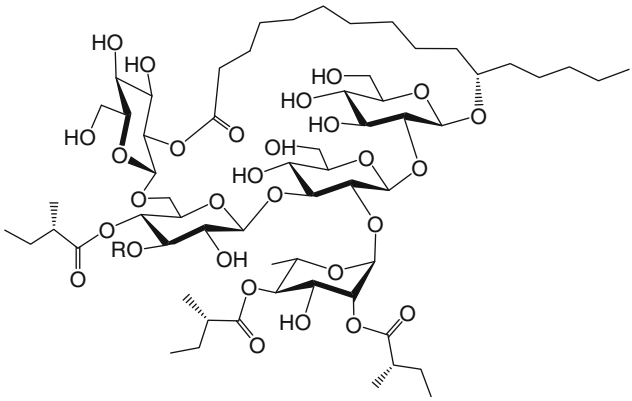

Compound	R
228	mba
229	iba

3.2.5. Hexasaccharides

Lonchophyllic Acid

Alkaline hydrolysis of the methanol-soluble resin glycosides from *Ipomoea lonchopylla* J. Black afforded a nonlinear hetero-hexasaccharide of ipurolic acid with two D-glucoses, one D-fucose, two D-quinovoses, and one L-rhamnose (tetradecanoic acid, (11*S*)-[(*O*-6-deoxy-*β*-D-glucopyranosyl-(1→2)-*O*-*β*-D-glucopyranosyl-(1→3)-*O*-[6-deoxy-α-L-mannopyranosyl-(1→4)]-*O*-6-deoxy-*β*-D-glucopyranosyl-(1→2)-*O*-*β*-D-glucopyranosyl-(1→2)-6-deoxy-*β*-D-galactopyranosyl)oxy]-(3*S*)-hydroxy) (*83*).

Operculinic Acid

Saponification of the diethyl ether-insoluble resin glycosides from *Ipomoea operculata* (Gomes) Martins, produced a glucorhamnohexasaccharide of 3,12-dihydroxypalmitic acid, operculinic acid (hexadecanoic acid, 12*S*-([*O*-6-deoxy-α-L-mannopyranosyl-(1→6)-*O*-[α-D-glucopyranosyl-(1→4)]-*O*-α-D-glucopyranosyl-(1→3)-*O*-6-deoxy-α-L-mannopyranosyl-(1→2)-*O*-[*β*-D-glucopyranosyl-(1→3)]-*β*-D-glucopyranosyl]oxy)-3-hydroxy) (*84*). This nonlinear glycosidic acid has four D-glucoses and two L-rhamnoses.

Pharbitic Acids B and D

Two glycosidic acids, pharbitic acids B and D, were isolated from alkaline hydrolysis of the ether-insoluble resin glycosides of *Ipomoea nil* (L.) Roth (syn. *Pharbitis nil* Choisy) seeds. Complete hydrolysis gave two D-glucoses, three L-rhamnoses, and one D-quinovose, with the only difference being found in the aglycone moiety, 3,11-dihydroxyhexadecanoic acid for pharbitic acid B (hexadecanoic acid, (11*S*)-[(*O*-6-deoxy-α-L-mannopyranosyl-(1→3)-*O*-6-deoxy-*β*-D-glucopyranosyl-(1→4)-*O*-6-deoxy-α-L-mannopyranosyl-(1→6)-*O*-[6-deoxy-α-L-mannopyranosyl-(1→2)-*O*-*β*-D-glucopyranosyl-(1→2)]-*β*-D-glucopyranosyl)oxy]-3-hydroxy) and ipurolic acid for pharbitic acid D (tetradecanoic acid, (11*S*)-[(*O*-6-deoxy-α-L-mannopyranosyl-(1→3)-*O*-6-deoxy-*β*-D-glucopyranosyl-(1→4)-*O*-6-deoxy-α-L-mannopyranosyl-(1→6)-*O*-[6-deoxy-α-L-mannopyranosyl-(1→2)-*O*-*β*-D-glucopyranosyl-(1→2)]-*β*-D-glucopyranosyl)oxy]-(3*S*)-hydroxy) (*85*, *86*).

Purgic Acids A and B

The authentic jalap root [*Ipomoea purga* (Wender) Hayne] MeOH-soluble resin glycosides have been found to be composed by two nonlinear hetero-hexasaccharides of convolvulinolic and jalapinolic acids, purgic acids A (tetradecanoic acid, (11*S*)-[(*O*-6-deoxy-*β*-D-glucopyranosyl-(1→2)-*O*-*β*-D-glucopyranosyl-(1→3)-*O*-[6-deoxy-*β*-D-galactopyranosyl-(1→4)]-*O*-6-deoxy-α-L-mannopyranosyl-(1→2)-*O*-*β*-D-glucopyranosyl-(1→2)-6-deoxy-*β*-D-glucopyranosyl)oxy]) and B (hexadecanoic acid, (11*S*)-[(*O*-6-deoxy-*β*-D-glucopyranosyl-(1→2)-*O*-*β*-D-glucopyranosyl-(1→3)-*O*-[6-deoxy-*β*-D-galactopyranosyl-(1→4)]-*O*-6-deoxy-α-L-mannopyranosyl-(1→2)-*O*-*β*-D-glucopyranosyl-(1→2)-6-deoxy-*β*-D-glucopyranosyl)oxy]) (*10*). The oligosaccharide core has two D-glucoses, two D-quinovoses, one D-fucose, and one L-rhamnose.

3.2.6. Ester-Type Oligomers

Batatins I and II

Batatins I (**230**) and II (**231**), two intact ester-type dimers of acylated pentasaccharides, were isolated by recycling HPLC from the *n*-hexane-soluble extract of the white-fleshed, and white-skinned staple-type cultivar of sweet potato (*Ipomoea batatas*). The glycosidic acid forming each branched pentasaccharide monomeric unit was confirmed as simonic acid B through saponification of pure **230** and **231**. The oligosaccharide core was esterified by three different fatty acids at the same positions on C-2 of the second rhamnose unit, as well as C-2 (or C-3) and C-4 of the third rhamnose moiety. The acylating residues were identified as (+)-(2*S*)-methylbutanoic, *n*-dodecanoic, and cinnamic acids. The site of lactonization by the aglycone in the macrocyclic unit was placed at C-3 of the second saccharide. The position for

the ester linkage for the noncyclic monomeric unit on the macrocyclic pentasaccharide was identified as C-3 of the terminal rhamnose (*78*). Both **230** and **231** represent dimers of batatinoside I (**187**).

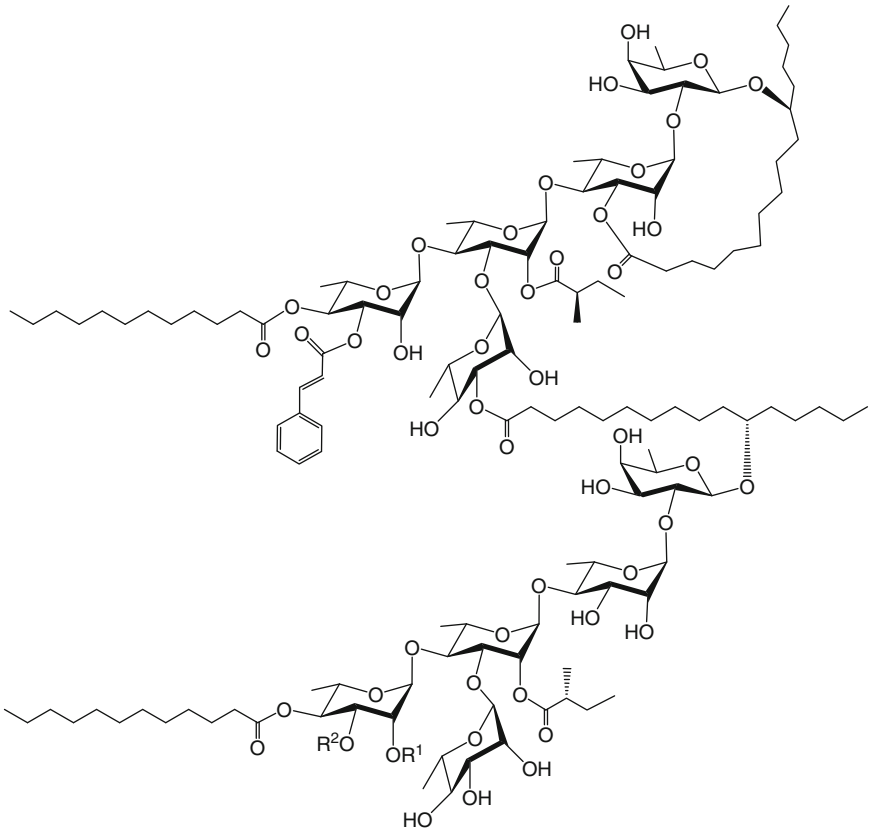

Compound	R^1	R^2
230	CA	H
231	H	CA

Batatins III and IV

As reported for all pentasaccharides from sweet potato (*64*, *86*), pure compounds **232** and **233** were also submitted to saponification yielding simonic acid B (*87*). The liberated fatty acids were identified as isobutyric, (2*S*)-methylbutanoic, *n*-decanoic, *n*-dodecanoic, and cinnamic acids. The site of lactonization by the aglycone in the macrocyclic unit was placed at C-2 of the second saccharide. The position of the ester linkage on the macrocyclic unit was C-2 of the terminal rhamnose. The acylations were identified as follows: for the macrocyclic unit at C-2 of the third saccharide (*n*-dodecanoic acid), and at C-3 and C-4 of the branched

terminal rhamnose ((2*S*)-methylbutyric or *n*-decanoic acids); for the glycosidic acid at C-2 of the third saccharide (*n*-decanoic acid), at C-2 or C-3 (cinnamic acid), and C-4 of the branched terminal rhamnose (isobutyric or (2*S*)-methylbutyric acids).

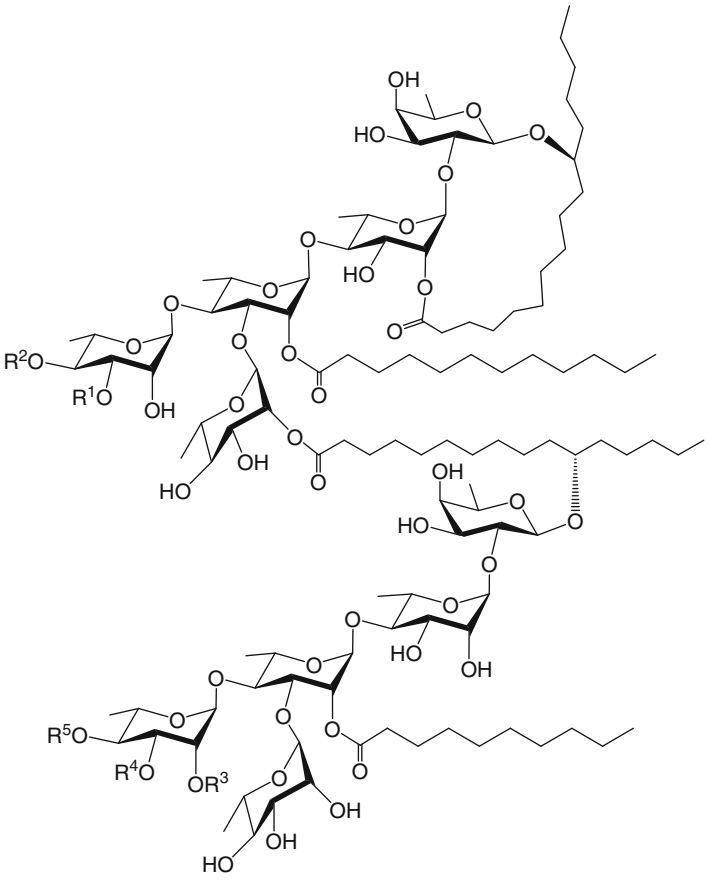

Compound	R^1	R^2	R^3	R^4	R^5
232	mba	deca	CA	H	iba
233	deca	mba	H	CA	mba

Batatins V and VI

Batatins V (**234**) and VI (**235**) are acylated tetrasaccharide ester-type dimers isolated from *Ipomoea batatas*, which yielded operculinic acid C through saponification. A mild alkaline hydrolysis of both afforded compound **30**, one of the monomeric units, identified by coelution in HPLC with natural batatinoside III (**31**), placing the lactonization at C-3 of the second saccharide in the macrocyclic portion. C-3 of the third saccharide unit was identified as the position for the ester linkage. Both dimers showed acylations at C-4 of the terminal rhamnose

(*n*-dodecanoic acid) on the macrocyclic unit and at C-3 of the second sugar on the glycosidic moiety (*n*-decanoic acid). Their diastereomeric structures, established by the acylation pattern differences, were a consequence of the presence of *n*-decanoic and *n*-dodecanoic acids at C-2 of the third sugar and C-4 of the terminal sugar on the glycosidic acid (*87*).

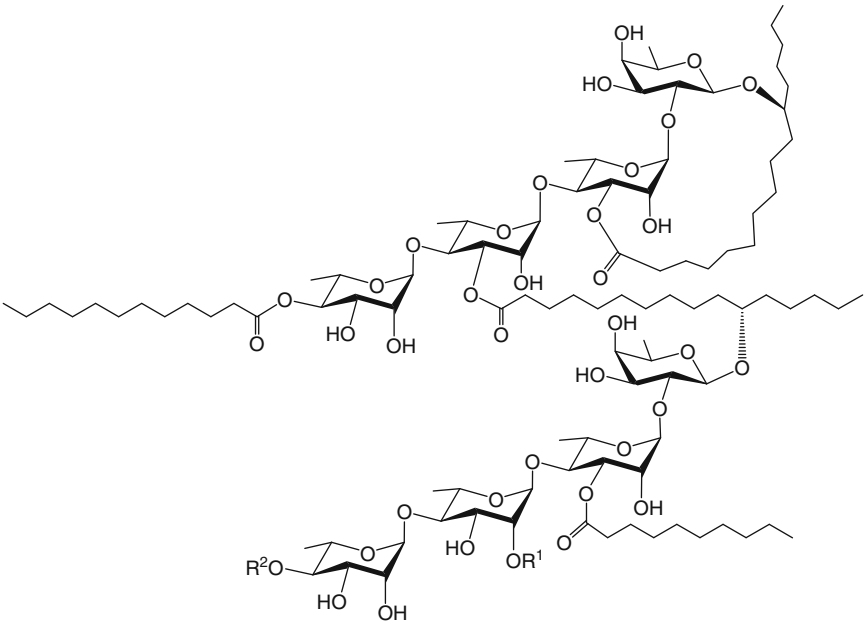

Compound	R^1	R^2
234	dodeca	deca
235	deca	dodeca

Merremin

The methanol extract of the fresh tuber of *Merremia hungaiensis* Lingelish and Borza was partitioned into a mixture of chloroform and water, and the chloroform-soluble resins were separated by silica gel and reversed-phase silica gel chromatography. Purification by HPLC provided merremin (**236**), as the first example of an ester-type dimer consisting of two units of operculinic acid A partially acylated by four residues of palmitic (*n*-hexadecanoic) acid. Mild alkaline hydrolysis of **236** gave tuguajalapin X (**175**) and its corresponding acylated glycosidic acid. The aglycone lactonization site was placed at C-2 of the first L-rhamnose unit in the macrolactone unit and the position for the glycosidic acid ester linkage at C-6 of the terminal glucose. Both pentasaccharide units were acylated at C-2 of the third sugar and C-4 of the branched terminal rhamnose (*88*).

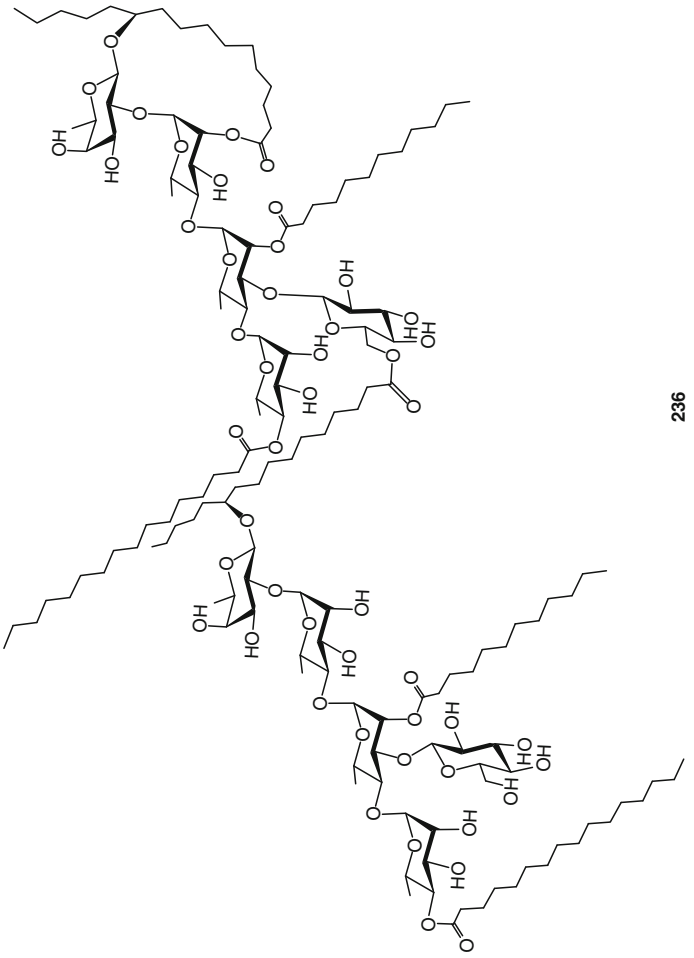

Tricolorins H–J

Investigation on the phytogrowth inhibitory polar fractions of heavenly-blue *Ipomoea tricolor* Cav. (syn. *Ipomoea violacea* L.) allowed the isolation of three ester-type heterohexasaccharides, tricolorins H–J (**237–239**), dimers of two trisaccharides, either tricolorins F (**10**) or G (**11**), and tricoloric acid C. Each of the monomeric units identified by coelution in HPLC with natural tricolorin G (**11**) and tricoloric acid C were obtained through mild alkaline hydrolysis of **237**. The aglycone lactonization site was placed at C-2 of the third monosaccharide in the macrolactone unit and the position for the glycosidic acid ester linkage at C-3 of the glucose unit. The terminal L-rhamnose in the macrocyclic oligosaccharide was acylated at C-4 by (2*S*)-methylbutyric acid. The diastereomeric structures of tricolorins I (**238**) and J (**239**) were dimers of tricoloric acid C, differing in the position of the ester linkage at C-3 or C-6

of the glucose unit. Each of the monomeric units was identified as tricolorin F (**10**) and tricoloric acid C through mild alkaline hydrolysis (*22*).

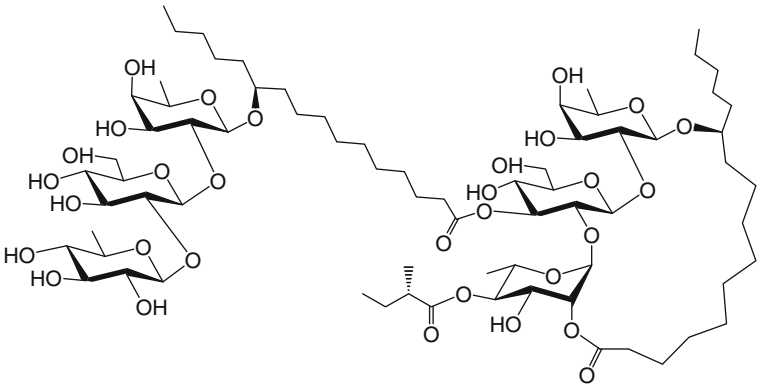

237

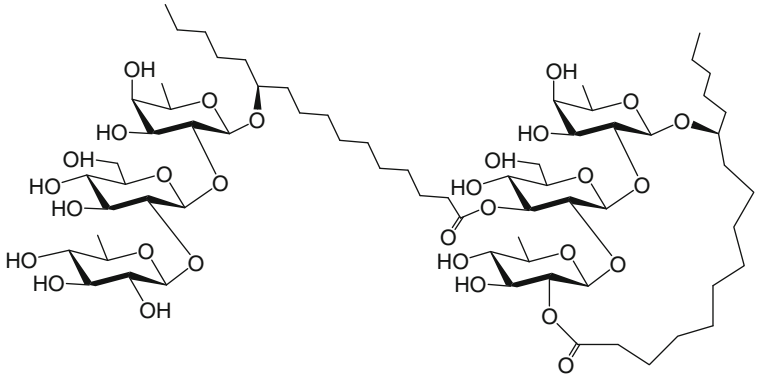

238

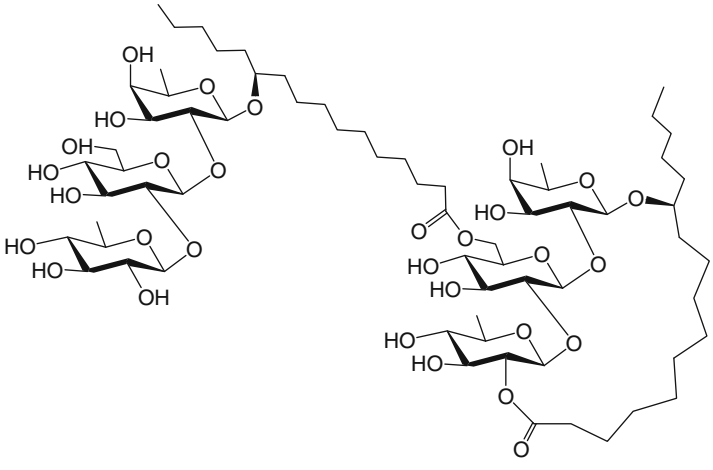

239

4. Isolation Techniques

Resin glycosides are amphiphilic compounds because of the presence of long aliphatic chains linked to a polar head. They are not very easy to isolate and purify for they are always present as complex mixtures of homologues having the same polar moiety but with alkyl substituents differing in chain length. Although a few reports of the isolation of glycolipids using silica gel TLC exist, this procedure is not suitable for purification of the individual constituents (*89*). Methods including open and low-pressure column chromatography using silica gel, Sephadex, ion exchange, and gel filtration were also conducted without successful results.

HPLC provides maximal resolution in a short-term analysis through the availability of small particle sizes (<25 μM in irregular and spherical shapes), pore sizes (60 and 130 Å), and modified (silica-gel bonded) stationary phases. The major technical challenges are finding the most favorable analytical factors (stationary and mobile phases, isocratic or gradient modes of elution, and maximum sample loading) and then scaling them into preparative conditions while retaining the resolution. Normal phase (*34*) and C_8 (*27*, *67*), C_{18} (*31*, *69*), cyano (*51*), and phenyl (*73*, *88*) silica gel bonded phases have been reported as being useful. As of now, the most successful and commonly employed phase is the amino column (aminopropylmethyl silica-bonded phase), a column also used for carbohydrate analysis. Using this column, several commercial samples of Mexican jalaps were assessed by generating HPLC profiles of their glycosidic acids, distinguishing the three herbal drugs currently in frequent use and serving as analytical tools for their authentication and quality control (*10*). Heart-cutting and peak shaving, singularly or combined, have been employed in the purification of individual resin glycosides. To achieve homogeneity, each peak collected is then recycled manually or using a recycling valve (*90*) until overlapped components separate, as demonstrated by the batatinoside (*64*), intrapilosin (*65*), murucoidin (*71*), orizabin (*45*), pescaprein (*49*), and tricolorin (*56*) series.

5. Structure Elucidation of Resin Glycosides

The main approaches for the structure elucidation of the resin glycosides involve the use of degradative chemical reactions or the application of high-resolution spectroscopic and spectrometric techniques and combining both has proven to be the best way for total characterization of these complex molecules.

5.1. Degradative Chemical Methods

Breaking up the large complex compounds by simple chemical reactions into smaller, more manageable molecules, has developed as a result of the difficulties

encountered in attempts to isolate the resin glycoside as intact constituents. Saponification of the crude material fragments the macrocyclic lactone and liberates the fatty acids that esterify the oligosaccharide core, which is then subjected to acid hydrolysis. Free fatty acids or their corresponding methyl or ethyl esters are analyzed by GC-MS (*10*). Total acid hydrolysis of the glycosidic acids releases the corresponding aglycone (hydroxylated C_{14} or C_{16} fatty acids) and monosaccharide units. Chain size and exact positions of hydroxylation are determined through direct EIMS analysis of the aglycone or GC-EIMS of its methyl ester and/or trimethylsilyl derivatives. The sugar units are converted into volatile derivatives by treatment with chlorotrimethylsilane and then analyzed by GC-MS. To avoid normal acid hydrolysis anomerization, silylation of the hydroxy groups and mercaptalation of the aldehyde functionalities is recommended (*55*). Liberated monosaccharides can also be detected by HPLC using a carbohydrate analytical column. Protocols are available for sugar analysis by either method (*91*). Permethylation of glycosidic acids followed by acid hydrolysis, pyranose reduction to the corresponding alditols, and acetylation may be used to establish the number and the relative positions of the glycosidic linkages (*83*). This allows the discrimination between free hydroxy groups (which are methylated in the alditol) and those involved in glycosidic bonds (acetylated in the alditols). Structure elucidation can also be approached through: (1) partial acid hydrolysis providing degraded identifiable products (di-, tri-, tetrasaccharides, etc.) (*33*); (2) partial basic hydrolysis of ester linkage in dimeric forms to correlate with natural monomers (*78*, *88*); and (3) total synthesis of the oligosaccharides (*24*, *25*).

5.2. Spectroscopic Methods

Complete structure elucidation of individual resin glycoside constituents is now achieved readily by the use of a combination of high-resolution mass spectrometry and NMR spectroscopy. These methods are applicable to the isolated natural products or to their peracetylated and methylated derivatives.

5.2.1. Mass Spectrometry

Natural glycoresins, even those having up to four acyl substituents, are polar solids with melting points generally above 100°C and are consequently non-volatile and quite difficult to vaporize in a standard electron-impact ion source without being thermally damaged. Electron ionization is not a suitable analytical method for these compounds even though their peracetyl and permethyl derivatives are easily volatilized and ionized (*59*, *86*, *92*). Soft ionization techniques, as fast-atom bombardment (FAB) and electrospray ionization (ESI), made a dramatic contribution to the field of resin glycoside characterization. The sample ions are formed as protonated

(positive mode) and deprotonated (negative mode) molecular species. The major breakthrough in FABMS analysis was due to the use of a liquid matrix, which facilitates production of molecular ions of the solute, helps in maintaining a persistent emission of these solute molecular ions, and allows dissipation of impact energy of the primary beam. Glycerol, the matrix most commonly used, is the best choice for underivatized oligosaccharides in the positive mode. Other alternative matrices for hydrophobic samples are 3-nitrobenzyl alcohol (3-NOBA), thioglycerol, and triethanolamine. Mass spectrometric quality depends on the *pH*, which is regulated by trace additions of HCl, and on the ionic force of the matrix, which may be increased by impregnation of the targeted sample with methanolic solutions of NH_4SCN, NaCl, or NaOAc. These additives promote the formation of abundant pseudo-molecular cations such as $[M + H]^+$, $[M + Na]^+$, and $[M + NH_4]^+$ or anions, such as $[M + SCN]^-$, and also facilitate the characteristic fragmentation of the glycosidic linkages for diagnostic purposes (*93*, *94*). The use of triethanolamine leads to a desirable extensive oligosaccharide fragmentation in the negative mode critical for identification of the glycosidation sequence (*49*, *64*). The numbers of units in these pure oligomers, as well as for total crude mixtures of resin glycosides, are obtainable through detection of molecular and fragment ions (*95*). Electrospray ionization also provides such structural information as composition, sequence, branching of the oligosaccharide, and type of sugar linkages. The reported mass spectra of batatins illustrate what can be expected from the analysis of an ester-type dimer in the negative mode (see Fig. 1): the $[M - H]^-$ anion, the glycosidic cleavage peaks, the fragments for the fatty acid elimination, and the $[M/2 - H]^-$ peak, representing the high-mass fragment ion for the two monomeric units (*78*).

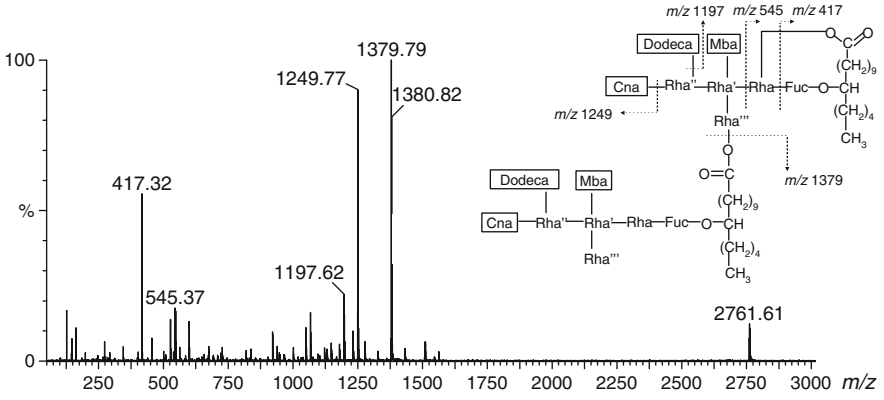

Fig. 1. Negative-ion MS/MS ESI−mass spectrum of batatin I (**230**). This technique provides an easily detectable $[M - H]^-$ peak (*m/z* 2761.61). All the characteristic ions resulting from glycosidic cleavage are clearly observed. The high-mass ion $[M/2 - H]^-$ (*m/z* 1379.79) corresponds to the ester cleavage of the dimeric structure. From *Escalante-Sánchez* and *Pereda-Miranda* (2007), with permission of the American Chemical Society (*78*)

5.2.2. Nuclear Magnetic Resonance

Due to extensive overlap within the region δ 3.0–4.5 ppm, ^{1}H NMR spectra of oligosaccharides in many cases produce complex patterns. In one-dimensional NMR analysis, the solvent pyridine-d_5 improves signal dispersion better than methanol-d_4 or acetone-d_6. For structural analysis, the following steps are suggested:

1. Estimation of sugar units: the anomeric protons around δ 4.4–6.5 ppm can be used as "structural reporter groups" for signals outside the bulk region. The integration of each of these resonances allows estimation of the number of different monosaccharide residues. The observed coupling constant values for the anomeric resonances are distinctive for each monosaccharide type: 1.0–3.0 Hz for rhamnose, 7.0–8.0 Hz for fucose, and 8.0–9.0 Hz for glucose and quinovose. In the ^{13}C NMR spectra, the anomeric signals in the δ 98–105 ppm region directly indicate the number of monosaccharide units. Sensitive 2D ^{13}C-^{1}H NMR experiments using HSQC, HMQC, or HMBC provide the same data. Profiling of the resin glycoside content of Mexican jalaps was assessed by generating ^{13}C NMR spectra of their glycosidic acid derivatives (*10*).
2. Identification of constitutive monosaccharides: two-dimensional homonuclear NMR techniques such as DQF-COSY and TOCSY are used to assign chemical-shift values for all C-bonded protons in each individual monosaccharide (*96*). One-dimensional NMR spectra provide useful information about the chemical shifts and scalar couplings of such well-resolved signals as methyl groups for 6-deoxy monosaccharides (fucose, quinovose, and rhamnose) at δ 1.1–1.3 ppm.
3. Characterization of anomeric configuration: in D-pyranoses in $^{4}C_1$ conformation, the α-anomer resonance appears downfield in comparison with the β-anomer (*96*). The vicinal coupling constant between the anomeric H-1 and H-2 protons indicates their relative orientation, i.e., a large coupling constant value (J = 7−8 Hz) for an *axial* orientation and smaller values for the *axial-equatorial* (J = 4 Hz) or *equatorial-equatorial* (J = <2 Hz) ones. The ^{13}C-^{1}H ($^{1}J_{CH}$) coupling constant is a more reliable criterion to determine conclusively the anomeric configuration in pyranoses. For D-sugars in the $^{4}C_1$ conformation, the α-anomeric configuration (β-*equatorial* C–H bond) has a $^{1}J_{CH}$ value of 170 Hz, which is 10 Hz higher than that observed ($^{1}J_{CH}$ = 160 Hz) for the β-anomer (α-*axial* C–H bond). This difference is reversed for L-sugars. One-bond rhamnose coupling constants correlate the anomeric configuration, which is impossible to deduce from the almost identical ^{1}H–^{1}H coupling values (^{3}J = >2 Hz) or the ^{13}C NMR chemical shifts for both anomers.
4. Elucidation of glycosidation sequence: the effect on the proton chemical shift of glycosylation is a typical deshielding (0.1–0.4 ppm) of the proton across the glycosidic bond (*97*). Glycosylation sites can be identified by comparison of ^{1}H NMR spectra of the native and the peracetylated oligosaccharide, since acylation of the free OH causes a downfield shift (0.5–1 ppm) of hydroxy-substituted geminal protons, whereas α-protons directly involved in the glycosidic linkage remain almost unaffected, permitting identification of both sites of

glycosylation as well as signals of terminal sugar residues. HMBC studies established the interglycosidic connectivities on the basis of long-range ($^3J_{CH}$) heteronuclear coupling correlations (*96*). Interresidue nuclear *Overhauser* effects in N*O*ESY and R*O*ESY experiments also provide glycosidic linkage and anomeric configuration. In addition, R*O*ESY crosspeaks discriminate between the α- and β-anomers of rhamnopyranosyl units (*96*).

Ester-type dimers illustrate the four-step approach for identification of carbohydrate structural elements in the oligosaccharide cores by NMR spectroscopy. For these type of compounds, edited ^{1}H NMR sub-spectra have permitted the assignment of all of the resonances in both monomeric units (*22*, *78*). Spectroscopic simulation of the coupling constants can be deduced for proton resonances with a non-first-order resolution. Figure 2 illustrates this approach for batatin I (**230**); the

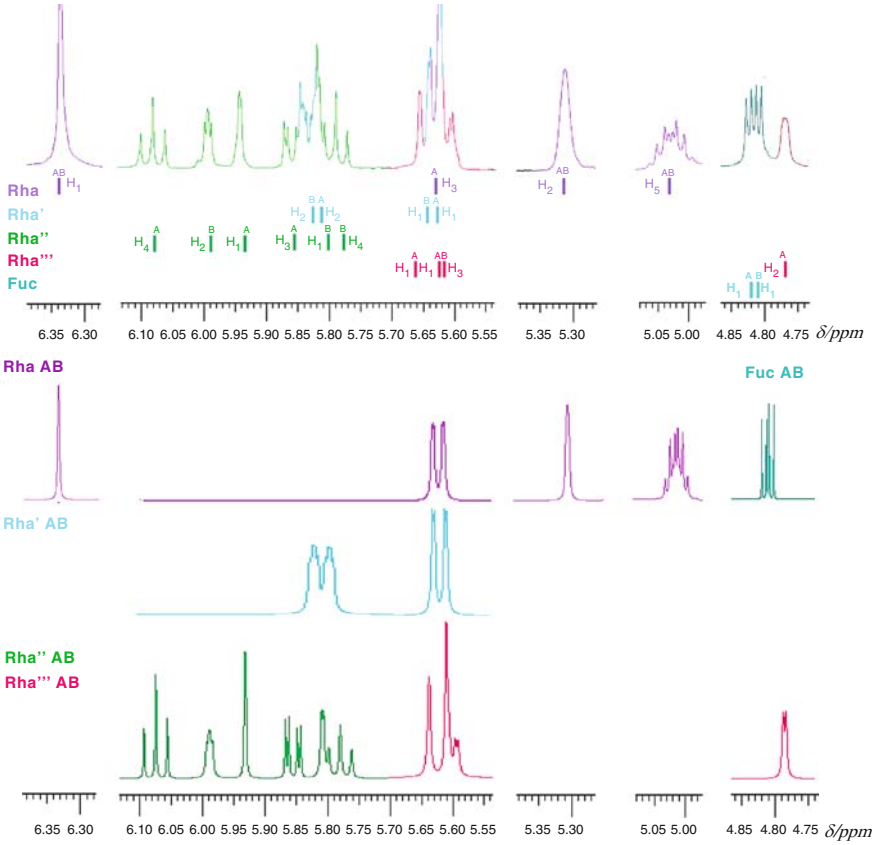

Fig. 2. Simulation of the anomeric region of the ^{1}H NMR spectrum of batatin I (**230**). The top trace is the measured 500 MHz spectrum, resolution enhanced. Actual chemical shifts are depicted along the bottom of the top plots. Below are the simulated spectra for each of the units. The H_n descriptors denote a specific position for each sugar unit. From *Escalante-Sánchez* and *Pereda-Miranda* (2007) with permission of the American Chemical Society (*78*)

coupling constants were varied by employing the MestRe-C program until an optimal agreement was achieved for the second-order analysis between measured and calculated spectra (*78*).

High-field NMR application of *Mosher*'s method was used to demonstrate that the absolute stereochemistry for all the hydroxy groups in the resin glycoside fatty acids correspond to the (*S*)-configuration (*70*, *98*), *e.g.*, (11*S*) for jalapinolic and convolvulinolic acids and (3*S*,11*S*) for dihydroxylated fatty acids such as ipurolic acid. This resulted in the revision of the (*R*)-configuration originally proposed by *Horeau*'s method for jalapinolic acid (*13*).

5.3. *Crystallographic Methods*

X-ray diffraction by single crystals is by far the most powerful experimental method for the characterization of atomic arrangements in molecules, providing accurate data concerning the conformation of carbohydrates. This information includes precise atomic coordinates, geometries, and crystal packing in the solid phase (*99*) and has the advantage over NMR spectroscopy in that it provides complete oligosaccharide conformation from experimental data. Its limitation is the requirement for regular crystals since few underivatized oligosaccharides crystallize uniformly due to their inherent flexibility. Obtaining a pure useable amount of an individual resin glycoside sample for crystal growth is a huge challenge and tricolorin A (**106**) is the only Convolvulaceous oligosaccharide that has been characterized crystallographically (*100*).

Four independent conformations were found in the asymmetric unit cell (see Fig. 3), but their superposition showed that all shared the same global shape (see Fig. 4), albeit with slightly different conformations for the externally placed L-rhamnopyranosyl-(1→3)-*O*-α-L-rhamnopyranoside moiety. The internal trisaccharide subunit, L-rhamnopyranosyl-(1→2)-*O*-β-D-glucopyranosyl-(1→2)-*O*-β-D-

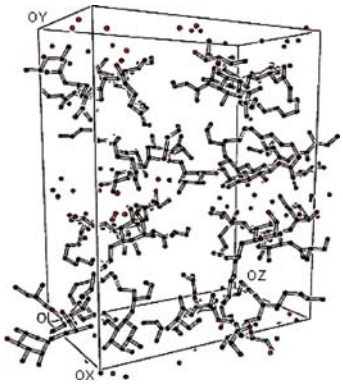

Fig. 3. Graphical representation of a unit cell showing the presence of 18 water molecules in the asymmetric unit in addition to the four independent tricolorin A (**106**) molecules

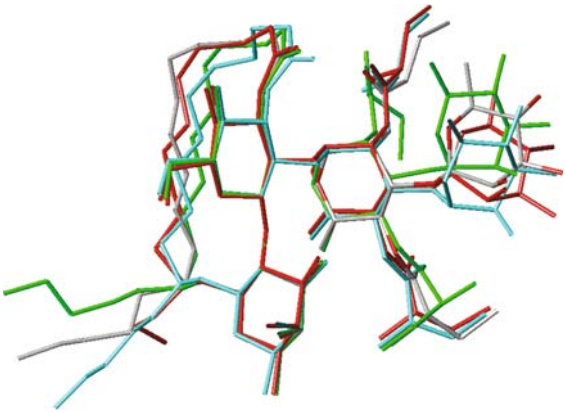

Fig. 4. Superposition of the four independent molecules of tricolorin A (**106**) showing that the internal trisaccharide subunit has limited conformational freedom due to its macrolactone structure

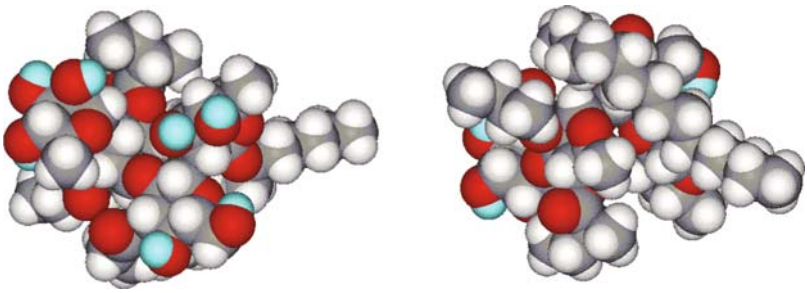

Fig. 5. Two different views (*ca.* 180°) of a single tricolorin A (**106**) molecule. Left, hydrophilic face. Right, hydrophobic face. Protons of hydroxyl groups are colored in cyan

fucopyranoside, has limited conformational freedom due to its macrolactone structure that spans the terminal two saccharide units reducing flexibility but allowing a uniform packing in the unit cell. The aglycone portion is well preserved in contrast to the flexibility for the terminal *n*-pentyl chain. Each molecule exhibits a hydrophobic wall formed by the aglycone unit, the methyl group of the fucose unit, and the three lipophilic residues on the inner rhamnose unit, i.e., the methyl group and the two esterified (2*S*)-methylbutyric acid groups. The other face presents two small hydrophilic areas: one composed of the hydroxy groups of the fucose and glucose residues and the other of the external rhamnose unit (see Fig. 5).

Notable in the tricolorin A (**106**) solid state is the presence of 18 water molecules in the unit cell, and an anisotropic repartitioning of the hydrophobic and hydrophilic sections. The water molecules form a dense network that creates a dividing layer between the hydrophilic faces (see Fig. 6). The high water content indicates that the conformation in the solid state is not dominated by intermolecular forces and could be indicative of a similar conformation in both solution and supermolecular

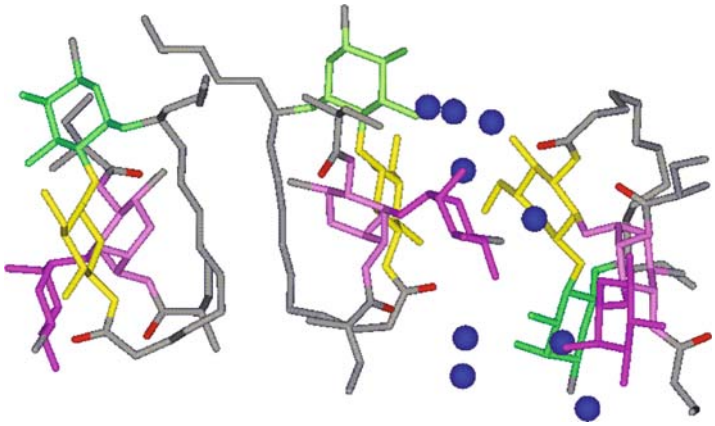

Fig. 6. Anisotropic repartitioning of the hydrophobic and hydrophilic interfaces observed in the crystal packing arrangement of tricolorin A (**106**)

aggregates. Conformational rigidity imposed by the macrolactone was also evident in the crystal structure of the synthetic substructure of tricolorin A, consisting of a protected disaccharide, 4,6-*O*-benzylidene-β-D-glucopyranosyl-(1→2)-(3,4-*O*-isopropylidene)-β-D-fucopyranoside. Five independent molecules were refined for the asymmetric unit of this analogue and confirmed the preservation of the macrocyclic moiety conformation. A piled parallel arrangement of the glycoside residues on one side and the macrolactone rings with alternating α- and β-faces on the other side was observed (*101*).

5.4. Molecular Modeling

Many force fields have been developed as well as protocols for modeling oligosaccharides (*99*, *102*), but it is necessary to modify them to include the *exo*-anomeric effect that largely determines the torsion angle ϕ of the glycosidic linkage (*103*). Although the X-ray ϕ/ψ plots indicate a wide range of glycosidic linkage conformations a smaller one might be adopted. For example, as dictated by the *exo*-anomeric effect, the energy maps of the three disaccharide subunits of tricolorin A (**106**) differ, and display low-energy regions centered around a ϕ-axis *gauche* conformation. A higher level of conformation freedom is apparent along the ψ axis with the lowest energy region between $-60°$ and $180°$ contrasting with the limited flexibility for the macrocyclic trisaccharide in this part of the 19-membered ring. Similar conclusions were obtained from the crystal structure of the synthetic dimeric subunit of tricolorin A since the glycosidic bond geometry in all five independent conformations was predicted by the *exo*-anomeric effect for the torsion angle ϕ. The other torsion angle populates the range $53°$–$76°$, limiting the flexibility of the macrolactone (*100*).

A combined approach is to use interproton distances determined by simulation and experimental N*O*E intensities to calculate the dynamic behavior of specific linkages in an oligosaccharide. The MM force field was employed for the computer simulation of calonyctin A_1 (**40**) where interglycosidic N*O*Es served as experimental distance restraints for the molecular dynamics (*104*).

6. Strategies for Synthesis

Resin glycoside macrolactone rings present a major challenge to develop methodologies for their synthesis. Initially, as employed for the total synthesis of calonyctin A_2 (**41**) (*105*), tricolorin A (**106**) (*106*, *107*), and tricolorin F (**10**) (*108*), these rings were prepared by conventional macrolactonization techniques, relying on the intrinsic differences in reactivities of the oligosaccharide core hydroxy groups and resulting in a regioselective process. This approach was obviously limited for the formation of a wide range of structural analogues since each new compound requires an independent multistep synthesis (coupling reactions of carbohydrate building blocks).

An alternative methodology takes advantage of the inherently modular character of ring-closing alkene or alkyne methathesis (RCM). Systematic variations of ring size and hence of target molecule lipophilicity are easy to produce by macrocyclization reactions via RCM using a ruthenium-based precatalyst compatible with the secondary hydroxy functions of sugars. The total syntheses using this approach of tricolorin A (**106**) (*109*), tricolorin G (**11**) (*110*), woodrosin I (**228**) (*111*, *112*), and ipomoeassins B (**3**), and E (**6**) (*113*) as well as the synthesis of the most frequently found disaccharide unit, L-Rha-(1→2)-D-Fuc, started with sugar building blocks (*i.e.,* L-rhamnose, D-fucose and/or D-glucose) and (6*S*)-undec-1-en-6-ol (*110*, *114*), with the latter readily accessible *via* asymmetric synthesis.

6.1. Tricolorin A

The total synthesis of tricolorin A (**106**) is an illustration of both synthetic approaches. The key disconnection for its retrosynthetic analysis (Scheme 1) has been the glycosidic linkage between glucose and rhamnose units. Coupling a rhamnose-rhamnose disaccharide glycosyl donor with a lactone disaccharide glycosyl acceptor has been used for the assembly of the entire tetrasaccharide skeleton of this target molecule. Both disaccharide subunits have been assembled via established glycosidation strategies. Due to the steric impediment that the large substituent at the anomeric position would present at the C-2 hydroxy group of the glucose unit, retrosynthesis of the lactone disaccharide fragment used the intrinsic differences in reactivities of the glucose hydroxy groups to selectively form the macrolactone at C-3 in the first approach, thus minimizing the number of protecting

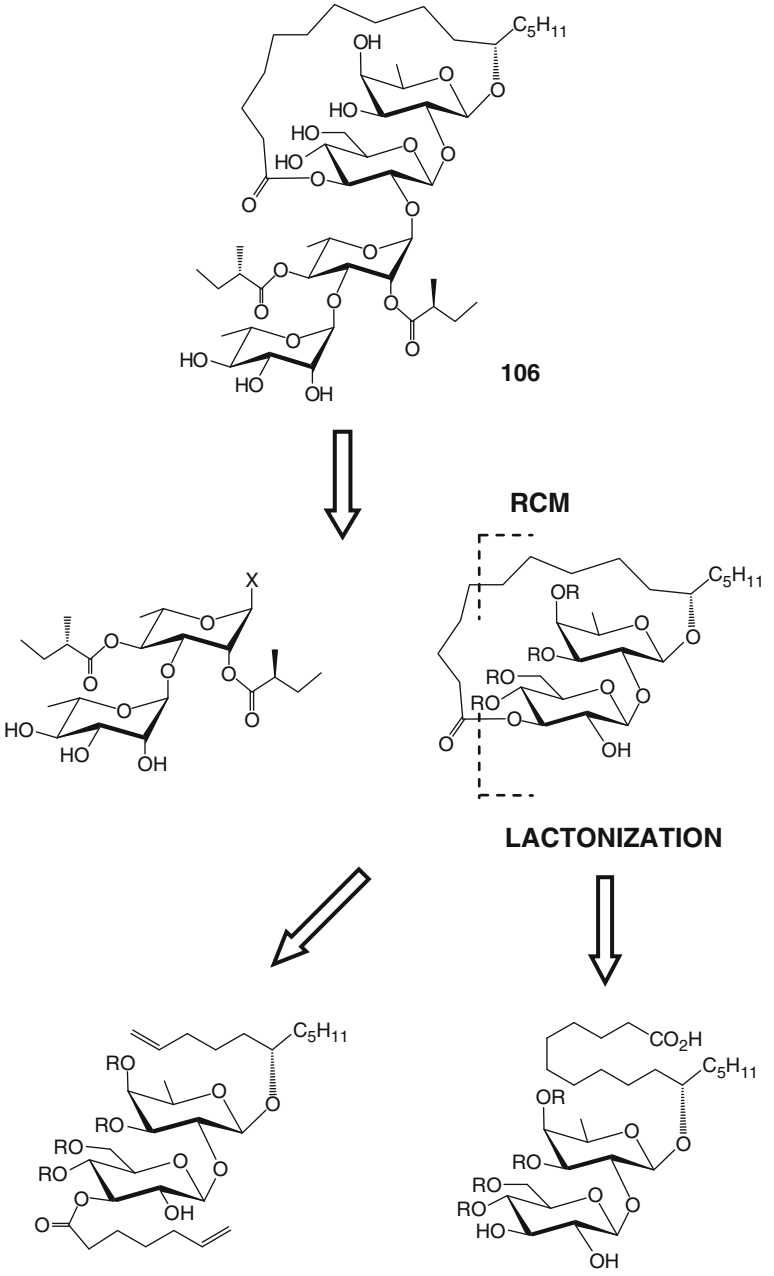

Scheme 1. Retrosynthetic analysis of tricolorin A (**106**)

groups. The RCM approach used an adequate diene as a cyclization precursor prepared by selective acylation with heptenoic acid of the corresponding diol at C-3 of glucose, in full accordance with the reactivity pattern described above.

6.1.1. Macrolactonization

The macrolactonization approach has been used by two different groups (*106*, *107*) to synthesize tricolorin A (**106**). Both approaches are similar and used as a key disconnection the glycosidic linkage between the glucose and rhamnose rings, and their goals were not to develop new synthetic methodologies for carbohydrates but rather to apply the known chemistry in an efficient manner. *Larson* and *Heathcock* started by coupling of the methyl ester derivative of jalapinolic acid with a protected D-fucosyl trichloroacetimidate to form fucoside **240** (*106*). Removal of the C-2 pivaloyl group from this derivative, followed by coupling with D-glucosyl trichloroacetimidate **241**, resulted in isolation of disaccharide **242**. The reaction of disaccharide glycosyl trichloroacetimidate **243** with disaccharide **242** was used to assemble the tetrasaccharide core. In preparation for the macrolactonization, the four ester groups were saponified to give acid triol **244**. Following the *Yonemitsu* protocol, the trihydroxy acid lactonized with a high degree of selectivity at the C-3 hydroxy position of the glucose ring instead of at the C-2 position, to afford the target diester lactone **245**, which was produced after addition of the chiral side chain acid. Synthetic tricolorin A (**106**) was obtained by deprotection of **245**. Starting from fucose, glucose, rhamnose, and (3*S*)-1-octyn-3-ol, the synthesis required 38 steps overall. The longest linear sequence was 14 steps, with an overall yield for this linear sequence of 6% (Scheme 2).

Coincidentally, *Lu* and co-workers employed a similar strategy for assembling the macrolactone disaccharide subunit (**246**) through a regioselective macrolactonization by the *Corey–Nicolaou* protocol (*107*). Macrolactone tetrasaccharide **245** was finally assembled by a facile one-pot, two-step glycosylation process with thioglycoside donors **247** and **248**. Alternatively, **245** was also constructed stepwise; disaccharide synthon **249**, the intermediate in the above one-pot protocol, was efficiently synthesized by a reaction of **247** and **248** involving the armed-disarmed glycosidation approach. Glycosylation of macrolactone disaccharide **246** by disaccharide donor **249** afforded the same important protected macrolactone precursor **245** of tricolorin A (**106**). This synthesis was achieved in a total of 45 steps, where the longest linear sequence consists of 20 steps, and the overall yield was 0.65% starting from D-(+)-mannitol (Scheme 3).

6.1.2. Ring-Closing Alkene Metathesis

RCM was also employed as a key design element for the synthesis of tricolorin A (**106**). This novel strategy demonstrated the efficiency of macrocyclizations using the standard ruthenimum catalysis either by the classical *Grubbs* carbene complex or the recently developed cationic ruthenium allenylidene complex as the

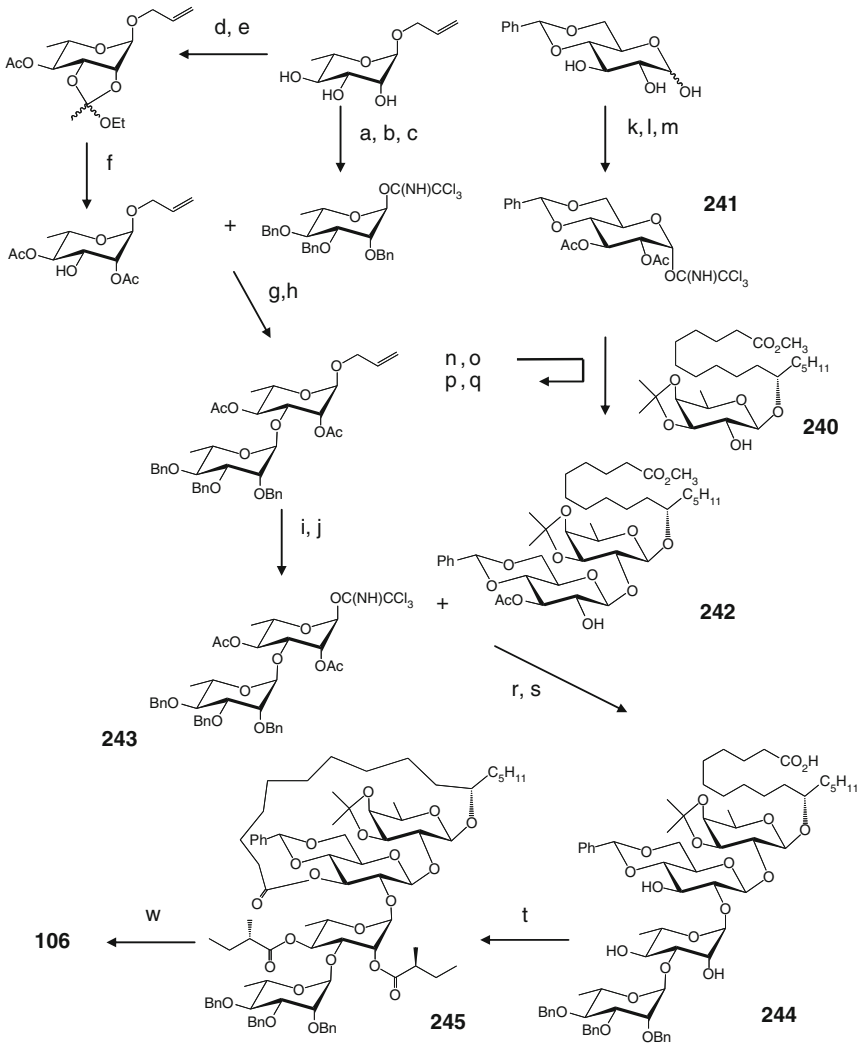

Scheme 2. Conditions: (a) BnBr, Bu_4NI, NaH, DMF; (b) (*i*) *t*-BuOK, DMSO, 100°C; (*ii*) 1*N* HCl, acetone, reflux; (c) Cl_3CCN, Cs_2CO_3, CH_2Cl_2, 76%; (d) $(EtO)_3CMe$, *p*-TsOH, CH_2Cl_2; (e) Ac_2O, Et_3N, DMAP, CH_2Cl_2; (f) HOAc, H_2O, 77%; (g) BF_3-Et_2O, CH_2Cl_2; (h) NaOMe, MeOH, 81%; (*i*) $(Ph_3P)_3RhCl$, *n*-BuLi, THF, reflux; (*ii*) HgO, $HgCl_2$, acetone, H_2O; (j) Cl_3CCN, Cs_2CO_3, CH_2Cl_2, 95%; (k) Ac_2O, Et_3N, DMAP, CH_2Cl_2; (l) (*i*) $BnNH_2$, THF; (*ii*) 1*N* HCl; (m) Cl_3CCN, Cs_2CO_3, CH_2Cl_2; (n) (*i*) **240** (*ii*) AgOTf, CH_2Cl_2; (o) LiOH, THF, H_2O; (p) Ac_2O (1 equiv), Et_3N, DMAP, CH_2Cl_2; (q) NaOMe, MeOH, MeOAc; (r) TMSOTf, CH_2Cl_2; (s) LiOH, THF, H_2O; (t) (*i*) 2,4,6-trichlorobenzoyl chloride, Et_3N, DMAP, benzene; (*ii*) (*S*)-2-methylbutyric acid; (w) $Pd(OH)_2$, H_2, HCl, MeOH

precatalysts (*110*). The required cyclization precursor **251** of the macrolactone disaccharide subunit **246** was assembled by established glycosidation methods from D-glucose, D-fucose, and (6*S*)-undec-1-en-6-ol (*109*). Diene **251a** cleanly

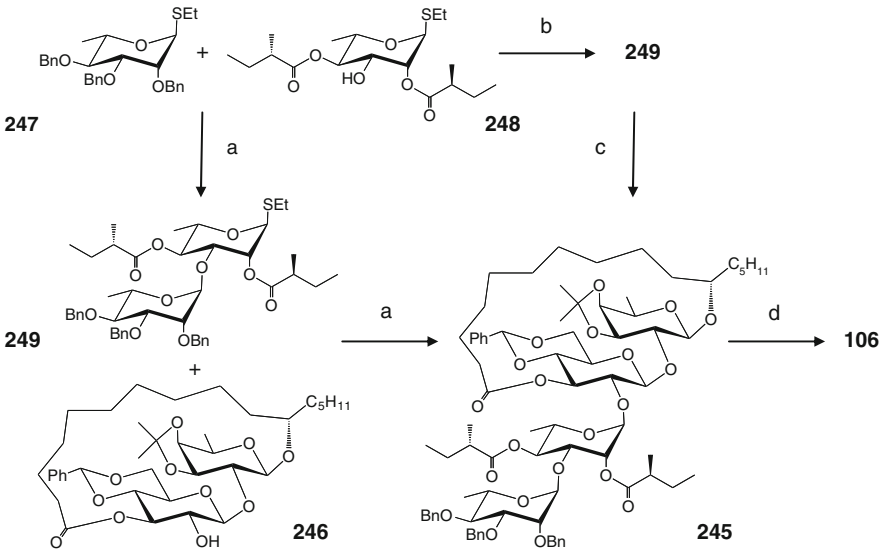

Scheme 3. Conditions: (a) **247** (1,2 equiv), **248** (1.0 equiv), NIS (1.4 equiv), TfOH (cat.), 4-Å molecular sieve, Et_2O, DCE (1:1; DCE = 1.2-dichloroethane), −15°C, 15 min, then **246** (1.6 equiv), NIS (1.4 equiv), TfOH (cat.), 4-Å molecular sieve, RT, 1 h, 43% (based on **246**); (b) IDCP (2.3 equiv), 4-Å molecular sieve, CH_2Cl_2, RT, 0.5 h, 98%; (c) (*i*) donor **246**, (*ii*) NIS (4.5 equiv), AgOTf (0.5 equiv, 4-Å molecular sieve, CH_2Cl_2, RT, 1 h, 86%; (d) two steps 1. DDQ (3.0 equiv), CH_3CN/H_2O (9/1), reflux, 4 h, 80%; 2. H_2 (6 Mpa), 10% Pd/C, 60°C, 7 h, 88%

cyclized to the desired 19-membered ring on reaction with the ruthenium carbene **252**. The fact that neither the free hydroxy group nor any other functional group in the substrate interfered with the RCM illustrated the selectivity of the *Grubbs* catalyst. Hydrogenation of the crude cycloalkene ((*E*)/(*Z*)-mixture) afforded disaccharide **246** in 77% yield over both steps. Since **246** was used as the key disaccharide subunit in the synthesis of **106** by the macrolactonization approach (see, Sect. 6.1.1), this RCM-based methodology completed a formal total synthesis of tricolorin A (Scheme 4). It should be mentioned that regioselective esterifications of diol **253**, in full accordance with *Heathcock*'s observations, with acids other that 4-pentenoic acid (**251a–251c**), permits a convenient entry into tricolorin A analogues differing from the parent macrolactone compound in their lipophilicity, as exemplified by the synthesis of compound **254** with a smaller macrocyclic structure, and **255** with an expanded lactone moiety.

6.2. Ipomoeassin E

The route for the cytotoxic ipomoeassin resin glycosides relied on the use of compound **256** as a new cinnamic acid surrogate with its trisubstituted double bond and meets the requirement of being hydrogenation resistant in the presence

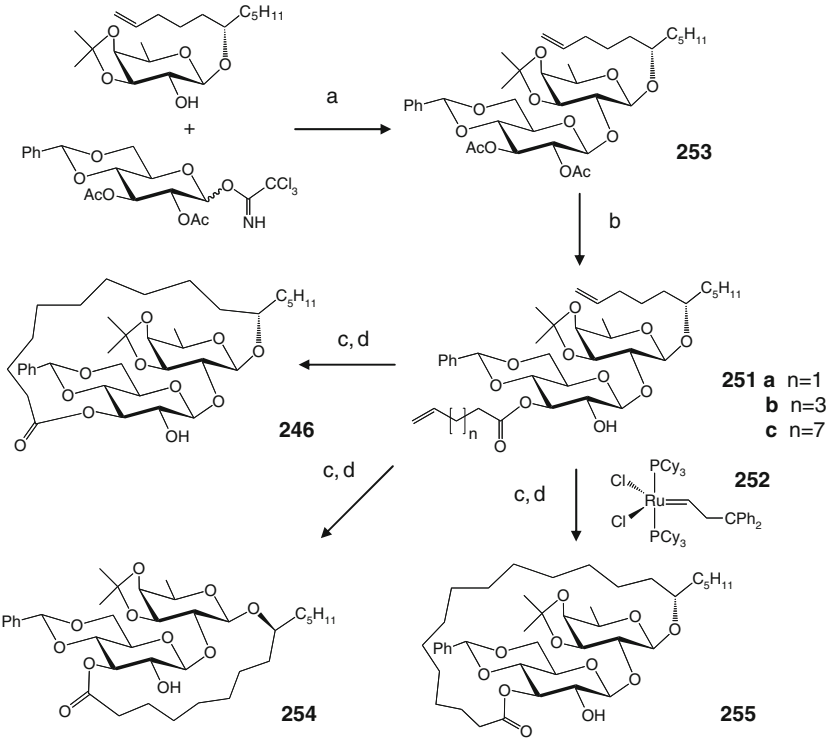

Scheme 4. Conditions: (a) $BF_3{\cdot}Et_2O$ cat., 20°C, CH_2Cl_2/*n*-hexane, 82%; (b) DCC, DMAP, CH_2Cl_2, **251a**, 4-pentenoic acid, 80%; **251b**: 6-heptenoic acid, 71%; **251c**: 10-undecenoic acid, 67%; (c) catalyst **252,** CH_2Cl_2, reflux; (d) H_2 (1 atm), Pd/C, EtOH, **246**: 77% (over both steps); **254**: 76% (over both steps); **255**: 76% (over both steps)

of homogeneous catalysts (*113*). As expected, acylation of disaccharide **257** with tiglic acid occured preferentially at the 3″-OH site (**258**). Reductive opening to the substituted benzylidene acetal in product **258** afforded the corresponding 6″-OPMB ether (**259**). Attachment of **256** to this derivative produced **260**, which was followed by oxidative cleavage of the -OPMB ether, released primary alcohol **261**. The subsequent following steps for the preparation of the required chiral acid segment for the esterification of this primary alcohol were: a *Sharpless*-type kinetic resolution of furyl alcohol (±)-**262**; oxidative rearrangement of (−)-**262**; oxidation of the hemiacetal in **263**; conjugate reduction of the resulting enone; opening of the

Scheme 5. Conditions: (a) Tiglic acid, DCC, DMAP, CH_2Cl_2, 55%; (b) $NaBH_3CN$, TMSCl, 4-Å molecular sieve, MeCN, 62%; (c) Acid **256**, 2,4,6-trichlorobenzoyl chloride, Et_3N, DMAP, toluene, 79% (over both steps from **258**); (d) DDQ, CH_2Cl_2/H_2O; (e) *t*-BuOOH, $VO(acac)_2$ (2%), CH_2Cl_2, 71%; (f) CrO_3, H_2SO_4, acetone, 0°C; (g) Zn, HOAc, CH_2Cl_2, 78% (over both steps); (h) (*i*) $HO(CH_2)_2SiMe_3$, *p*-TsOH cat., CH_2Cl_2; (*ii*) Ac_2O, DMAP cat., CH_2Cl_2, 93% (over both steps); (i) TASF, DMF, 68%; (j) compound **261**, 2,4,6-trichlorobenzoyl chloride, Et_3N, DMAP, toluene, 87%; (k) complex **268** (10%), CH_2Cl_2, reflux, 85%; (l) H_2 (1 atm), RhCl $(PPh_3)_3$ (20%), EtOH, 83%; (m) TASF, MeCN; (n) TFA, CH_2Cl_2, 63% (over both steps)

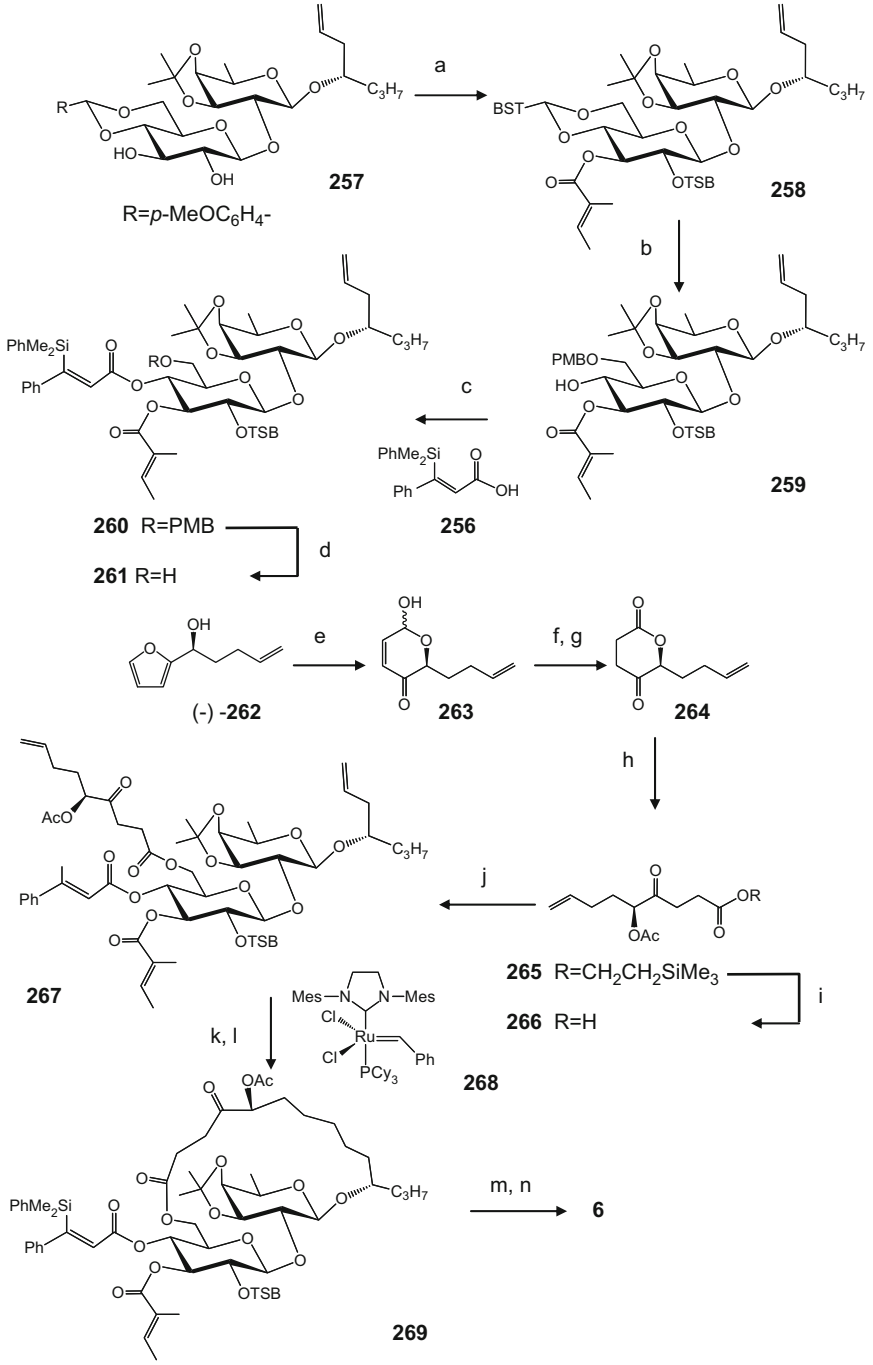
a
R=p-MeOC6H4-
257
BST
OTSB
258
b
PMBO
HO
259
c
PhMe2Si
Ph
OH
256
RO
260 R=PMB
d
261 R=H
OH
e
(-) -262
263
f, g
264
h
AcO
OR
OAc
265 R=CH2CH2SiMe3
i
266 R=H
j
267
Mes—N N—Mes
Cl
Ru
Cl
Ph
PCy3
268
k, l
OAc
m, n
6
269

lactone **264**; and cleavage of ester **265**, producing a good overall yield of acid **266** without racemization of the rather labile center at C-5. Esterification of **266** with disaccharide **261** afforded the precursor **267** for RCM macrolactonization using the ruthenium carbene **268**. Hydrogenation of the resulting (*E*)/(*Z*) mixture afforded macrolactone **269** which, after simultaneous cleavage of the C-silyl and O-silyl groups as well as final deprotection of the isopropylidene acetal, afforded ipomeassin E (**6**) in high overall yield (Scheme 5).

6.3. Woodrosin I

This particular branched oligosaccharide is certainly the structurally most demanding resin glycoside to have been totally synthesized (*111*, *112*). The particular challenges were: (1) the large macrolide ring spanning four glucose units; (2) the complementary acylation pattern at its periphery which seriously restricted the choices for protecting groups; (3) the pentasaccharide core entailing severe steric hindrance among hydroxy groups at vicinal positions at the branching site. Treatment of substrate **270** with tichloroacetimidate **271** resulted in a regioseletive reaction of the glycosyl acceptor's vicinal diol unit. Surprisingly, the reaction exclusively delivered the orthoester **272** by participation of the adjacent chloroacetyl moiety rather than the expected β-glycoside. Inspections of models suggested that the trajectory of a glycosyl donor towards the hidden 2″-OH group might be more favorable after closing the macrocyclic ring. Therefore, the completion of the oligosaccharide core was postponed after the RCM reation. Diene **272** was treated with catalytic amounts of the ruthenium indenylidene complex **273** resulting in an efficient ring closure which afforded cycloalkene **274** in 94% yield, (*E*):(*Z*) = 9:1 (Scheme 6). An inverse glycosylation procedure was used for the condensation of alcohol **274** and donor compound **275**. This method allowed for the attachment of the missing rhamnose unit to the oligosaccharide backbone as well as for the concomitant rearrangement of the orthoester to the required β-glycosidic linkage in the isolated product **276**, which was then easily elaborated into woodrosin I (**228**) (Scheme 6).

7. Significance

Little is known about either the mechanism of the purgative action caused by resin glycosides of the morning glory family or their ecological significance for the producing plants. The discovery of physiological effects with therapeutic potential

Scheme 6. Conditions: (a) donor **271**, TMSOTf cat., CH_2Cl_2, 84%; (b) complex **273** cat., CH_2Cl_2, reflux, 94%; (c) donor **275**, TMSOTf cat., Et_2O, 0°C, 60%; (d) hydrazinium acetate, DMF, −10→0°C; (e) H_2, Pd/C, MeOH, 84% (over both steps)

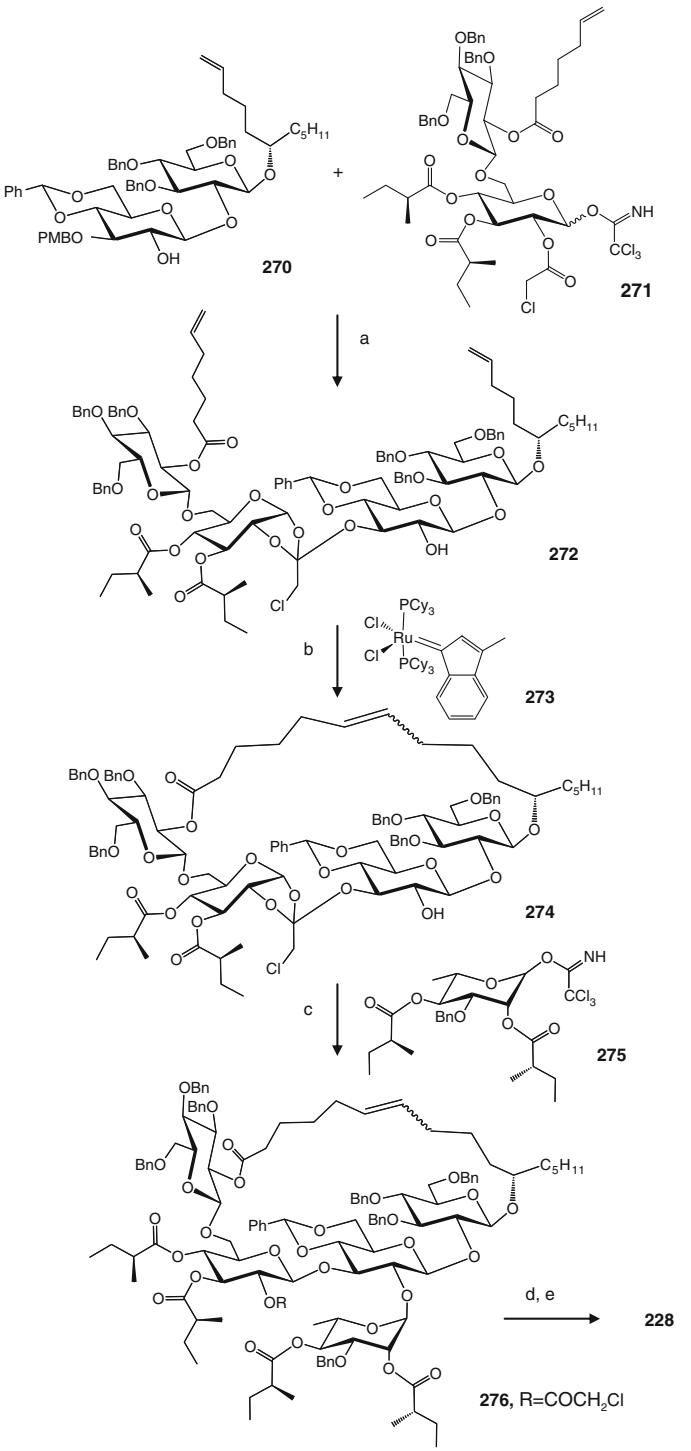
270
271
a
272
b
273
274
c
275
d, e
228
276, R=COCH2Cl

has stimulated a scientific revival of chemical research and biological evaluation of these principles. As of now, nothing is known about the biosynthesis of these compounds and all that can be said is that they are secondary metabolites derived from the assembly of products of primary metabolism such as sugars and fatty acids.

7.1. Traditional Medicine and Morning Glories

Morning glories have worldwide recognition in traditional medicine for the treatment of several illnesses apart from their purgative properties. Following is a description of the most interesting ethnobotanical information concerning resin glycoside-containing species.

In the Old World, several species are included in the contemporary health care systems of countries like the People's Republic of China and India, which have a long history of traditional use of herbal drugs. For example, the seeds of *Cuscuta chinensis* and *C. japonica* are used as tonics in mainland China (*14*). *Merremia hungaiensis* is the Chinese crude drug "Tu Gua" and used for the treatment of chronic hepatitis, hernia, and dealing with the tantrums of children (*73*). In the Unani system of India, *C. chinensis* is also considered to have antitumor activity. The seeds of *I. nil* are regarded as diuretics and antihelminthics as well as being prescribed for edema, constipation, and to promote menstruation (*77*, *86*). In India, the seeds of *I. turbinata* and *I. hederacea* are also used as laxatives and carminatives. In Indonesia, the tuber of *I. mammosa* is used to treat diabetes and illnesses involving the throat and the respiratory system as well as for burns, dysentery, edema, fever, and snake bites (*24*). *Convolvulus microphyllus* is reported to be a prominent memory-improving drug and used as a psychostimulant and tranquilizer as well as to reduce mental tension (*61*). In Europe, *Calystegia soldanella* has been used to cure hydropsy, paralysis, rheumatism, and scurvy (*81*). Worldwide, *Ipomoea pes-caprae*, commonly called "railroad vine" or "beach morning glory", is used in infusions for urinary or kidney complaints, hypertension, and scrofula and in decoctions to treat functional digestive disorders, internal pain, colic, dysentery, lumbago, and arthritis, rheumatism and other inflammatory conditions (*29*, *49*, *76*, *80*).

In the New World, several morning glories have been used since pre-Hispanic times. Native Americans used primarily the roots of *I. leptophylla*, *e.g.*, the Pawnee tribe dried the roots, burned them, and inhaled the smoke for treatment of nervousness and the Lakota people ate portions of the roots for stomach ailments (*66*). In Mexico, the roots of *I. orizabensis* have been employed as a vermifuge, for abdominal inflammation, dysentery, epilepsy, hydrocephaly, meningitis, and tumors (*44*). The roots of *I. stans* have been used to treat convulsions, hypertension, epilepsy, St. Vitus' dance and other nervous afflictions (*53*). There are 13 tree-like morning glory species belonging to the series *Arborescentes* with most confined to Mexico and nearby Central America. *I. murucoides* represents the signature species

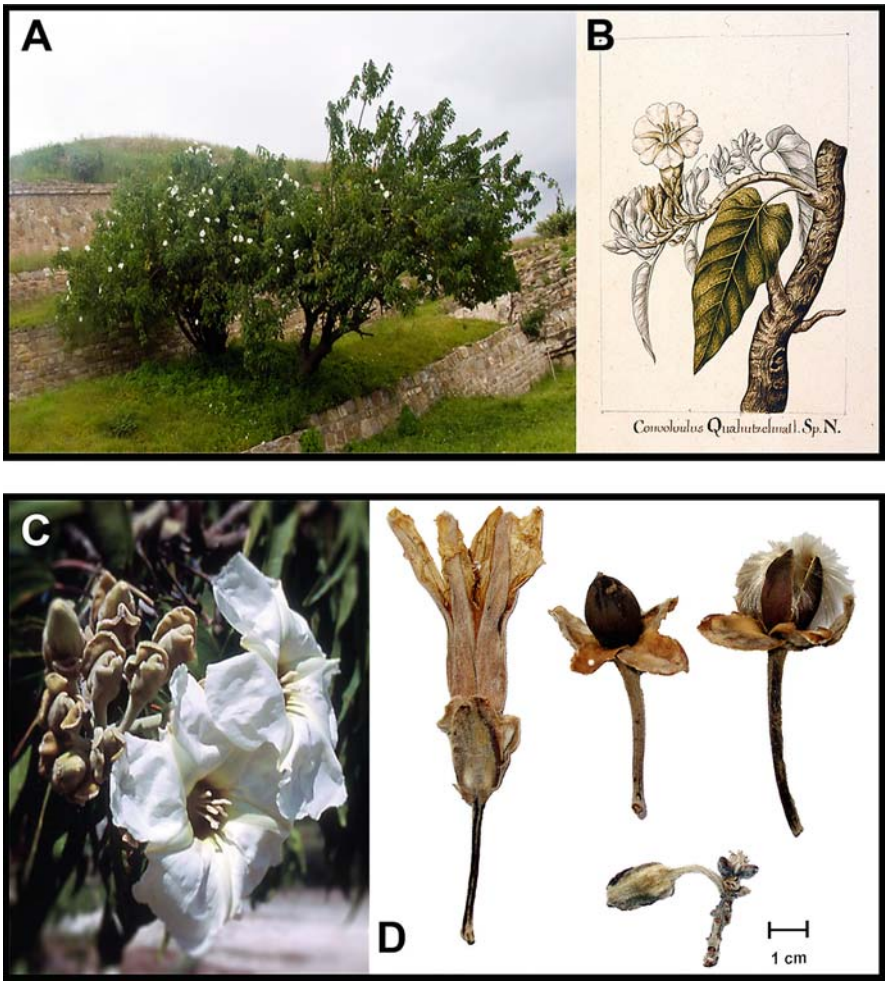

Plate 3. Arborescent morning glory species. The 13 species are confined to Mexico and nearby Central America and have long been of medicinal and economic interest (A: flowering tree in the archeological zone of Monte Alban, Oaxaca, Mexico). In central Mexico, six species collectively called "cazahuate" are a conspicuous floristic element of the Seasonal Dry Tropical Forest (B: Watercolor from eighteenth century Spanish Royal Botanical Expedition to the New World where the native name "Quahutzehuatl" was used to identified *Ipomoea murucoides*, the signature species of this medicinal plant complex. Courtesy of Hunt Institute for Botanical Documentation, Carnegie Mellon University, Pittsburgh, PA. Torner Collection of Sessé and Mociño Biological Illustrations). These trees share the morphological features of large white flowers and funnel-shaped corollas (C), as well as the same therapeutic uses such as treating itching and rashes by rubbing the raw flowers directly on the skin. Dried flowers with fruits (D)

of the "cazahuate" medicinal plant complex, a Nahuatl word (Aztec language) for "tree to cure mange" (Plate 3). This vernacular name in contemporary Mexican Spanish is used for all medicinal arborescent morning glories that share two

therapeutic properties: the raw flowers, used antiseptically, are rubbed directly on skin infections, itches and rashes, and as decoctions, plasters, and poultices for rheumatism, inflammation, and muscular pain (*70*). *I. arborescens* is another member of the "cazahuate" complex also known in several states of Western Mexico as "palo bobo". Some communities use an aqueous infusion of the bark against snake and scorpion bites, and to prevent hair loss (*58*). Infusions prepared from leaves are used as an anti-inflammatory agent and to treat stomachache. *I. intrapilosa* is endemic to the "Sierra Madre Occidental" (Western Sierra Madre, Mexico) and also grows in the central volcanic region that includes the states of Michoacán and Morelos. An infusion of the flowers of this "cazahuate" is used topically to treat rheumatism and ear pain, and the bark is chewed for toothache as well as burned to repel insects (*65*).

Native to tropical America, sweet potato (*I. batatas*) is a perennial morning glory vine that has been cultivated for over 5,000 years for its edible tubers in Mexico, Central and lowland South America, and the West Indies. Today, sweet potato is cultivated around the world, especially in developing countries (Plate 4). A decoction made from the leaves of this plant is used in folk remedies as a gargle to treat mouth and throat tumors, and poultices are prepared for inflammatory tumors (*64*). In Mexico, leaf decoctions are considered to be of "cold nature", to reduce excessive body heat, contemporarily defined as such illnesses as diarrhea, dysentery, heart disease, stomach distress, fever, and gastrointestinal infection. In Chinese traditional medicine, the tubers have been used as a medicinal herb to eliminate secretion in perceived abnormal quantities of blood or other body fluids (*79*).

7.2. Biological Activities

Selected resin glycosides isolated from medicinal morning glory species have recently been evaluated in several bioassays. In an effort to identify selective antifungal agents, the inhibitory potential of the tricolorin and orizabin series was evaluated on (1,3)-β-D-glucan synthase activity since the general structure of these series resembles that of papaculacandins, which are potent in vitro and in vivo inhibitors of this enzyme. Results showed that all the resin glycosides exhibited an inhibitory activity (IC_{50} = 0.06–0.18 μg/mm^3) comparable to that of papulacandin B (IC_{50} = 0.100 μg/mm^3) (*115*).

The cytotoxic potential of several resin glycosides has been evaluated against mammalian cancer cultured cell lines. For tricolorin A (**106**), the most potent cytotoxic activity (ED_{50} 2.2 μg/cm^3) was observed with human breast cancer and

Plate 4. Sweet potato. The roots of *Ipomoea batatas,* known in Mexico as "camote" (*camohtli* in Nahuatl, edible root), is an important contribution to world nutrition in addition to have been used by the native population as a "cold nature" remedy to reduce excessive body heat (A: The Latin description in this illustration from the *Badianus* Manuscript reads *Contra cordis calorem*, "for heat in the heart"; *Libellus de Medicinalibus Indorum Herbis*, 1552. Fol. 28v. CONACULTA-INAH-MEX, with permission of the "Instituto Nacional de Antropología e Historia", Mexico).

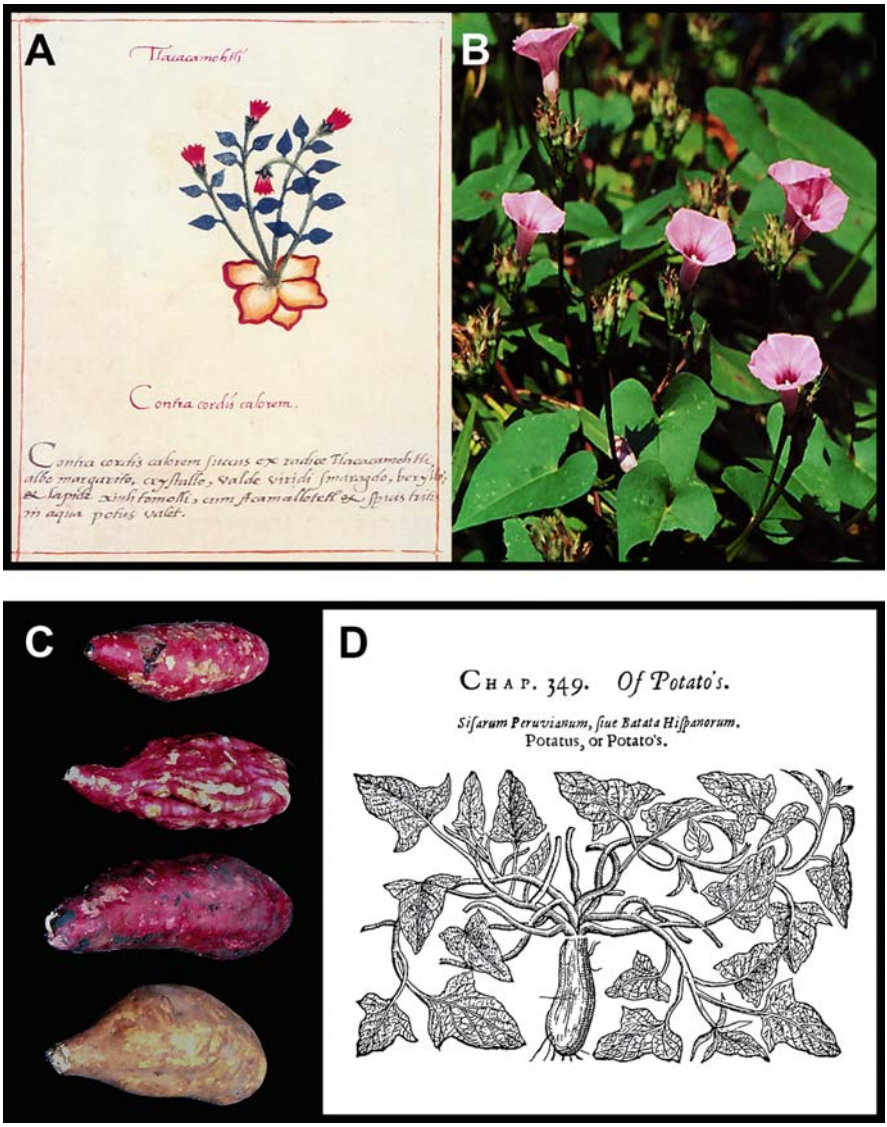

Plate 4. (*continued*) Aerial parts of commercially cultivated varieties are used to produce the crude drug (B). The edible varieties derived from the wild *Ipomoea tiliacea* were cultivated by careful selection by early native inhabitants of the tropical areas of the Americas (C: The varieties planted in Mexico include those with white, yellow, orange, red and purple pulp and skin colors). Although the sweet potato was introduced in Europe in early sixteenth century its importance was not properly appreciated due a confusion perpetuated by herbals (D: In *Gerald*'s *Herbal*, an Andean origin was ascertained to the sweet potato (*Sisarum peruvianum*) while claiming that the ordinary potato originated in the English colony of Virginia (*Battata virginiana*) and calling them both potato. Reproduced from reference (7) with permission of Dover Publications, Inc.)

P-388 cells (*55*). All members of the tricolorin and orizabin series also exhibited a weak cytotoxicity against colon carcinoma, squamous cell cervix carcinoma, and ovarian cancer cell lines (ED_{50} 4–20 μg/cm^3), but a more potent effect was observed when tested against oral epidermoid carcinoma (KB, ED_{50} 1–5 μg/cm^3). The potency displayed for triacetylated orizabins, *i.e.*, orizabins V–VII (**69–71**; KB, ED_{50} 7–10 μg/cm^3), was greater than the values reported for the more polar isolates with one or two acylating substituents (*44*, *45*). Similar results were described for the stansin series, which are composed of the same basic tetrasaccharide as the orizabins (*53*), and they displayed moderate to marginal cytotoxic activity against ovarian and cervical carcinoma cell lines (ED_{50} 1.5–24 μg/cm^3). All glycosidic acids, i.e., tricoloric, tyrianthinic, and scammonic acids, were inactive against all the cell lines tested, suggesting that the biological activity is associated with the macrocyclic structure of these glycoresins (*116*).

The highly lipophilic arboresin, intrapilosin, murucin, murucoidin, and pescaprein series were found to be weakly cytotoxic or inactive in cytotoxicity assays, *e.g.*, murucoidin IV (**162**) exhibited marginal activity againts Hep-2 laryngeal carcinoma cells (ED_{50} 4 μg/cm^3). The most potent of all resin glycosides is ipomoeassin F that inhibits A2780 human ovarian cancer cell line with a value as low as 0.37 μM (0.30 μg/cm^3). The available data with the ipomoeassin series suggest that minor variations in the peripherial oxygenation of the aglycone and acylation pattern of the oligosaccharide core modulate the cytotoxicity of these compounds to a significant extent (*15*, *16*).

Quantitative antimicrobial assays against *Staphylococcus aureus* led to the determination of a *MIC* (minimum inhibitory concentration) of 1.8 μg/cm^3 for tricolorin A (**106**). Tricolorin B (**107**) displayed a *MIC* of 8.7 μg/cm^3 while the values for the other tetrasaccharides of the tricolorin series were higher (*MIC* = 40–70 μg/cm^3). A moderate activity was also recorded for all these compounds against *Mycobacterium tuberculosis* (*MIC* = 16–32 μg/cm^3) (*117*). Convolvulaceous oligosaccharides selected from the tricolorin, scammonin, orizabin, and murucoidin series were evaluated for activity against a panel of *Staphylococcus aureus* strains possessing specific efflux pumps (*71*, *118*). The *MIC* values for most of the amphipatic compounds ranged from 4 to 32 μg/cm^3 against XU−212 (possessing the TetK multidrug efflux pump) and SA−1199B (overexpressing the NorA multidrug efflux pump), compared with 64 and 0.25 μg/cm^3, for tetracycline. This activity was shown to be bactericidal. Two microbiologically inactive members of the orizabin series, orizabins IX (**72**) and XIX (**82**), increased norfloxacin susceptibility of strain SA−1199B (*118*). Compound **72** at 25 μg/cm^3 reversed norfloxacin resistance fourfold (8 *vs.* 32 μg/cm^3) for SA−1199B, while **82** at 1 μg/cm^3 completely inhibited SA−1199B growth in the presence of norfloxacin (2 μg/cm^3). All of the murucoidins strongly potentiated the action of norfloxacin against this NorA over-expressing strain (*71*). They exerted a potentiation effect that increased the activity of norfloxacin by fourfold (8 μg/cm^3 from 32 μg/cm^3) at concentrations of 5–25 μg/cm^3; stoloniferin I (**224**) enhanced norfloxacin activity eightfold when incorporated at a concentration of 5 μg/cm^3. Orizabin IX (**72**) and reserpine were nearly equipotent with respect to the inhibition of ethidum bromide

efflux by SA−1199B, which is a substrate for many multidrug efflux pumps, including NorA of *S. aureus* (*118*). From these results, there seems to be a correlation between lipophilicity and antibacterial activity where the more lipophilic compounds displayed significantly more activity than their polar analogues. The size of the lactone ring was not crucial for antibacterial activity. The amphipathic properties of these compounds resulting from the acylation of some of the free hydroxy groups of the oligosaccharide core and the lipophilic alkyl chains of their aglycones would seem to be important in facilitating cellular uptake to its multidrug resistance pump target. It is possible that non-polar compounds will not interact with the membrane efflux pumps and those that are polar poorly penetrate membranes. In relation to the alleviation of refractive infections caused by effluxing staphylococci, the most important result from the standpoint of the potential use of resin glycosides as therapeutic agents is in combining these plant non-cytotoxic products with commercial antibiotics.

The formation of complex resin glycoside aggregates or micelles explains, in part, the cytotoxicity of this class of glycolipids with the potential to induce membrane perturbation provoking an imbalance of cellular homeostasis. The interactions of selected members of the tricolorin series with Sf9 cell membranes of the insect *Spodoptera frugiperda* were studied in an attempt to unravel the mechanism of action of these compounds. Tricolorin A (**106**) and all compounds evaluated with an intact macrolactone-type structures showed the ability to increase the membrane permeability for both cations (K^+ and Na^+) and anions (Cl^-) in a dose-dependent fashion, without any measurable delay, suggesting a membrane disruption induced by the amphiphilic properties of these molecules (*119*). The mammoside and merremoside series exhibited ionophoric activity against Na^+, K^+, and Ca^{2+} ions in human erythrocyte membranes (*24*, *25*, *120*). The ion-transport activities were completely lost by cleavage of the macrocyclic structure. A speculative model of transmembrane channel formation based on the crystal structure of tricolorin A (**106**) has been proposed to explain the interactions of the resin glycoside aggregates with their target cell membranes (*100*).

7.3. Pharmacology and Toxicology

The purgative effect of resin glycosides is confined to the whole molecule, presumably bound to the intact complex mixture of glycoconjugates, since their glycosidic acids are inactive. Resin glycosides induce peristalsis in the small intestine resulting in water elimination and numerous bowel movements within 1–2 h even after moderate dosages. It has been proposed that these compounds dissolve lecithin from the epithelial cells of the intestine resulting in its irritation (*2*).

Since even low overdoses cause severe inflammation of the mucous membranes of both the small intestine and the colon, the past medicinal importance of the Convolvulaceous resin glycosides as purgative herbal drugs has now been supplanted by the introduction of alternative phytopharmaceuticals with less severe

effects. Resin glycoside mixtures also display a saponin-like effect, as reported for a 38,000-fold dilution of jalapin, which caused a total hemolysis of human blood (*2*).

The effect of tricolorin A (**106**) on intestinal and arterial smooth muscle contractility was evaluated. This compound elicited a concentration-dependent stimulation of spontaneous contractions of the guinea pig ileum (EC_{50} = 6.99 ± 1.08 μg/cm^3) and a concentration-dependent vasorelaxation of the isolated intact rat aorta (EC_{50} = 4.63 ± 1.1 mg/cm^3). Both effects were completely abolished in the absence of extracellular Ca^{2+}. Verapamil (1 μM), a L-type voltage-dependent Ca^{2+} channel blocker, significantly inhibited the contractile response produced by tricolorin A (**106**) on the ileum, though it did not affect the vasodilatory actions. These findings suggest that the contractions induced on the ileum are caused mainly by an increase in Ca^{2+} permeability that occurs through L-type voltage-dependent Ca^{2+} channels found in the cell membrane. It seems that the influx of Ca^{2+} through voltage-dependent Ca^{2+} channels does not participate prominently in the vasorelaxant effect. This vascular relaxation was endothelium-dependent and significantly decreased in the presence of nitric oxide synthase and soluble guanylate cyclase inhibitors, and a NO scavenger. These results suggest that the vasodilatation is mainly due to activation of the NO/cGMP pathway (*121*).

Merremosides B (**13**) and D (**15**) exhibited antiserotonergic activity in mice with ED_{80} values of 10 μg/cm^3 and 2 μg/cm^3, (*cf.*, promethazine, ED_{80} 2 μg/cm^3) (*24*). Intraperitoneal administration to mice of tyrianthins VI (**91**), VIII (scammonin VI, **68**), and IX (**93**) resulted in antidepressant activity. Also, the activities of tryanthinic acids I (**94**) and II (**95**), and the macrolactones scammonins I (**63**) and II (**64**), and tyrianthins VI (**91**), VIII (**68**), and IX (**93**) exhibited dose-dependent protective effects against pentylenetetrazole-induced seizures. Tyrianthin VI (**91**) and scammonin II (**64**) produced relaxant effects on spontaneous contractions in the isolated rat ileum. Finally, the administration of compounds **68** and **93–95** to mouse brain slices induced increments in the release of GABA and glutamic acid (*48*).

7.4. Chemical Ecology

The morning glory heavenly blue (*I. tricolor*) was the first Convolvulaceous plant material subjected to activity-guided fractionation to identify its allelopathic constituents (*55*). The phytotoxicity was traced to the resin glycosides present in $CHCl_3$-soluble extracts. Further chromatographic analysis of this active fraction by reversed-phase HPLC yielded tricolorin A (**106**) as the main constituent (63%). Studies on the inhibition induced by the glycoside mixture on H^+-ATPase indicated that the activity was mainly caused by tricolorin A (**106**), for this compound strongly inhibited radicle growth of *Amaranthus leucocarpus* and *Echinochloa crus-galli* (IC_{50} 12–36 μM). Polar extracts prepared from the sweet potato root periderm also inhibited germination of several species but attempts to isolate the phytotoxic principles were unsuccessful (*122*). The $CHCl_3$ maceration of powdered sweet potatoes also afforded a bioactive residue, which clearly showed a defined

zone of phytotoxicity by means of a preliminary bioautographic TLC. Separation of this toxic band by preparative TLC and further purification by reversed-phase HPLC proved that the active constituents were a resin glycoside mixture with simonin IV (**185**, 48%) as the major principle (IC_{50} 50–90 μM) (*123*). Tricolorin A (**106**) has also been shown to uncouple photophosphorylation in spinach chloroplasts and to inhibit electron transport in photosystem II and ATP-synthesis, probably by interfering directly with the thylakoidal membrane and depending on the macrolactone-type structure for activity (*124*). The extracts from leaves of *Caloncyction aculeatum,* known in Chinese as "yue-guang-hua" (moonlight flower), showed a promoting effect on the growth and yield of various crops, such as yams, peanuts, beans, and wheat. The plant growth regulator was separated into components **40** and **41** by HPLC (*36*). The wide range of antimicrobial activity displayed by these compounds is an example of synergy between related components occurring in the same medicinal crude drug extract, *i.e.*, microbiologically inactive components disabling a resistance mechanism and potentiating the antibiotic properties of the active substances (*71*, *118*). Thus, morning glories may elaborate an array of amphipathic mixtures of glycolipids to confer selective advantages against microbial infections through a combination of several mechanisms of action, *e.g.*, cytotoxicity and modulation of multidrug resistance pumps. Intoxication of livestock has been attributed to both the resin glycoside and alkaloidal contents of several morning glories, providing evidence for their protective potential against vertebrate herbivores (*2*, *83*).

Acknowledgements. The corresponding author would like to express his gratitude to both the "Consejo Nacional de Ciencia y Tecnología" and the "Dirección General de Asuntos del Personal Académico" (UNAM) for their support of the chemical investigations of the morning glories used in Mexican traditional medicine through a series of grants over the past decade.

References

1. Langenheim JH (2003) Plant Resins. Chemistry, Evolution, Ecology, and Ethnobotany. Timber Press, Portland, Oregon, p 418
2. Eich E (2008) Solanaceae and Convolvulaceae: Secondary Metabolites. Biosynthesis, Chemotaxonomy, Biological and Economic Significance (A Handbook). Springer, Heidelberg, p 532
3. Pereda-Miranda R, Bah M (2003) Biodynamic Constituents in the Mexican Morning Glories: Purgative Remedies Transcending Boundaries. Curr Top Med Chem **3**: 111
4. Huguet-Termes T (2001) New World Materia Medica in Spanish Renaissance Medicine: From Scholarly Reception to Practical Impact. Medical History **45**: 359
5. Worth Estes J (2000) The Reception of American Drugs in Europe, 1500-1650. In: Varey S, Chabrán R, Weiner DB (eds) Searching for the Secrets of Nature. The Life and Works of Dr. Francisco Hernández. Stanford University Press, Stanford, California, p 111
6. Gunther RT (1968) The Greek Herbal of Dioscorides. Hafner, London, p 571
7. Gerard J (1975) The Herbal or General History of Plants. Dover, New York, p 872
8. Frampton J (1925) Joyfull Newes out of the Newe Founde World Written in Spanish by Nicholas Monardes, vol 1. Constable, London, p 54

9. Linares A, Rico-Gray V, Carrión G (1994) Traditional Production System of the Root of Jalap, *Ipomoea purga* (Convolvulaceae), in Central Veracruz, Mexico. Econ Bot **48**: 84
10. Pereda-Miranda R, Fragoso-Serrano M, Escalante-Sánchez E, Hérnandez-Carlos B, Linares E, Bye R (2006) Profiling of the Resin Glycoside Content of Mexican Jalap Roots with Purgative Activity. J Nat Prod **69**: 1460
11. Wagner H (1973) The Chemistry of Resin Glycosides of the Convolvulaceae Family. In: Bendz G, Santensson J (eds) Medicine and Natural Sciences. Chemistry in Botanical Classification. Academic Press, New York, p 235
12. Mannich C, Schumann P (1938) Über Jalapenharz und dessen Hauptbestandteil, das Convolvulin. Arch Pharm Ber Dtsch Pharm Ges **276**: 211
13. Noda N, Ono M, Miyahara K, Kawasaki T, Okabe M (1987) Resin Glycosides. I. Isolation and Structure Elucidation of Orizabin-I, II, III and IV, Genuine Resin Glycosides from the Root of *Ipomoea orizabensis*. Tetrahedron **43**: 3889
14. Umehara K, Nemoto K, Ohkubo T, Miyase T, Degawa M, Noguchi H (2004) Isolation of a New 15-Membered Macrocyclic Glycolipid Lactone, Cuscutic Resinoside A from the Seeds of *Cuscuta chinensis*: A Stimulator of Breast Cancer Cell Proliferation. Planta Med **70**: 299
15. Cao S, Guza RC, Wisse JH, Miller JS, Evans R, Kingston DGI (2005) Ipomoeassins A–E, Cytotoxic Macrocyclic Glycoresins from the Leaves of *Ipomoea squamosa* from the Suriname Rainforest. J Nat Prod **68**: 487
16. Cao S, Norris A, Wisse JH, Miller JS, Evans R, Kingston DGI (2007) Ipomoeassin F, a New Cytotoxic Macrocyclic Glycoresin from the Leaves of *Ipomoea squamosa* from the Suriname Rainforest. Nat Prod Res **21**: 872
17. Misra AL, Tewari JD (1952) Chemical Examination of Seeds of *Ipomoea muricata*. III. J Indian Chem Soc **29**: 430
18. Misra AL, Tewari JD (1953) Chemical Examination of *Ipomoea muricata* Seeds. IV. J Indian Chem Soc **30**: 391
19. Khanna SN, Gupta PC (1967) Structure of Muricatin. Phytochemistry **6**: 735
20. Miyahara K, Du XM, Watanabe M, Sugimura C, Yahara S, Nohara T (1996) Resin Glycosides XXIII. Two Novel Acylated Trisaccharides Related to Resin Glycoside from the Seeds of *Cuscuta chinensis*. Chem Pharm Bull **44**: 481
21. Du X-M, Sun N-Y, Nishi M, Kawasaki T, Guo Y-T, Miyahara K (1999) Components of the Ether-Insoluble Resin Glycoside Fraction from the Seed of *Cuscuta australis*. J Nat Prod **62**: 722
22. Bah M, Pereda-Miranda R (1997) Isolation and Structural Characterization of New Glycolipid Ester Type Dimers from the Resin of *Ipomoea tricolor* (Convolvulaceae). Tetrahedron **53**: 9007
23. Du XM, Kohinata K, Kawasaki T, Guo YT, Miyahara K (1998) Resin Glycosides XXVI. Components of the Ether-Insoluble Glycoside-Like Fraction from *Cuscuta chinensis*. Phytochemistry **48**: 843
24. Kitagawa I, Baek N-I, Kawashima K, Yokokawa Y, Yoshikawa M, Ohashi K, Shibuya H (1996) Indonesian Medicinal Plants XV. Chemical Structures of Five New Resin-Glycosides, Merremosides A, B, C, D, and E, from the Tuber of *Merremia mammosa* (Convolvulaceae). Chem Pharm Bull **44**: 1680
25. Kitagawa I, Ohashi K, In N, Sakagami M, Yoshikawa M, Shibuya H (1997) Indonesian Medicinal Plants. XIX. Chemical Structures of Four Additional Resin-Glycosides, Mammosides A, B, H_1 and H_2, from the Tuber of *Merremia mammosa* (Convolvulaceae). Chem Pharm Bull **45**: 786
26. Ono M, Kawasaki T, Miyahara K (1989) Resin Glycosides. V. Identification and Characterization of the Component Organic and Glycosidic Acids of the Ether-Soluble Crude Resin Glycosides ("Jalapin") from Rhizoma Jalapae Brasiliensis (Roots of *Ipomoea operculata*). Chem Pharm Bull **37**: 3209

27. Ono M, Fujimoto K, Kawata M, Fukunaga T, Kawasaki T, Miyahara K (1992) Resin Glycosides. XIII. Operculins VI, XI, XII, XIII, XIV and XV, the Ether-Soluble Resin Glycosides ("Jalapin") from Rhizoma Jalapae Brasiliensis (Roots of *Ipomoea operculata*). Chem Pharm Bull **40**: 1400
28. Noda N, Takahashi N, Miyahara K, Yang CR (1998) Stoloniferins VIII–XII, Resin Glycosides from *Ipomoea stolonifera*. Phytochemistry **48**: 837
29. Escobedo-Martínez C, Pereda-Miranda R (2007) Resin Glycosides from *Ipomoea pes-caprae*. J Nat Prod **70**: 974
30. Chérigo L, Pereda-Miranda R, Gibbons S (2009) Bacterial Resistance Modifying Tetrasaccharide Agents from *Ipomoea murucoides*. Phytochemistry **70**: 222
31. Noda N, Yoda S, Kawasaki T, Miyahara K (1992) Resin Glycosides XV. Simonins I–V, Ether-Soluble Resin Glycosides (Jalapins) from the Roots of *Ipomoea batatas* (cv. Simon). Chem Pharm Bull **40**: 3163
32. Noda N, Horiuchi Y (2008) The Resin Glycosides from the Sweet Potato (*Ipomoea batatas* L. Lam.). Chem Pharm Bull **56**: 1607
33. Noda N, Kobayashi H, Miyahara K, Kawasaki T (1988) Resin Glycosides II. Identification and Characterization of the Component Organic and Glycosidic Acids of the Crude Resin Glycosides from the Seeds of *Ipomoea muricata*. Chem Pharm Bull **36**: 627
34. Noda N, Kobayashi H, Miyahara K, Kawasaki T (1988) Resin Glycosides III. Isolation and Structural Study of the Genuine Resin Glycosides, Muricatins I–VI, from the Seeds of *Ipomoea muricata*. Chem Pharm Bull **36**: 920
35. Noda N, Nishi M, Miyahara K, Kawasaki T (1988) Resin Glycosides IV. Two New Resin Glycosides, Muricatins VII and VIII, from the Seeds of *Ipomoea muricata*. Chem Pharm Bull **36**: 1707
36. Fang Y, Chai W, Chen S, He Y, Zhao L, Peng J, Huang H, Xin B (1993) On the Structure of Calonyctin A, a Plant Growth Regulator. Carbohyd Res **245**: 259
37. Ono M, Fukunaga T, Kawasaki T, Miyahara K (1990) Resin Glycosides VIII. Four New Glycosidic Acids, Operculinic Acids D, E, F, and G, of the Ether-Soluble Crude Resin Glycosides ("Jalapin") from Rhizoma Jalapae Brasiliensis (Roots of *Ipomoea operculata*). Chem Pharm Bull **38**: 2650
38. Ono M, Ueguchi T, Murata H, Kawasaki T, Miyahara K (1992) Resin Glycosides XVI. Marubajalapins I–VII, New Ether-Soluble Resin Glycosides from *Pharbitis purpurea*. Chem Pharm Bull **40**: 3169
39. Ono M, Ueguchi T, Kawasaki T, Miyahara K (1992) Resin Glycosides XVII. Marubajalapins VIII–XI, Jalapins from the Aerial Part of *Pharbitis purpurea*. Yakugaku Zasshi **112**: 866
40. Yin Y-Q, Wang J-S, Luo J-G , Kong L-Y (2009) Novel acylated lipo-oligosaccharides from the tubers of *Ipomoea batatas*. Carbohyd Res **344**: 466
41. Noda N, Kogetsu H, Kawasaki T, Miyahara K (1992) Scammonins VII and VIII. Two Resin Glycosides from *Convolvulus scammonia*. Phytochemistry **31**: 2761
42. Noda N, Kogetsu H, Kawasaki T, Miyahara K (1990) Scammonins I and II. The Resin Glycosides of Radix Scammoniae from *Convolvulus scammonia*. Phytochemistry **29**: 3565
43. Kogetsu H, Noda N, Kawasaki T, Miyahara K (1991) Scammonins III–VI. Resin Glycosides of *Convolvulus scammonia*. Phytochemistry **30**: 957
44. Hernández-Carlos B, Bye R, Pereda-Miranda R (1999) Orizabins V–VIII. Tetrasaccharide Glycolipids from the Mexican Scammony Root (*Ipomoea orizabensis*). J Nat Prod **62**: 1096
45. Pereda-Miranda R, Hernández-Carlos B (2002) HPLC Isolation and Structural Elucidation of Diastereomeric Niloyl Ester Tetrasaccharides from Mexican Scammony Root. Tetrahedron **58**: 3145
46. Austin DF, Huáman Z (1996) A Synopsis of *Ipomoea* (Convolvulaceae) in the Americas. Taxon **45**: 3
47. Mirón-López G, Herrera-Ruiz M, Estrada-Soto S, Aguirre-Crespo F, Vásquez-Navarrete L, León-Rivera I (2007) Resin Glycosides from the Roots of *Ipomoea tyrianthina* and Their Biological Activity. J Nat Prod **70**: 557

48. León-Rivera I, Mirón-López G, Molina-Salinas GM, Herrera-Ruiz M, Estrada-Soto S, Gutierrez M, Alonso-Cortes D, Navarrete-Vásquez G, Ríos M, Said-Fernández S (2008) Tyrianthinic Acids from *Ipomoea tyrianthina* and Their Antimycobacterial Activity, Cytotoxicity and Effects on the Central Nervous System. J Nat Prod **71**: 1686
49. Pereda-Miranda R, Escalante-Sánchez E, Escobedo-Martínez C (2005) Characterization of Lipophilic Pentasaccharides from Beach Morning Glory (*Ipomoea pes-caprae*). J Nat Prod **68**: 226
50. Calis I, Sezgin Y, Dönmez AA, Rüedi P, Tasdemir D (2007) Crypthophilic Acids A, B, and C: Resin Glycosides from Aerial Parts of *Scrophularia crypthophila*. J Nat Prod **70**: 43
51. Enriquez RG, Leon I, Perez F, Walls F, Carpenter KA, Puzzuoli FV, Reynolds WF (1992) Characterization, by Two-Dimensional NMR Spectroscopy, of a Complex Tetrasaccharide Glycoside Isolated from *Ipomoea stans*. Can J Chem **70**: 1000
52. Reynolds WF, Yu M, Enriquez RG, Gonzalez H, Leon I, Magos G, Villareal ML (1995) Isolation and Characterization of Cytotoxic and Antibacterial Tetrasaccharide Glyclosides from *Ipomoea stans*. J Nat Prod **58**: 1730
53. León I, Enriquez RG, Gnecco D, Villareal ML, Cortés DA, Reynolds WF, Yu M (2004) Isolation and Characterization of Five New Tetrasaccharide Glycosides from the Roots of *Ipomoea stans* and Their Cytotoxic Activity. J Nat Prod **67**: 1552
54. Gaspar EMM (2001) Soldanelline B, the First Acylated Nonlinear Tetrasaccharide Macrolactone from the European Convolvulaceae *Calystegia soldanella*. Eur J Org Chem **2001**: 369
55. Pereda-Miranda R, Mata R, Anaya AL, Wickramaratne DBM, Pezzuto JM, Kinghorn AD (1993) Tricolorin A, Major Phytogrowth Inhibitor from *Ipomoea tricolor*. J Nat Prod **56**: 571
56. Bah M, Pereda-Miranda R (1996) Detailed FAB-Mass Spectrometry and High Resolution NMR Investigations of Tricolorins A–E, Individual Oligosaccharides from the Resins of *Ipomoea tricolor* (Convolvulaceae). Tetrahedron **52**: 13063
57. Wagner H, Wenzel G, Chari VM (1978) The Turpethinic Acids of *Ipomoea turphetum* L. Planta Med **33**: 144
58. León I, Mirón G, Alonso D (2006) Characterization of Pentasaccharide Glycosides from the Roots of *Ipomoea arborescens*. J Nat Prod **69**: 896
59. Harrison DA, Madhusudan KP, Kulshreshtha DK (1985) Structure of Dichroside D, a Fatty Acid Glycoside from *Ipomoea dichroa*. Carbohyd Res **143**: 207
60. Kitagawa I, In N, Ykokawa Y, Yoshikawa M (1996) Chemical Structures of Four New Resin-Glycosides, Meremosides F, G, H_1, and H_2, from the Tuber of *Merremia mammosa* (Convolvulaceae). Chem Pharm Bull **44**: 1693
61. Wagner H, Schwarting G (1997) Struktur der Microphyllinsäure aus dem Harz von *Convolvulus microphyllus*. Phytochemistry **16**: 715
62. Ono M, Honda F, Karahashi A, Kawasaki T, Miyahara K (1997) Resin Glycosides XXV. Multifidins I and II, New Jalapins, from the seed of *Quamoclit* x *multifida*. Chem Pharm Bull **45**: 1955
63. León I, Enriquez RG, Nieto DA, Alonso D, Reynolds WF, Aranda E, Villa J (2005) Pentasaccharide Glycosides from the Roots of *Ipomoea murucoides*. J Nat Prod **68**: 1141
64. Escalante-Sánchez E, Rosas-Ramírez D, Linares E, Bye R, Pereda-Miranda R (2008) Batatinosides II−VI, Acylated Lipooligosaccharides from the Resin Glycosides of Sweet Potato. J Agric Food Chem **56**: 9423
65. Bah M, Chérigo L, Cardoso A, Fragoso-Serrano M, Hammond GB, Pereda-Miranda R (2007) Intrapilosins I-VII, Pentasaccharides from the Seeds of *Ipomoea intrapilosa*. J Nat Prod **70**: 1153
66. Barnes CC, Smalley MK, Manfredi KP, Kindscher K, Loring H, Sheeley DM (2003) Characterization of an Anti-tuberculosis Resin Glycoside from the Prairie Medicinal Plant *Ipomoea leptophylla*. J Nat Prod **66**: 1457

67. Ono M, Kubo K, Miyahara K, Kawasaki T (1989) Operculin I and II, New Ether-Soluble Resin Glycosides ("Jalapin") with Fatty Acid Ester Groups from Rhizoma Jalapae Braziliensis (Roots of *Ipomoea operculata*). Chem Pharm Bull **37**: 241
68. Ono M, Kawasaki T, Miyahara K (1991) Resin Glycosides XI. Operculins III, IV, IX, X, XVI, XVII and XVIII. New Ether-Soluble Resin Glycosides of Rhizoma Jalapae Braziliensis (Root of *Ipomoea operculata*). Chem Pharm Bull **39**: 2534
69. Noda N, Takahashi T, Kawasaki T, Miyahara K, Yang CR (1994). Stoloniferins I-VII, Resin Glycosides from *Ipomoea stolonifera*. Phytochemistry **36**: 365
70. Chérigo L, Pereda-Miranda R (2006) Resin Glycosides from the Flowers of *Ipomoea murucoides*. J Nat Prod **69**: 595
71. Chérigo L, Pereda-Miranda R, Fragoso-Serrano M, Jacobo-Herrera N, Kaatz GW, Gibbons S (2008) Inhibitors of Bacterial Multidrug Efflux Pumps from the Resin Glycosides of *Ipomoea murucoides*. J Nat Prod **71**: 1037
72. Ono M, Kuwabata K, Kawasaki T, Miyahara K (1992) Resin Glycosides XVI. Quamoclins I-IV, New Ether-Soluble Resin Glycosides (Jalapin) from the Seeds of *Quamoclit pennata*. Chem Pharm Bull **40**: 2674
73. Noda N, Tsuji K, Miyahara K, Yang CR (1994) Resin Glycosides XXI. Tuguajalapins I–X, the Resin Glycosides Having Long-Chain Fatty Acid Groups from the Root of *Merremia hungaiensis*. Chem Pharm Bull **42**: 2011
74. Ono M, Fukuda H, Murata H, Miyahara K (2009) Resin glycosides from the leaves and stems of *Ipomoea digitata*. J Nat Med **63**: 176
75. Escobedo-Martínez C (2007) Resinas Glicosídicas de la Planta Medicinal *Ipomoea pes-caprae*. PhD Thesis, Universidad Nacional Autónoma de México, p 71
76. Srivastava R, Sachdev K, Madhusudanan KP, Kulshreshtha D (1991) Structure of Pescaproside E, Fatty Acid Glycoside from *Ipomoea pes-caprae*. Carbohyd Res **212**: 169
77. Ono M, Noda N, Kawasaki T, Miyahara K (1990) Resin Glycosides. VII. Reinvestigation of the Component Organic and Glycosidic Acids of Pharbitin, the Crude Ether-Insoluble Resin Glycoside ("Convolvulin") of Pharbitis Semen (Seeds of *Pharbitis nil*). Chem Pharm Bull **38**: 1892
78. Escalante-Sánchez E, Pereda-Miranda R (2007) Batatins I and II, Ester-Type Dimers of Acylated Pentasaccharides from the Resin Glycosides of Sweet Potato. J Nat Prod **70**: 1029
79. Yin Y, Li Y, Kong L (2008) Pentasaccharide Glycosides from the Tubers of Sweet Potato (*Ipomoea batatas*). J Agric Food Chem **56**: 2363
80. Tao H, Hao X, Liu J, Ding J, Fang Y, Gu Q, Zhu W (2008) Resin Glycoside Constituents of *Ipomoea pes-caprae* (Beach Morning Glory). J Nat Prod **71**: 1998
81. Gaspar E (1999) New Pentasaccharide Macrolactone from the European Convolvulaceae *Calystegia soldanella*. Tetrahedron Lett **40**: 6861
82. Ono M, Nakagawa T, Kawasaki T, Miyahara K (1993) Woodrosins I and II, Ether-Insoluble Resin Glycosides from the Stems of *Ipomoea tuberosa*. Chem Pharm Bull **41**: 1925
83. MacLeod JK, Ward A, Oelrichs PB (1997) Structural Investigation of Resin Glycosides from *Ipomoea lonchophylla*. J Nat Prod **60**: 467
84. Wagner H, Kazmaier P (1977) Struktur der Operculinsäure aus dem Harz von *Ipomoea operculata*. Phytochemistry **16**: 711
85. Okabe H, Kawasaki T (1972) Studies on Resin Glycosides III. Complete Structures of Pharbitic Acids C and D. Chem Pharm Bull **20**: 514
86. Yin Y-Q, Huang X-F, Kong L-Y, Niwa M (2008) Three New Pentasaccharide Resin Glycosides from the Roots of Sweet potato (*Ipomoea batatas*). Chem Pharm Bull **56**: 1670
87. Escalante-Sánchez E (2007) Caracterización de la Composición Química de las Resinas Glicosídicas de Tres Remedios Herbolarios Purgantes del Género *Ipomoea* (Convolvulaceae). PhD Thesis, Universidad Nacional Autónoma de México, p 153

88. Noda N, Tsuji K, Kawasaki T, Miyahara K, Hanazono H, Yang CR (1995) A Novel Resin Glycoside, Merremin (Tuguajalapin X Dimer), from *Merremia hungaiensis*. Chem Pharm Bull **43**: 1061
89. Okabe H, Koshito N, Tanaka K, Kawasaki T (1971) Studies on Resin Glycosides. II. Unhomogeneity of "Pharbitic Acid" and Isolation and Partial Structures of Pharbitic Acids C and D, the Major Constituents of "Pharbitic Acid". Chem Pharm Bull **19**: 2394
90. Kubo I, Nakatsu T (1990) Recent Examples of Preparative-Scale Recycling High Performance Liquid Chromatography in Natural Products Chemistry. LC-GC **8**: 933
91. White CA, Kennedy JF (1986) Oligosaccharides. In: Chaplin MF, Kennedy JF (eds) Carbohydrate Analysis. A Practical Approach. IRL Press, Oxford, UK p 37
92. Okabe H, Kawasaki T (1970) Structures of Pharbitic Acids C and D. Tetrahedron Lett **36**: 3123
93. Wolter MA, Engels JW, Montanarella L, Tilio R, Faccheti S (1995) Influence of Matrix on FAB-MS of Oligonucleotides. J Mass Spectrom **30**: 485
94. Dass C (1996) The Role of a Liquid Matrix in Controlling FAB-Induced Fragmentation. J Mass Spectrum **31**: 77
95. Du XM, Sun NY, Nishi M, Kawasaki T, Guo YT, Miyahara K (1999) Components of the Ether-Insoluble Resin Glycoside Fraction from the Seed of *Cuscuta australis*. J Nat Prod **62**: 722
96. Duus JØ, Gotfredsen CH, Bock K (2000) Carbohydrate Structural Determination by NMR Spectroscopy: Modern Methods and Limitations. Chem Rev **100**: 4589
97. Agrawal PK, Pathak AK (1996) Nuclear Magnetic Resonance Spectroscopic Approaches for the Determination of Interglycosidic Linkage and Sequence in Oligosaccharides. Phytochem Anal **7**: 113
98. Ono M, Yamada F, Noda N, Kawasaki T, Miyahara K (1993) Resin Glycosides. XVIII. Determination by Mosher's Method of the Absolute Configurations of Mono- and Dihydroxyfatty Acids Originated from Resin Glycosides. Chem Pham Bull **41**: 1023
99. Imberty A, Pérez S (2000) Structure, Conformation, and Dynamic of Bioactive Oligosaccharides: Theoretical Approaches and Experimental Validations. Chem Rev **100**: 4567
100. Rencurosi A, Mitchell EP, Cioci G, Pérez S, Pereda-Miranda R, Imberty A (2004) Crystal Structure of Tricolorin A: Molecular Rationale for the Biological Properties of Resin Glycosides Found in Some Mexican Herbal Remedies. Angew Chem Int Ed **43**: 5918
101. Lehmann CW, Fürstner A, Müller T (2000) Macrocyclic Substructure of Tricolorin A. The First Crystal Structure of a Resin Glycoside. Z Kristallogr **215**: 114
102. Wormald MR, Petrescu AJ, Pao YL, Glithero A, Elliot T, Dwek RA (2002) Conformational Studies of Oligosaccharides and Glycopeptides: Complementarity of NMR, X-Ray Crystallography, and Molecular Modelling. Chem Rev **102**: 371
103. Meyer B (1990) Conformational Aspects of Oligosaccharides. Topics Curr Chem **154**: 141
104. Jiang ZH, Geyer A, Schmidt RR (1995) The Macrolidic Glycolipid Calonyctin A, a Plant Growth Regulator: Synthesis, Structural Assignment, and Conformational Analysis in Micellar Solution. Angew Chem Int Ed Engl **34**: 2520
105. Furukawa J-I, Kobayashi S, Nomizu M, Nishi N, Sakairi N (2000) Total Synthesis of Calonyctin A_2, a Macrolidic Glycolipid with Plant Growth-Promoting Activity. Tetrahedron Lett **41**: 3453
106. Larson DP, Heathcock CH (1997) Total Synthesis of Tricolorin A. J Org Chem **62**: 8406
107. Lu S-F, O'yang Q, Guo Z-W, Yu B, Hui Y-Z (1997) Total Synthesis of Tricolorin A. J Org Chem **62**: 8400
108. Brito-Arias M, Pereda-Miranda R, Heathcock CH (2004) Synthesis of Tricolorin F. J Org Chem **69**: 4567
109. Fürstner A, Müller T (1998) Metathesis Route to Resin Glycosides: Formal Total Synthesis of Tricolorin A. J Org Chem **63**: 424
110. Fürstner A, Müller T (1999) Efficient Total Syntheses of Resin Glycosides and Analogues by Ring-Closing Olefin Metathesis. J Am Chem Soc **121**: 7814

111. Fürstner A, Jeanjean F, Razon P, Wirtz C, Mynott R (2003) Total Synthesis of Woodrosin I—Part 1: Preparation of the Building Blocks and Evaluation of the Glycosylation Strategy. Chem Eur J **9**: 307
112. Fürstner A, Jeanjean F, Razon P (2002) Total Synthesis of Woodrosin I. Angew Chem Int Ed **41**: 2097
113. Fürstner A, Nagano T (2007) Total Syntheses of Ipomoeassin B and E. J Am Chem Soc **129**: 1906
114. Fürstner A (2004) Total Syntheses and Biological Assessment of Macrocyclic Glycolipids. Eur J Org Chem **2004**: 943
115. Castelli MV, Cortés JCG, Escalante AM, Bah M, Pereda-Miranda R, Ribas JC, Zacchino SA (2002) Inhibition of (1,3)-β-Glucan Synthase by Glycoresins from Convolvulaceous Plants. Planta Med **68**: 739
116. Pereda-Miranda R (1995) Bioactive Natural Products from Traditionally Used Mexican Plants. In: Arnason JT, Mata R, Romeo JT (eds) Phytochemistry of Medicinal Plants. Plenum Press, New York, p 83
117. Rivero-Cruz I, Acevedo L, Guerrero JA, Martínez S, Bye R, Pereda-Miranda R, Franzblau S, Timmermann BN, Mata R (2005) Antimycobacterial Agents from Selected Mexican Medicinal Plants. J Pharm Pharmacol **57**: 1117
118. Pereda-Miranda R, Kaatz GW, Gibbons S (2006) Polyacylated Oligosaccharides from Medicinal Mexican Morning Glory Species as Antibacterials and Inhibitors of Multidrug Resistance in *Staphylococcus aureus*. J Nat Prod **69**: 406
119. Pereda-Miranda R, Villatoro-Vera R, Bah M, Lorence A (2009) Pore-Forming Activity of Morning Glory Resin Glycosides in Model Membranes. Rev Latinoamer Quimica **37**: 144
120. Kitagawa I, Ohashi K, Kawanishi H, Shibuya H, Shinkai K, Akedo H (1989) Ionophoretic Activities of Oligopeptide Lactones and Resin-Glycosides in Human Erythrocytes. Chem Pharm Bull **37**: 1679
121. Hernández R, Vuelvas A, García A, Fragoso M, Pereda R, Ibarra C, Rojas A (2008) Calcium-Dependent Effect of Tricolorin A on Intestinal and Arterial Smooth Muscle Contractility. 7th Joint Meeting of AFERP, ASP, GA, PSE and SIF. Planta Med **74**: 973
122. Peterson JK, Harrison HF (1991) Isolation of Substance from Sweet Potato (*Ipomoea batatas*) Periderm Tissue that Inhibits Seed Germination. J Chem Ecol **17**: 943
123. Mata R, Pereda-Miranda R, Lotina-Hennsen B (1996) Natural Products from Mexican Plants as a Source of Potential Herbicide Agents. In: Rodríguez-Hahn L, Pandalai SG (eds) Secondary Metabolites from Mexican Plants: Chemistry and Biological Properties. Research Signpost, Trivandrum, India p 59
124. Achnine L, Pereda-Miranda R, Iglesias-Prieto R, Moreno-Sánchez R, Lotina-Hennsen B (1999) Tricolorin A, a Potent Natural Uncoupler and Inhibitor of Photosystem II Acceptor Side of Spinach Chloroplasts. Physiol Plant **106**: 246

Author Index

C

D

H

L

M

N

S

T

Subject Index